New perspectives for the management of Duchenne Muscular Dystrophy

Nicolas Dubuisson

Thèse présentée en vue de l'obtention du grade

de docteur en sciences de la santé

Promotors: Pr Sonia Brichard and Pr Peter Van den Bergh
Endocrinology, Diabetes and nutrition unit (EDIN)
Institute of Expiremental and Clinical research (IREC)
Université Catholique de Louvain

October 2024

Jury Members

Promotors

Pr Sonia Brichard: Endocrinology, Diabetes and nutrition unit (EDIN), Institute of Expiremental and Clinical research (IREC), Université Catholique de Louvain, Brussels, Belgium

Pr Peter Van den Bergh: Neuromuscular Reference Center, Neurology department, Cliniques universitaires St-Luc, Brussels, Belgium

Co-Promotor

Pr Philippe Gailly : Cellular and Molecular Division, institute of Neuroscience, Université Catholique de Louvain, Brussels, Belgium

Jury President

Pr Yves Vandermeeren: Institute of Neuroscience (IONS), Clinical neuroscience, Université Catholique de Louvain, Brussels, Belgium

Internal Jury members

Pr Olivier Devuyst : Pôle néphrologie, Institute of Expiremental and Clinical research (IREC), Université Catholique de Louvain, Brussels, Belgium

Pr Nathalie Goemans: Department of Child Neurology, University Hospitals Leuven, Leuven, Belgium

Pr Jean-Paul Thissen : Endocrinology, Diabetes and nutrition unit (EDIN), Institute of Expiremental and Clinical research (IREC), Université Catholique de Louvain, Brussels, Belgium

External Jury members

Pr Nicolas Deconinck: Neuromuscular Reference Center, UZ Gent, Ghent, Belgium

Pr Annamaria De Luca : Department of Pharmacy-Drug Sciences, University of Bari "Aldo Moro", Bari, Italy

Remerciements

Je tiens à exprimer mes plus sincères remerciements à ma superviseure, la professeure Sonia Brichard, pour son soutien inestimable, ses conseils avisés et sa patience tout au long de cette thèse. Votre encadrement m'a permis de grandir en tant que chercheur et d'atteindre mes objectifs. Je retiendrai aussi votre rigueur, notamment en ce qui concerne réalisation des powerpoints où l'alignement au millimètre près, ainsi que l'utilisation de couleurs « sexy » pour illustrer les présentations étaient indispensables. Vous avez créé une excellente ambiance au sein du laboratoire, et je vous remercie pour ces cinq années passées à vos côtés.

Je souhaite également remercier chaleureusement les membres de mon jury. Tout d'abord le Professeur Gailly qui a accepté d'être mon superviseur à l'éméritat du Professeur Brichard. Mais aussi le Professeur Thissen, le Professeur Devuyst, le Professeur Vandermeeren, et le Professeur Goemans pour leurs précieux conseils et leurs remarques constructives qui ont grandement amélioré la qualité de ce travail.

Je voulais également remercier le Professeur Van den Bergh, sans qui cette thèse n'aurait pas pu se faire. Véritable mentor depuis le début de mon assistanat en neurologie, c'est vous qui avez fait naitre en moi cette passion pour les pathologies neuromusculaires et je vous en remercie.

Merci également au Professeur De Luca et au Professeur Deconinck d'avoir accepté de relire mon travail et d'avoir contribué à son amélioration.

Merci à tous les membres du labo EDIN pour m'avoir accueilli dans cette unité.

Un grand merci à mes collègues/amis de laboratoire pour leur soutien quotidien et leur aide précieuse. Michel, qui a toujours répondu à toutes mes questions, même lorsque je passais 100 fois par jour dans son bureau. Camille, merci pour ta patience et ta disponibilité chaque fois que je te demandais où se trouvait quelque chose. Laurence, qui m'a énormément aidé pour mes expériences, ta compétence et ta gentillesse ont été d'un grand secours. Maya, merci pour ton enthousiasme, tes idées novatrices, ton soutien indéfectible et ton aide précieuse pour toute la section imagerie, je te suis très reconnaissant. Romain, le spécialiste des western

blot et du welsh, et accessoirement le rigolo de la bande, merci pour ton expertise et pour avoir su rendre l'ambiance du laboratoire si agréable.

Je remercie également mes amis et ma famille qui m'ont soutenu tout au long de ce parcours. Plus particulièrement je souhaite remercier mes parents, qui m'ont donné le gout du travail bien fait, mes frères, même s'ils n'ont pas fait grand-chose, mes beaux-frères et belles-sœurs en or, Philippe pour son soutien et sa disponibilité sans faille, ma belle-mère Nathalie qui nous a malheureusement quitté trop tôt, ainsi que Fabienne et Baudouin, qui ont fait de leur foyer respectif un havre de paix.

Sans oublier mon grand-père Joseph, qui lira certainement cette thèse jusqu'au dernier mot et ma grand-mère Monique connue pour sa gentillesse sans limite. J'ai également une pensée pour ma grand-mère Yvonne et mon grand-père Francis qui ne sont plus avec nous aujourd'hui.

Un immense merci à ma femme pour son soutien constant et infaillible. Tes encouragements m'ont aidé à surmonter les moments difficiles, et ce n'est que le début, puisque notre projet à l'étranger vient tout juste de commencer. De très belles années nous attendent encore...

Et pour terminer un grand merci à mes trois enfants, qui ont été une source inestimable de bonheur et de motivation.

À tous, merci du fond du cœur.

Table of contents

Chapter 1: Introduction

Chapter 1: Introduction

Part I: Skeletal and cardiac muscle

Overview

The human body is composed by three different kinds of muscle tissue: skeletal, cardiac and smooth muscles. In this chapter, we will discuss the structural, physiological, and endocrine properties of the skeletal and cardiac muscles while focusing on inflammation and regeneration.

Skeletal muscle, also referred to as striated muscle, is connected to bones via tendons and it is responsible for executing voluntary movements of the body. When the muscle contracts, it pulls on the attached tendons, initiating movement in the corresponding bone, facilitating specific actions or movements, and providing postural support. Consequently, its primary role is to convert chemical energy into mechanical energy [4]. Additionally, skeletal muscle serves other functions such as being a reservoir for amino acids and carbohydrates and acting as a source of thermogenesis to regulate body temperature [6]. Skeletal muscle also functions as an endocrine organ capable of secreting various peptides and cytokines known as myokines. These myokines exert autocrine, paracrine, and endocrine effects [7-9]. Pathological conditions affecting the skeletal muscle are called myopathies. They are characterized by abnormalities in skeletal muscle structure or function, leading to muscle weakness, stiffness, or wasting. These disorders can be genetic, acquired, or idiopathic, affecting individuals of all ages and often resulting in significant disability [10]. In this work, we will focus on Duchenne Muscular dystrophy (DMD) a particular type of inherited myopathy.

Cardiac muscle, on the other hand, is responsible for the pumping mechanism of the heart. Unlike skeletal muscle, cardiac muscle contracts involuntarily, allowing the rhythmic beating of the heart. The heart rate is regulated by pacemaker cells that spontaneously generate electrical impulses, known as action potentials, which trigger contractions and relaxations in cardiac muscle cells. Cardiac muscle has also endocrine properties [13] and exhibits remarkable resistance to fatigue maintaining continuous contraction without exhaustion [14]. Dysfunction in cardiac muscle can

result in various cardiovascular diseases that hinder heart contractile function, a condition referred to as cardiomyopathy. In DMD, cardiomyopathy is the leading cause of death and is characterized by cardiac fibrosis, arrhythmias, and heart failure [16].

Structure

Skeletal muscle

Starting from the external layer, skeletal muscles are enclosed by dense connective tissue known as fascia, which surrounds each individual muscle, separating it from neighbouring muscles and providing structural support. Beneath the fascia, each skeletal muscle is closely enveloped by a larger layer of connective tissue called the epimysium. Further inward, the muscle tissue is partitioned into smaller sections known as fascicles by layers of connective tissue called perimysium. Fascicles are essentially bundles of multiple muscle fibres, which are each enveloped by a thin layer of connective tissue called endomysium. This organizational structure allows for relative independent movement of the muscle components. Numerous blood vessels and nerves traverse through these connective tissue layers, facilitating muscle function. Additionally, the connective tissues may extend beyond the muscle to form cord-like tendons that attach the muscle to bone [18] (Figure 1).

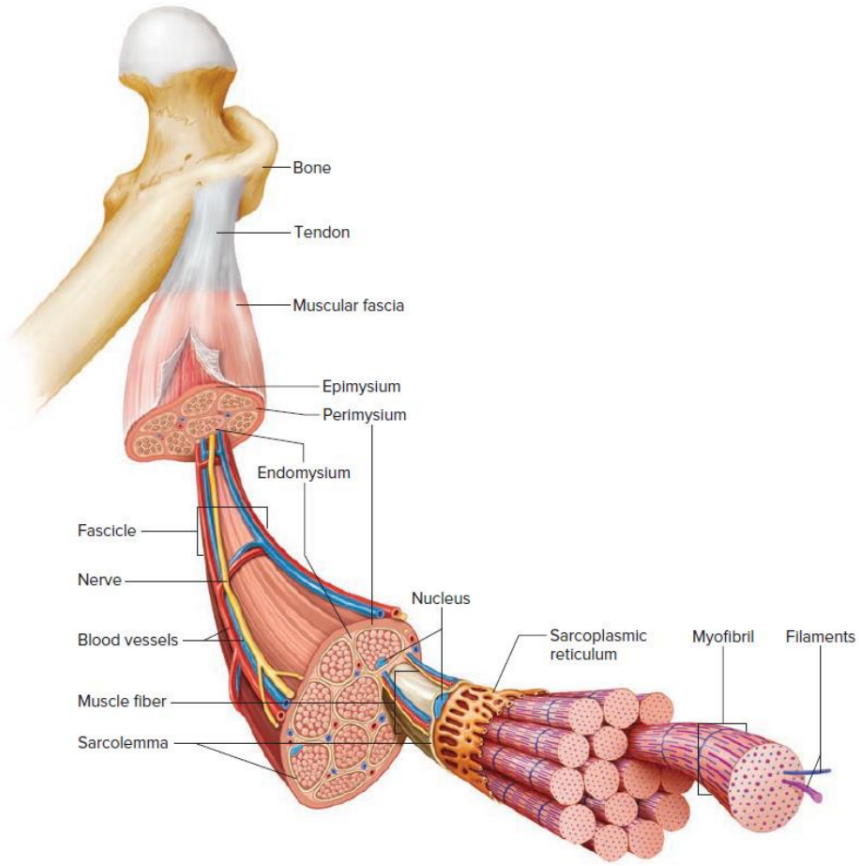

Figure 1. Skeletal muscle structure and its connective tissue. *Figure taken from Hole's Essentials of Human Anatomy and Physiology (13th edition) 2017 [1]*

Muscle tissue is composed by a bunch of fascicles, and fascicles by a bunch of myofibres. The latter, also called a muscle cell, are the basic structural unit of skeletal muscle. Myofibres are elongated and multinucleated cells, containing mitochondria and surrounded by a plasma membrane called the sarcolemma. Inside the muscle fibre, there are numerous cylindrical structures called myofibrils. Myofibrils are composed of repeating units called sarcomeres, which are the smallest functional units of muscle contraction. The shortening of sarcomeres generates force via the "sliding mechanism" of the myosin rich thick filament over the actin-rich thin filament after neuronal activation [2, 3]. The size of a muscle is determined mostly by the number and size of individual muscle fibres although pathological infiltration by fat and fibrotic tissues may alter this relationship [5].

Cardiac muscle

The human heart is a muscular organ divided into four chambers (two atria and two ventricles), enclosed within a protective pericardial sac that surrounds and lubricates it. The heart wall consists of three layers of tissue: the outer epicardium, the middle myocardium, and the inner endocardium. The endocardium lines the chambers of the heart, covers the cardiac valves, and links with the endothelium lining the blood vessels connected to the heart. The myocardium is composed of cardiomyocytes, or cardiac muscle cells, each containing a single centrally located nucleus and surrounded by a specialized cell membrane called the sarcolemma, while the epicardium serves as a protection layer. Cardiomyocytes are distinguished by their branched fibres, which interconnect to facilitate the coordinated propagation of action potentials, leading to synchronized contraction [11].

These cardiomyocytes form multiple layers or sheets of muscle, and when these sheets contract in unison, they enable the ventricle to contract in various directions simultaneously: longitudinally (shortening from apex to base), radially (narrowing from side to side), and with a twisting motion (akin to wringing out a damp cloth). This coordinated contraction maximizes the amount of blood ejected from the heart with each heartbeat [12]. Besides cardiomyocytes, the heart comprises various cell types and relies on the interaction between them to fulfil its vital functions. Studies have revealed that the heart consists of approximately 70% non-cardiomyocytes and 30% cardiomyocytes [15]. Non-cardiomyocytes predominantly consist of cardiac fibroblasts, endothelial cells, immune cells, neurons (pacemaker cells), adipocytes, smooth muscle cells and pericytes. Together, these cells form the four chambers of the heart, each with distinct morphologies and functions, contributing to the systemic circulation of blood [17] (Figure 2).

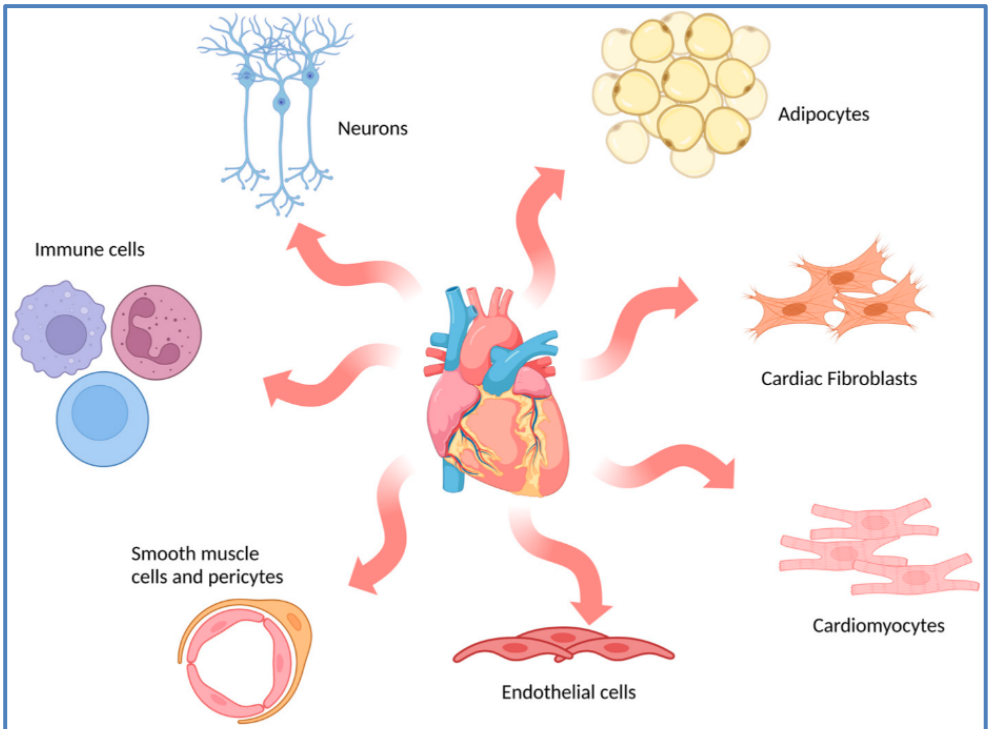

Figure 2. Main cell types in the human heart. *Figure taken from Baena-Montes et al. 2023 [19]*

Type of fibres

While cardiomyocytes can be divided into atrial and ventricular myocytes, distinguished by their location, size and electrophysiological properties [20], skeletal muscles have historically been categorized based on their colour or contractile characteristics, classifying them as either fast or slow. However, in recent decades, there has been significant advancement in understanding skeletal muscle fibre type diversity, resulting in the recognition of several major fibre types, each characterized by a unique myosin composition [21].

In this classification, there are three main categories of muscle fibre types. Type I fibres, known as slow oxidative fibres, are characterized by their slow-twitching nature. They express myosin heavy chain beta (MyHC- β) encoded by the MYH7 gene. They are the smallest type of fibre and have a low glycogen content. Type I fibres exhibit a low rate of fatigue and slow contractile speed, making them well-

suited for endurance activities like maintaining posture and marathon running. Type IIa fibres, also called fast oxidative fibres, are fast-twitching fibres. They are most suitable for activities of medium duration and moderate intensity, such as walking and biking. Both Type I and IIa fibres are often referred to as red fibres due to their high myoglobin content. On the other hand, Type IIx fibres, known as fast glycolytic fibres, are fast-twitching fibres characterized by their large diameter and high density of actin and myosin proteins. They are rich in MyHC-2x encoded by the MYH1 gene [22]. These fibres are termed white fibres due to their low myoglobin content. Mice have a much higher proportion of fast-twitch glycolytic fibres than humans, and they also have an additional myosin heavy chain isoform type IIb fibres, which are not present in human muscle [23]. Both type IIx and IIb fibres are best suited for short-duration, high-intensity activities such as sprinting and weightlifting [7, 21]. Lastly, mixed or hybrid fibres also exist. These fibres express more than one type of MyHCs and have been observed to proliferate with exercise, aging, and disease [24].

Muscle inflammation

The cardiac and skeletal muscles serve as a target for numerous cytokines that regulate various physiological and pathological functions. However, the muscle itself has the capacity to generate and release a multitude of myokines [8, 13, 25], the expression and secretion of which are tightly regulated by factors such as exercise and disease [26, 27]. Many of these myokines play roles in inflammatory responses, exhibiting either pro-inflammatory effects [28] or possessing anti-inflammatory properties [27-29]. Consequently, injured muscles can act as a source of inflammatory responses of varying intensity and duration, which can either aid in tissue repair and restoration of homeostasis or exacerbate the injury itself [30]. At the core of these processes lies the pleiotropic transcription factor called nuclear factor kappa B (NF-κB), which governs inflammation, immunity, and tissue remodelling [31, 32].

Immune Cells

Muscle damage triggers the release of numerous damage-associated molecular patterns (DAMPs), recognized by resident sentinel cells within the muscle [33-35], which respond by promptly secreting proinflammatory cytokines such as tumour necrosis factor alpha (TNFα), leading to the recruitment of leukocytes to the site of

injury [25, 36]. Neutrophils are typically the first to infiltrate the damaged area, where they engage in phagocytosis of cellular debris, secrete cytokines, and facilitate the recruitment of blood monocytes [37]. Monocytes undergo maturation on-site, transitioning into proinflammatory M1 macrophages. These cells produce abundant inflammatory cytokines such as TNFα and IL-1β and support the regeneration program by stimulating myoblast proliferation in skeletal muscle [38], In cardiac muscle, they promote myofibroblast accumulation, angiogenesis and deposition of collagen [39]. M1 macrophages are the predominant cell type present within the first 24 to 48 hours post-injury, but subsequently undergo polarization toward M2 macrophages, characterized by their anti-inflammatory profile [38]. M2 macrophages secrete high levels of IL-10 to dampen further leukocyte infiltration, halt muscle cells proliferation, and promote their differentiation to facilitate the regeneration process [40, 41]. Additionally, lymphocytes and dendritic cells can be observed in the injured tissue [34]. While T cells exhibit elevated levels of Interferon gamma (IFNγ) and contribute to maintaining the pro-inflammatory phenotype of macrophages, regulatory T cells (Tregs) infiltrate the site of injury, where they promote the transition of M1 to M2 macrophages, facilitating the resolution of inflammation and initiation of muscle regeneration [30, 42]. However, persistent presence of these various cell types can lead to chronic and severe inflammation that hinders muscle regeneration. Successive muscle injuries, such as those observed in muscular dystrophies, result in ongoing cycles of myofibre degeneration/regeneration, culminating in tissue necrosis, persistent inflammation, and fibrosis [16, 43].

Inflammatory Myokines Controlling NF-κB Signalling

TNFα, an inflammatory cytokine generated by both immune cells and myofibres or cardiomyocytes during acute or chronic inflammation, orchestrates a wide array of signalling cascades leading to cell necrosis or apoptosis [43-45]. Upon binding to its receptor, TNFR, TNFα triggers activation of the classical NF-κB pathway [46]. This activation promotes muscle wasting and cachexia by enhancing protein degradation through NF-κB activation [31, 47, 48]. Additionally, TNFα contributes to the onset of insulin resistance in skeletal muscle [49]. Moreover, TNFα stimulates endothelial cells to produce adhesion molecules, which facilitate leukocyte retention and accumulation at the site of inflammation [36].

IL-1β, is produced by various cell types, including skeletal muscle cells [50], endothelial cells and cardiac fibroblasts [51]. IL-1β acts as a pivotal cytokine in both local and systemic inflammation and plays critical pathogenic roles across a spectrum of inflammatory diseases [52, 53]. Like TNFα, the primary role of IL-1β is to perpetuate the ongoing inflammatory response [54] by inducing NF-κB activation. Once activated, NF-κB promotes the expression of the proinflammatory cytokines IL-1β and TNF-α, leading to a positive feed-back loop and a consequent overstimulation of NF-κB signalling hence causing muscle wasting [55].

NF-κB transcription factors, comprising homo- and hetero-dimers from the Rel/NF-κB family of proteins, are typically sequestered in the cytoplasm in inactive states through interaction with inhibitor protein IκB [56]. Activation of the NF-κB pathway occurs via diverse extracellular ligand-binding receptors, notably TNFR, IL-1R, and Toll-Like receptors (TLR). These canonical stimulatory signals trigger ubiquitination and proteasomal degradation of IκB [32, 57]. Subsequent loss of IκB permits nuclear accumulation of NF-κB and subsequent transcription of numerous genes, particularly those involved in inflammatory and acute stress responses [58, 59]. Inactivation of the pathway entails re-synthesis of IκB proteins by NF-κB, leading to displacement of NF-κB dimers from DNA and transcriptional coactivators [32, 57]. While the NF-κB pathway regulates cell survival, differentiation, and proliferation [57], chronic activation is often implicated in the pathophysiology of various diseases, including muscular dystrophies [60], where it is associated with severe muscle wasting [61], atrophy [62], chronic inflammation [60], impaired muscle regeneration [63] and cardiac dysfunction [64].

On the other hand, skeletal muscles also release myokines with anti-inflammatory effects. As such, adiponectin (ApN) plays a major role in mitigating inflammation and promoting tissue regeneration in cardiac and skeletal muscles [65, 66]. Part III of this manuscript delves extensively into ApN, a central theme of my thesis.

Muscle degeneration-regeneration

Muscle repair follows a highly coordinated process consisting of two distinct phases: a degenerative and a regenerative phase [3, 67]. While the degenerative phase share similarities between cardiac and skeletal muscle, the regenerative capacity differs significantly. Unlike skeletal muscles, cardiac muscle exhibits a more modest regenerative phase, as it does not fully restore its functional capacity [67].

The Degenerative Phase

Commencing within minutes of injury and lasting up to two weeks, this phase is marked by disruption of the sarcolemma, resulting in increased myofibre and cardiomyocytes permeability. In both skeletal and cardiac muscles, elevated serum levels of muscle proteins, such as creatine kinase (CK), indicative of sarcolemma disruption, are observed [3, 68]. Inflammatory cells infiltrate the affected site, secreting cytokines to amplify the inflammatory response and facilitate debris clearance [69]. Neutrophils and monocytes invade the site shortly after injury onset, engaging in proteolysis, oxidation, and phagocytosis of necrotic fibres [70]. Macrophages play a pivotal role by promoting muscle stem cell growth, preventing apoptosis, and facilitating recruitment to the lesion site [71].

The Regenerative Phase in skeletal muscle

Initiated during the first week post-injury and peaking at week two, muscle repair entails satellite cell activation and expansion to generate myoblasts for muscle regeneration.

Satellite cells, also known as skeletal muscle stem cells, are dormant mononucleated myogenic cells situated between the basement membrane and the sarcolemma of myofibres [72, 73]. Upon injury, they undergo proliferation and generate myoblasts, which subsequently differentiate into myotubes. These myotubes then fuse to either restore damaged fibres or form new ones [69]. A subset of proliferating satellite cells returns to a quiescent state via asymmetric divisions, replenishing the satellite cell reservoir [3]. Satellite cell activity is governed by a gene regulatory network involving the paired bow transcription factors Pax3 and Pax7, and several myogenic regulatory factors (MRFs) such as Myf5, MyoD, Myogenin, and Mrf4. Pax3 plays an important role in establishing the satellite cell niche during development, while Pax7 is essential for prenatal and postnatal growth [69]. MRFs are sets of transcription factors that activate muscle-specific gene expression. Upregulation of Myf5 and MyoD triggers the activation and proliferation of quiescent satellite cells, leading to myoblast formation. Myogenin upregulation initiates myogenic differentiation, followed by the appearance of Mrf4 during myotube fusion. This differentiation process culminates in the activation of muscle-specific proteins (MyHCs) and myotube fusion into myofibres [74, 75] (Figure 3). Importantly, M1 macrophages promote myoblast

proliferation by releasing pro-inflammatory cytokines such as TNFα and IFNγ [76]. Subsequently, M1 macrophages transition to an anti-inflammatory M2 phenotype, secreting IL-4 and IL-10, which promote myoblast differentiation and fusion into myofibres [38]. Remodelling is regulated by the transforming growth factor-beta (TGFβ) and insulin-like growth factor 1 (IGF-1) pathways, promoting hyperplasia and hypertrophy [69]. The TGFβ/Smad pathway restricts myoblast differentiation to favour satellite cell expansion during early muscle repair, while IGF-1 induces muscle hypertrophy by modulating protein synthesis and degradation [77]. The regenerated muscle exhibits morphological and functional similarity to undamaged muscle under normal conditions [3, 68].

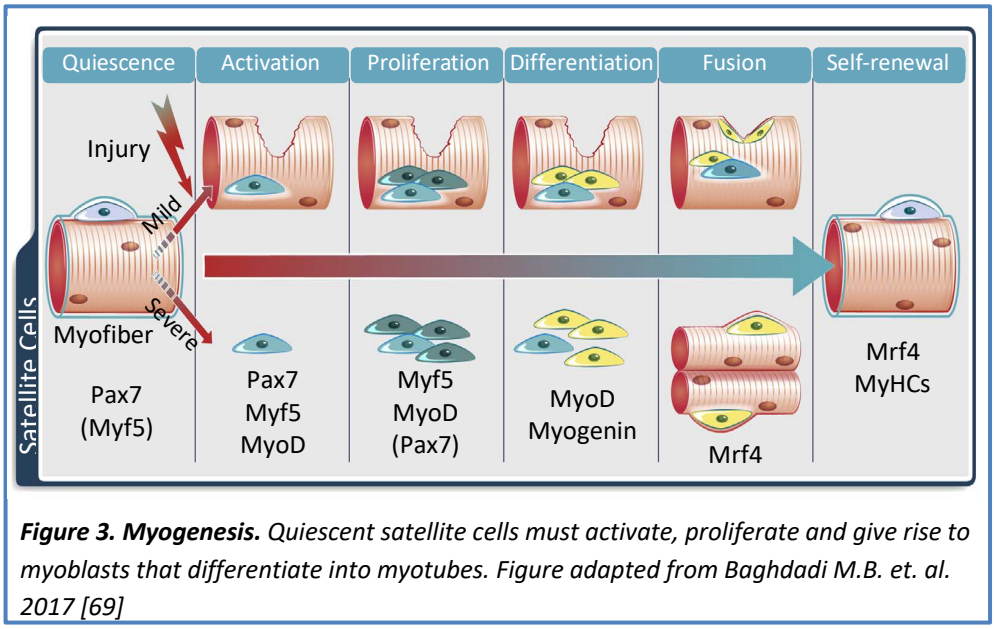

Figure 3. Myogenesis. *Quiescent satellite cells must activate, proliferate and give rise to myoblasts that differentiate into myotubes. Figure adapted from Baghdadi M.B. et. al. 2017 [69]*

The Regenerative Phase in cardiac muscle

During this phase, cardiac fibroblasts undergo trans-differentiation into secretory and contractile cells known as myofibroblasts, under the influence of IL-10, an anti-inflammatory cytokine, and active TGF-β1, a highly pleiotropic cytokine playing an important role in wound healing and in the production of extracellular matrix [78]. These myofibroblasts then secrete heightened levels of collagens and other extracellular matrix (ECM) proteins to uphold structural integrity and prevent myocardial dysfunction [79]. Following the proliferative stage, a maturation phase

ensues, during which a scar forms with a cross-linked extracellular matrix. However, the excessive deposition of ECM proteins and collagens, coupled with a scarcity of functional regenerating cardiomyocytes, results in ventricular stiffness, potentially leading to contractile dysfunction [80, 81] and elevating the risk of arrhythmogenesis and mortality [82, 83] (Figure 4).

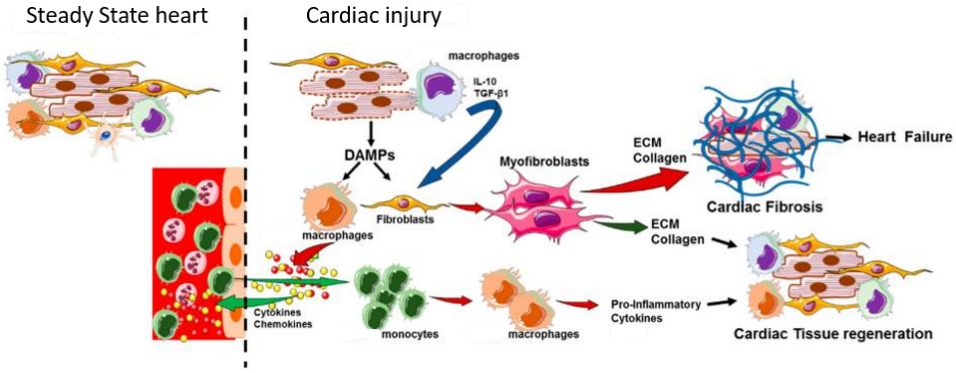

Figure 4. Cardiac immune response during injury and tissue repair. *Adapted from Lafuse et al 2020.*

Part II: Duchenne Muscular Dystrophy (DMD)

Overview

Duchenne Muscular Dystrophy (DMD) is named after the French neurologist Guillaume Duchenne, who first described the disease in the 1860s [84]. It is a lethal neuromuscular disorder with an X-linked recessive pattern of inheritance. DMD arises from mutations in the dystrophin gene, leading to the absence or inadequate production of functional dystrophin—a crucial cytoskeletal protein essential for the strength, stability, and functionality of myofibres. DMD stands as the most common hereditary neuromuscular disease with an incidence estimated at 1 in 5000 to 1 in 6000 male infants [85], moreover some studies evaluated the global prevalence of DMD as 2.8 per 100,000 inhabitants [86]. Progressive damage and degeneration of muscles characterize the disease, resulting in muscular weakness, motor delays, loss of ambulation, respiratory impairment, and cardiomyopathy. Although the clinical course of skeletal muscle and cardiac involvement may vary, fatalities invariably occur between the ages of 20 and 40, primarily due to cardiac or respiratory complications.

Cause

DMD is caused by genetic mutations affecting the dystrophin gene, situated on chromosome Xp21. This condition follows an X-linked recessive inheritance pattern [87]. Therefore, DMD predominantly affects male children, while females are likely to be asymptomatic “healthy carriers” [88]. Remarkably, the dystrophin gene ranks among the largest in the human genome, comprising 79 exons in its coding sequence and spanning 2.5 Mb of DNA. The gene contains 7 promoters and two polyadenylation signal sequences which orchestrate expression of 17 known isoforms. Muscle isoform (Dp427m) is the most characterized and widely studied due to its crucial role in DMD manifestation. Most mutations involve deletions and duplications, accounting for 65% to 75% of cases, while point mutations, small deletions and insertions occur in 20% of patients [89]. Importantly, around 30% of cases are secondary to spontaneous mutations [90]. These mutations lead to a group of disorders called dystrophinopathies, encompassing both DMD and Becker muscular dystrophy (BMD). The difference between these two entities lies in the fact that DMD is often associated with mutations disrupting the reading frame of

the gene, thereby leading most of the time to an absent dystrophin protein. BMD, on the other hand, may involve in-frame mutations or partial gene deletions that allow for the production of a partially functional dystrophin protein [91], therefore resulting in a less severe phenotype [92].

Dystrophin associated protein complex

Dystrophin is a crucial structural protein, which plays a pivotal role in maintaining the integrity and stability of muscle fibre membranes. Indeed, dystrophin is a cytoskeletal protein which links cytoskeletal F-actin with its actin-binding domain (ABD) and the extracellular matrix via its cysteine rich (CR) and C-terminal (CT) domains, thereby improving the interactions between the cytoskeleton, the cell membrane, and the extracellular matrix [93] (Figure 5). Collectively, dystrophin and its binding partners form the dystrophin-associated protein complex (DAPC) [94]. The DAPC is composed by multiple proteins such as dystrophin, the dystroglycan subcomplex (α-dystroglycan and β-dystroglycan), the sarcoglycan subcomplex (α-sarcoglycan, β-sarcoglycan, γ-sarcoglycan and δ-sarcoglycan), sarcospan, syntrophin, and dystrobrevin [95].

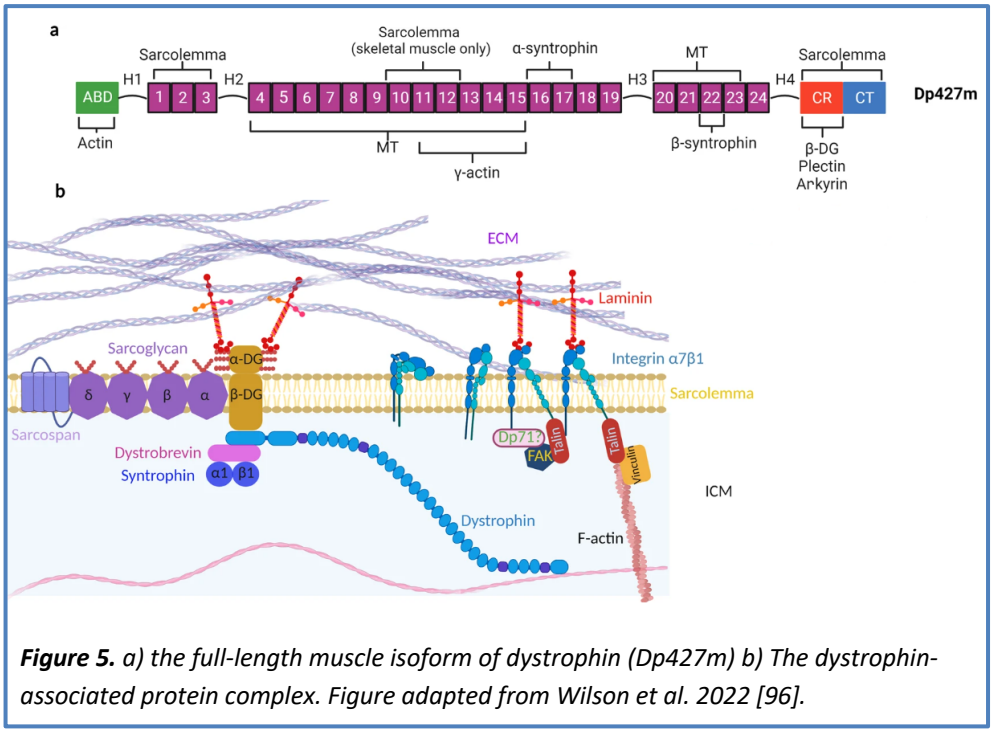

Figure 5. *a) the full-length muscle isoform of dystrophin (Dp427m) b) The dystrophin-associated protein complex. Figure adapted from Wilson et al. 2022 [96].*

The DAPC possesses important mechanical properties and transfer the force of the contractile apparatus to the extracellular matrix. It also has signalling roles in maintaining muscle cell structural integrity and contractile activity [97]. Once a genetic mutation occurs in the DMD gene, the diminished dystrophin synthesis leads to a loss of contractile function combined with excessive membrane fragility and permeability [98], alongside disruptions in calcium homeostasis [99], functional ischemia [100] and free radical damages [101]. This renders muscles more susceptible to damage during contraction, instigating a cycle of myofibre necrosis and subsequent regeneration. Over time, as individuals with DMD progress in age, the regenerative potential of muscles appears to wane, gradually supplanted by connective and adipose tissues replacing muscle fibres [43, 102].

Notably, dystrophin expression extends beyond muscle tissue to include the cardiac muscles, as well as the brain and retina. Although its presence in the brain is comparatively lower, this distribution partly elucidates the central nervous system manifestations observed in this disease [103].

Signs and Symptoms

DMD usually presents in early childhood, typically between the ages of 2 and 6. Initially, children may struggle with activities like climbing stairs, running, rising from seated or lying positions. They also exhibit toe walking, waddling gait while suffering from frequent falls. All these symptoms are the result of progressive muscle weakness, primarily affecting proximal muscles of the lower limb more than the upper limb, then extending to the distal muscles, the neck, and other regions [104]. Delayed achievement of motor milestones, including walking, is common. Additionally, calf muscles may exhibit enlargement (known as pseudohypertrophy), while enlargement of the tongue and muscles of the forearm may be seen but are less classical.

Other symptoms and/or complications include contractures often accompanied by lumbar lordosis and scoliosis [105], gastrointestinal symptoms resulting from visceral smooth muscle involvement [106], intellectual impairment [107], epilepsy [108], and in rare instances, autism-like behaviours [109].

Typically, in later stages, complications such as cardiomyopathy and respiratory issues may arise. Cardiomyopathy symptoms may emerge during adolescence and are typically evident in all patients by their twenties. Persistent tachycardia and

heart failure sometimes present as initial symptoms. Dilated cardiomyopathy in DMD is characterised by considerable fibrosis in left ventricular free wall [16].

Around 10 to 12 years of age, most patients require wheelchair assistance, and at the age of 20, many may necessitate assisted ventilation (Figure 6). Despite optimal management, the majority of individuals with DMD succumb between the ages of 20 and 40 due to cardiac and/or respiratory failure. Interestingly, DMD patient life expectancy has increased over time; being estimated at 25.77 years for people born before 1970 and 40.95 years for those born after 1970 [110], certainly thanks to the more developed symptom management techniques.

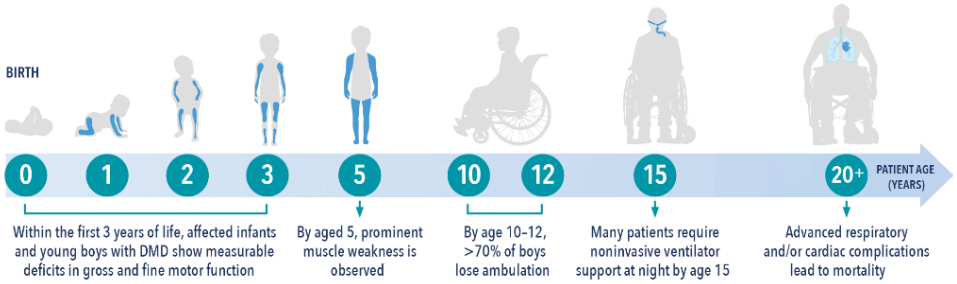

Figure 6. Duchenne Muscular Dystrophy, signs and symptoms. *Figure adapted from takeonduchenne.eu.*

Diagnosis

Diagnosis of DMD typically involves a combination of clinical evaluation, blood tests, genetic testing, and rarely muscle biopsy. Specific guidelines for DMD diagnosis are available [104].

Clinical evaluation

DMD should be considered in young males, typically between the ages of 2 and 4, who exhibit delayed achievement of motor milestones, muscle weakness, hypertrophic calves, and Gowers sign. The Gowers sign refers to the characteristic

manoeuvre where patients use their hands pushing on their legs to ascend from a squatting position due to weakness. Furthermore, it's important to note that approximately 30% of individuals with DMD may present with cognitive impairment, while speech delay is frequently observed. Therefore, the presence of cognitive deficits or speech delay alongside the aforementioned symptoms should raise suspicion for DMD [111].

Blood test

In boys exhibiting symptoms suggestive of DMD, it is recommended to measure plasma creatine kinase (CK) levels. Elevated CK levels are a result of muscle tissue damage or injury, leading to its release into the bloodstream as part of the cellular response. Additionally, plasma levels of aspartate transaminase (AST) and alanine transaminase (ALT) are elevated due to ongoing muscle damage and the abundant presence of these enzymes in skeletal muscle. However, they are less specific of muscle damage than CK [112].

Genetic testing

Genetic testing is essential for confirming a clinical diagnosis of DMD. While sequencing the DMD gene to identify disease-causing mutations is anticipated to become the gold standard in the future, this method remains relatively costly. Currently, a stepwise approach is recommended. Initially, testing for deletions or duplications within the DMD gene, which accounts for approximately 70% of cases, is advised [113, 114]. If deletion or duplication testing yields negative results, subsequent genetic sequencing should be pursued to screen for other types of mutations. These may include point mutations (nonsense or missense), small deletions, and small duplications or insertions, which can be detected using next-generation sequencing [115]. The identification of the mutation then triggers familial genetic counselling and testing. [116]. In addition, prenatal testing can be performed during pregnancy to determine if the foetus is affected by DMD. This procedure allows couples to select unaffected embryos for implantation, reducing the risk of passing on DMD to offspring [117].

Muscle biopsy

For the majority of patients, a muscle biopsy is not necessary to diagnose DMD and is only recommended when no mutations are identified through genetic testing. In

such instances, the muscle biopsy serves to evaluate the localization of dystrophin, utilizing techniques like immunohistochemistry analysis with specific antibodies targeting dystrophin, to determine if it is properly localized or absent/reduced (Figure 7). Absent levels of dystrophin are indicative of DMD [118].

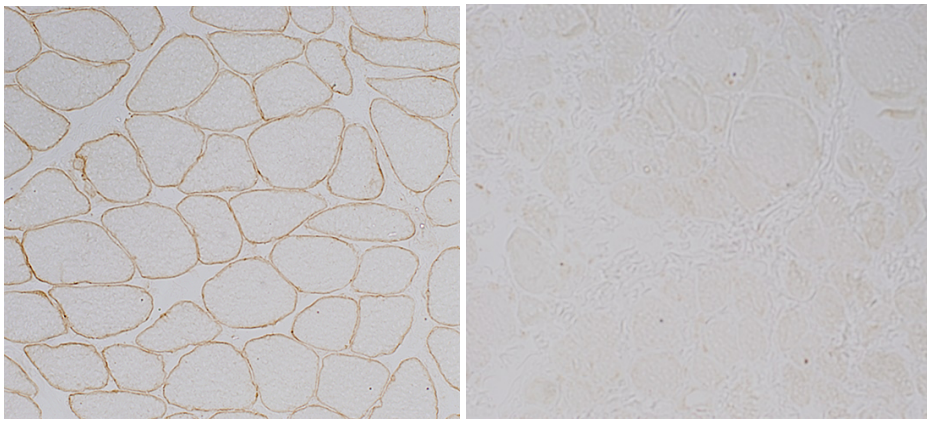

Figure 7. Immunohistochemical analysis of muscle biopsy sections. *A healthy control (left panel), and a DMD patient (right panel) are shown. Figure from https://neuromuscular.wustl.edu/pathol/dmdpath.htm.*

Secondary Processes

Besides dystrophin deficiency which represent the primary cause of DMD, membrane instability, calcium dysregulation, mitochondria dysfunction, oxidative stress, persistent inflammation, fibrosis impaired muscle regeneration and muscle atrophy are likely to be other events that exacerbate the disease progression [43]. Herein is an outline of some of the mechanisms involved these processes.

Membrane instability

In DMD, the absence of dystrophin leads to the disruption of the physical linkage between the sarcolemma, cytoskeleton, and ECM. Consequently, the sarcolemma becomes permeable and vulnerable to injury [119, 120]. This mechanism is confirmed by several findings such as the presence of sarcolemmal tears on electronic microscopy (referred to as "delta" lesions) [98], elevated levels of CK and permeability to albumin and Evans blue dye into the muscle [119, 120].

Calcium dysregulation and mitochondrial dysfunction

Following a mechanical stress (eccentric contraction) occurring on dystrophin-deficient fibres, intracellular calcium levels increased in muscle cells [121], causing the malfunction of a great variety of proteins and channels responsible for the correct storage and release of calcium. Activated by calcium, proteases and lipases inflict damage upon various components of the muscle, including the contractile apparatus, mitochondria, sarcoplasmic reticulum, and muscle membrane [122]. Furthermore, the influx of calcium dysregulates several oxidative phosphorylation enzymes, resulting in dysfunction of ATP synthase. Consequently, this process amplifies the production of reactive oxygen species (ROS) while reducing energy production mediated by ATP [123]. Moreover, the muscle's repair capacity is constrained due to the energy-intensive nature of cellular proliferation [122] (Figure 8).

This results in an abnormal environment that is not favourable for mitochondrial homeostasis. Morphologically, mitochondria in dystrophin-deficient muscle display decreased size and sparse cristae formation, which are attributed to an increased mitochondrial fission/fusion cycle. In addition, the process of mitophagy is also affected [124], leading mitochondria to swell, dysfunction and eventually burst [125].

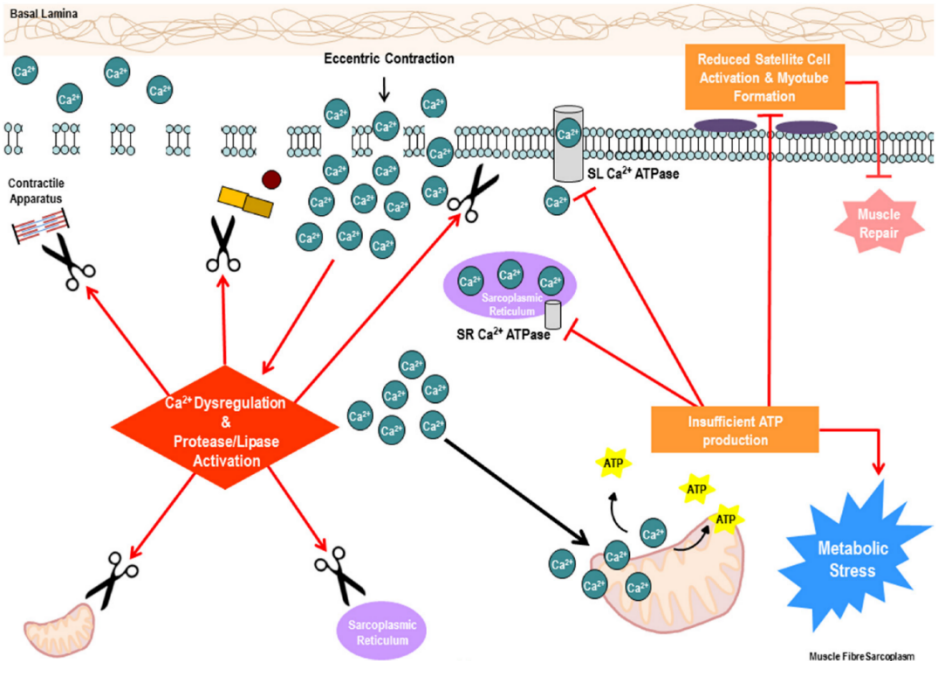

Figure 8. Calcium dysregulation, oxidative stress and mitochondria dysfunction in DMD
Figure from Rybalka et al. 2015 [122]. SR: Sarcoplasmic Reticulum ; SL: Sarcolemma

Oxidative stress

Dysfunction in mitochondria results in the overproduction of reactive oxygen species (ROS). Notably, studies have shown a significant increase in Complex I-supported maximal H_2O_2 production in skeletal muscle from young mdx mice, the best-known mouse model of DMD [126]. In individuals with DMD, the excessive ROS production surpasses the capacity of natural antioxidants, causing a redox imbalance that leads to contractile dysfunction [127] and potential cell death [128].

Inflammation

The persistent leakage of cytoplasmic contents from dystrophic muscle cells, caused by membrane instability, also triggers activation of the innate immune system. Upon release into the extracellular space DAMPs and pro-inflammatory cytokines such as TNFα and IL-1β bind to specific receptors such as TLRs and other pattern recognition receptors (PRRs) [129], which will in turn activate NLRP3

inflammasome, thereby increasing pro-inflammatory cytokine secretion and leading to a phenomenon called pyroptosis [130]. Pyroptosis causes the rupture of the cell membrane via pore formation and induces the release of mature inflammatory cytokines, DAMPs and ASC inflammasome specks into the extracellular compartment where they remain active, ultimately resulting in an amplification of the inflammatory response [131, 132].

The presence of pro-inflammatory cytokines will also lead to a coordinated vascular response, mononuclear cell accumulation and myofibre proteolysis [133]. In addition to white blood cells, NF-κB plays a central role in maintaining a chronic inflammatory state by orchestrating the transcription of pro-inflammatory cytokines, which can, in turn, stimulate NF-κB itself. This vicious cycle contributes to a severe and persistent state of inflammation [134].

The initiation of the innate immune response plays a crucial role in clearing necrotic fibres and facilitating full regeneration in normal muscle [81]. However, in dystrophic muscle, persistent myofibre degeneration prolongs the inflammatory process, leading to a chronic state that ultimately results in myofibre death, fibrosis, and muscle atrophy.

Impaired regeneration

NF-κB also plays a negative role in muscle regeneration by suppressing regenerative factors like MyoD [47], an essential myogenic factor, and limiting the participation of satellite cells. This results in reduced proliferation of myoblasts and inhibition of myogenic differentiation [60]. After several rounds of muscle degeneration, inflammation becomes chronic and the continuous process of satellite cell activation exhausts the muscle intrinsic regenerative capacity, provoking the replacement of muscle fibres by fibrotic and adipose tissue, resulting in muscle weakness and dysfunction.

Fibrosis

Inflammation combined with impaired regeneration will initiate the production of fibrotic tissue. More specifically muscle injury and inflammation, leads to the recruitment of fibro-adipogenic progenitors (FAPs), which differentiate into fibroblasts via the action of TGF-β, thereby increasing the deposition of connective tissues [135, 136]. TGF-β is a major mediator of the fibrotic response and acts via

its effector, the phosphorylated and active form of Smad2, which can then promote the excessive production of extracellular matrix (ECM) rich in type I and type III collagen [137, 138]. This fibrosis ultimately impairs contractile function and reduces the pool of healthy muscle available for therapy [139]. Moreover, several other molecules contribute to the regulation of fibrogenic processes in muscle cells. For instance, Myostatin stimulates muscle fibroblasts to produce ECM proteins [140]. Additionally, molecules such as angiotensin II, collagen triple helix repeat-containing 1 (Cthrc1) protein, and Wnt signalling also play roles in modulating fibrosis [141-143].

Treatment

While there is currently no cure for DMD, various treatment options aim to manage symptoms, slow down disease progression, and improve quality of life. These include glucocorticosteroids (GCs) and multidisciplinary management.

Glucocorticosteroids

GCs are the mainstay of treatment in DMD due to their immunosuppressive and anti-inflammatory properties. GCs act as ligands for the glucocorticoid receptor (GR) present in muscle cells. Upon binding to the GR, the GC/GR complex translocate to the nucleus and subsequently bind to the glucocorticoid response elements (GREs) in the promotor region of specific targets genes, thereby modifying their transcription either positively (transactivation) or negatively (transrepression) [144]. The process of transactivation is responsible for the upregulation of anti-inflammatory genes such as IL-10 and IκB [145], while transrepression is acting on nuclear factor-kappa B (NF-κB), activator protein-1 (AP-1), and other nuclear coactivators involved in the inflammatory response [144]. NF-κB being a master regulator of inflammation by modulating the expression of genes encoding pro-inflammatory cytokines, chemokines, and adhesion molecules, its transrepression will therefore reduce the production of pro-inflammatory mediators, thereby attenuating inflammation and immune cell infiltration in muscle tissue [146]. Finally, GCs also exerts non-genomic properties which include, among others, non-specific interactions with the cell membrane, the activation of mitogen-activated protein kinase (MAPK) pathway, the modulation of ion channels, and calcium signalling [147].

The latest guidelines strongly advocate for the lifelong administration of glucocorticosteroids once the motor development halts or begins to regress [104]. Typically, treatment initiation occurs around 4 to 5 years of age. Once started, GCs have been shown to slow down the progression of muscle degeneration and improve muscle strength and function [148]. However, uncertainty persists regarding the selection of the drug (prednisolone vs deflazacort), regimen (daily vs intermittent), and dosage to achieve optimal results with minimal adverse events [149]. While, some studies suggest that deflazacort shows superior outcomes in terms of survival [150] and also presents a more favourable adverse event profile than prednisolone [151], the FOR DMD study (NCT01603407), comparing these medications in a randomized controlled trial, demonstrated the equivalence between both medications. The same study also showed the superiority of the daily dosing over the intermittent regimen in enhancing motor function, pulmonary function, and overall treatment satisfaction [148].

Unfortunately, the clinical use of glucocorticoids in DMD is associated with a large spectrum of potential adverse reactions, including osteoporosis, obesity, growth retardation, delayed puberty, cataracts, cushingoid facies, diabetes, glaucoma, acne, hypertension, immunosuppression, adrenal insufficiency and further muscle damage [152, 153]. These adverse events mainly stem from transactivation, which amplifies the expression of genes involved in metabolic processes [154]. Management of these complications primarily involves preventative measures and symptomatic treatments. In cases where side effects become unmanageable or intolerable, a reduction in glucocorticoid dosage by 25-33% is recommended. If dose adjustments prove ineffective, discontinuation of treatment is necessary, irrespective of the individual's motor function status [155].

Currently, there is a lack of alternative to GCs, underscoring the necessity for new medications that match the efficacy of GCs in addressing the inflammatory component while offering a superior safety profile.

Multidisciplinary management

An integrated medical, surgical, and rehabilitative strategy addressing the symptoms of DMD can modify the disease's natural progression, enhancing both quality of life and lifespan [156]. This approach requires a core group of healthcare professionals specializing in DMD patients, including physicians, nurses,

physiotherapists, speech therapists, psychologists, occupational therapists, social workers and dieticians, all of them playing a pivotal role in both preventing and managing symptoms associated with the condition [157].

While physical therapy and mobility aids to maintain flexibility, strength, and independence, assistive devices, such as braces, orthopaedic supports, and wheelchairs, aid mobility, avert the development of significant deformities and prevent falls [158].

Importantly, cardiac annual monitoring via physical examination, electrocardiography, echocardiography or, when possible, cardiac MRI, combined with cardiac medication help to manage heart function and prevent complications associated with cardiomyopathy [159]. Finally, respiratory support, including mechanically assisted coughing and mechanical ventilation, assist patients with breathing as respiratory muscles weaken [160].

Clinical trials and perspectives

Over the past decade, there has been a significant emergence of new treatments in the landscape of DMD therapies. These approaches can be broadly categorized into two main groups: those aimed at restoring dystrophin production (Figure 9) and those focused on mitigating the secondary effects resulting from dystrophin deficiency. Importantly, restoring dystrophin production will not restore lost muscle tissue and function, therefore, it is probable that a combination of approaches will be employed in the future to restore dystrophin levels, preserve muscle quality, and minimize disease progression.

Restoration of dystrophin progression

-Ribosomal read-through strategy: Ataluren is small molecule that induces ribosomal read-through of a premature “STOP” codon caused by a nonsense mutation. Despite receiving provisional acceptance from the European Medicines Agency (EMA) in 2014 [161], a subsequent study compared patients from the STRIDE registry who were treated with Ataluren for an average of 5.5 years (between 2015 and 2022) with untreated patients from the Cooperative International Neuromuscular Research Group (CINRG) Duchenne natural history study (DNHS) registry, followed between 2006 and 2016. This study revealed no

significant effects of the medication, ultimately resulting in the non-renewal of EMA authorization in January 2024 [162].

-Exon-skipping therapies works by essentially "skipping" over the mutated exon during the process of protein production, allowing the remaining exons to be spliced together to form a functional, albeit shorter, dystrophin protein. This technology is possible via Antisense oligonucleotides (ASOs) which are small pieces of modified RNA designed to target the splice sites flanking the mutated exon, thus blocking its inclusion in the final mRNA transcript [163]. While exon-skipping is a promising therapeutic approach, it is important to note that it is mutation-specific. Four ASOs have been developed yet, namely casimersen targeting exon 45, eteplirsen targeting exon 51 [164], golodirsen [165] and viltolarsen targeting exon 53 [166]. All of them have demonstrated potential in inducing dystrophin restoration in small patient groups. Some of these ASOs have received conditional approval from the Food and Drug Administration (FDA) (eteplirsen, golodirsen, and viltolarsen) and the Japanese Ministry of Health, Welfare, and Labour (viltolarsen). Ongoing confirmatory studies are still conducted to evaluate their clinical benefits.

-Gene therapy: While ASO technology provides a flexible and reversible approach by modulating gene expression, gene therapy aims for a more permanent solution by correcting the genetic defect itself. It involves replacing the defective dystrophin gene (DMD gene) with a therapeutic gene encoding a microdystrophin, delivered to the muscles via a vector, most commonly an adeno-associated viral (AAV) vector. Microdystrophin has been selected for gene transfer because the entire DMD gene is too large for the small AAV virus. It contains all the functional parts necessary for its function in muscle cells. While three phase II trials (GNT-0004, SGT-001, RGX-202) and one phase III trial (PF-06939926) are ongoing, the SRP-9001 is the first microdystrophin gene therapy treatment to receive conditional market authorization in the United States in June 2023, under the name Elevidys®, for boys with DMD aged 4 to 5 years. However, the initial efficacy results unveiled in October 2023 are still pending further confirmation. Trials evaluating the effectiveness of SRP-9001 are ongoing.

-Stem cells therapy: The concept of stem cell transplantation for DMD holds great promise, as transplanted cells carry a functional copy of the DMD gene and are anticipated to contribute to muscle repair post-transplantation. Various cell types

are under investigation for transplantation as part of DMD therapy such as satellite cells (myoblasts), mesenchymal stem cells or induced pluripotent stem cells (iPSCs). CAP-1002 is a product containing cardiac stem cells from donors, which, when administered to patients with DMD, promote cardiac muscle regeneration and showed interesting results in two phase II clinical trials (NCT02485938 and NCT04428476) [167]. Another cellular therapy called DT-DEC01 involves the use of chimeric cells expressing dystrophin, created by fusing two myoblasts, one from a healthy donor expressing dystrophin and the other from each DMD patient, who will subsequently be treated with the obtained chimeric cells. A pilot study confirms the safety and efficacy of DEC01 treatment with absent adverse events [168].

-Genome editing (Crispr-Cas9): Theoretically, a single infusion of CRISPR genome-editing components could correct genetic mutations at the genome level, offering a promising therapeutic strategy for addressing genetic disorders like DMD in the long term [169, 170]. Both in vitro and in vivo studies utilizing CRISPR-mediated gene editing for DMD have been conducted. These studies have demonstrated therapeutic efficacy in human cells as well as in various animal models, including mice, rats, dogs, and piglets with different DMD mutations [171-173]. However, before clinical translation can proceed, deeper insights into sequence-humanized animal models will be necessary. These models will provide crucial information such as the optimal dose, delivery method, administration route, and the threshold levels required for functional dystrophin restoration [169, 174]. Concerns regarding off-target effects also need to be addressed before advancing to human trials.

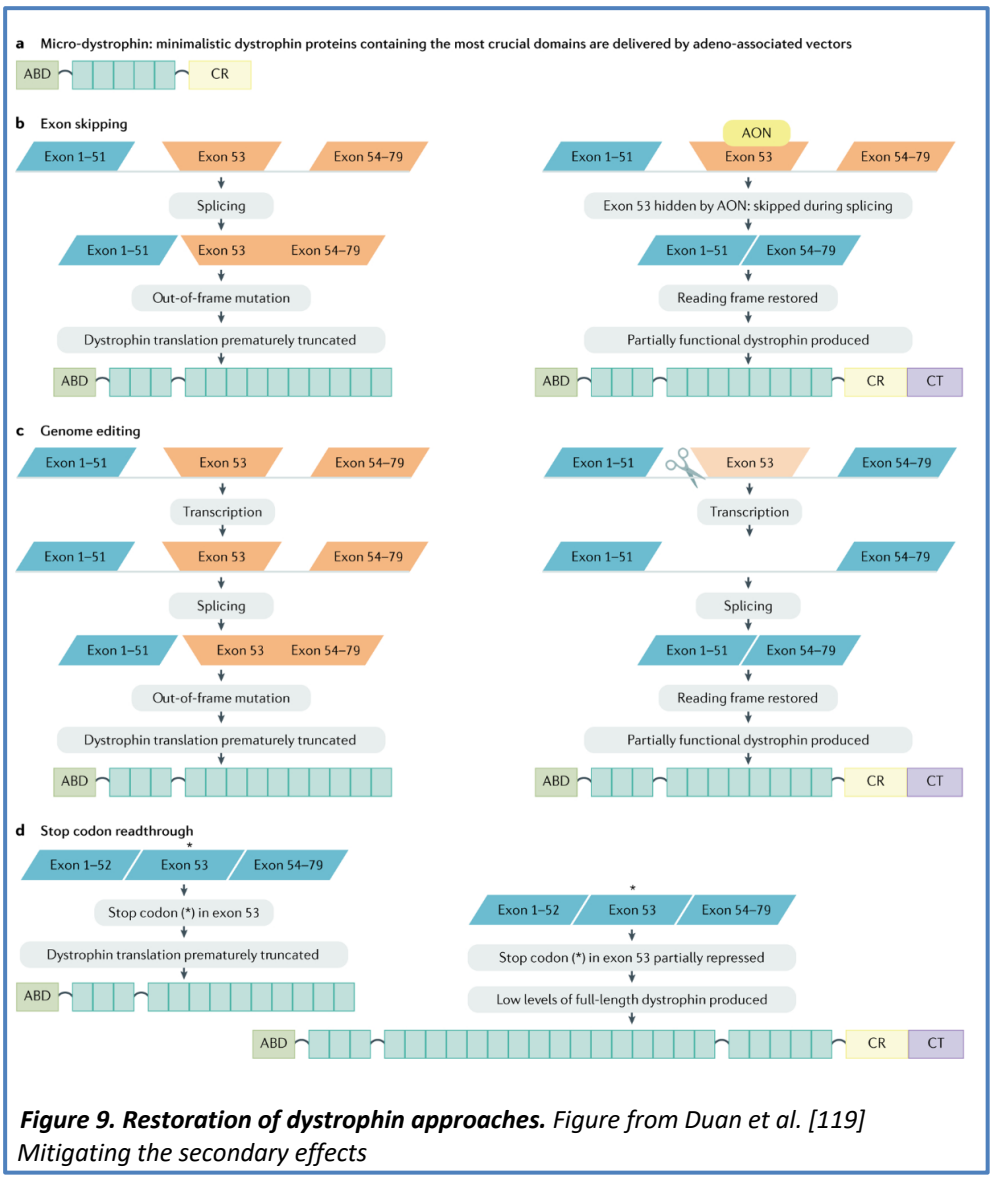

Figure 9. Restoration of dystrophin approaches. *Figure from Duan et al. [119]*

Mitigating the secondary effects

-Vamorolone is a synthetic steroid targeting the same receptors as corticosteroids and sharing its anti-inflammatory properties. Yet, it possesses a distinct chemical structure and divergent mechanism of action. Unlike corticosteroids, vamorolone exhibits reduced positive gene transcriptional activity (transactivation) while maintaining its ability to inhibit proinflammatory pathways mediated by NF-κB

(transrepression). In addition, vamorolone functions as a potent antagonist of the mineralocorticoid receptor, distinguishing it from most corticosteroids, which mainly act as agonists [175]. In a randomized clinical trial, vamorolone was shown to be effective and safe in the treatment of boys with DMD over a 24-week treatment period. Importantly, it showed normal growth trajectories and a better bone health in comparison with glucocorticoids [176]. Nonetheless, vamorolone is associated with some residual adverse effects, including minimal delay in bone age, undesired weight gain, and adrenal suppression [176, 177]. Moreover, the available long-term safety and efficacy data remain limited. As a result, while vamorolone is a valid alternative to conventional corticosteroids (prednisone, prednisolone, deflazacort), there is a necessity for extensive real-world experience to further elucidate its profile. Vamorolone has just been authorized in the United States and in Europe starting from the age of two.

-Copolymers: A novel therapeutic approach involves the use of synthetic membrane stabilizers to mitigate muscle damage by directly fortifying the dystrophin-deficient muscle membrane [178]. Recently, the amphiphilic properties of poloxamer 188 (P188) have demonstrated a protective effect on the cell membrane both in vitro and in vivo [179]. P188 also mitigated cardiomyopathy induced by isoproterenol in mdx mice, the most used mice model of DMD [180]. A Phase 2 single-site, open-labelled trial to evaluate the efficacy of membrane stabilizers in skeletal limb, cardiac, and respiratory muscle endpoints in non-ambulatory DMD patients has been initiated (ClinicalTrials.gov Identifier: NCT03558958).

-Utrophin modulation: Utrophin, an autosomal paralog of dystrophin encoded by the *UTRN* gene [181], shares structural and functional similarities with dystrophin. Initially, ezutromid (SMTC1100) emerged as the first orally bioavailable utrophin regulator. However, it failed to meet both primary (changes in leg muscle magnetic resonance parameters) and secondary (increased utrophin levels and decreased muscle damage) endpoints [182]. Recently, several preclinical investigations involving "micro-utrophin" (μUtrn) gene delivery have been conducted, with some studies reporting restoration of the dystrophin-glycoprotein complex (DGC), prevention of myofibre degeneration, normalization of serum CK levels, and improvement in muscle function [183]. Nonetheless, further research is necessary before utrophin-based therapies can be applied to patients with DMD and BMD.

-α7-Integrin upregulation: The α7β1 integrin protein functions as a mechano-signalling anchor, connecting laminin in the ECM to the intracellular actin [184]. Notably, there is an increase in α7-integrin expression at the sarcolemma in both mdx mice and individuals with DMD [185]. Moreover, knockout of both dystrophin and α7 integrin leads to a significantly more severe dystrophic phenotype, suggesting that upregulation of integrin may serve as a compensatory mechanism in the absence of dystrophin [186]. Consequently, akin to utrophin, the exploration of small compound screens for α7-integrin modulators presents a promising avenue [187].

-Muscle growth strategies: Myostatin, a member of the transforming growth factor-β-superfamily, serves as a negative regulator of skeletal muscle growth [188]. Unfortunately, clinical trials in humans testing myostatin inhibitors have yielded disappointing outcomes, characterized by a lack of improvement in muscle strength [189] or the emergence of adverse effects [190, 191].

-Givinostat is believed to increase muscle mass and reduce muscle fibrosis and inflammation. Results from the EPIDYS trial in ambulatory patients (aged 6 to 17 years) indicate a trend towards lesser decline in motor abilities [192].

-EDG-5506 is a small molecule thought to protect muscle fibres from damage, particularly fast fibres, it is being evaluated in several international trials (LYNX trial, FOX trial for patients already treated with gene therapy).

Animal Models

Non-mammalian models

As previously discussed, the current strategies for DMD therapy are numerous and varied. All these methodologies require testing in animal models, and it's essential to recognize that animal models are also indispensable for gaining a deeper understanding of the disease's pathophysiology.

Thus, throughout the years different models were developed, each of them having their own advantages and drawbacks. The emergence of non-mammalian DMD models has facilitated the exploration of high-throughput, high-content screening of extensive chemical compound libraries. These models encompass organisms like *Caenorhabditis elegans* (C. elegans), *Drosophila melanogaster*, and zebrafish. They offer advantages such as straightforward maintenance, short life cycles, large progeny size, genetic manipulability, and readily observable phenotypes. However, their inability to fully replicate the intricate pathophysiology of the disease observed in humans, along with the absence of pertinent anatomical and physiological features such as genetic composition, metabolism, and immune responses, poses significant limitations [193].

Mammalian models

In terms of mammalian models, mdx mice are probably the most widely used and well described model. It consists of C57BL/10ScSn mouse line, which harbours a spontaneous nonsense point mutation (C to T transition) in exon 23 of the *dmd* gene, resulting in the absence of full-length dystrophin [194, 195] Mutant mice displayed characteristics reminiscent of human DMD, including elevated plasma pyruvate kinase and CK levels, as well as histological abnormalities in skeletal muscles. Indeed, histopathological abnormalities become notable in mdx muscles around 3–4 weeks of age, while extensive necrosis followed by regeneration in skeletal muscles has been documented in mdx mice as early as 16–17 days [196]. Similarly, the heart, another affected muscular organ in mdx mice akin to DMD patients, shows signs of cardiomyopathy on echocardiography after approximately 8 months of age, with histological evidence of interstitial cardiac fibrosis becoming apparent around 17 months [197]. However, while DMD is marked by muscle atrophy in the later stages of the disease, in mdx mice, myofibres undergo

progressive hypertrophy from week 24 until the end of life, with no signs of atrophy [198]. In addition, their phenotype differs from that of humans, exhibiting only moderate muscle weakness in the extremities. This variation could be attributed to a sustained capacity for muscle regeneration, partly due to increased expression of utrophin and of the laminin receptor α7β1 integrin [185, 199].

To address these discrepancies with the human disease, numerous animal models exhibiting more severe phenotypes have been developed. N-ethylnitrosourea (ENU) mutagenesis has been employed resulting in mdx2Cv, mdx3Cv, mdx4Cv, mdx5Cv mouse models [200, 201]. Other approaches include crossbreeding mdx mice with different genetic backgrounds. Among them the resulting DBA/2-mdx mice developed cardiomyopathy and cardiac fibrosis at an earlier age than mdx mice, [202]. Double knockout dystrophin/utrophin (mdx/Utrn−/−) or α7-integrin/dystrophin mice have also been developed, both of which display more severe symptoms than mdx mice, often succumbing to respiratory insufficiency by 20 weeks of age [203, 204]. Alternatively, the dup2 mouse model was specifically engineered to study exon 2 duplication, accounting for approximately 11% of DMD causative mutations [205].

While these phenotypic mouse models offer a closer resemblance to patients, they have not yet become the predominant model in DMD research. This is due to several reasons. Firstly, many of these models lack comprehensive natural history data. Secondly, some are challenging to establish and maintain as colonies. Additionally, concerns arise regarding data interpretation with double knockout mice, as human patients typically do not carry mutations in the second gene that is inactivated in mice.

Among non-rodent mammals, the golden retriever muscular dystrophy dog model is the most extensively studied. This model more faithfully replicates human DMD, with cardiomyopathy and respiratory failure as primary causes of mortality, typically occurring around 3 years of age, representing a 75% reduction in normal life expectancy [206]. Additionally, other canine models of DMD, such as the Beagle-based canine X-linked muscular dystrophy model, have also been utilized in research [207]. However, dog models present significant drawbacks including high cost, breeding challenges, ethical issues and limited availability, thereby restricting the reliability of statistical analyses.

Part III: Adiponectin (ApN) and its mimics[1]

Overview

Structure

Adiponectin (ApN) is a hormone secreted by adipocytes, consisting of 244 amino acids and encoded by the ADIPOQ gene [208]. ApN is initially synthesized as a monomeric peptide comprising four domains; namely a signal sequence, a short variable region, a collagenous stalk and a C-terminal globular domain [209, 210]. ApN monomers can self-assemble into complexes ranging up to 18 mers. Consequently, ApN circulates in the bloodstream in various forms, including low-molecular-weight (LMW; trimer), middle-molecular-weight (MMW, hexamer), and high-molecular-weight (HMW, 12–18 mers)[66]. Notably, both the total ApN levels and the distribution of its complex forms contribute to the hormone's biological effects, with HMW ApN exerting the most potent insulin-sensitizing effects [211]. Additionally, ApN can undergo cleavage into a smaller globular fragment (gApN) by leukocyte elastases secreted from activated monocytes and neutrophils [212, 213] (Figure 10).

[1] Some portions of this section have been adapted from a review article 166. Abou-Samra, M., et al., Adiponectin and Its Mimics on Skeletal Muscle: Insulin Sensitizers, Fat Burners, Exercise Mimickers, Muscling Pills … or Everything Together? Int J Mol Sci, 2020. 21(7). in which I contributed as a co-author.

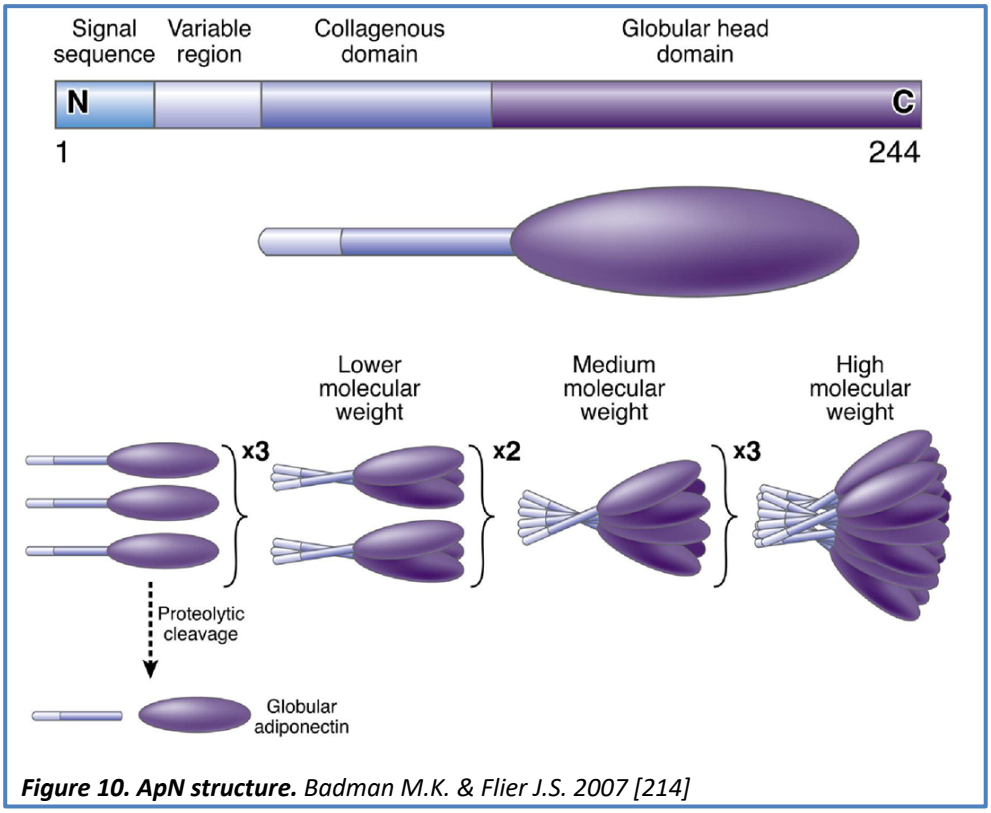

Figure 10. ApN structure. *Badman M.K. & Flier J.S. 2007 [214]*

ApN Receptors

AdipoR1 and AdipoR2 serve as the primary adiponectin receptors [215]. They are characterized by their seven transmembrane domains, which are structurally and functionally distinct from G-protein coupled receptors. While AdipoR1 finds predominant expression in skeletal muscle, AdipoR2 is primarily expressed in the liver [216]. AdipoR1 plays a pivotal role in activating AMP-activated protein kinase (AMPK) pathways, whereas AdipoR2 appears to be more closely associated with peroxisome proliferator-activated receptor (PPAR)-α pathways [215, 217]. AdipoR1 acts as a high-affinity receptor for gApN and demonstrates the capability to bind full-length ApN. Conversely, AdipoR2 exhibits intermediate affinity for both the globular and full-length forms [216]. T-cadherin, acts as an additional binding partner for MMW and HMW isoforms of adiponectin [218]. T-cadherin is a glycosylphosphatidylinositol (GPI)-anchored structure lacking transmembrane and cytosolic domains. T-cadherin finds expression in the heart, aorta, and skeletal muscle. In these tissues, adiponectin could potentially stimulate exosome

production, thereby enhancing whole-body metabolism [219]. Furthermore, T-cadherin mediates cardiovascular protection [220, 221] and skeletal muscle regeneration induced by HMW adiponectin [222].

Pleiotropic effects

ApN serves as a crucial messenger facilitating communication between adipose tissue and other metabolically relevant organs [223] (Figure 11). In the liver, ApN promotes fatty acid oxidation [224] and diminishes glucose production, thus exerting insulin-sensitizing effects on this organ [225]. Within adipose tissue, ApN demonstrates insulin-sensitizing properties by combining anti-inflammatory actions with enhanced glucose uptake [226-228]. In the pancreas, ApN enhances glucose-induced insulin secretion by activating fatty acid oxidation [229] and safeguarding beta cells against apoptosis [230]. Additionally, ApN regulates food intake, energy expenditure, and lipid and glucose metabolism by acting on the hypothalamus [231, 232]. It also demonstrates antidepressant effects by enhancing hippocampal neurogenesis and reducing neuroinflammation [233-235]. Furthermore, ApN exhibits renoprotective effects against oxidative stress and apoptosis [236]. Ultimately, ApN may play a protective role against cancer progression in various obesity-related cancer types, including colorectal and breast cancers, by inducing apoptosis and limiting cell proliferation and angiogenesis [237]. Finally, the impact of ApN on skeletal and cardiac muscles will be thoroughly discussed in the next section.

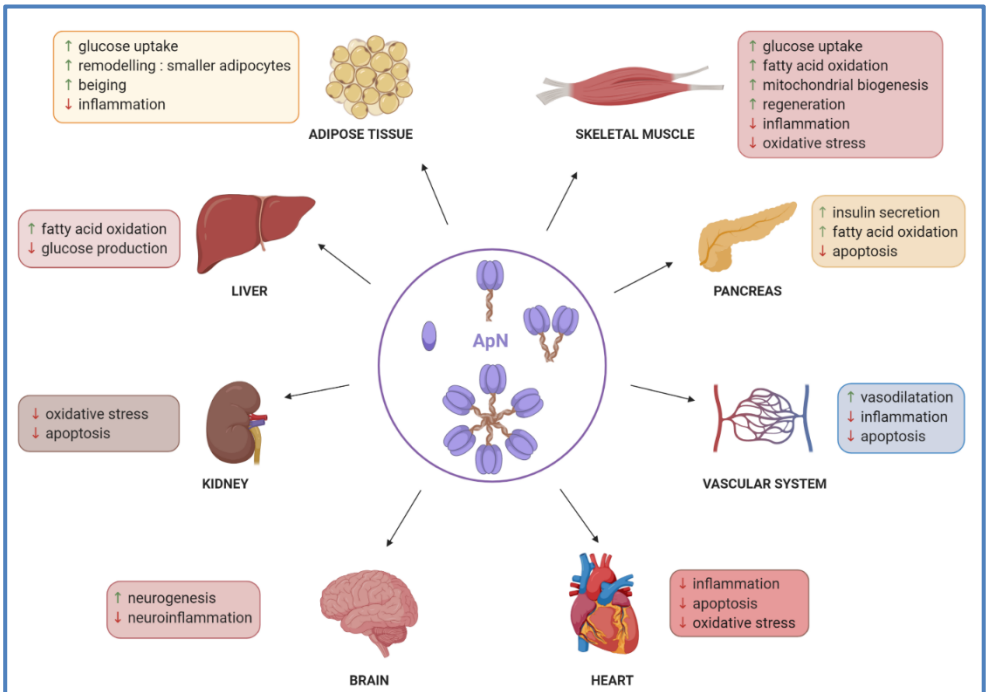

Figure 11. Pleiotropic effects of adiponectin. *Abou-Samra M. et al. 2020 [238].*

Adiponectin in normal muscle

Overview

Skeletal muscle is described as an endocrine organ capable of producing and releasing myokines, [8, 9]. Among these myokines, ApN plays a central role as an energy metabolism regulator and as a local protective mechanism against excessive inflammatory responses, and oxidative stress [66].

The ApN properties discussed herein have been investigated primarily in rodent models in vivo. However, many findings from mouse studies have been validated in vitro using human muscle cells.

Metabolic Effects

AdipoR1-AMPK-SIRT1-PGC-1α pathway

ApN primarily exerts its metabolic effects on skeletal muscle by activating the AMPK signalling pathway (Figure 12). AMPK serves as a pivotal sensor of cellular energy status, crucial for maintaining systemic energy balance. Upon binding to AdipoR1, ApN triggers the recruitment of the adaptor protein APPL1, which acts as an anchor, tethering Liver kinase B1 (LKB1) [239]. Additionally, ApN may induce calcium influx, thus activating Ca(2+)/calmodulin-dependent protein kinase kinase β (CaMKKβ), leading to increased expression of peroxisome proliferator-activated receptor γ coactivator-1α (PGC-1α), a pivotal regulator of mitochondrial function and biogenesis [240, 241]. Both LKB1 and CaMKKβ fully activate AMPK.

Subsequently, phosphorylated AMPK (P-AMPK) phosphorylates PGC-1α, and indirectly upregulate the expression of a deacetylase, sirtuin-1 (SIRT1). SIRT1, in turn, fully activates PGC-1α through deacetylation. Thus, ApN stimulates both the expression and activation of PGC-1α. Consequently, PGC-1α enhances the activity of several transcription factors (TF), leading to the upregulation of target genes associated with mitochondrial biogenesis and a shift towards oxidative metabolism [217].

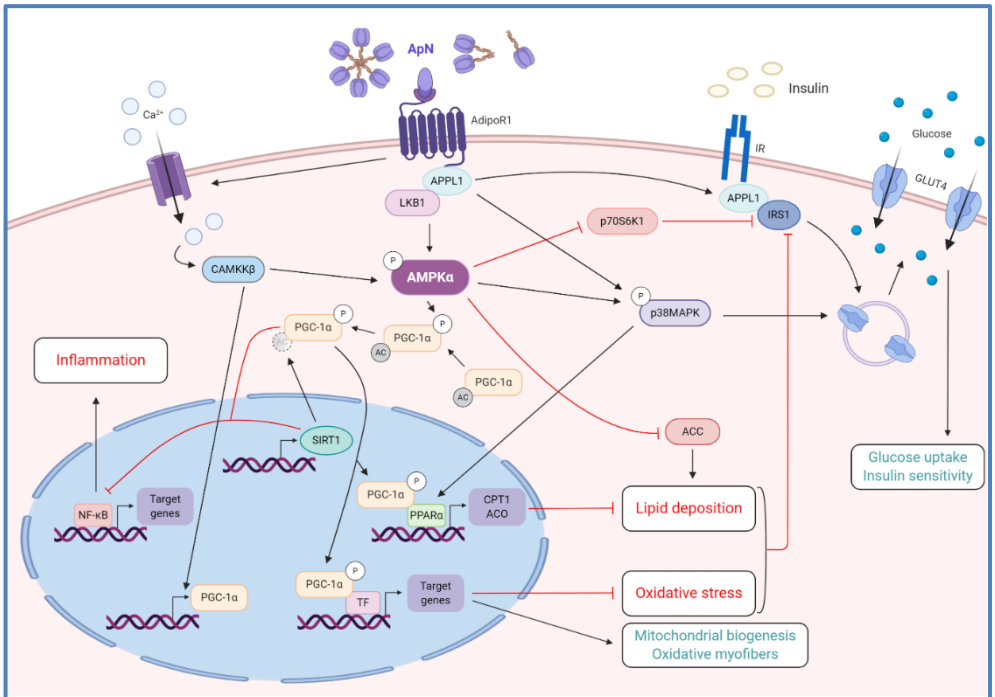

Figure 12. Adiponectin properties on healthy skeletal muscle. *Boxes with processes in green represent net beneficial effects of ApN, while boxes with processes in red represent metabolic dysfunctions counteracted by ApN. Dashed and blurred circle represents removal of the indicated residue. TF: transcription factors. Abou-Samra M. et al. 2020 [238].*

Fatty-Acid oxidation

AMPK is also involved in the sequential activation of peroxisome proliferator-activated receptor alpha (PPARα) (Figure 12). Through this mechanism, ApN enhances the transcriptional activity of PPARα and upregulates the expression of its target genes, which are involved in fatty acid transport into the mitochondria like carnitine palmitoyltransferase 1 (CPT1), or in oxidation, such as acyl-CoA oxidase (ACO) [242]. Furthermore, AMPK promotes fatty acid oxidation by phosphorylating and inhibiting acetyl-CoA carboxylase 2 (ACC2) [243].

Insulin-sensitizing action

Another fundamental protective mechanism of adiponectin (ApN) against metabolic syndrome arises from its insulin-sensitizing properties. Various in vivo studies have illustrated the substantial improvement in insulin signalling facilitated by ApN. Administration of ApN resulted in decreased blood glucose levels and alleviated insulin resistance in mice fed a high-fat diet [244]. Similarly, mice engineered to overexpress ApN (ApN-Tg) exhibited enhanced insulin sensitivity [228], whereas ApN knockout (ApN-KO) mice displayed heightened resistance to insulin [245].

In skeletal muscle, ApN modulates insulin sensitivity through diverse mechanisms. Firstly, ApN activates AMPK signalling, leading to the inhibition of p70 ribosomal S6 kinase 1 (p70S6K1). This enzyme phosphorylates insulin receptor substrate-1 (IRS-1) on serine residues, thus impeding the insulin signalling cascade [246]. Secondly, activation of PGC-1α enhances the expression of several enzymes involved in oxidative stress detoxification and fatty acid oxidation [241, 247]. As oxidative stress and elevated triglyceride levels are associated with insulin resistance via inhibitory phosphorylation of IRS-1, ApN serves as a sensitizing agent [248, 249]. Thirdly, ApN promotes the translocation of glucose transporter type 4 (GLUT4) to the plasma membrane, facilitating glucose uptake. This beneficial action is mediated by p38MAPK and by a direct action on the insulin receptor to boost insulin signalling [216, 250] (Figure 12).

Anti-inflammatory and anti-oxidative effects

In previous studies, our group demonstrated that muscles of ApN-deficient mice showed increased susceptibility to oxidative stress, inflammation, and apoptosis. These abnormalities were further aggravated by acute (lipopolysaccharide/LPS) or chronic (obesogenic diet) inflammatory challenges but were mitigated by local electro-transfer of the ApN gene [29, 251]. Additionally, mice with muscle-specific disruption of AdipoR1 exhibited a localized decrease in oxidative stress-detoxifying enzymes [217]. Furthermore, ApN displayed potent anti-inflammatory properties in human myotubes when subjected to an inflammatory challenge [252].

ApN also played a role in modulating local inflammation by directly regulating macrophage phenotype, favouring a shift from a pro-inflammatory M1-like state to

an anti-inflammatory M2-like state, as evidenced in both in vivo and in vitro studies [253]. M2 cells are known to secrete the anti-inflammatory cytokine IL-10 and down-regulate the production of pro-inflammatory cytokines [253]. Thus, ApN appears to play a crucial role in controlling inflammation and oxidative stress in muscle. Mechanistically, the anti-inflammatory effects of ApN in human "healthy" myotubes were linked to the activation of the AdipoR1-AMPK-SIRT1-PGC-1α pathway [252]. The AMPK pathway is known to inhibit inflammation and oxidative stress by suppressing the activity of NF-κB, a key inducer of inflammatory responses [254]. Indeed, both PGC-1α and SIRT1 have been shown to repress NF-κB activity by inhibiting its transcriptional activity and thereby reducing the expression of pro-inflammatory genes [255, 256].

Additionally, a strong microRNA candidate, miR-711, was identified to mediate the anti-inflammatory action of ApN on mouse and human skeletal muscles [257]. ApN upregulated the expression of miR-711, which in turn suppressed NF-κB as well as the inflammasome complex [257, 258].

Moreover, as previously mentioned, PGC-1α also regulates cellular oxidant-antioxidant homeostasis by upregulating the expression of several antioxidant enzymes such as superoxide dismutase-2, catalase, and glutathione peroxidase [241] (Figure 12).

Pro-Myogenic effects

Following acute (reversible) injury, skeletal muscle demonstrates an impressive ability to initiate rapid and extensive regeneration, often accompanied by varying degrees of inflammatory response [69]. As mentioned before, the regeneration of skeletal muscle relies heavily on muscle stem cells, known as satellite cells, which remain quiescent in healthy muscle tissue [69]. Upon injury, immune cells, including M1 macrophages, are recruited to the site of injury, where they secrete elastases that cleave native ApN into its globular ApN form (gApN) [213]. Both M1 macrophages and gApN play pivotal roles in activating satellite cells and initiating the process of muscle regeneration [30, 259]. Once activated, satellite cells undergo migration, proliferation, and differentiation into myoblasts, which subsequently fuse to repair damaged fibres or generate new ones [69] (Figure 13).

Additionally, ApN is implicated in regulating various stages of the repair process by activating diverse signalling pathways, including p38MAPK and AMPK [259], and various myogenic transcription factors such as Myf5, MyoD, Myogenin, and Mrf4 [252]. Firstly, ApN upregulates Myf5 expression in skeletal muscle [252], promoting the activation of satellite cells and their commitment to muscle regeneration [75]. Furthermore, gApN induces a specific motility program in satellite cells by stimulating the production of specific metalloproteases, facilitating their migration to the injury site through the degradation of the surrounding extracellular matrix [71].

Secondly, gApN triggers the expression of MyoD, facilitating myoblast proliferation and differentiation [252, 260, 261]. Additionally, gApN stimulates autophagy in myoblasts through an AMPK-dependent mechanism, promoting cell survival and inhibiting apoptosis [262]. Thirdly, ApN coordinates the final step of skeletal muscle regeneration by activating the expression of key muscle differentiation factors, Myogenin and Mrf4 [252], which are crucial for cell fusion into multinucleated myotubes [75] (Figure 13). Muscle regeneration is a highly intricate process that occasionally involves non-resident progenitor cells possessing myogenic properties, such as mesoangioblasts. Following injury, these cells are drawn to the damaged area, where they have the capability to differentiate or merge with existing myofibres. [263]. gApN serves as a positive regulator in mesoangioblasts homing to injured or diseased muscles in mice, driving their commitment to the skeletal muscle lineage [264]. There is an interplay among the three major functions of ApN in skeletal muscle, as it coordinates inflammation resolution and energy metabolism for efficient muscle regeneration. ApN promotes the conversion of M1 to M2 macrophages, facilitating inflammation resolution [253]. Simultaneously, ApN enhances PGC-1α expression and activity, promoting oxidative metabolism to meet the high energy demand required for tissue healing and regeneration [265]. Thus, the controlled accumulation of immune cells and increased energy metabolism are crucial for proper muscle tissue remodelling [30] (Figure 13).

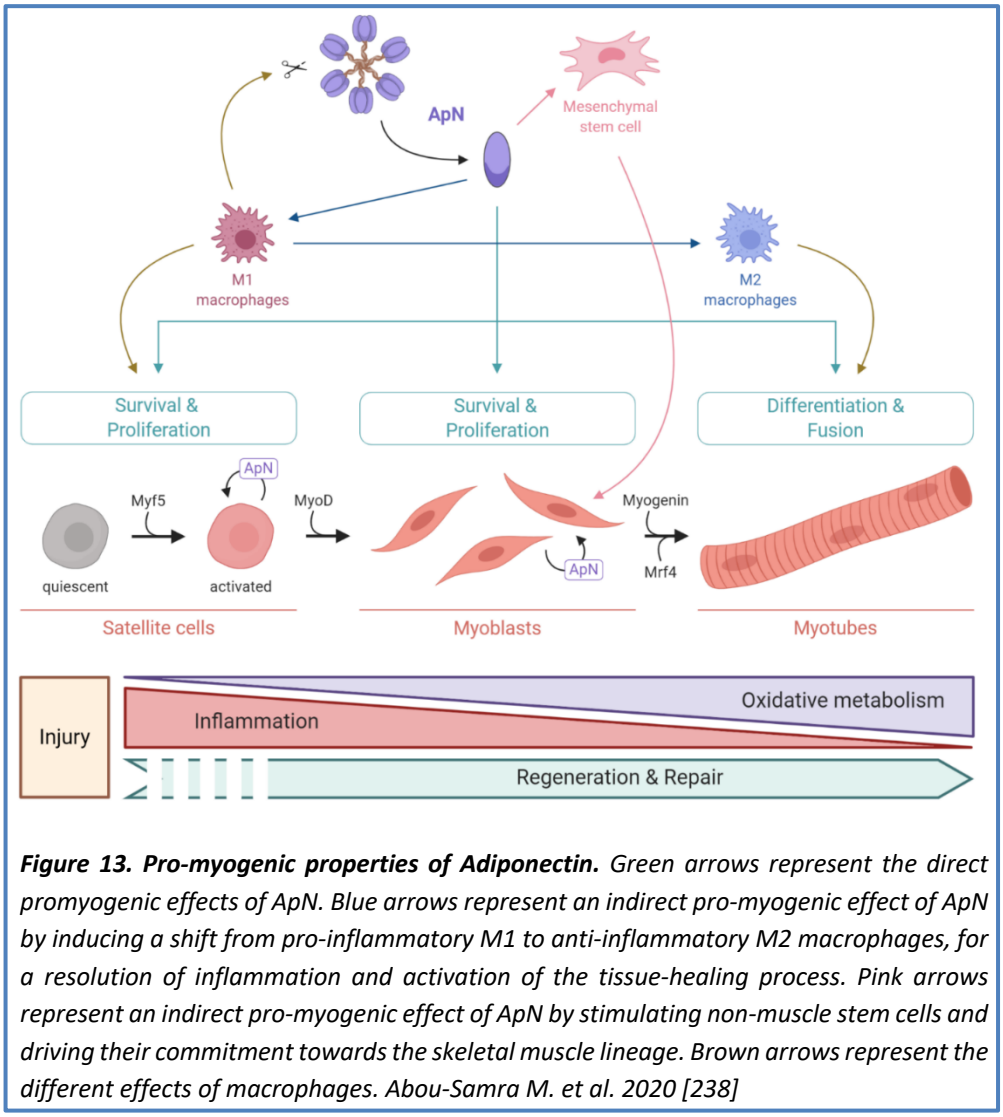

Figure 13. Pro-myogenic properties of Adiponectin. *Green arrows represent the direct promyogenic effects of ApN. Blue arrows represent an indirect pro-myogenic effect of ApN by inducing a shift from pro-inflammatory M1 to anti-inflammatory M2 macrophages, for a resolution of inflammation and activation of the tissue-healing process. Pink arrows represent an indirect pro-myogenic effect of ApN by stimulating non-muscle stem cells and driving their commitment towards the skeletal muscle lineage. Brown arrows represent the different effects of macrophages. Abou-Samra M. et al. 2020 [238]*

Cardio-protective effect

In addition to its pleiotropic effects on skeletal muscle, ApN also confers several additional benefits to the cardiac muscle (Figure 14). ApN plays a key role as anti-inflammatory agent [266] and in maintaining energy homeostasis in the heart through the AMPK axis by facilitating glucose and fatty acid uptake in cardiomyocytes [267]. ApN can also decrease myocardial cell apoptosis through pathways involving AMPK and Akt activation [268]. While AMPK activation can

enhance cellular antioxidant defences, thereby protecting against oxidative stress-induced apoptosis, ApN also protects against palmitate-induced cardiomyocyte apoptosis by activating the Sphingosine kinase 1 (SphK-1) via the Akt signalling pathway. SphK-1 will in turn converts sphingosine to S1P, which has anti-apoptotic properties, thereby promoting myocyte survival [269].

Overexpression or supplementation of ApN has been shown to improve myocardial hypertrophy and diastolic dysfunction in a rat model of heart failure with preserved ejection fraction (HFpEF), irrespective of its effect on blood pressure [270]. Observational studies have also revealed that higher levels of ApN are associated with a reduced left ventricular mass. [271]. These direct anti-hypertrophic effects are mediated by the AMPK and extracellular signal-regulated kinases (ERK) signalling pathways [272, 273], as demonstrated *in vitro* in mice [273, 274]. Additionally, ApN's also exerts indirect antihypertrophic effects by other mechanisms such as ameliorating hyperglycemia-induced cardiac hypertrophy and dysfunction by activating nuclear factor (erythroid-derived 2)-like 2 (Nrf2) and the brahma-related gene 1 protein (Brg1) to induce heme oxygenase-1 (HO-1) expression [275], or by attenuating Angiotensin II-induced cardiac hypertrophic signals, partly through the Akt pathway [276].

The anti-hypertrophic properties of ApN were also associated with the regulation of myocardial autophagy through AMPK activation. Autophagy is an intracellular process involving the bulk degradation of unwanted cellular components via the PI3K/Akt/mTor pathway, and it is crucial for maintaining cellular homeostasis. By inducing autophagy, ApN has been shown indirectly prevents myocardial hypertrophy in rodent models of type II diabetes [277-279].

Furthermore, ApN displays anti-fibrotic properties through the hlu of the TGF-β/smad2/3 pathway as demonstrated in left ventricles of rats submitted to chronic intermittent hypoxia [280]. Moreover, Ad-KO mice submitted to angiotensin-II showed higher levels of collagen I and III and TGF-β1, as well as more severe cardiac fibrosis in comparison with WT mice. These changes were ameliorated by ApN re-expression using adenovirus [281]

Finally, ApN exhibits antiatherosclerotic [282], and proangiogenic [283], properties, thereby improving overall cardiovascular function.

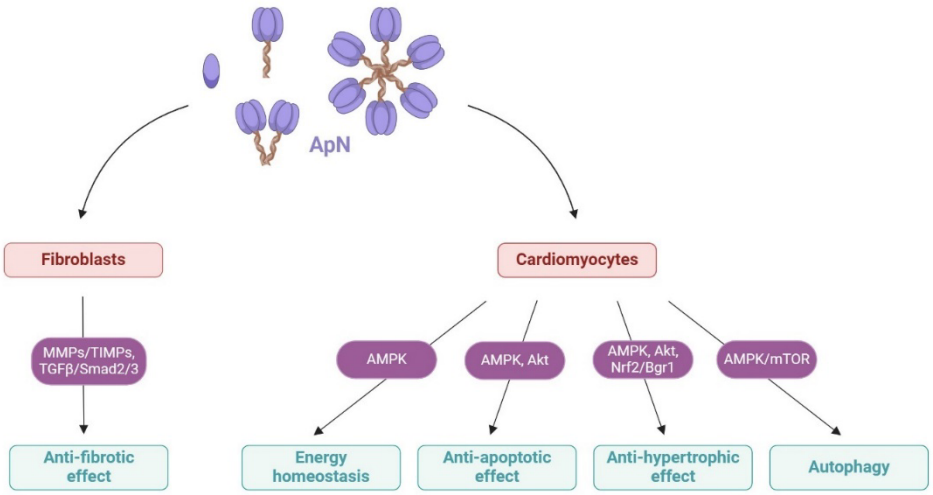

Figure 14. Cardio-protective effects of Adiponectin. *Figure adapted from Peng and al. 2023 [284].*

Adiponectin in DMD

Muscle may be a site of a severe form of chronic inflammation, which in turn plays a central role in the development or evolution of several myopathies [43, 60]. Because of its anti-inflammatory and pro-myogenic properties [285], ApN could offer interesting therapeutic prospects for managing muscle diseases such as DMD.

Our group and others have observed significant reductions in circulating levels of ApN in mdx mice [252, 286]. This observation has also been validated in human patients [287]. Additionally, myotubes derived from DMD patients have been found to lack the ability to produce ApN for local protection [28], unlike non-dystrophic myotubes exposed to inflammation [288]. Therefore, there may be a rationale for therapeutically addressing the low levels of ApN in individuals with dystrophy. Replenishing ApN through transgenesis or gene electro-transfer has been shown to ameliorate the dystrophic phenotype in mdx mice [252, 289]. Our work involving the generation of transgenic mdx mice overexpressing ApN (mdx-ApN mice) demonstrated that ApN can serve as a preventive agent, delaying disease progression [252].

First, restoring ApN levels reduced the expression of pro-inflammatory cytokines such as TNF-α and IL-1β, along with oxidative stress markers including

peroxiredoxin (an antioxidant enzyme) and 4-hydroxynonenal (a lipid peroxidation product). Dystrophic muscles from mdx-ApN mice also exhibited reduced infiltration by T-lymphocytes and M1 (pro-inflammatory) macrophages. [252]. Second, ApN significantly enhanced the skeletal muscle's myogenic program as demonstrated by the increased expression of muscle proliferation (Myf5 and MyoD) and muscle differentiation factors (Myogenin and Mrf4) [75, 252]. Third, mdx-ApN mice demonstrated a shift towards a more oxidative and resilient myofibre phenotype (type 1). Fourth, ApN upregulated utrophin, a protein analogous to dystrophin, which partially compensated for the deficiency of this structural protein. As a result, mdx-ApN mice showed improved overall muscle strength and endurance, coupled with reduced muscle damage [252].

Conversely, an opposite trend was observed through a contrasting approach. When mdx mice were bred with ApN-knockout mice, the mdx phenotype deteriorated. These mice exhibited diminished overall muscle strength and endurance, alongside increased muscle damage compared to regular mdx mice. However, supplementation of ApN through muscular gene electro-transfer counteracted all abnormalities, even after the onset of the disease. This suggests that ApN can serve not only as a preventive, but also as a therapeutic agent [289].

Some of the beneficial effects observed with ApN have been extended to human subjects. Our studies revealed that supplementation with ApN preserved its anti-inflammatory attributes in DMD human myotubes [28, 252, 290], fostering a shift in the secretion profile of downstream myokines toward a less inflammatory state. Specifically, analysis of the myotube secretome showed that ApN down-regulated the secretion of two pro-inflammatory factors (TNFα and IL-17A), one soluble receptor (soluble tumor necrosis factor receptor type II/sTNFRII), and one chemokine (CCL28)[28].

The mechanisms leading to the protective effects of ApN in DMD involved the activation of the AdipoR1-AMPK-SIRT1-PGC-1α axis both in vivo (mdx mice) or in vitro (human dystrophic myotubes) [28, 252, 290] (Figure 11). Silencing any component of this cascade nullified the effects of ApN. Among them, LKB1, a regulator of AMPK phosphorylation, has been shown to be reduced in mdx mice, supporting this impairment as a key feature of muscular dystrophy. However, a significant basal increase of AMPK phosphorylation [291, 292] has been observed

on dystrophic muscles, which is probably a compensatory mechanism due to the reduction of LKB1. This compensation might be explained by the existence of additional mechanisms responsible for AMPK phosphorylation, such as CaMKKβ, which is known to be overexpressed and overactive in DMD due to alterations in calcium homeostasis [293]. In contrast, in conditions of energetic stress caused by physical exercise, impaired LKB1 signaling fails to efficiently transduce mechanical-metabolic coupling, leading to an insufficient stimulation of AMPK in dystrophic myofibres [294]. To date, very little is known about upstream regulation of LKB1, a role for epigenetic control by miRNAs cannot be ruled out, which will require further investigation

The anti-inflammatory properties of ApN in DMD are attributed to NF-κB inhibition by PGC-1α dephosphorylation, SIRT1 deacetylation [252], and miR-711 up-regulation [257]. Additionally, PPARα may contribute to NF-κB repression [256]. Furthermore, restoration of the myogenic program could stem from inflammation attenuation [252, 290] as well as from insulin-sensitizing properties or p38 MAPK activation [71, 260].

Ultimately, the heightened activity of PGC-1α orchestrated by ApN in DMD results in the up-regulation of several target genes, contributing to its protective effects. Firstly, antioxidant detoxifying enzymes may mitigate oxidative stress. Secondly, the promotion of mitochondrial biogenesis and oxidative metabolism induces a shift towards an oxidative and more resilient fibre phenotype [252, 289]. Thirdly, the up-regulation of utrophin partly compensates for dystrophin deficiency [28, 252]. Fourthly, the elevation of miR-711, another target gene of PGC-1α (Collagen VII alpha-1) [257], may mitigate inflammation through the suppression of NF-κB and NLRP3 inflammasome activation [258] (Figure 15).

The continuous inflammation and necrosis characteristic of DMD also occurs within the heart, where it stimulates compensatory mechanisms by promoting hypertrophic signalling pathways and remodelling processes, leading to fibrosis, cardiac dysfunction, and ultimately heart failure [295]. To our knowledge, ApN has not been directly tested on dystrophic hearts. However, its documented beneficial effects on the cardiac muscle imply potential benefits for enhancing the condition of individuals with DMD.

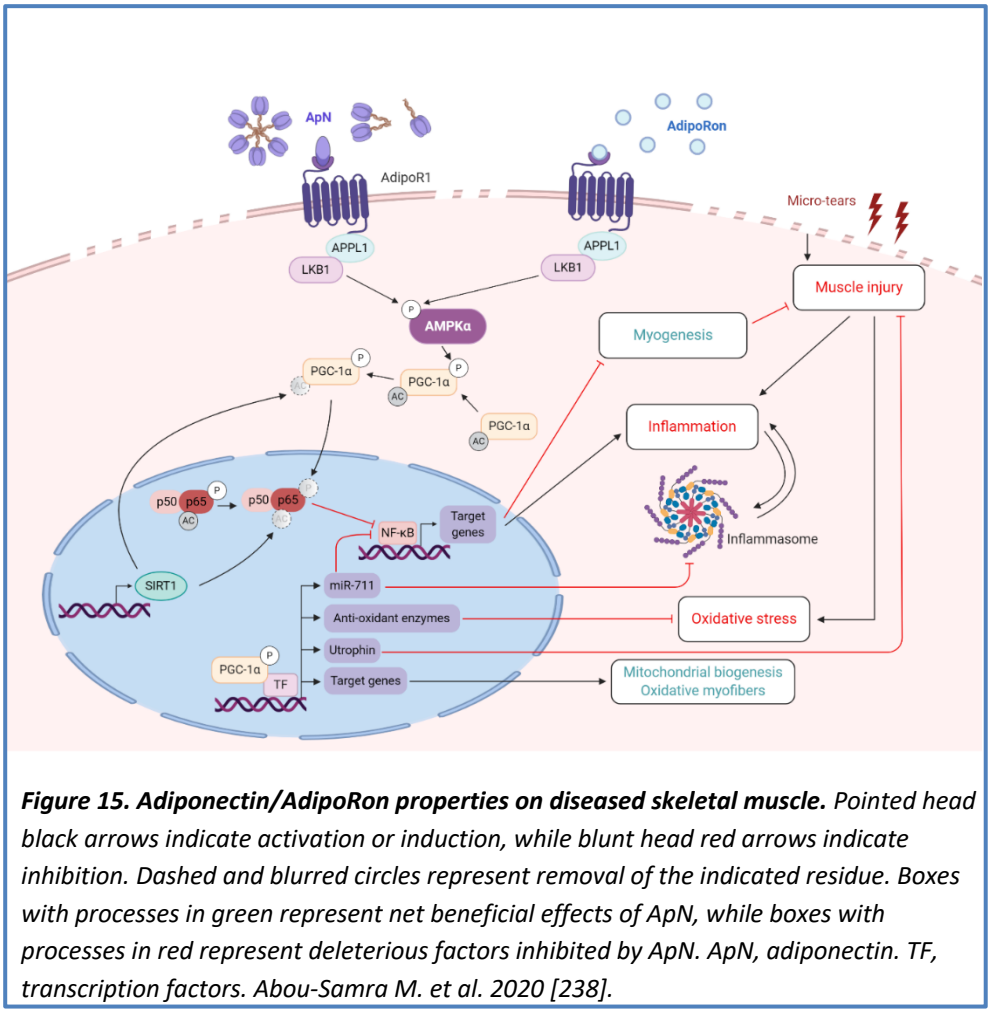

Figure 15. Adiponectin/AdipoRon properties on diseased skeletal muscle. *Pointed head black arrows indicate activation or induction, while blunt head red arrows indicate inhibition. Dashed and blurred circles represent removal of the indicated residue. Boxes with processes in green represent net beneficial effects of ApN, while boxes with processes in red represent deleterious factors inhibited by ApN. ApN, adiponectin. TF, transcription factors. Abou-Samra M. et al. 2020 [238].*

Adiponectin mimics

Due to its plethora of beneficial effects, ApN has garnered significant interest, fostering hopes for its therapeutic application in various diseases [238]. However, employing ApN directly as a therapeutic agent presents several challenges. Indeed, ApN possesses complex three-dimensional structures, circulates at high concentrations in plasma, and, like other peptides, requires injection for administration. Therefore, numerous short peptides and small molecules have been identified to target ApN receptors (AdipoRs) and replicate some of the effects

of ApN. These receptor agonists can initiate similar downstream signalling cascades as ApN, including AMPK, p38MAPK, and PPARα pathways [296]. The following section will provide a review of adipoR agonists, with particular emphasis on Adiporon and ALY688 (Table 1).

GTDF is a flavonoid-type compound, which was shown to attenuate the diabetic phenotype and its complications in obese db/db mice, through an AdipoR1-dependent mechanism [297]. GTDF also protected against skeletal muscle atrophy, by increasing myoblast differentiation and suppressing the expressions of atrophy markers, such as atrogin-1 and MuRF1, in models of steroid, cytokine and starvation-induced muscle atrophy [298].

Tiliroside is a plant derived glycosidic flavonoid with ApN-like effect. It was shown to stimulate fatty-acid oxidation in liver and skeletal muscle in obese-diabetic mice, and attenuate obesity-induced metabolic disorders [299].

JT003 is a synthetic AdipoR1/AdipoR2 dual agonists based on gApN. JT003 exhibited significant anti-lipogenic and anti-fibrogenic properties in both nonalcoholic steatohepatitis (NASH) and fibrotic mice, as well as a longer half-life duration than first generation AdipoRs agonists [300].

Table 1. Adiponectin mimics. Compounds that specifically bind to AdipoRs and greatly mimic several beneficial and protective effects of ApN.

Compound	Nature	Effets	Tested on SM	Pre-clinical models	References
GTDF	Flavonoid	Pro-metabolic and anti-atrophic	+	T2D, sarcopenia	[297, 298]
Tiliroside		Lipid metabolism	+	Metabolic disorders	[299]
JT003	Small synthetic molecule	Lipid metabolism and anti-fibrotic	-	NASH	[300]
AdipoRon		Pleiotropic effects similar to ApN	+	Metabolic disorders, cancer, systemic sclerosis, depression anxiety, PTSD, cardiac fibrosis, cerebral ischemia, DMD	[290, 301, 302]
AdipoAI			-	Obesity, perionditis	[303-305]
AdipoRaMab	Monoclonal antibody	Anti-inflammatory and antifibrotic	-	T2D, NASH	[306]
Osmotin	Protein	Pro-metabolic and neuroprotective	+	Obesity, T2D cardiovascular diseases, AD, PD	[307-311]
Pep70	Peptide	Anti-fibrotic	-	-	[312]
PEGylated BHD1028		Glucose, lipid metabolism and anti-inflammatory	+	Dry eyed disease, T2D	[313-315]
ADP-1	Short peptide	Glucose and lipid metabolism	+	T2D	[316]
ADP355		Suppress cancer cells proliferation	-	Cancer	[317]
ALY688		Anti-fibrotic, pro-metabolic and anti-inflammatory	+	Dry eyed disease, T2D, heart failure, obesity, DMD	[318-320]

AD: Alzheimer disease; NASH: non-alcoholic steatohepatitis; PD: Parkinson disease; PTSD: Post-traumatic stress disorder SM : skeletal muscle; T2D: Type 2 Diabetes.

AdipoRon, discovered in 2013 by Okada-Iwabu et al., is an orally active synthetic small-molecule agonist of AdipoRs, identified through screening a compound library. AdipoRon binds to AdipoRs and primarily exerts its biological effects by activating AMPK [301].

In vitro, and more specifically in C2C12 cells, AdipoRon was shown to promote AMPK activation and enhances PGC-1α expression, leading to an improved mitochondrial biogenesis. In vivo, AMPK and PPAR-α pathways were also activated, enhancing glucose, lipid metabolism, muscle endurance and alleviating insulin resistance, myosteatosis and muscle degenerative markers in high-fat diet-fed mice [321]. Furthermore, it improves diabetes and extends the lifespan of db/db mice [301, 322]. Specifically, in skeletal muscle, AdipoRon promotes mitochondrial biogenesis, reduces tissue triglyceride content, alleviates oxidative stress and prevent sarcopenia [302].
Based on these interesting results, AdipoRon has first been proposed for the treatment of type 2 diabetes and other obesity-related disorders in mice [301, 323-327]. Since then, its beneficial effects have also been demonstrated in other non-metabolic conditions such as cancer [328, 329], bone repair [330], systemic sclerosis [331], neuroinflammation, depression [323, 332], anxiety [333, 334], post-traumatic stress disorder [335], cardiac fibrosis [336] and cerebral ischemia [337].

Our latest study has brought to light the beneficial and protective effects of AdipoRon on the dystrophic skeletal muscle in mdx mice and in human DMD myotubes. Indeed, AdipoRon, mainly though AdipoR1-AMPK signalling, significantly mitigated skeletal muscle inflammation, oxidative stress, and damage, while markedly improving its regeneration and function [290]. To date, AdipoRon has not been tested in humans. However, a recent study has confirmed the effectiveness of AdipoRon on the human receptor AdipoR1 [338], therefore suggesting that adipoRon could be effective for clinical application. However, even though AdipoRon has been commercially available for a decade, it has only been used for research purposes and no human clinical trials have been conducted yet.

An analogue of AdipoRon called AdipoAI (adipo anti-inflammation agonist), was recently identified [303]. Remarkably, AdipoAI exhibits an anti-inflammatory effectiveness approximately eightfold greater than that of AdipoRon in macrophages. Subsequently, AdipoAI has demonstrated the capacity to improve insulin sensitivity in diet-induced obesity (DIO) mice models [304] and to mitigate periodontitis in diabetic rats [305].

AdipoRaMab, is a monoclonal antibody activating AdipoRs, that demonstrated promising effects in preclinical studies. It also improved glucose intolerance in high-fat diet-fed mice, and showed anti-inflammatory and antifibrotic effects in a NASH mouse model. Moreover, the study suggested that AdipoRaMab could maintain therapeutic efficacy even with a once-monthly dosing schedule due to its humanization [306].

Osmotin is a plant protein possessing structural and functional similarities to ApN [339]. It can also induce the phosphorylation of AMPK in C2C12 myotubes [310]. Several in vitro and in vivo experiments revealed its potential effects for counteracting obesity, diabetes and cardiovascular diseases [307-309]. Moreover, other studies have demonstrated its neuroprotective effects by preventing memory impairment and neuroinflammation induced by either amyloid or LPS injections [340] and by improving the neuropathological deficits of Parkinson's [341] and Alzheimer's disease [311, 342]. These findings position it as an interesting candidate for the treatment of neurological disorders [343].

In silico studies have further identified additional AdipoR activating peptides, including Pep70 and PEGylated BHD1028 [296]. Pep70 has demonstrated significant inhibition of cell proliferation and suppression of collagen type I alpha1 and TGF-β1 expression, thereby offering protection against fibrotic responses [312]. PEGylated BHD1028 exhibits high-affinity binding to both AdipoR1 and AdipoR2, making it a promising candidate for diabetes treatment [313]. It has demonstrated the ability to enhance glucose uptake, fatty acid β-oxidation, and mitochondrial biogenesis by stimulating AMPK phosphorylation, as evidenced in mouse C2C12 cells [314]. Furthermore, in both rabbit and mouse models of dry eye disease, it notably improved tear volumes, reduced inflammation, and ameliorated corneal status within a span of 10 days [315].

ADP-1 is a highly conserved 13-residue segment peptide from ApN's collagen domain, with similar positive effects on glucose and fatty-acid metabolism. In addition, it was shown to increase glucose uptake in rat skeletal muscle cells lines and improved glucose tolerance in db/db mice [316].

ADP355 is a synthetic decapeptide AdipoRs agonist derived from the active site of human gApN, and which can bind both AdipoRs with a better affinity to AdipoR1. This first-in-class small peptide agonist was discovered as an inhibitor of cancer cell

growth that was more potent than gApN [317, 344, 345]. Several other beneficial effects were observed both in vitro and in vivo. More specifically, when administered to mice, ADP355 reduced inflammation and fibrosis after toxic liver or heart injury [346-348]; its antifibrotic properties were probably the most striking ones and were also confirmed in a mouse model of keloid and systemic sclerosis [349, 350]. ADP355 was also capable of inhibiting atherosclerosis in apoE-deficient mice [351] and to improve neurocognitive performance in mice treated with HIV protease inhibitors [352]. Thereafter, ADP355 structure underwent further refinement to achieve an optimal size and configuration. This process led to the development of the peptide ALY688, which demonstrated enhanced potency in activating both AdipoR1 and AdipoR2 compared to the original peptide. Additionally, ALY688 exhibited increased resistance to degradation and a favourable safety profile [353].

ALY688 attenuated insulin resistance induced by a high-fat/high-sucrose diet in muscle cells [318], and act favourably on glucose and fat metabolism in rat adipocytes [319]. On a mouse model of heart failure with reduced ejection fraction (HFrEF), ALY688 was also able to reduce cardiac hypertrophy, inflammation and fibrosis [320].

Importantly, ALY688 is available in two distinct formulations. The first is a conventional formulation, employed for in vitro and in vivo studies. It was first tested with success in a mouse model of experimental dry eye [354] then recently evaluated in a Phase 1/2a clinical trial to assess its safety and efficacy in individuals with xerophthalmia (dry eyes). Results from this study showed consistent improvements in ocular surface staining (both cornea and conjunctiva) as well as symptom relief within just 2 weeks of treatment initiation (as reported in an abstract presented at the 2023 Association for Research in Vision and Ophthalmology Annual Meeting). Encouraged by these results, a Phase IIb/III trial involving 900 participants is currently underway, with data expected in 2024 (NCT04899518). The second formulation is an extended-release (ER) variant of ALY688, known as ALY688ER, which is administered subcutaneously and has primarily been developed to target inflammatory, fibrotic, and metabolic conditions. This formulation has shown improvement in recognition memory and hippocampal mitochondrial status in young D2.mdx mice [355]. Additionally, our research has demonstrated improved physical performance in mdx mice treated

with ALY688ER, along with potent anti-inflammatory, anti-oxidative, and anti-fibrotic effects on dystrophic muscle [356]. These findings will be further elaborated in the results section. Currently, a Phase 1 study utilizing the ER formulation is underway in overweight and obese healthy adults (NCT04855565).

Considerable efforts have been dedicated to identifying and optimizing AdipoR agonists as potential therapeutic agents. However, only ALY688 yet advanced to the stage of clinical adoption. This could be attributed to the interindividual variations in endogenous ApN and AdipoR expression levels, as well as the intricate molecular networks formed around its signalling pathway. Moreover, the development of ApN resistance in certain disease states, possibly stemming from reduced expression or altered post-translational modification of AdipoRs or adaptor proteins like APPL1, may significantly impact the efficacy of AdipoR agonists [357, 358].

In summary, ALY688 is a strong candidate for clinical evaluation in the near future as a promising therapeutic. In addition, no toxicity signals have been observed yet. However, while already tested in a DMD mouse model, its potential anti-inflammatory, promyogenic and anti-fibrotic properties have not been evaluated in skeletal muscle and a fortiori not in the dystrophic muscle.

Part IV: Inflammasome[2]

NLRP3 inflammasome

Structure and components of NLRP3 inflammasome

Inflammation is a natural process which aim to defend our body against infection or damages. Typically, the innate immune system is the first to react and can trigger sterile inflammation through specific pattern-recognition receptors (PRRs), such as the nucleotide binding domain leucine-rich repeat-containing receptor (NLR) [359].

NLRP3, also known as NALP3, is the most extensively characterized NLR and is encoded by the Nlrp3 (CIAS1) gene. NLRP3 protein consists of an amino-terminal pyrin domain (PYD), a central nucleotide-binding domain (NACHT) containing extended Walker A and Walker B sites capable of accommodating ADP in the inactive, closed state, and ATP (or dATP) in the active, open state of NLRP3, and a C-terminal leucine-rich repeat (LRR) motif [360, 361]. Activation of the NLRP3 inflammasome necessitates a complex interplay of specific proteins (Figure 12).

Initially, LRR domain of NLRP3 detects danger signals, leading to the oligomerisation of NLRP3 monomers. Then, interaction occurs between NLRP3 and the apoptosis-associated speck-like protein containing a C-terminal caspase recruitment domain (ASC) [361]. ASC is a cytosolic protein featuring a C-terminal caspase recruitment domain (CARD) and a PYD, pivotal for activating the inflammasome complex by bridging NLRP3 proteins and pro-caspase-1 [362, 363]. Furthermore, the interaction of NEK7 with the LRR domain of NLRP3 is crucial for complete inflammasome activation [364]. NEK7 belongs to the NIMA-related serine-threonine kinase family and comprises a catalytic domain with a 30–40 amino acid N-terminal extension [365].

[2] Some portions of this section have been adapted from a review article published by our team: 132. Dubuisson, N., et al., *Walking down Skeletal Muscle Lane: From Inflammasome to Disease.* Cells, 2021. **10**(11).

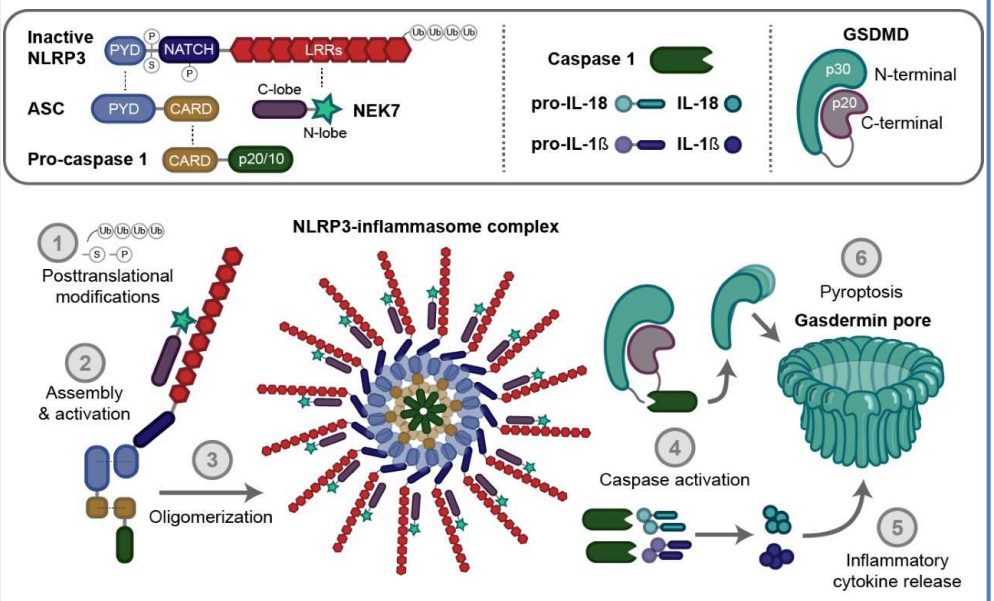

Figure 16. The nucleotide-binding oligomerization domain like receptor family (NOD-like) pyrin domain containing 3 (NLRP3) inflammasome complex. *Dubuisson et al 2021 [132].*

Once activated, caspase-1 subsequently cleaves pro-interleukin-1β (pro-IL1β), pro-interleukin-18 (pro-IL-18), and Gasdermin D (GSDMD) into their active mature forms [366, 367]. Caspases constitute a family of proteolytic enzymes responsible for the degradation of cellular components during programmed cell death. They are categorized into three groups: apoptosis-related caspases (2, 3, 6, 7, 8, 9, and 10), inflammation-related caspases (1, 4, 5, 11, and 12), and a third category consisting of caspases with unknown functions (13, 14, and 16) [368, 369].

IL-1β serves as a central proinflammatory cytokine orchestrating inflammation across diverse cell types and tissues. Its levels and functions are intimately linked with the development of numerous autoinflammatory and autoimmune diseases. Intriguingly, IL-1β can also exhibit anti-inflammatory properties and regulate adaptive immune responses [370], suggesting that the primary physiological role of

NLRP3 is to eliminate harmful substances and modulate metabolism and inflammation [371].

Belonging to the same family of IL-1 cytokines, IL-18 shares similar mechanisms of activation, receptor structure, and signal transduction pathways [372]. IL-18, a pleiotropic cytokine, serves as a crucial link between the innate and adaptive immune responses, influencing their regulation [373]. Depending on the host microenvironment, IL-18 can act as a potent activator of CD4 T helper (Th) 1 lymphocytes and natural killer cells, while also modulating Th2 and Th17 cell responses, along with the activity of CD8 cytotoxic cells and neutrophils [373].

Notably, IL-1 family members lack a specific secretion signal peptide and are not secreted via exocytosis. Consequently, pore formation via GSDMD activation is necessary for IL-1 release [374].

GSDMD, a protein comprising a 31 kDa N-terminal (GSDMD-N) and a 22 kDa C-terminal (GSDMD-C) domain, plays a crucial role in the pyroptosis process. Upon recruitment by NLRP3 inflammasomes, GSDMD undergoes proteolytic cleavage by caspase-1 (canonical) or by caspases 4, 5, and murine caspase 11 (noncanonical) during inflammasome activation [375]. Both pathways end up with the release of GSDMD-N, which in turn oligomerizes with other GSDMD-N molecules, forming a complex capable of creating nonselective pores in the plasma membrane. This process ultimately leads to pyroptosis and the release of IL-1β and IL-18 [366, 376] (Figure 16).

Pyroptosis is defined as a form of necrotic cell death facilitated by GSDMD and differing from other modes of cell demise like necrosis and apoptosis. In addition, the recently discovered nerve injury-induced protein 1 (NINJ1) [377], creates bigger pores than GSDMD-N, for the release of larger DAMPs such as HMGB1, LDH and polymerized ASC proteins, called ASC specks, into the extracellular space [378]. Once released extracellularly, these components remain active, thereby fuelling an escalation of the inflammatory response [131, 379, 380]. Recent research suggests that GSDMD-N can also puncture the mitochondrial membrane thereby inducing the release of mitochondrial DAMPs, such as mitochondrial double-stranded DNA (mtDNA) and reactive oxygen species (ROS), into the cytosol [381]. While pyroptosis may serve as a physiological mechanism during acute inflammatory responses by maintaining cellular homeostasis and curbing excessive cell proliferation, its

occurrence under chronic disease conditions can lead to uncontrolled inflammation, heightened cell death, and tissue remodelling [382, 383].

NLRP3 inflammasome activation

Regulation of NLRP3 inflammasome activation occurs at both transcriptional and posttranslational levels. Initially, NLRP3 activation is triggered by a priming signal initiated by TNFα, pathogen-associated molecular patterns (PAMPs), or IL-1β [378]. These signals operate via the NF-κB pathway, which subsequently upregulates the expression of pro-IL-1β, pro-IL-18, and NLRP3 genes within the cells, as their baseline levels are relatively low in numerous cell types [384-386]. Apart from innate immunity effectors like myeloid cells (monocytes and macrophages), muscle cells also harbour NLRP3 inflammasomes, actively contributing to the immune response and ultimately leading to myofibre damage [387, 388]. These priming signals additionally induce posttranslational modifications such as NLRP3 deubiquitination, along with ASC ubiquitination and phosphorylation, facilitating inflammasome complex assembly [389].

Following the initial priming signal, a second stimulus is transmitted through various activators, including PAMPs and DAMPs [35, 390]. DAMPs encompass a wide range of entities such as viruses [391], adenosine triphosphate (ATP) [392], the glycosaminoglycan hyaluronan found in the ECM [393], amyloid-beta fibrils [394], crystalline structures (like silica, asbestos, aluminum salt, uric acid, and calcium pyrophosphate dehydrate (CPPD)) [395, 396], ultraviolet irradiation [397], albumin [398], dietary saturated fatty acids [399], numerous pore-forming toxins [400], and aggregates [390]. Various molecular mechanisms have been proposed to initiate NLRP3 inflammasome oligomerization. These mechanisms include the activation of ATP-dependent P2X purino-receptor 7 receptor (P2 × 7R), which triggers both calcium and sodium influxes, subsequently enhancing potassium (K+) efflux through the opening of the two-pore potassium channel 2 (TWIK-2) [401, 402]. Moreover, pore formation induced by bacterial toxins also results in increased K+ efflux [403].

Lysosomal alterations [404, 405] and mitochondrial ROS [406] generation also contribute to the assembly of the inflammasome complex. Specifically, ROS rigger NLRP3 activation through different mechanisms. Firstly, ROS induce dissociation of thioredoxin-interacting protein (TXNIP) from thioredoxin (TRX), facilitating

interaction between TXNIP and NLRP3 [407]. Secondly, ROS promote the release of mitochondrial DNA into the cytosol, ultimately leading to NLRP3 inflammasome activation. Additionally, ROS enhance NF-κB activity, thereby augmenting NLRP3 priming and activation [408].

Besides the canonical activation of the NLRP3 inflammasome acting by its effector caspase-1, there is a noncanonical activation operating independently of the Toll-like receptor (TLR)/NF-κB pathway and triggered upon cytosolic detection of LPS. NLRP3 is then activated both by a K+ efflux resulting from the opening of the pannexin-1 (panx-1) channel subsequently activating of the ATP-gated cation channel receptor (P2 × 7R) [409, 410] and also by the direct cleavage of GSDMD into GSDMD-N and GSDMD-C by Caspases 4, 5, and 11 (Figure 17).

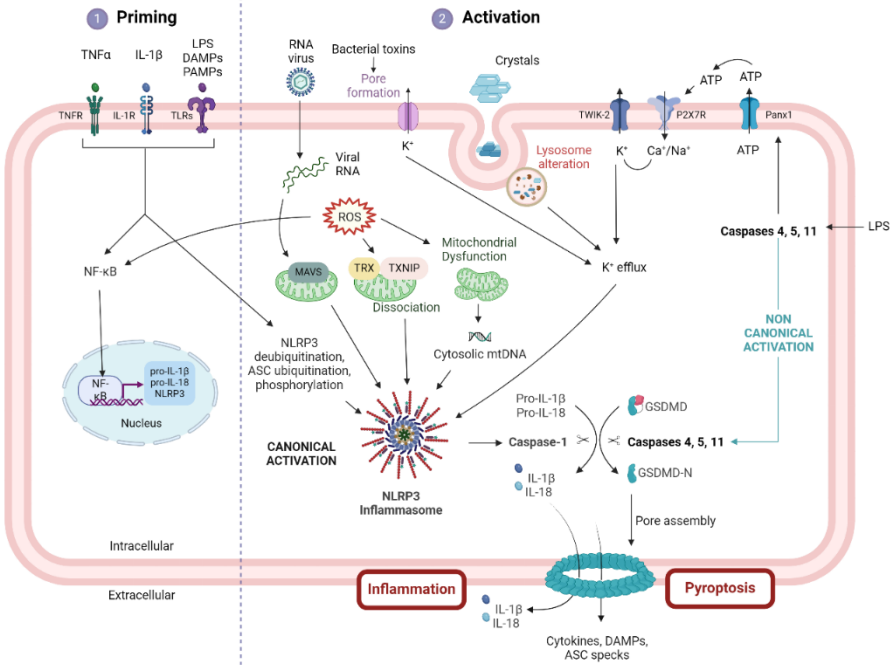

Figure 17. NLRP3 priming and activation. *Dubuisson et al 2021 [132].*

NLRP3 inflammasome regulation

Excessive NLRP3 inflammasome activation could lead to several diseases [411, 412], therefore, the activation of this inflammasome should be tightly regulated to prevent cell damage and excessive inflammation. The regulation of NLRP3 is carried out by many post-translational modifications, such as ubiquitination, phosphorylation, sumoylation and s-nitrosylation [413]. Various regions of the NLRP3 protein can undergo post-translational modifications, resulting in distinct profiles of NLRP3 that can either activate or inhibit its function. Furthermore, the impact of these modifications on NLRP3 is specific to different tissues [414]. Apart from post-translational modifications, NLRP3 is also regulated through interactions with regulatory partners. Many of these regulators promote NLRP3 activation, including TXNIP [407], guanylate binding protein 5 (GBP5) [415], double-stranded RNA-dependent protein kinase (PKR) [416, 417], migration inhibitory factor (MIF)[418], microtubule affinity-regulating kinase 4 (MARK4) [419], as well as Hsp90 and its cochaperone SGT1 [420], with the latter also playing a role in protecting NLRP3 from degradation. In contrast, certain regulators are involved in inhibiting NLRP3, such as pyrin-only protein 1 (POP1) [421], pyrin-only protein 2 (POP2) [422], and inhibitory CARD (INCA, also known as CARD17) [423].

Role of NLRP3 inflammasome in DMD

DMD is characterized by progressive muscle weakness and atrophy, accompanied by pronounced and persistent muscle inflammation, which holds a pivotal role in the initiation and advancement of the disease [43, 258, 290]. Several studies have indicated that the NLRP3 inflammasome instigates a pathogenic inflammatory response in several inherited myopathies, including DMD [130, 258], valosin-containing protein (VCP) associated diseases [424], inclusion body myositis [425] and limb girdle muscular dystrophy type 2B (LGMD2B) [388]. Rawat and colleagues were the first to demonstrate that, in addition to immune cells, primary skeletal muscle cells express TLRs and can effectively produce and release IL-1β under stressful conditions. They also observed a significant upregulation of inflammasome components in dysferlin-deficient muscle cells, which likely contributed to the pathogenesis of LGMD2B [388].

Our research on DMD revealed significant upregulation of NLRP3 and IL-1β expression, not only in inflammation-challenged C2C12 murine cell lines but also in

human primary cultured myotubes obtained from DMD patients. Similarly, all components of the inflammasome showed increased levels in the skeletal muscles of mdx mice, indicating an overactivation of the complex [258]. Targeted depletion of NLRP3 in mdx mice resulted in marked protection of skeletal muscle against inflammation, oxidative stress, and injury, while concurrently enhancing its strength and endurance, thus contributing to the amelioration of the dystrophic phenotype [130, 258].

Inflammasome inhibitors

The activation of the NLRP3 inflammasome has been recognized as a pathogenic mechanism in a range of cell-based and preclinical in vivo models of autoinflammatory, autoimmune, metabolic, neurodegenerative and muscle disorders. As a result, treatments targeting the NLRP3/caspase-1/IL-1β axis are expected to improve our drug arsenal to combat a plethora of disease acting either directly on NLRP3 protein (direct inhibitors) or interacting with the upstream or downstream NLRP3 signalling pathways (indirect inhibitors) (Figure 18).

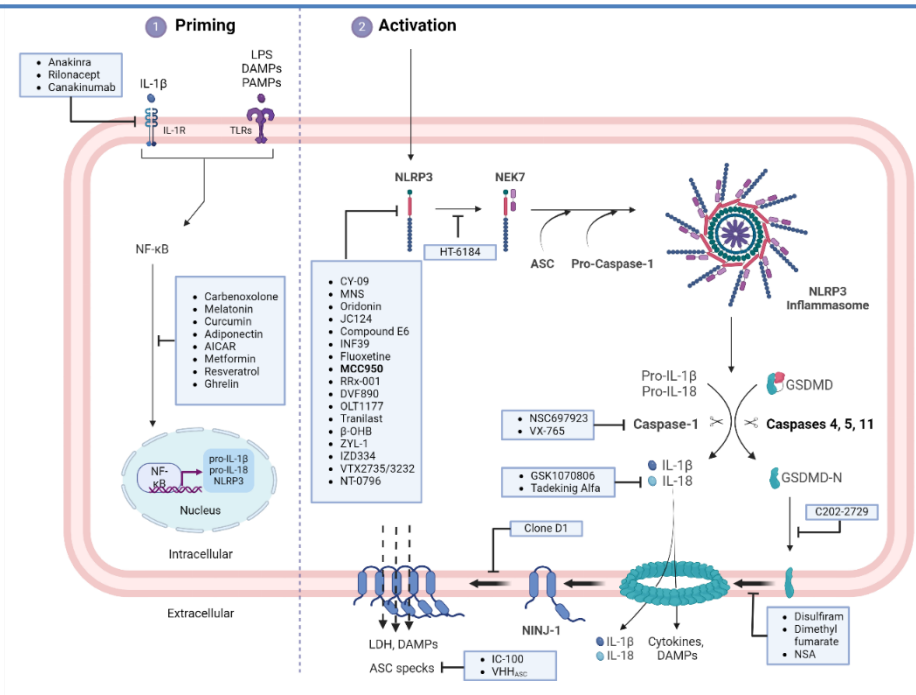

Figure 18. Targets of NLRP3 direct and indirect inhibitors

NLRP3 Direct Inhibitors

Direct inhibitors are separated into 2 groups, based on their preclinical (Table 2) or clinical applications (Table 3). Among them, I will focus on one highly interesting inhibitor, MCC950, which has been extensively studied in muscle-related disorders and is very relevant to my studies.

Table 2. Direct NLRP3 inhibitors in preclinical studies. Mechanisms of action and involvement in diseases.

Agent	Target site	Inhibitory Effect	Tested on SM	Diseases	References
Cy-09	NLRP3 NACHT Domain	NLRP3 ATPase activity	-	Gout, T2D, CAPS, seizure and NAFLD	([426-429]
MNS			-	Wound healing, colitis and osteosarcoma tumors	[430-432]
Oridonin		NLRP3 oligomerization	-	TBI, T2D, gout, AD, cardiac hypertrophy, methicillin-resistant Staphylococcus aureus (MRSA), pulmonary fibrosis, cancer, and more	[433, 434]
JC124			-	TBI, AD	[435, 436]
Compound E6			-	Colitis	[437]
INF39	Unknown	NLRP3 ATPase activity and oligomerization	-	Inflammatory bowel disease	[438]

AD: Alzheimer disease; ALS: amyotrophic lateral sclerosis; CAPS: cryopyrin associated periodic syndrome; Cy-09: glitazone; MNS: 3,4-methylenedioxy-beta-nitrostyrene; NAFLD: non-alcoholic fatty liver disease; NLRP3: NOD-like receptor family, pyrin domain containing 3; SM: skeletal muscle; TBI: traumatic brain injury; T2D: Type 2 Diabetes; VCP: valosin-containing protein; +: validated; -: absence;

Table 3. Direct NLRP3 inhibitors tested in clinical trials or repurposed drugs. Mechanisms of action and involvement in diseases.

Agent	Target site	Inhibitory effect	Tested on SM	Preclinical studies	Clinical trials	References
Fluoxetine			+	Macular degeneration	-	[439]
MCC950			**+**	**MS, AD, Parkinson, stroke, MI, CAPS, Ischemia, CLI, VCP, DMD**	RA, Phase II	**[130, 440, 441]**
RRx-001			-	Inflammatory diseases, Cancer, Parkinson's disease, ALS, AD	SCLC, Phase III; Mucositis, Phase II	[442, 443]
IFM 2427/DFV890	NLRP3 NACHT Domain	NLRP3 ATPase activity	-	Inflammatory diseases	FCAS, Phase II; knee arthritis, Phase II; Coronary disease Phase II	[444]
OLT1177			+	Inflammatory diseases	Arthritis, Phase II; Gout Phase II; Heart failure Phase Ib; Covid19, Phase II; Schnitzler's syndrome, Phase II	[445-447],
Tranilast			-	Gout, T2D, CAPS, atherosclerosis	RA, Phase II; Hyperuricemia, Phase II; CAPS, Phase II	[448, 449]
β-OHB		NLRP3 oligomerization	+/*	ALS, stress-related mood disorders, hypertension, seizures, gout	ALS, Phase II	[450-454]
ZYIL1			-	-	CAPS, Phase II	[444]
IZD334	Unknown	Unknown	-	-	CAPS, Phase Ib Colitis, Phase Ib COPD, Phase Ib	No publication
VTX2735			-	-	CAPS, Phase I completed, Phase II underway	No publication
VTX3232			-	-	Phase I underway	No publication
NT-0796			-	-	Obesity, Phase I	No publication
HT-6184			-	-	Phase I completed, Pain, Phase II	No publication

*β-OHB: β-hydroxybutyrate; AD: Alzheimer disease; ALS: amyotrophic lateral sclerosis; CAPS: cryopyrin associated periodic syndrome; CLI: chronic limb ischemia; COPD: chronic obstructive pulmonary disease; FCAS: Familial cold autoinflammatory syndrome; MI: Myocardial infarction; MS: Multiple Sclerosis; NLRP3: NOD-like receptor family, pyrin domain containing 3; OLT1177: Dapansutrile; RA: Rhumatoid arthritis, SCLC: small cell lung cancer; SM : skeletal muscle; T2D: Type 2 Diabetes; VCP: valosin-containing protein; .+: validated; -: absence; *: Not directly demonstrated*.

MCC950 also known as CP-456,773 or CRID-3, is a diaryl sulfonylurea-containing compound which stands out as an exceptionally potent inhibitor of NLRP3, exerting its action by reversibly binding to the Walker B site of the NLRP3 NACHT domain, responsible for ATP binding and hydrolysis. Therefore, MCC950 prevents structural conformational changes and ATP hydrolysis hence maintaining NLRP3 in an inactive state [455, 456]. In preclinical studies, MCC950 demonstrated remarkable efficacy, rescuing neonatal lethality in a mouse model featuring an activating mutation in NLRP3, which was not possible by targeted blockade of IL-1β alone. Notably, this compound exhibited activity in ex vivo samples from patients exhibiting similar gain-of-function mutations [457, 458].

MCC950 has been employed in various experimental contexts, demonstrating its ability to inhibit NLRP3-mediated pathology across numerous preclinical in vivo models. These include the experimental autoimmune encephalomyelitis (EAE) model of multiple sclerosis, the APP/PS1 model of Alzheimer's disease, several in vivo models of Parkinson's disease, preclinical models of myocardial infarction, atherosclerosis, stroke, asthma, allergic airway inflammation, and inflammatory arthritis [440]. In the skeletal muscle, studies in mice revealed that MCC950 enhances blood flow and capillary density, underscoring the significance of NLRP3 in ischemic muscle diseases [459]. Moreover, in a mouse model of VCP myopathy, MCC950 showcased the ability to enhance physical performance and notably reduce the expression of NLRP3, caspase 1, IL-1β, and IL-18 [424]. Similarly, MCC950 reduces muscle atrophy in a mouse model of diabetes type II, its effect was even potentialized when combined with exercise [460].

In addition, investigations into the role of MCC950 in the pathogenesis of DMD have yielded promising results, demonstrating improvements in muscle performance and protection against muscle inflammation [130]. As such, NLRP3 inhibitors emerge as a potential therapeutic avenue for various muscle disorders.

Due to its exceptional selectivity and potency, MCC950 continues to serve as the primary tool compound for inhibiting NLRP3 in preclinical disease models. However, when MCC950 was evaluated in a phase II clinical trial for the treatment of rheumatoid arthritis, elevation of serum liver enzyme levels, indicative of potential liver toxicity was observed [461]. This setback forced Pfizer to halt further clinical translation of MCC950 [441]. To account for these side effects, researchers investigated the off-target effects of MCC950 and recently discovered its non-competitive inhibition of the esterase activity of carbonic anhydrase 2 [462]. However, it remains unclear whether this off-target inhibition contributes to the reported liver injury induced by MCC950 in early human studies. Notably, carbonic anhydrase inhibitors are commonly used clinically as diuretic medications, and no adverse effects on the liver have been reported [463].

MCC950-derived analogues with improved potency and pharmacological profiles are currently being developed and clinically evaluated. Apart from compounds specifically designed for treating CAPS, autoimmune disorders, and metabolic conditions with peripheral effects, there is a growing focus on developing inhibitors capable of penetrating the blood-brain barrier. These inhibitors are being explored for the treatment of neurodegenerative diseases such as Alzheimer's disease, Parkinson's disease, and other central nervous system disorders [464].

NLRP3 indirect inhibitors

Targeting upstream signals

NF-κB modulators have displayed promising outcomes in inflammatory skeletal muscle models. Triptolide prevented muscle atrophy in LPS-challenged mice [465], carbenoxolone reduced metabolic abnormalities like liver and muscle steatosis in HFD-mice [466], while melatonin exhibited an intriguing anti-inflammatory effect and preserved normal muscular structure and function in a sarcopenic mouse model [467-470]. Curcumin decreased ROS levels and proinflammatory cytokines in C2C12 muscle cells subjected to palmitate-induced inflammation [471] and demonstrated favourable effects on dystrophic skeletal muscle by reducing TNFα and IL-1β levels and enhancing cell membrane integrity when administered to mdx mice [472].

Several other compounds and drugs primarily activating AMPK signalling, such as AICAR (an adenosine monophosphate analogue), resveratrol (a natural polyphenolic compound), and metformin (used in type 2 diabetes treatment), have demonstrated mitigation of DMD features in cell cultures and animal models [473-476]. Metformin was also evaluated in a Phase III clinical trial NCT01995032 in combination with L-citrulline for DMD treatment, showing a modest reduction in motor function decline in the stable subgroup of treated patients. These interventions exert their beneficial effects, in part, by reducing inflammation and inhibiting the inflammasome [252, 477].

Similarly, ghrelin, a circulating gastric peptide known as the "hunger hormone," exhibited anti-inflammatory effects when administered to mdx mice, improving muscle performance and alleviating muscle pathology by inhibiting NLRP3 inflammasome activation and subsequent IL-1β maturation [478, 479]. Shikonin, a Chinese medicine inhibitor of pyruvate kinase M2 (PKM2), demonstrated NLRP3 inhibitory activation and protected against pyroptosis in muscle cells [480, 481]. In addition, human subjects on a high palmitate diet (saturated fatty acids/SFA) exhibited elevated levels of NLRP3 mRNAs in their skeletal muscle biopsies, while transitioning to an oleate-rich diet (monounsaturated fatty acids/MUFA) decreased NLRP3 priming and activation [482]. Trimetazidine was effective in reducing dexamethasone-induced muscle atrophy [483]. Two compounds act on the P2X7/K+ channel activation pathway: bright blue G (BBG) [484-486] and glyburide

(a sulfonylurea currently used in T2D) [484, 487], both demonstrating a restoration of muscle strength in idiopathic inflammatory myositis mouse models. While indirect inhibitors can suppress NLRP3 inflammasome activation, they often necessitate high doses, rendering direct inhibitors more precise and effective. Moreover, the mechanisms of action for some of these compounds may be tissue-specific, limiting their efficacy in diseases affecting multiple organs and tissues. Therefore, direct targeting of NLRP3 likely presents the optimal therapeutic strategy for muscle diseases with an inflammatory component.

Targeting downstream signals

Other drugs and molecules could act downstream of the NLRP3 inflammasome to inhibit pyroptosis and/or inflammation. The downstream signals of NLRP3 include inhibition of caspase-1, IL-1β/IL-1R, IL-18, gasdermin D pore formation, and ASC specks released.

Inhibitors of caspase-1 encompass NSC697923 and VX-765. NSC697923 notably suppressed caspase-1-mediated gasdermin D cleavage and pyroptosis in macrophages. Moreover, in an animal model of gouty arthritis, NSC697923 demonstrated efficacy in reducing joint swelling, IL-1β release, and NLRP3 inflammasome activation [488]. VX765 inhibits both caspase 1 and NLRP3 inflammasome assembly/activation [489]. It shows interesting results in inflammatory diseases such as preclinical models of Alzheimer disease, HIV, sepsis and atherosclerosis [490-493].

Anti-IL-1β therapies (anakinra, rilonacept and canakinumab) were the first to be tested in humans and showed efficacy in several inflammatory diseases. Anakinra is currently approved for the treatment of rheumatoid arthritis and CAPS [494, 495], while rilonacept having a longer half-life than anakinra, got an approval for CAPS and recurrent pericarditis [496, 497]. Finally, canakinumab, a human monoclonal antibody targeting IL-1β is the preferred treatment option for CAPS, juvenile idiopathic arthritis, rare periodic fever syndromes, and adult-onset Still's disease (AOSD) [498-501]. However, their effects in metabolic disorders were less evident [502-504], and even absent for sporadic inclusion body myositis (sIBM), an inflammatory muscle disease [505]. Moreover, the use of canakinumab, was also associated with increased susceptibility to infection [506].

Anti-IL-18 therapies are currently in development for different inflammatory diseases. Tadekinig Alfa, is a recombinant human IL-18 binding protein, being tested in AOSD [507, 508] in a phase II trial (NCT02398435) and in NLRC4 related macrophage activation syndrome, an inflammatory diseases associated with high plasma IL-18 levels, in a phase III trial (NCT03113760) [509]. In addition, GSK1070806, a humanized antibody targeting IL-18, is currently being tested in a phase 1 trial for atopic dermatitis (NCT04975438), and in phase II trials for delayed graft function (NCT02723786) [510], Crohn disease (NCT03681067), and Behcet's disease (NCT03522662).

GSDMD targeted therapies includes disulfiram, an approved medication for the treatment of alcoholism, which inhibits GSDMD pore formation, leading to a decrease in levels of inflammatory cytokines in a mouse model of sepsis and an extension of their survival rate [511]. Necrosulfonamide (NSA) acts by a similar mechanism and also demonstrated efficacy in LPS-induced sepsis [512]. Finally, dimethyl fumarate, a drug used in routine clinical practice in multiple sclerosis and psoriasis, has been shown to inhibit GSDMD-induced cell death, while protecting mice from endotoxic shock [513]. Moreover, it reduces GSDMD-N, IL-1β and IL-18 in the hippocampus following status epilepticus [514]. However, these three GSDMD modulators exert additional effect on other pathways thereby limiting their specificity [515-517]. To overcome this caveat, a compound called C202-2729 has been discovered and is thought to have a more specific mode of action has shown by his potent anti-inflammatory properties in both endotoxin shock and EAE mouse models [488]. In summary, inhibiting GSDMD has emerged as a promising approach for treating both acute and chronic inflammatory diseases. However, evidence suggests the presence of redundant mechanisms, such as crosstalk between pyroptosis and apoptosis [518], aimed at safeguarding IL-1β release following intense inflammation. This phenomenon limiting the effectiveness of drugs targeting this specific pathway [519].

Neutralizing ASC specks that are released extracellularly during pyroptosis that contribute to the propagation of the inflammatory response, represents another approach to act on downstream effectors of the NLRP3 inflammasome. Two molecules have been developed to target this specific pathway namely IC-100 and VHH_{ASC}. IC-100 is a humanized antibody that targets human ASC, that demonstrated therapeutic potential in the EAE mouse model [520]. VHH_{ASC} is a single-chain antibody specifically targeting and neutralizing extracellular ASC specks. When administered systemically, VHH_{ASC} reduced inflammatory pathology in mouse models of gout and antigen-induced arthritis [521].

Lastly, a new strategy targeting NINJ1, a small plasma membrane protein responsible for the extracellular release of DAMPs that are too large to pass through GSDMD pores, has been developed [377]. Although the exact mechanism leading to NINJ1 conformational changes and polymerization is not yet elucidated, a NINJ1-neutralizing monoclonal antibody named ‘clone D1’ was recently tested. It showed a reduction cell lysis and liver injury in mouse models of acute hepatitis

[522]. To our knowledge, none of these medications have been tested on skeletal muscle related disorders yet.

Future of therapy

Traditional pharmaceutical development has long adhered to the concept where one drug targets one disease through one specific mechanism. However, with increasing recognition of chronic inflammation as a central player in numerous diseases, the potential of inflammasome inhibitors to serve as broad-spectrum treatment options is becoming apparent.

Arguably, the only other class of pharmaceuticals with comparable versatility is glucocorticoids. Introduced in the 1950s and initially hailed as "wonder drugs," glucocorticoids remain widely used across various medical fields to manage acute and chronic inflammation. However, unlike glucocorticoids, which come with a range of potential side effects, many direct inflammasome inhibitors have shown promising safety profiles.

This suggests the potential for their use not only as standalone therapies but also in combination with glucocorticoids, non-steroidal anti-inflammatory drugs (NSAIDs), other inflammasome direct or indirect inhibitors. In an optimistic scenario, such combination therapies could collectively address a wide range of medical conditions.

Part V: References

1. David Shier, J.B., Ricki Lewis, *Hole's essentials of Human Anatomy & Physiology 13th edition*. 2017.
2. Rassier, D.E., *Sarcomere mechanics in striated muscles: from molecules to sarcomeres to cells.* Am J Physiol Cell Physiol, 2017. **313**(2): p. C134-c145.
3. Chargé, S.B. and M.A. Rudnicki, *Cellular and molecular regulation of muscle regeneration.* Physiol Rev, 2004. **84**(1): p. 209-38.
4. Dave, H.D., M. Shook, and M. Varacallo, *Anatomy, Skeletal Muscle*, in *StatPearls*. 2024, StatPearls Publishing
5. Javan, R., et al., *Generating color-coded anatomic muscle maps for correlation of quantitative magnetic resonance imaging analysis with clinical examination in neuromuscular disorders.* Muscle Nerve, 2013. **48**(2): p. 293-5.
6. Periasamy, M., J.L. Herrera, and F.C.G. Reis, *Skeletal Muscle Thermogenesis and Its Role in Whole Body Energy Metabolism.* Diabetes Metab J, 2017. **41**(5): p. 327-336.
7. Frontera, W.R. and J. Ochala, *Skeletal muscle: a brief review of structure and function.* Calcif Tissue Int, 2015. **96**(3): p. 183-95.
8. Giudice, J. and J.M. Taylor, *Muscle as a paracrine and endocrine organ.* Curr Opin Pharmacol, 2017. **34**: p. 49-55.
9. Pedersen, B.K. and M.A. Febbraio, *Muscles, exercise and obesity: skeletal muscle as a secretory organ.* Nat Rev Endocrinol, 2012. **8**(8): p. 457-65.
10. Nagy, H. and K.D. Veerapaneni, *Myopathy*, in *StatPearls*. 2024, StatPearls Publishing
11. Kanno, S. and J.E. Saffitz, *The role of myocardial gap junctions in electrical conduction and arrhythmogenesis.* Cardiovasc Pathol, 2001. **10**(4): p. 169-77.
12. Stöhr, E.J., et al., *Left ventricular twist mechanics in the context of normal physiology and cardiovascular disease: a review of studies using speckle tracking echocardiography.* Am J Physiol Heart Circ Physiol, 2016. **311**(3): p. H633-44.
13. Ogawa, T. and A.J. de Bold, *The heart as an endocrine organ.* Endocr Connect, 2014. **3**(2): p. R31-44.
14. Saxton, A., M.A. Tariq, and B. Bordoni, *Anatomy, Thorax, Cardiac Muscle*, in *StatPearls*. 2024, StatPearls Publishing
15. Nag, A.C., *Study of non-muscle cells of the adult mammalian heart: a fine structural analysis and distribution.* Cytobios, 1980. **28**(109): p. 41-61.

16. Schultz, T.I., F.J. Raucci, Jr., and F.N. Salloum, *Cardiovascular Disease in Duchenne Muscular Dystrophy: Overview and Insight Into Novel Therapeutic Targets.* JACC Basic Transl Sci, 2022. **7**(6): p. 608-625.
17. Tucker, N.R., et al., *Transcriptional and Cellular Diversity of the Human Heart.* Circulation, 2020. **142**(5): p. 466-482.
18. Purslow, P.P., *The Structure and Role of Intramuscular Connective Tissue in Muscle Function.* Front Physiol, 2020. **11**: p. 495.
19. Baena-Montes, J.M., et al., *In Vitro Models for Improved Therapeutic Interventions in Atrial Fibrillation.* J Pers Med, 2023. **13**(8).
20. Ng, S.Y., C.K. Wong, and S.Y. Tsang, *Differential gene expressions in atrial and ventricular myocytes: insights into the road of applying embryonic stem cell-derived cardiomyocytes for future therapies.* Am J Physiol Cell Physiol, 2010. **299**(6): p. C1234-49.
21. Ahmetov, II, O.L. Vinogradova, and A.G. Williams, *Gene polymorphisms and fiber-type composition of human skeletal muscle.* Int J Sport Nutr Exerc Metab, 2012. **22**(4): p. 292-303.
22. Chal, J. and O. Pourquié, *Making muscle: skeletal myogenesis in vivo and in vitro.* Development, 2017. **144**(12): p. 2104-2122.
23. Augusto V, P.C., Campos GER. , *Skeletal Muscle Fiber Types in C57BL6J Mice.* Braz J Morphol Sci, 2004. **21**: p. 89–94.
24. Andersen, J.L., *Muscle fibre type adaptation in the elderly human muscle.* Scand J Med Sci Sports, 2003. **13**(1): p. 40-7.
25. Aoyagi, T. and T. Matsui, *The Cardiomyocyte as a Source of Cytokines in Cardiac Injury.* J Cell Sci Ther, 2011. **2012**(S5).
26. Schnyder, S. and C. Handschin, *Skeletal muscle as an endocrine organ: PGC-1α, myokines and exercise.* Bone, 2015. **80**: p. 115-125.
27. Berezin, A.E., A.A. Berezin, and M. Lichtenauer, *Myokines and Heart Failure: Challenging Role in Adverse Cardiac Remodeling, Myopathy, and Clinical Outcomes.* Dis Markers, 2021. **2021**: p. 6644631.
28. Lecompte, S., et al., *Skeletal muscle secretome in Duchenne muscular dystrophy: a pivotal anti-inflammatory role of adiponectin.* Cell Mol Life Sci, 2017. **74**(13): p. 2487-2501.
29. Jortay, J., et al., *Local induction of adiponectin reduces lipopolysaccharide-triggered skeletal muscle damage.* Endocrinology, 2010. **151**(10): p. 4840-51.
30. Dufresne, S.S., J. Frenette, and N.A. Dumont, *[Inflammation and muscle regeneration, a double-edged sword].* Med Sci (Paris), 2016. **32**(6-7): p. 591-7.
31. Fiordelisi, A., et al., *NFkappaB is a Key Player in the Crosstalk between Inflammation and Cardiovascular Diseases.* Int J Mol Sci, 2019. **20**(7).

32. Leeman, J.R. and T.D. Gilmore, *Alternative splicing in the NF-kappaB signaling pathway.* Gene, 2008. **423**(2): p. 97-107.
33. Epelman, S., P.P. Liu, and D.L. Mann, *Role of innate and adaptive immune mechanisms in cardiac injury and repair.* Nat Rev Immunol, 2015. **15**(2): p. 117-29.
34. Brigitte, M., et al., *Muscle resident macrophages control the immune cell reaction in a mouse model of notexin-induced myoinjury.* Arthritis Rheum, 2010. **62**(1): p. 268-79.
35. Rubartelli, A. and M.T. Lotze, *Inside, outside, upside down: damage-associated molecular-pattern molecules (DAMPs) and redox.* Trends Immunol, 2007. **28**(10): p. 429-36.
36. Collins, R.A. and M.D. Grounds, *The role of tumor necrosis factor-alpha (TNF-alpha) in skeletal muscle regeneration. Studies in TNF-alpha(-/-) and TNF-alpha(-/-)/LT-alpha(-/-) mice.* J Histochem Cytochem, 2001. **49**(8): p. 989-1001.
37. Scapini, P., et al., *The neutrophil as a cellular source of chemokines.* Immunol Rev, 2000. **177**: p. 195-203.
38. Arnold, L., et al., *Inflammatory monocytes recruited after skeletal muscle injury switch into antiinflammatory macrophages to support myogenesis.* J Exp Med, 2007. **204**(5): p. 1057-69.
39. Nahrendorf, M., et al., *The healing myocardium sequentially mobilizes two monocyte subsets with divergent and complementary functions.* J Exp Med, 2007. **204**(12): p. 3037-47.
40. Dumont, N. and J. Frenette, *Macrophages protect against muscle atrophy and promote muscle recovery in vivo and in vitro: a mechanism partly dependent on the insulin-like growth factor-1 signaling molecule.* Am J Pathol, 2010. **176**(5): p. 2228-35.
41. Gao, Y., et al., *The Roles of Macrophages in Heart Regeneration and Repair After Injury.* Front Cardiovasc Med, 2021. **8**: p. 744615.
42. Lafuse, W.P., D.J. Wozniak, and M.V.S. Rajaram, *Role of Cardiac Macrophages on Cardiac Inflammation, Fibrosis and Tissue Repair.* Cells, 2020. **10**(1).
43. De Paepe, B. and J.L. De Bleecker, *Cytokines and chemokines as regulators of skeletal muscle inflammation: presenting the case of Duchenne muscular dystrophy.* Mediators Inflamm, 2013. **2013**: p. 540370.
44. Idriss, H.T. and J.H. Naismith, *TNF alpha and the TNF receptor superfamily: structure-function relationship(s).* Microsc Res Tech, 2000. **50**(3): p. 184-95.
45. Comstock, K.L., et al., *LPS-induced TNF-alpha release from and apoptosis in rat cardiomyocytes: obligatory role for CD14 in mediating the LPS response.* J Mol Cell Cardiol, 1998. **30**(12): p. 2761-75.

46. Hoesel, B. and J.A. Schmid, *The complexity of NF-κB signaling in inflammation and cancer.* Mol Cancer, 2013. **12**: p. 86.
47. Guttridge, D.C., et al., *NF-kappaB-induced loss of MyoD messenger RNA: possible role in muscle decay and cachexia.* Science, 2000. **289**(5488): p. 2363-6.
48. Reid, M.B. and Y.P. Li, *Tumor necrosis factor-alpha and muscle wasting: a cellular perspective.* Respir Res, 2001. **2**(5): p. 269-72.
49. Steinberg, G.R., et al., *Tumor necrosis factor alpha-induced skeletal muscle insulin resistance involves suppression of AMP-kinase signaling.* Cell Metab, 2006. **4**(6): p. 465-74.
50. Dinarello, C.A., *Biologic basis for interleukin-1 in disease.* Blood, 1996. **87**(6): p. 2095-147.
51. Kawaguchi, M., et al., *Inflammasome activation of cardiac fibroblasts is essential for myocardial ischemia/reperfusion injury.* Circulation, 2011. **123**(6): p. 594-604.
52. Dinarello, C.A. and J.W. van der Meer, *Treating inflammation by blocking interleukin-1 in humans.* Semin Immunol, 2013. **25**(6): p. 469-84.
53. Benny Klimek, M.E., et al., *Effect of the IL-1 Receptor Antagonist Kineret® on Disease Phenotype in mdx Mice.* PLoS One, 2016. **11**(5): p. e0155944.
54. Gabay, C., C. Lamacchia, and G. Palmer, *IL-1 pathways in inflammation and human diseases.* Nat Rev Rheumatol, 2010. **6**(4): p. 232-41.
55. Li, H., S. Malhotra, and A. Kumar, *Nuclear factor-kappa B signaling in skeletal muscle atrophy.* J Mol Med (Berl), 2008. **86**(10): p. 1113-26.
56. Karin, M. and Y. Ben-Neriah, *Phosphorylation meets ubiquitination: the control of NF-[kappa]B activity.* Annu Rev Immunol, 2000. **18**: p. 621-63.
57. Hayden, M.S. and S. Ghosh, *NF-κB, the first quarter-century: remarkable progress and outstanding questions.* Genes Dev, 2012. **26**(3): p. 203-34.
58. Ghosh, S., M.J. May, and E.B. Kopp, *NF-kappa B and Rel proteins: evolutionarily conserved mediators of immune responses.* Annu Rev Immunol, 1998. **16**: p. 225-60.
59. Baldwin, A.S., Jr., *Series introduction: the transcription factor NF-kappaB and human disease.* J Clin Invest, 2001. **107**(1): p. 3-6.
60. Acharyya, S., et al., *Interplay of IKK/NF-kappaB signaling in macrophages and myofibers promotes muscle degeneration in Duchenne muscular dystrophy.* J Clin Invest, 2007. **117**(4): p. 889-901.
61. Cai, D., et al., *IKKbeta/NF-kappaB activation causes severe muscle wasting in mice.* Cell, 2004. **119**(2): p. 285-98.
62. Hunter, R.B. and S.C. Kandarian, *Disruption of either the Nfkb1 or the Bcl3 gene inhibits skeletal muscle atrophy.* J Clin Invest, 2004. **114**(10): p. 1504-11.

63. Langen, R.C., et al., *Tumor necrosis factor-alpha inhibits myogenic differentiation through MyoD protein destabilization.* Faseb j, 2004. **18**(2): p. 227-37.
64. Peterson, J.M., et al., *NF-κB inhibition rescues cardiac function by remodeling calcium genes in a Duchenne muscular dystrophy model.* Nat Commun, 2018. **9**(1): p. 3431.
65. Lei, X., et al., *Adiponectin and metabolic cardiovascular diseases: Therapeutic opportunities and challenges.* Genes Dis, 2023. **10**(4): p. 1525-1536.
66. Kadowaki, T., et al., *Adiponectin and adiponectin receptors in insulin resistance, diabetes, and the metabolic syndrome.* J Clin Invest, 2006. **116**(7): p. 1784-92.
67. Mercola, M., P. Ruiz-Lozano, and M.D. Schneider, *Cardiac muscle regeneration: lessons from development.* Genes Dev, 2011. **25**(4): p. 299-309.
68. Ceafalan, L.C., B.O. Popescu, and M.E. Hinescu, *Cellular players in skeletal muscle regeneration.* Biomed Res Int, 2014. **2014**: p. 957014.
69. Baghdadi, M.B. and S. Tajbakhsh, *Regulation and phylogeny of skeletal muscle regeneration.* Dev Biol, 2018. **433**(2): p. 200-209.
70. Tidball, J.G. and S.A. Villalta, *Regulatory interactions between muscle and the immune system during muscle regeneration.* Am J Physiol Regul Integr Comp Physiol, 2010. **298**(5): p. R1173-87.
71. Fiaschi, T., et al., *Globular adiponectin activates motility and regenerative traits of muscle satellite cells.* PLoS One, 2012. **7**(5): p. e34782.
72. Mauro, A., *Satellite cell of skeletal muscle fibers.* J Biophys Biochem Cytol, 1961. **9**(2): p. 493-5.
73. Rumman, M., J. Dhawan, and M. Kassem, *Concise Review: Quiescence in Adult Stem Cells: Biological Significance and Relevance to Tissue Regeneration.* Stem Cells, 2015. **33**(10): p. 2903-12.
74. Hernández-Hernández, J.M., et al., *The myogenic regulatory factors, determinants of muscle development, cell identity and regeneration.* Semin Cell Dev Biol, 2017. **72**: p. 10-18.
75. Zammit, P.S., *Function of the myogenic regulatory factors Myf5, MyoD, Myogenin and MRF4 in skeletal muscle, satellite cells and regenerative myogenesis.* Semin Cell Dev Biol, 2017. **72**: p. 19-32.
76. Lu, H., et al., *Acute skeletal muscle injury: CCL2 expression by both monocytes and injured muscle is required for repair.* Faseb j, 2011. **25**(10): p. 3344-55.
77. Schiaffino, S. and C. Mammucari, *Regulation of skeletal muscle growth by the IGF1-Akt/PKB pathway: insights from genetic models.* Skelet Muscle, 2011. **1**(1): p. 4.

78. Wagner, M.J., M. Khan, and S. Mohsin, *Healing the Broken Heart; The Immunomodulatory Effects of Stem Cell Therapy.* Front Immunol, 2020. **11**: p. 639.
79. Travers, J.G., et al., *Cardiac Fibrosis: The Fibroblast Awakens.* Circ Res, 2016. **118**(6): p. 1021-40.
80. Chaturvedi, R.R., et al., *Passive stiffness of myocardium from congenital heart disease and implications for diastole.* Circulation, 2010. **121**(8): p. 979-88.
81. Espira, L. and M.P. Czubryt, *Emerging concepts in cardiac matrix biology.* Can J Physiol Pharmacol, 2009. **87**(12): p. 996-1008.
82. Wang, J., et al., *Cardiac regeneration: Options for repairing the injured heart.* Front Cardiovasc Med, 2022. **9**: p. 981982.
83. Spach, M.S. and J.P. Boineau, *Microfibrosis produces electrical load variations due to loss of side-to-side cell connections: a major mechanism of structural heart disease arrhythmias.* Pacing Clin Electrophysiol, 1997. **20**(2 Pt 2): p. 397-413.
84. Lhermitte, J., *[Duchenne de Boulogne in his time].* Prog Med (Paris), 1946. **74**(24): p. 596-602.
85. Ryder, S., et al., *The burden, epidemiology, costs and treatment for Duchenne muscular dystrophy: an evidence review.* Orphanet Journal of Rare Diseases, 2017. **12**(1): p. 79.
86. Crisafulli, S., et al., *Global epidemiology of Duchenne muscular dystrophy: an updated systematic review and meta-analysis.* Orphanet J Rare Dis, 2020. **15**(1): p. 141.
87. Cai, A. and X. Kong, *Development of CRISPR-Mediated Systems in the Study of Duchenne Muscular Dystrophy.* Hum Gene Ther Methods, 2019. **30**(3): p. 71-80.
88. Giliberto, F., et al., *Symptomatic female carriers of Duchenne muscular dystrophy (DMD): genetic and clinical characterization.* J Neurol Sci, 2014. **336**(1-2): p. 36-41.
89. Aartsma-Rus, A., et al., *Entries in the Leiden Duchenne muscular dystrophy mutation database: an overview of mutation types and paradoxical cases that confirm the reading-frame rule.* Muscle Nerve, 2006. **34**(2): p. 135-44.
90. Garcia, S., et al., *Identification of de novo mutations of Duchénnè/Becker muscular dystrophies in southern Spain.* Int J Med Sci, 2014. **11**(10): p. 988-93.
91. Monaco, A.P., et al., *An explanation for the phenotypic differences between patients bearing partial deletions of the DMD locus.* Genomics, 1988. **2**(1): p. 90-5.
92. Mercuri, E., C.G. Bönnemann, and F. Muntoni, *Muscular dystrophies.* Lancet, 2019. **394**(10213): p. 2025-2038.

93. Zhao, J., et al., *Dystrophin contains multiple independent membrane-binding domains.* Hum Mol Genet, 2016. **25**(17): p. 3647-3653.
94. Gao, Q.Q. and E.M. McNally, *The Dystrophin Complex: Structure, Function, and Implications for Therapy.* Compr Physiol, 2015. **5**(3): p. 1223-39.
95. Ervasti, J.M. and K.J. Sonnemann, *Biology of the striated muscle dystrophin-glycoprotein complex.* Int Rev Cytol, 2008. **265**: p. 191-225.
96. Wilson, D.G.S., A. Tinker, and T. Iskratsch, *The role of the dystrophin glycoprotein complex in muscle cell mechanotransduction.* Commun Biol, 2022. **5**(1): p. 1022.
97. Blake, D.J., et al., *Function and genetics of dystrophin and dystrophin-related proteins in muscle.* Physiol Rev, 2002. **82**(2): p. 291-329.
98. Mokri, B. and A.G. Engel, *Duchenne dystrophy: electron microscopic findings pointing to a basic or early abnormality in the plasma membrane of the muscle fiber.* Neurology, 1975. **25**(12): p. 1111-20.
99. Allen, D.G., N.P. Whitehead, and S.C. Froehner, *Absence of Dystrophin Disrupts Skeletal Muscle Signaling: Roles of Ca2+, Reactive Oxygen Species, and Nitric Oxide in the Development of Muscular Dystrophy.* Physiol Rev, 2016. **96**(1): p. 253-305.
100. Sander, M., et al., *Functional muscle ischemia in neuronal nitric oxide synthase-deficient skeletal muscle of children with Duchenne muscular dystrophy.* Proc Natl Acad Sci U S A, 2000. **97**(25): p. 13818-23.
101. Kim, J.H., et al., *Contribution of oxidative stress to pathology in diaphragm and limb muscles with Duchenne muscular dystrophy.* J Muscle Res Cell Motil, 2013. **34**(1): p. 1-13.
102. Bello, L. and E. Pegoraro, *The "Usual Suspects": Genes for Inflammation, Fibrosis, Regeneration, and Muscle Strength Modify Duchenne Muscular Dystrophy.* J Clin Med, 2019. **8**(5).
103. Jones, D., *Duchenne muscular dystrophy awaits gene therapy.* Nat Biotechnol, 2019. **37**: p. 335–337.
104. Birnkrant, D.J., et al., *Diagnosis and management of Duchenne muscular dystrophy, part 1: diagnosis, and neuromuscular, rehabilitation, endocrine, and gastrointestinal and nutritional management.* Lancet Neurol, 2018. **17**(3): p. 251-267.
105. Skalsky, A.J. and C.M. McDonald, *Prevention and management of limb contractures in neuromuscular diseases.* Phys Med Rehabil Clin N Am, 2012. **23**(3): p. 675-87.
106. Lo Cascio, C.M., et al., *Gastrointestinal Dysfunction in Patients with Duchenne Muscular Dystrophy.* PLoS One, 2016. **11**(10): p. e0163779.
107. Thangarajh, M., et al., *Relationships between DMD mutations and neurodevelopment in dystrophinopathy.* Neurology, 2019. **93**(17): p. e1597-e1604.

108. Ramani, P.K., et al., *Epilepsy Characteristics in Duchenne and Becker Muscular Dystrophies.* Child Neurol Open, 2023. **10**: p. 2329048x231159484.
109. Snow, W.M., J.E. Anderson, and L.S. Jakobson, *Neuropsychological and neurobehavioral functioning in Duchenne muscular dystrophy: a review.* Neurosci Biobehav Rev, 2013. **37**(5): p. 743-52.
110. Kieny, P., et al., *Evolution of life expectancy of patients with Duchenne muscular dystrophy at AFM Yolaine de Kepper centre between 1981 and 2011.* Ann Phys Rehabil Med, 2013. **56**(6): p. 443-54.
111. Aartsma-Rus, A., et al., *Evidence-Based Consensus and Systematic Review on Reducing the Time to Diagnosis of Duchenne Muscular Dystrophy.* J Pediatr, 2019. **204**: p. 305-313.e14.
112. Zatz, M., et al., *Serum creatine-kinase (CK) and pyruvate-kinase (PK) activities in Duchenne (DMD) as compared with Becker (BMD) muscular dystrophy.* J Neurol Sci, 1991. **102**(2): p. 190-6.
113. Sansović, I., I. Barišić, and K. Dumić, *Improved detection of deletions and duplications in the DMD gene using the multiplex ligation-dependent probe amplification (MLPA) method.* Biochem Genet, 2013. **51**(3-4): p. 189-201.
114. Hegde, M.R., et al., *Microarray-based mutation detection in the dystrophin gene.* Hum Mutat, 2008. **29**(9): p. 1091-9.
115. Wang, Y., et al., *Whole dystrophin gene analysis by next-generation sequencing: a comprehensive genetic diagnosis of Duchenne and Becker muscular dystrophy.* Mol Genet Genomics, 2014. **289**(5): p. 1013-21.
116. Helderman-van den Enden, A.T., et al., *Recurrence risk due to germ line mosaicism: Duchenne and Becker muscular dystrophy.* Clin Genet, 2009. **75**(5): p. 465-72.
117. Grimm, T., et al., *Risk assessment and genetic counseling in families with Duchenne muscular dystrophy.* Acta Myol, 2012. **31**(3): p. 179-83.
118. Aartsma-Rus, A., I.B. Ginjaar, and K. Bushby, *The importance of genetic diagnosis for Duchenne muscular dystrophy.* J Med Genet, 2016. **53**(3): p. 145-51.
119. Duan, D., et al., *Duchenne muscular dystrophy.* Nature Reviews Disease Primers, 2021. **7**(1): p. 13.
120. Houang, E.M., et al., *Muscle membrane integrity in Duchenne muscular dystrophy: recent advances in copolymer-based muscle membrane stabilizers.* Skelet Muscle, 2018. **8**(1): p. 31.
121. Mareedu, S., et al., *Abnormal Calcium Handling in Duchenne Muscular Dystrophy: Mechanisms and Potential Therapies.* Front Physiol, 2021. **12**: p. 647010.

122. Rybalka, E., et al., *Metabogenic and Nutriceutical Approaches to Address Energy Dysregulation and Skeletal Muscle Wasting in Duchenne Muscular Dystrophy.* Nutrients, 2015. **7**(12): p. 9734-67.
123. Timpani, C.A., A. Hayes, and E. Rybalka, *Revisiting the dystrophin-ATP connection: How half a century of research still implicates mitochondrial dysfunction in Duchenne Muscular Dystrophy aetiology.* Med Hypotheses, 2015. **85**(6): p. 1021-33.
124. Pant, M., et al., *Metabolic dysfunction and altered mitochondrial dynamics in the utrophin-dystrophin deficient mouse model of duchenne muscular dystrophy.* PLoS One, 2015. **10**(4): p. e0123875.
125. Petrof, B.J., *Molecular pathophysiology of myofiber injury in deficiencies of the dystrophin-glycoprotein complex.* Am J Phys Med Rehabil, 2002. **81**(11 Suppl): p. S162-74.
126. Hughes, M.C., et al., *Early myopathy in Duchenne muscular dystrophy is associated with elevated mitochondrial H(2) O(2) emission during impaired oxidative phosphorylation.* J Cachexia Sarcopenia Muscle, 2019. **10**(3): p. 643-661.
127. Terrill, J.R., et al., *Oxidative stress and pathology in muscular dystrophies: focus on protein thiol oxidation and dysferlinopathies.* Febs j, 2013. **280**(17): p. 4149-64.
128. Powers, S.K., et al., *Reactive oxygen species: impact on skeletal muscle.* Compr Physiol, 2011. **1**(2): p. 941-69.
129. Henriques-Pons, A., et al., *Role of Toll-like receptors in the pathogenesis of dystrophin-deficient skeletal and heart muscle.* Hum Mol Genet, 2014. **23**(10): p. 2604-17.
130. Dubuisson, N., et al., *Inhibiting the inflammasome with MCC950 counteracts muscle pyroptosis and improves Duchenne muscular dystrophy.* Front Immunol, 2022. **13**: p. 1049076.
131. Shi, J., W. Gao, and F. Shao, *Pyroptosis: Gasdermin-Mediated Programmed Necrotic Cell Death.* Trends Biochem Sci, 2017. **42**(4): p. 245-254.
132. Dubuisson, N., et al., *Walking down Skeletal Muscle Lane: From Inflammasome to Disease.* Cells, 2021. **10**(11).
133. Porter, J.D., et al., *A chronic inflammatory response dominates the skeletal muscle molecular signature in dystrophin-deficient mdx mice.* Human Molecular Genetics, 2002. **11**(3): p. 263-272.
134. Kumar, A. and A.M. Boriek, *Mechanical stress activates the nuclear factor-kappaB pathway in skeletal muscle fibers: a possible role in Duchenne muscular dystrophy.* Faseb j, 2003. **17**(3): p. 386-96.
135. Biferali, B., et al., *Fibro-Adipogenic Progenitors Cross-Talk in Skeletal Muscle: The Social Network.* Front Physiol, 2019. **10**: p. 1074.

136. Tidball, J.G., *Regulation of muscle growth and regeneration by the immune system.* Nat Rev Immunol, 2017. **17**(3): p. 165-178.
137. Meng, X.M., D.J. Nikolic-Paterson, and H.Y. Lan, *TGF-β: the master regulator of fibrosis.* Nat Rev Nephrol, 2016. **12**(6): p. 325-38.
138. Lieber, R.L. and S.R. Ward, *Cellular mechanisms of tissue fibrosis. 4. Structural and functional consequences of skeletal muscle fibrosis.* Am J Physiol Cell Physiol, 2013. **305**(3): p. C241-52.
139. Kharraz, Y., et al., *Understanding the process of fibrosis in Duchenne muscular dystrophy.* Biomed Res Int, 2014. **2014**: p. 965631.
140. Li, Z.B., H.D. Kollias, and K.R. Wagner, *Myostatin directly regulates skeletal muscle fibrosis.* J Biol Chem, 2008. **283**(28): p. 19371-8.
141. Bedair, H.S., et al., *Angiotensin II receptor blockade administered after injury improves muscle regeneration and decreases fibrosis in normal skeletal muscle.* Am J Sports Med, 2008. **36**(8): p. 1548-54.
142. Cisternas, P., C.P. Vio, and N.C. Inestrosa, *Role of Wnt signaling in tissue fibrosis, lessons from skeletal muscle and kidney.* Curr Mol Med, 2014. **14**(4): p. 510-22.
143. Li, J., et al., *Collagen triple helix repeat containing-1 inhibits transforming growth factor-b1-induced collagen type I expression in keloid.* Br J Dermatol, 2011. **164**(5): p. 1030-6.
144. Ehrchen, J.M., J. Roth, and K. Barczyk-Kahlert, *More Than Suppression: Glucocorticoid Action on Monocytes and Macrophages.* Front Immunol, 2019. **10**: p. 2028.
145. Ehrchen, J., et al., *Glucocorticoids induce differentiation of a specifically activated, anti-inflammatory subtype of human monocytes.* Blood, 2007. **109**(3): p. 1265-74.
146. Cain, D.W. and J.A. Cidlowski, *Immune regulation by glucocorticoids.* Nat Rev Immunol, 2017. **17**(4): p. 233-247.
147. Panettieri, R.A., et al., *Non-genomic Effects of Glucocorticoids: An Updated View.* Trends Pharmacol Sci, 2019. **40**(1): p. 38-49.
148. Guglieri, M., et al., *Effect of Different Corticosteroid Dosing Regimens on Clinical Outcomes in Boys With Duchenne Muscular Dystrophy: A Randomized Clinical Trial.* Jama, 2022. **327**(15): p. 1456-1468.
149. Matthews, E., et al., *Corticosteroids for the treatment of Duchenne muscular dystrophy.* Cochrane Database Syst Rev, 2016. **2016**(5): p. Cd003725.
150. McDonald, C.M., et al., *Long-term effects of glucocorticoids on function, quality of life, and survival in patients with Duchenne muscular dystrophy: a prospective cohort study.* Lancet, 2018. **391**(10119): p. 451-461.

151. Biggar, W.D., et al., *Deflazacort in Duchenne muscular dystrophy: a comparison of two different protocols.* Neuromuscul Disord, 2004. **14**(8-9): p. 476-82.
152. Moxley, R.T., 3rd, et al., *Change in natural history of Duchenne muscular dystrophy with long-term corticosteroid treatment: implications for management.* J Child Neurol, 2010. **25**(9): p. 1116-29.
153. Schakman, O., et al., *Glucocorticoid-induced skeletal muscle atrophy.* Int J Biochem Cell Biol, 2013. **45**(10): p. 2163-72.
154. Schäcke, H., W.D. Döcke, and K. Asadullah, *Mechanisms involved in the side effects of glucocorticoids.* Pharmacol Ther, 2002. **96**(1): p. 23-43.
155. Bushby, K., et al., *Diagnosis and management of Duchenne muscular dystrophy, part 1: diagnosis, and pharmacological and psychosocial management.* Lancet Neurol, 2010. **9**(1): p. 77-93.
156. Eagle, M., et al., *Managing Duchenne muscular dystrophy--the additive effect of spinal surgery and home nocturnal ventilation in improving survival.* Neuromuscul Disord, 2007. **17**(6): p. 470-5.
157. Chabrol, B. and M. Mayer, *[Principles of multidisciplinary management of Duchenne muscular dystrophy].* Arch Pediatr, 2015. **22**(12 Suppl 1): p. 12s69-72.
158. Apkon, S.D., et al., *Orthopedic and Surgical Management of the Patient With Duchenne Muscular Dystrophy.* Pediatrics, 2018. **142**(Suppl 2): p. S82-s89.
159. Buddhe, S., et al., *Cardiac Management of the Patient With Duchenne Muscular Dystrophy.* Pediatrics, 2018. **142**(Suppl 2): p. S72-s81.
160. Finder, J.D., et al., *Respiratory care of the patient with Duchenne muscular dystrophy: ATS consensus statement.* Am J Respir Crit Care Med, 2004. **170**(4): p. 456-65.
161. Haas, M., et al., *European Medicines Agency review of ataluren for the treatment of ambulant patients aged 5 years and older with Duchenne muscular dystrophy resulting from a nonsense mutation in the dystrophin gene.* Neuromuscul Disord, 2015. **25**(1): p. 5-13.
162. *(https://www.ema.europa.eu/en/news/ema-confirms-recommendation-non-renewal-authorisation-duchenne-muscular-dystrophy-medicine-translarna).* [cited 2024 02/05/24].
163. Niks, E.H. and A. Aartsma-Rus, *Exon skipping: a first in class strategy for Duchenne muscular dystrophy.* Expert Opin Biol Ther, 2017. **17**(2): p. 225-236.
164. Alfano, L.N., et al., *Long-term treatment with eteplirsen in nonambulatory patients with Duchenne muscular dystrophy.* Medicine (Baltimore), 2019. **98**(26): p. e15858.

165. Frank, D.E., et al., *Increased dystrophin production with golodirsen in patients with Duchenne muscular dystrophy.* Neurology, 2020. **94**(21): p. e2270-e2282.
166. Roshmi, R.R. and T. Yokota, *Viltolarsen for the treatment of Duchenne muscular dystrophy.* Drugs Today (Barc), 2019. **55**(10): p. 627-639.
167. McDonald, C.M., et al., *Repeated intravenous cardiosphere-derived cell therapy in late-stage Duchenne muscular dystrophy (HOPE-2): a multicentre, randomised, double-blind, placebo-controlled, phase 2 trial.* Lancet, 2022. **399**(10329): p. 1049-1058.
168. Heydemann, A., et al., *Dystrophin Expressing Chimeric (DEC) Cell Therapy for Duchenne Muscular Dystrophy: A First-in-Human Study with Minimum 6 Months Follow-up.* Stem Cell Rev Rep, 2023. **19**(5): p. 1340-1359.
169. Olson, E.N., *Toward the correction of muscular dystrophy by gene editing.* Proc Natl Acad Sci U S A, 2021. **118**(22).
170. Chen, G., et al., *CRISPR-Based Therapeutic Gene Editing for Duchenne Muscular Dystrophy: Advances, Challenges and Perspectives.* Cells, 2022. **11**(19).
171. Young, C.S., et al., *A Single CRISPR-Cas9 Deletion Strategy that Targets the Majority of DMD Patients Restores Dystrophin Function in hiPSC-Derived Muscle Cells.* Cell Stem Cell, 2016. **18**(4): p. 533-40.
172. Duchêne, B.L., et al., *CRISPR-Induced Deletion with SaCas9 Restores Dystrophin Expression in Dystrophic Models In Vitro and In Vivo.* Mol Ther, 2018. **26**(11): p. 2604-2616.
173. Pickar-Oliver, A., et al., *Full-length dystrophin restoration via targeted exon integration by AAV-CRISPR in a humanized mouse model of Duchenne muscular dystrophy.* Mol Ther, 2021. **29**(11): p. 3243-3257.
174. Aartsma-Rus, A. and M. van Putten, *The use of genetically humanized animal models for personalized medicine approaches.* Dis Model Mech, 2019. **13**(2).
175. Liu, X., et al., *Disruption of a key ligand-H-bond network drives dissociative properties in vamorolone for Duchenne muscular dystrophy treatment.* Proc Natl Acad Sci U S A, 2020. **117**(39): p. 24285-24293.
176. Guglieri, M., et al., *Efficacy and Safety of Vamorolone vs Placebo and Prednisone Among Boys With Duchenne Muscular Dystrophy: A Randomized Clinical Trial.* JAMA Neurol, 2022. **79**(10): p. 1005-1014.
177. Smith, E.C., et al., *Efficacy and safety of vamorolone in Duchenne muscular dystrophy: An 18-month interim analysis of a non-randomized open-label extension study.* PLoS Med, 2020. **17**(9): p. e1003222.
178. Houang, E.M., et al., *Membrane-stabilizing copolymers confer marked protection to dystrophic skeletal muscle in vivo.* Mol Ther Methods Clin Dev, 2015. **2**: p. 15042.

179. Yasuda, S., et al., *Dystrophic heart failure blocked by membrane sealant poloxamer.* Nature, 2005. **436**(7053): p. 1025-9.
180. Spurney, C.F., et al., *Membrane sealant Poloxamer P188 protects against isoproterenol induced cardiomyopathy in dystrophin deficient mice.* BMC Cardiovasc Disord, 2011. **11**: p. 20.
181. Love, D.R., et al., *An autosomal transcript in skeletal muscle with homology to dystrophin.* Nature, 1989. **339**(6219): p. 55-8.
182. Soblechero-Martín, P., et al., *Utrophin modulator drugs as potential therapies for Duchenne and Becker muscular dystrophies.* Neuropathol Appl Neurobiol, 2021. **47**(6): p. 711-723.
183. Ebihara, S., et al., *Differential effects of dystrophin and utrophin gene transfer in immunocompetent muscular dystrophy (mdx) mice.* Physiol Genomics, 2000. **3**(3): p. 133-44.
184. Hynes, R.O., *Integrins: versatility, modulation, and signaling in cell adhesion.* Cell, 1992. **69**(1): p. 11-25.
185. Hodges, B.L., et al., *Altered expression of the alpha7beta1 integrin in human and murine muscular dystrophies.* J Cell Sci, 1997. **110 (Pt 22)**: p. 2873-81.
186. Rooney, J.E., et al., *Severe muscular dystrophy in mice that lack dystrophin and alpha7 integrin.* J Cell Sci, 2006. **119**(Pt 11): p. 2185-95.
187. Gurpur, P.B., et al., *Valproic acid activates the PI3K/Akt/mTOR pathway in muscle and ameliorates pathology in a mouse model of Duchenne muscular dystrophy.* Am J Pathol, 2009. **174**(3): p. 999-1008.
188. McPherron, A.C., A.M. Lawler, and S.J. Lee, *Regulation of skeletal muscle mass in mice by a new TGF-beta superfamily member.* Nature, 1997. **387**(6628): p. 83-90.
189. Wagner, K.R., et al., *A phase I/IItrial of MYO-029 in adult subjects with muscular dystrophy.* Ann Neurol, 2008. **63**(5): p. 561-71.
190. Attie, K.M., et al., *A single ascending-dose study of muscle regulator ACE-031 in healthy volunteers.* Muscle Nerve, 2013. **47**(3): p. 416-23.
191. Lee, S.J., et al., *Challenges and Future Prospects of Targeting Myostatin/Activin A Signaling to Treat Diseases of Muscle Loss and Metabolic Dysfunction.* J Gerontol A Biol Sci Med Sci, 2023. **78**(Suppl 1): p. 32-37.
192. Mercuri, E., et al., *Safety and efficacy of givinostat in boys with Duchenne muscular dystrophy (EPIDYS): a multicentre, randomised, double-blind, placebo-controlled, phase 3 trial.* Lancet Neurol, 2024. **23**(4): p. 393-403.
193. Wasala, N.B., S.J. Chen, and D. Duan, *Duchenne muscular dystrophy animal models for high-throughput drug discovery and precision medicine.* Expert Opin Drug Discov, 2020. **15**(4): p. 443-456.

194. McGreevy, J.W., et al., *Animal models of Duchenne muscular dystrophy: from basic mechanisms to gene therapy.* Dis Model Mech, 2015. **8**(3): p. 195-213.
195. Sicinski, P., et al., *The molecular basis of muscular dystrophy in the mdx mouse: a point mutation.* Science, 1989. **244**(4912): p. 1578-80.
196. Muntoni, F., et al., *Muscular weakness in the mdx mouse.* J Neurol Sci, 1993. **120**(1): p. 71-7.
197. Quinlan, J.G., et al., *Evolution of the mdx mouse cardiomyopathy: physiological and morphological findings.* Neuromuscular Disorders, 2004. **14**(8): p. 491-496.
198. Massopust, R.T., et al., *Lifetime analysis of mdx skeletal muscle reveals a progressive pathology that leads to myofiber loss.* Sci Rep, 2020. **10**(1): p. 17248.
199. Tinsley, J.M., et al., *Primary structure of dystrophin-related protein.* Nature, 1992. **360**(6404): p. 591-3.
200. Chapman, V.M., et al., *Recovery of induced mutations for X chromosome-linked muscular dystrophy in mice.* Proc Natl Acad Sci U S A, 1989. **86**(4): p. 1292-6.
201. Ramos, J.N., et al., *Development of Novel Micro-dystrophins with Enhanced Functionality.* Mol Ther, 2019. **27**(3): p. 623-635.
202. van Putten, M., et al., *Natural disease history of the D2-mdx mouse model for Duchenne muscular dystrophy.* Faseb j, 2019. **33**(7): p. 8110-8124.
203. Deconinck, A.E., et al., *Utrophin-dystrophin-deficient mice as a model for Duchenne muscular dystrophy.* Cell, 1997. **90**(4): p. 717-27.
204. Yucel, N., et al., *Humanizing the mdx mouse model of DMD: the long and the short of it.* NPJ Regen Med, 2018. **3**: p. 4.
205. Vulin, A., et al., *The first exon duplication mouse model of Duchenne muscular dystrophy: A tool for therapeutic development.* Neuromuscul Disord, 2015. **25**(11): p. 827-34.
206. Kornegay, J.N., *The golden retriever model of Duchenne muscular dystrophy.* Skelet Muscle, 2017. **7**(1): p. 9.
207. Yu, X., et al., *Dystrophin-deficient large animal models: translational research and exon skipping.* Am J Transl Res, 2015. **7**(8): p. 1314-31.
208. Whitehead, J.P., et al., *Adiponectin--a key adipokine in the metabolic syndrome.* Diabetes Obes Metab, 2006. **8**(3): p. 264-80.
209. Hu, E., P. Liang, and B.M. Spiegelman, *AdipoQ is a novel adipose-specific gene dysregulated in obesity.* J Biol Chem, 1996. **271**(18): p. 10697-703.
210. Scherer, P.E., et al., *A novel serum protein similar to C1q, produced exclusively in adipocytes.* J Biol Chem, 1995. **270**(45): p. 26746-9.

211. Pajvani, U.B., et al., *Complex distribution, not absolute amount of adiponectin, correlates with thiazolidinedione-mediated improvement in insulin sensitivity.* J Biol Chem, 2004. **279**(13): p. 12152-62.
212. Fruebis, J., et al., *Proteolytic cleavage product of 30-kDa adipocyte complement-related protein increases fatty acid oxidation in muscle and causes weight loss in mice.* Proc Natl Acad Sci U S A, 2001. **98**(4): p. 2005-10.
213. Waki, H., et al., *Generation of globular fragment of adiponectin by leukocyte elastase secreted by monocytic cell line THP-1.* Endocrinology, 2005. **146**(2): p. 790-6.
214. Badman, M.K. and J.S. Flier, *The adipocyte as an active participant in energy balance and metabolism.* Gastroenterology, 2007. **132**(6): p. 2103-15.
215. Yamauchi, T., et al., *Targeted disruption of AdipoR1 and AdipoR2 causes abrogation of adiponectin binding and metabolic actions.* Nat Med, 2007. **13**(3): p. 332-9.
216. Yamauchi, T., et al., *Cloning of adiponectin receptors that mediate antidiabetic metabolic effects.* Nature, 2003. **423**(6941): p. 762-9.
217. Iwabu, M., et al., *Adiponectin and AdipoR1 regulate PGC-1alpha and mitochondria by Ca(2+) and AMPK/SIRT1.* Nature, 2010. **464**(7293): p. 1313-9.
218. Hug, C., et al., *T-cadherin is a receptor for hexameric and high-molecular-weight forms of Acrp30/adiponectin.* Proc Natl Acad Sci U S A, 2004. **101**(28): p. 10308-13.
219. Kita, S., et al., *Native adiponectin in serum binds to mammalian cells expressing T-cadherin, but not AdipoRs or calreticulin.* Elife, 2019. **8**.
220. Denzel, M.S., et al., *T-cadherin is critical for adiponectin-mediated cardioprotection in mice.* J Clin Invest, 2010. **120**(12): p. 4342-52.
221. Parker-Duffen, J.L., et al., *T-cadherin is essential for adiponectin-mediated revascularization.* J Biol Chem, 2013. **288**(34): p. 24886-97.
222. Tanaka, Y., et al., *Adiponectin promotes muscle regeneration through binding to T-cadherin.* Sci Rep, 2019. **9**(1): p. 16.
223. Wang, Z.V. and P.E. Scherer, *Adiponectin, the past two decades.* J Mol Cell Biol, 2016. **8**(2): p. 93-100.
224. Yamauchi, T., et al., *Adiponectin stimulates glucose utilization and fatty-acid oxidation by activating AMP-activated protein kinase.* Nat Med, 2002. **8**(11): p. 1288-95.
225. Combs, T.P. and E.B. Marliss, *Adiponectin signaling in the liver.* Rev Endocr Metab Disord, 2014. **15**(2): p. 137-47.

226. Wu, X., et al., *Involvement of AMP-activated protein kinase in glucose uptake stimulated by the globular domain of adiponectin in primary rat adipocytes.* Diabetes, 2003. **52**(6): p. 1355-63.
227. Ge, Q., et al., *Adipokines identified as new downstream targets for adiponectin: lessons from adiponectin-overexpressing or -deficient mice.* Am J Physiol Endocrinol Metab, 2011. **301**(2): p. E326-35.
228. Bauche, I.B., et al., *Overexpression of adiponectin targeted to adipose tissue in transgenic mice: impaired adipocyte differentiation.* Endocrinology, 2007. **148**(4): p. 1539-49.
229. Patané, G., et al., *Adiponectin increases glucose-induced insulin secretion through the activation of lipid oxidation.* Acta Diabetol, 2013. **50**(6): p. 851-7.
230. Wijesekara, N., et al., *Adiponectin-induced ERK and Akt phosphorylation protects against pancreatic beta cell apoptosis and increases insulin gene expression and secretion.* J Biol Chem, 2010. **285**(44): p. 33623-31.
231. Kubota, N., et al., *Adiponectin stimulates AMP-activated protein kinase in the hypothalamus and increases food intake.* Cell Metab, 2007. **6**(1): p. 55-68.
232. Quaresma, P.G., et al., *Pioglitazone treatment increases food intake and decreases energy expenditure partially via hypothalamic adiponectin/adipoR1/AMPK pathway.* Int J Obes (Lond), 2016. **40**(1): p. 138-46.
233. Chabry, J., et al., *Enriched environment decreases microglia and brain macrophages inflammatory phenotypes through adiponectin-dependent mechanisms: Relevance to depressive-like behavior.* Brain Behav Immun, 2015. **50**: p. 275-287.
234. Yau, S.Y., et al., *Physical exercise-induced hippocampal neurogenesis and antidepressant effects are mediated by the adipocyte hormone adiponectin.* Proc Natl Acad Sci U S A, 2014. **111**(44): p. 15810-5.
235. Zhang, D., X. Wang, and X.Y. Lu, *Adiponectin Exerts Neurotrophic Effects on Dendritic Arborization, Spinogenesis, and Neurogenesis of the Dentate Gyrus of Male Mice.* Endocrinology, 2016. **157**(7): p. 2853-69.
236. Kim, Y., et al., *The Adiponectin Receptor Agonist AdipoRon Ameliorates Diabetic Nephropathy in a Model of Type 2 Diabetes.* J Am Soc Nephrol, 2018. **29**(4): p. 1108-1127.
237. Dalamaga, M., K.N. Diakopoulos, and C.S. Mantzoros, *The role of adiponectin in cancer: a review of current evidence.* Endocr Rev, 2012. **33**(4): p. 547-94.
238. Abou-Samra, M., et al., *Adiponectin and Its Mimics on Skeletal Muscle: Insulin Sensitizers, Fat Burners, Exercise Mimickers, Muscling Pills … or Everything Together?* Int J Mol Sci, 2020. **21**(7).

239. Zhou, L., et al., *Adiponectin activates AMP-activated protein kinase in muscle cells via APPL1/LKB1-dependent and phospholipase C/Ca2+/Ca2+/calmodulin-dependent protein kinase kinase-dependent pathways.* J Biol Chem, 2009. **284**(33): p. 22426-22435.
240. Lin, J., C. Handschin, and B.M. Spiegelman, *Metabolic control through the PGC-1 family of transcription coactivators.* Cell Metab, 2005. **1**(6): p. 361-70.
241. Kang, C. and L. Li Ji, *Role of PGC-1α signaling in skeletal muscle health and disease.* Ann N Y Acad Sci, 2012. **1271**(1): p. 110-7.
242. Yoon, M.J., et al., *Adiponectin increases fatty acid oxidation in skeletal muscle cells by sequential activation of AMP-activated protein kinase, p38 mitogen-activated protein kinase, and peroxisome proliferator-activated receptor alpha.* Diabetes, 2006. **55**(9): p. 2562-70.
243. Marcinko, K. and G.R. Steinberg, *The role of AMPK in controlling metabolism and mitochondrial biogenesis during exercise.* Exp Physiol, 2014. **99**(12): p. 1581-5.
244. Yamauchi, T., et al., *The fat-derived hormone adiponectin reverses insulin resistance associated with both lipoatrophy and obesity.* Nat Med, 2001. **7**(8): p. 941-6.
245. Maeda, N., et al., *Diet-induced insulin resistance in mice lacking adiponectin/ACRP30.* Nat Med, 2002. **8**(7): p. 731-7.
246. Wang, C., et al., *Adiponectin sensitizes insulin signaling by reducing p70 S6 kinase-mediated serine phosphorylation of IRS-1.* J Biol Chem, 2007. **282**(11): p. 7991-6.
247. Civitarese, A.E., et al., *Role of adiponectin in human skeletal muscle bioenergetics.* Cell Metab, 2006. **4**(1): p. 75-87.
248. Houstis, N., E.D. Rosen, and E.S. Lander, *Reactive oxygen species have a causal role in multiple forms of insulin resistance.* Nature, 2006. **440**(7086): p. 944-8.
249. Tuncman, G., et al., *A genetic variant at the fatty acid-binding protein aP2 locus reduces the risk for hypertriglyceridemia, type 2 diabetes, and cardiovascular disease.* Proc Natl Acad Sci U S A, 2006. **103**(18): p. 6970-5.
250. Tomas, E., et al., *Enhanced muscle fat oxidation and glucose transport by ACRP30 globular domain: acetyl-CoA carboxylase inhibition and AMP-activated protein kinase activation.* Proc Natl Acad Sci U S A, 2002. **99**(25): p. 16309-13.
251. Jortay, J., et al., *Adiponectin and skeletal muscle: pathophysiological implications in metabolic stress.* Am J Pathol, 2012. **181**(1): p. 245-56.
252. Abou-Samra, M., Sophie Lecompte, Olivier Schakman, Laurence Noel, Marie C. Many, Philippe Gailly, and Sonia M. Brichard, *Involvement of*

Adiponectin in the Pathogenesis of Dystrophinopathy. Skeletal Muscle, 2015. **5**: p. 25.
253. Ohashi, K., et al., *Adiponectin promotes macrophage polarization toward an anti-inflammatory phenotype.* J Biol Chem, 2010. **285**(9): p. 6153-60.
254. Salminen, A., J.M. Hyttinen, and K. Kaarniranta, *AMP-activated protein kinase inhibits NF-κB signaling and inflammation: impact on healthspan and lifespan.* J Mol Med (Berl), 2011. **89**(7): p. 667-76.
255. Yang, X.D., E. Tajkhorshid, and L.F. Chen, *Functional interplay between acetylation and methylation of the RelA subunit of NF-kappaB.* Mol Cell Biol, 2010. **30**(9): p. 2170-80.
256. Eisele, P.S., et al., *The peroxisome proliferator-activated receptor γ coactivator 1α/β (PGC-1) coactivators repress the transcriptional activity of NF-κB in skeletal muscle cells.* J Biol Chem, 2013. **288**(4): p. 2246-60.
257. Boursereau, R., et al., *New targets to alleviate skeletal muscle inflammation: role of microRNAs regulated by adiponectin.* Sci Rep, 2017. **7**: p. 43437.
258. Boursereau, R., et al., *Downregulation of the NLRP3 inflammasome by adiponectin rescues Duchenne muscular dystrophy.* BMC Biol, 2018. **16**(1): p. 33.
259. Fiaschi, T., et al., *Adiponectin as a tissue regenerating hormone: more than a metabolic function.* Cell Mol Life Sci, 2014. **71**(10): p. 1917-25.
260. Fiaschi, T., et al., *Globular adiponectin induces differentiation and fusion of skeletal muscle cells.* Cell Res, 2009. **19**(5): p. 584-97.
261. Riuzzi, F., et al., *Cellular and molecular mechanisms of sarcopenia: the S100B perspective.* J Cachexia Sarcopenia Muscle, 2018. **9**(7): p. 1255-1268.
262. Gamberi, T., et al., *Activation of autophagy by globular adiponectin is required for muscle differentiation.* Biochim Biophys Acta, 2016. **1863**(4): p. 694-702.
263. Minasi, M.G., et al., *The meso-angioblast: a multipotent, self-renewing cell that originates from the dorsal aorta and differentiates into most mesodermal tissues.* Development, 2002. **129**(11): p. 2773-83.
264. Fiaschi, T., et al., *Globular adiponectin as a complete mesoangioblast regulator: role in proliferation, survival, motility, and skeletal muscle differentiation.* Mol Biol Cell, 2010. **21**(6): p. 848-59.
265. Eming, S.A., T.A. Wynn, and P. Martin, *Inflammation and metabolism in tissue repair and regeneration.* Science, 2017. **356**(6342): p. 1026-1030.
266. Hopkins, T.A., et al., *Adiponectin actions in the cardiovascular system.* Cardiovasc Res, 2007. **74**(1): p. 11-8.
267. Nakamura, K., J.J. Fuster, and K. Walsh, *Adipokines: a link between obesity and cardiovascular disease.* J Cardiol, 2014. **63**(4): p. 250-9.

268. Konishi, M., et al., *Adiponectin protects against doxorubicin-induced cardiomyopathy by anti-apoptotic effects through AMPK up-regulation.* Cardiovasc Res, 2011. **89**(2): p. 309-19.
269. Holland, W.L., et al., *Receptor-mediated activation of ceramidase activity initiates the pleiotropic actions of adiponectin.* Nat Med, 2011. **17**(1): p. 55-63.
270. Tanaka, K., et al., *Effects of adiponectin on calcium-handling proteins in heart failure with preserved ejection fraction.* Circ Heart Fail, 2014. **7**(6): p. 976-85.
271. McManus, D.D., et al., *Relations of circulating resistin and adiponectin and cardiac structure and function: the Framingham Offspring Study.* Obesity (Silver Spring), 2012. **20**(9): p. 1882-6.
272. Xiao, L., et al., *MEK1/2-ERK1/2 mediates alpha1-adrenergic receptor-stimulated hypertrophy in adult rat ventricular myocytes.* J Mol Cell Cardiol, 2001. **33**(4): p. 779-87.
273. Shibata, R., et al., *Adiponectin-mediated modulation of hypertrophic signals in the heart.* Nat Med, 2004. **10**(12): p. 1384-9.
274. Aoki, H., et al., *Specific role of the extracellular signal-regulated kinase pathway in angiotensin II-induced cardiac hypertrophy in vitro.* Biochem J, 2000. **347 Pt 1**(Pt 1): p. 275-84.
275. Li, H., et al., *Adiponectin ameliorates hyperglycemia-induced cardiac hypertrophy and dysfunction by concomitantly activating Nrf2 and Brg1.* Free Radic Biol Med, 2015. **84**: p. 311-321.
276. Fujishima, Y., et al., *Effect of adiponectin on cardiac β-catenin signaling pathway under angiotensin II infusion.* Biochem Biophys Res Commun, 2014. **444**(2): p. 224-9.
277. Guo, R., et al., *Adiponectin knockout accentuates high fat diet-induced obesity and cardiac dysfunction: role of autophagy.* Biochim Biophys Acta, 2013. **1832**(8): p. 1136-48.
278. Xie, Z., et al., *Improvement of cardiac functions by chronic metformin treatment is associated with enhanced cardiac autophagy in diabetic OVE26 mice.* Diabetes, 2011. **60**(6): p. 1770-8.
279. Hu, N., et al., *Deficiency in adiponectin exaggerates cigarette smoking exposure-induced cardiac contractile dysfunction: Role of autophagy.* Pharmacol Res, 2015. **100**: p. 175-89.
280. Ding, W.X., et al., *Adiponectin protects rat heart from left ventricular remodeling induced by chronic intermittent hypoxia via inhibition of TGF-β/smad2/3 pathway.* J Thorac Dis, 2014. **6**(9): p. 1278-84.
281. Fujita, K., et al., *Adiponectin protects against angiotensin II-induced cardiac fibrosis through activation of PPAR-alpha.* Arterioscler Thromb Vasc Biol, 2008. **28**(5): p. 863-70.

282. Wang, X., et al., *Adiponectin improves NF-κB-mediated inflammation and abates atherosclerosis progression in apolipoprotein E-deficient mice.* Lipids Health Dis, 2016. **15**: p. 33.
283. Ouchi, N., et al., *Adiponectin stimulates angiogenesis by promoting cross-talk between AMP-activated protein kinase and Akt signaling in endothelial cells.* J Biol Chem, 2004. **279**(2): p. 1304-9.
284. Peng, J., Q. Chen, and C. Wu, *The role of adiponectin in cardiovascular disease.* Cardiovascular Pathology, 2023. **64**: p. 107514.
285. Gamberi, T., F. Magherini, and T. Fiaschi, *Adiponectin in Myopathies.* Int J Mol Sci, 2019. **20**(7).
286. Hathout, Y., et al., *Discovery of serum protein biomarkers in the mdx mouse model and cross-species comparison to Duchenne muscular dystrophy patients.* Hum Mol Genet, 2014. **23**(24): p. 6458-69.
287. Hathout, Y., et al., *Disease-specific and glucocorticoid-responsive serum biomarkers for Duchenne Muscular Dystrophy.* Sci Rep, 2019. **9**(1): p. 12167.
288. Delaigle, A.M., et al., *Induction of adiponectin in skeletal muscle by inflammatory cytokines: in vivo and in vitro studies.* Endocrinology, 2004. **145**(12): p. 5589-97.
289. Abou-Samra, M., Raphaël Boursereau, Sophie Lecompte, Laurence Noel, and Sonia M. Brichard, *Potential Therapeutic Action of Adiponectin in Duchenne Muscular Dystrophy.* The American Journal of Pathology 2017. **187**(7): p. 1577–85.
290. Abou-Samra, M., et al., *AdipoRon, a new therapeutic prospect for Duchenne muscular dystrophy.* J Cachexia Sarcopenia Muscle, 2020. **11**(2): p. 518-533.
291. Capogrosso, R.F., et al., *Contractile efficiency of dystrophic mdx mouse muscle: in vivo and ex vivo assessment of adaptation to exercise of functional end points.* J Appl Physiol (1985), 2017. **122**(4): p. 828-843.
292. Mantuano, P., et al., *Effect of a long-term treatment with metformin in dystrophic mdx mice: A reconsideration of its potential clinical interest in Duchenne muscular dystrophy.* Biochem Pharmacol, 2018. **154**: p. 89-103.
293. Ye, C., et al., *CaMKK2 Suppresses Muscle Regeneration through the Inhibition of Myoblast Proliferation and Differentiation.* Int J Mol Sci, 2016. **17**(10).
294. Boccanegra, B., et al., *LKB1 signaling is altered in skeletal muscle of a Duchenne muscular dystrophy mouse model.* Dis Model Mech, 2023. **16**(7).
295. Schade van Westrum, S.M., et al., *Cardiac abnormalities in a follow-up study on carriers of Duchenne and Becker muscular dystrophy.* Neurology, 2011. **77**(1): p. 62-6.

296. Liu, Y., V. Vu, and G. Sweeney, *Examining the Potential of Developing and Implementing Use of Adiponectin-Targeted Therapeutics for Metabolic and Cardiovascular Diseases.* Front Endocrinol (Lausanne), 2019. **10**: p. 842.
297. Singh, A.K., et al., *Orally active osteoanabolic agent GTDF binds to adiponectin receptors, with a preference for AdipoR1, induces adiponectin-associated signaling, and improves metabolic health in a rodent model of diabetes.* Diabetes, 2014. **63**(10): p. 3530-44.
298. Singh, A.K., et al., *Small molecule adiponectin receptor agonist GTDF protects against skeletal muscle atrophy.* Mol Cell Endocrinol, 2017. **439**: p. 273-285.
299. Goto, T., et al., *Tiliroside, a glycosidic flavonoid, ameliorates obesity-induced metabolic disorders via activation of adiponectin signaling followed by enhancement of fatty acid oxidation in liver and skeletal muscle in obese-diabetic mice.* J Nutr Biochem, 2012. **23**(7): p. 768-76.
300. Xu, H., et al., *AdipoR1/AdipoR2 dual agonist recovers nonalcoholic steatohepatitis and related fibrosis via endoplasmic reticulum-mitochondria axis.* Nat Commun, 2020. **11**(1): p. 5807.
301. Okada-Iwabu, M., et al., *A small-molecule AdipoR agonist for type 2 diabetes and short life in obesity.* Nature, 2013. **503**(7477): p. 493-9.
302. Balasubramanian, P., et al., *Adiponectin receptor agonist AdipoRon improves skeletal muscle function in aged mice.* Elife, 2022. **11**.
303. Qiu, W., et al., *Identification and characterization of a novel adiponectin receptor agonist adipo anti-inflammation agonist and its anti-inflammatory effects in vitro and in vivo.* Br J Pharmacol, 2021. **178**(2): p. 280-297.
304. Ahuja, A., et al., *Antidiabetic features of AdipoAI, a novel AdipoR agonist.* Cell Biochem Funct, 2024. **42**(1): p. e3910.
305. Qiu, W., et al., *The adiponectin receptor agonist AdipoAI attenuates periodontitis in diabetic rats by inhibiting gingival fibroblast-induced macrophage migration.* Br J Pharmacol, 2023. **180**(18): p. 2436-2451.
306. Asahara, N., et al., *A monoclonal antibody activating AdipoR for type 2 diabetes and nonalcoholic steatohepatitis.* Sci Adv, 2023. **9**(45): p. eadg4216.
307. Ahmad, A., et al., *Adiponectin homolog novel osmotin protects obesity/diabetes-induced NAFLD by upregulating AdipoRs/PPARα signaling in ob/ob and db/db transgenic mouse models.* Metabolism, 2019. **90**: p. 31-43.
308. Liu, J., et al., *Osmotin Protects H9c2 Cells from Simulated Ischemia-Reperfusion Injury through AdipoR1/PI3K/AKT Signaling Pathway.* Front Physiol, 2017. **8**: p. 611.

309. Takahashi, Y., et al., *Novel phytopeptide osmotin mimics preventive effects of adiponectin on vascular inflammation and atherosclerosis.* Metabolism, 2018. **83**: p. 128-138.
310. Narasimhan, M.L., et al., *Osmotin is a homolog of mammalian adiponectin and controls apoptosis in yeast through a homolog of mammalian adiponectin receptor.* Mol Cell, 2005. **17**(2): p. 171-80.
311. Shah, S.A., et al., *Novel osmotin inhibits SREBP2 via the AdipoR1/AMPK/SIRT1 pathway to improve Alzheimer's disease neuropathological deficits.* Mol Psychiatry, 2017. **22**(3): p. 407-416.
312. Ma, L., et al., *A potent peptide as adiponectin receptor 1 agonist to against fibrosis.* J Enzyme Inhib Med Chem, 2017. **32**(1): p. 624-631.
313. Kim, S., et al., *Discovery of a novel potent peptide agonist to adiponectin receptor 1.* PLoS One, 2018. **13**(6): p. e0199256.
314. Lee, I.K., et al., *PEG-BHD1028 Peptide Regulates Insulin Resistance and Fatty Acid β-Oxidation, and Mitochondrial Biogenesis by Binding to Two Heterogeneous Binding Sites of Adiponectin Receptors, AdipoR1 and AdipoR2.* Int J Mol Sci, 2021. **22**(2).
315. Lee, I.K., et al., *Enhanced Immunomodulation, Anti-Apoptosis, and Improved Tear Dynamics of (PEG)-BHD1028, a Novel Adiponectin Receptor Agonist Peptide, for Treating Dry Eye Disease.* Pharmaceutics, 2022. **15**(1).
316. Sayeed, M., et al., *A collagen domain-derived short adiponectin peptide activates APPL1 and AMPK signaling pathways and improves glucose and fatty acid metabolisms.* J Biol Chem, 2018. **293**(35): p. 13509-13523.
317. Otvos, L., Jr., et al., *Design and development of a peptide-based adiponectin receptor agonist for cancer treatment.* BMC Biotechnol, 2011. **11**: p. 90.
318. Sung, H.K., et al., *ALY688 elicits adiponectin-mimetic signaling and improves insulin action in skeletal muscle cells.* Am J Physiol Cell Physiol, 2022. **322**(2): p. C151-c163.
319. Da Eira, D., et al., *Effects of the adiponectin mimetic compound ALY688 on glucose and fat metabolism in visceral and subcutaneous rat adipocytes.* Adipocyte, 2020. **9**(1): p. 550-562.
320. Cho, S., et al., *Cardioprotection by the adiponectin receptor agonist ALY688 in a preclinical mouse model of heart failure with reduced ejection fraction (HFrEF).* Biomed Pharmacother, 2024. **171**: p. 116119.
321. Selvais, C.M., et al., *AdipoRon enhances healthspan in middle-aged obese mice: striking alleviation of myosteatosis and muscle degenerative markers.* J Cachexia Sarcopenia Muscle, 2023. **14**(1): p. 464-478.
322. Okada-Iwabu, M., et al., *Perspective of Small-Molecule AdipoR Agonist for Type 2 Diabetes and Short Life in Obesity.* Diabetes Metab J, 2015. **39**(5): p. 363-72.

323. Nicolas, S., et al., *Adiporon, an adiponectin receptor agonist acts as an antidepressant and metabolic regulator in a mouse model of depression.* Transl Psychiatry, 2018. **8**(1): p. 159.
324. Wang, Y., et al., *Small-molecule agonist AdipoRon alleviates diabetic retinopathy through the AdipoR1/AMPK/EGR4 pathway.* J Transl Med, 2024. **22**(1): p. 2.
325. Hong, K., et al., *Adiponectin Receptor Agonist, AdipoRon, Causes Vasorelaxation Predominantly Via a Direct Smooth Muscle Action.* Microcirculation, 2016. **23**(3): p. 207-20.
326. Wang, Y., et al., *Hepatoprotective effects of AdipoRon against d-galactosamine-induced liver injury in mice.* Eur J Pharm Sci, 2016. **93**: p. 123-31.
327. Zhang, Y., et al., *AdipoRon, the first orally active adiponectin receptor activator, attenuates postischemic myocardial apoptosis through both AMPK-mediated and AMPK-independent signalings.* Am J Physiol Endocrinol Metab, 2015. **309**(3): p. E275-82.
328. Akimoto, M., et al., *Antidiabetic adiponectin receptor agonist AdipoRon suppresses tumour growth of pancreatic cancer by inducing RIPK1/ERK-dependent necroptosis.* Cell Death Dis, 2018. **9**(8): p. 804.
329. Messaggio, F., et al., *Adiponectin receptor agonists inhibit leptin induced pSTAT3 and in vivo pancreatic tumor growth.* Oncotarget, 2017. **8**(49): p. 85378-85391.
330. Wu, X., et al., *AdipoRon accelerates bone repair of calvarial defect in diet-induced obesity mice.* Heliyon, 2023. **9**(3): p. e13975.
331. Yamashita, T., et al., *An orally-active adiponectin receptor agonist mitigates cutaneous fibrosis, inflammation and microvascular pathology in a murine model of systemic sclerosis.* Sci Rep, 2018. **8**(1): p. 11843.
332. Fang, Q., et al., *AdipoRon Engages Microglia to Antinociception through the AdipoR1/AMPK Pathway in SNI Mice.* Mediators Inflamm, 2023. **2023**: p. 7661791.
333. Sun, F., et al., *Adiponectin modulates ventral tegmental area dopamine neuron activity and anxiety-related behavior through AdipoR1.* Mol Psychiatry, 2019. **24**(1): p. 126-144.
334. Formolo, D.A., et al., *Increasing Adiponectin Signaling by Sub-Chronic AdipoRon Treatment Elicits Antidepressant- and Anxiolytic-Like Effects Independent of Changes in Hippocampal Plasticity.* Biomedicines, 2023. **11**(2).
335. Zhang, D., et al., *Adiponectin regulates contextual fear extinction and intrinsic excitability of dentate gyrus granule neurons through AdipoR2 receptors.* Mol Psychiatry, 2017. **22**(7): p. 1044-1055.

336. Zhang, N., et al., *AdipoRon, an adiponectin receptor agonist, attenuates cardiac remodeling induced by pressure overload.* J Mol Med (Berl), 2018. **96**(12): p. 1345-1357.
337. Liu, B., et al., *Adiponectin Protects Against Cerebral Ischemic Injury Through AdipoR1/AMPK Pathways.* Front Pharmacol, 2019. **10**: p. 597.
338. Iwabu, M., et al., *AdipoR agonist increases insulin sensitivity and exercise endurance in AdipoR-humanized mice.* Commun Biol, 2021. **4**(1): p. 45.
339. Anil Kumar, S., et al., *Osmotin: a plant sentinel and a possible agonist of mammalian adiponectin.* Front Plant Sci, 2015. **6**: p. 163.
340. Ali, T., et al., *Adiponectin-mimetic novel nonapeptide rescues aberrant neuronal metabolic-associated memory deficits in Alzheimer's disease.* Mol Neurodegener, 2021. **16**(1): p. 23.
341. Park, J.S., et al., *Neuroprotective effects of osmotin in Parkinson's disease-associated pathology via the AdipoR1/MAPK/AMPK/mTOR signaling pathways.* J Biomed Sci, 2023. **30**(1): p. 66.
342. Yoon, G., et al., *The Adiponectin Homolog Osmotin Enhances Neurite Outgrowth and Synaptic Complexity via AdipoR1/NgR1 Signaling in Alzheimer's Disease.* Mol Neurobiol, 2018. **55**(8): p. 6673-6686.
343. Amin, F.U., et al., *Osmotin-loaded magnetic nanoparticles with electromagnetic guidance for the treatment of Alzheimer's disease.* Nanoscale, 2017. **9**(30): p. 10619-10632.
344. Otvos, L., Jr., *Potential Adiponectin Receptor Response Modifier Therapeutics.* Front Endocrinol (Lausanne), 2019. **10**: p. 539.
345. Philp, L.K., et al., *Adiponectin receptor activation inhibits prostate cancer xenograft growth.* Endocr Relat Cancer, 2020. **27**(12): p. 711-729.
346. Kumar, P., et al., *Adiponectin modulates focal adhesion disassembly in activated hepatic stellate cells: implication for reversing hepatic fibrosis.* Faseb j, 2014. **28**(12): p. 5172-83.
347. Wang, H., et al., *Adiponectin-derived active peptide ADP355 exerts anti-inflammatory and anti-fibrotic activities in thioacetamide-induced liver injury.* Sci Rep, 2016. **6**: p. 19445.
348. Zhao, D., et al., *Adiponectin agonist ADP355 ameliorates doxorubicin-induced cardiotoxicity by decreasing cardiomyocyte apoptosis and oxidative stress.* Biochem Biophys Res Commun, 2020. **533**(3): p. 304-312.
349. Darmawan, C.C., et al., *Adiponectin-Based Peptide (ADP355) Inhibits Transforming Growth Factor-β1-Induced Fibrosis in Keloids.* Int J Mol Sci, 2020. **21**(8).
350. Marangoni, R.G., et al., *Adiponectin is an endogenous anti-fibrotic mediator and therapeutic target.* Scientific Reports, 2017. **7**(1): p. 4397.

351. Sun, L., et al., *Activation of Adiponectin Receptor Regulates Proprotein Convertase Subtilisin/Kexin Type 9 Expression and Inhibits Lesions in ApoE-Deficient Mice.* Arterioscler Thromb Vasc Biol, 2017. **37**(7): p. 1290-1300.
352. Pepping, J.K., et al., *Designer adiponectin receptor agonist stabilizes metabolic function and prevents brain injury caused by HIV protease inhibitors.* J Neuroimmune Pharmacol, 2014. **9**(3): p. 388-98.
353. Otvos, L., Jr., et al., *Development of second generation peptides modulating cellular adiponectin receptor responses.* Front Chem, 2014. **2**: p. 93.
354. Li, Y., et al., *Therapeutic Effect of Topical Adiponectin-Derived Short Peptides Compared with Globular Adiponectin in Experimental Dry Eye and Alkali Burn.* J Ocul Pharmacol Ther, 2020. **36**(2): p. 88-96.
355. Bellissimo, C.A., et al., *Memory impairment in the D2.mdx mouse model of Duchenne muscular dystrophy is prevented by the adiponectin receptor agonist ALY688.* Exp Physiol, 2023.
356. Dubuisson, N., et al., *The Adiponectin Receptor Agonist, ALY688: A Promising Therapeutic for Fibrosis in the Dystrophic Muscle.* Cells, 2023. **12**(16).
357. Mullen, K.L., et al., *Adiponectin resistance precedes the accumulation of skeletal muscle lipids and insulin resistance in high-fat-fed rats.* Am J Physiol Regul Integr Comp Physiol, 2009. **296**(2): p. R243-51.
358. Tsuchida, A., et al., *Insulin/Foxo1 pathway regulates expression levels of adiponectin receptors and adiponectin sensitivity.* J Biol Chem, 2004. **279**(29): p. 30817-22.
359. Martinon, F., K. Burns, and J. Tschopp, *The inflammasome: a molecular platform triggering activation of inflammatory caspases and processing of proIL-beta.* Mol Cell, 2002. **10**(2): p. 417-26.
360. Liu, J. and X. Cao, *Cellular and molecular regulation of innate inflammatory responses.* Cell Mol Immunol, 2016. **13**(6): p. 711-721.
361. Xiao, L., V.G. Magupalli, and H. Wu, *Cryo-EM structures of the active NLRP3 inflammasome disc.* Nature, 2023. **613**(7944): p. 595-600.
362. Schroder, K. and J. Tschopp, *The inflammasomes.* Cell, 2010. **140**(6): p. 821-32.
363. Compan, V., et al., *Apoptosis-associated speck-like protein containing a CARD forms specks but does not activate caspase-1 in the absence of NLRP3 during macrophage swelling.* J Immunol, 2015. **194**(3): p. 1261-73.
364. Shi, H., et al., *NLRP3 activation and mitosis are mutually exclusive events coordinated by NEK7, a new inflammasome component.* Nat Immunol, 2016. **17**(3): p. 250-8.

365. Kandli, M., et al., *Isolation and characterization of two evolutionarily conserved murine kinases (Nek6 and nek7) related to the fungal mitotic regulator, NIMA.* Genomics, 2000. **68**(2): p. 187-96.
366. Pandey, A., et al., *Cell biology of inflammasome activation.* Trends Cell Biol, 2021. **31**(11): p. 924-939.
367. Brydges, S.D., et al., *Divergence of IL-1, IL-18, and cell death in NLRP3 inflammasomopathies.* J Clin Invest, 2013. **123**(11): p. 4695-705.
368. McIlwain, D.R., T. Berger, and T.W. Mak, *Caspase functions in cell death and disease.* Cold Spring Harb Perspect Biol, 2013. **5**(4): p. a008656.
369. Shalini, S., et al., *Old, new and emerging functions of caspases.* Cell Death Differ, 2015. **22**(4): p. 526-39.
370. O'Neill, L.A., *The interleukin-1 receptor/Toll-like receptor superfamily: 10 years of progress.* Immunol Rev, 2008. **226**: p. 10-8.
371. Moreno-García, L., et al., *Inflammasome in ALS Skeletal Muscle: NLRP3 as a Potential Biomarker.* Int J Mol Sci, 2021. **22**(5).
372. Arend, W.P., G. Palmer, and C. Gabay, *IL-1, IL-18, and IL-33 families of cytokines.* Immunol Rev, 2008. **223**: p. 20-38.
373. Wawrocki, S., et al., *Interleukin 18 (IL-18) as a target for immune intervention.* Acta Biochim Pol, 2016. **63**(1): p. 59-63.
374. Kuriakose, T. and T.D. Kanneganti, *Gasdermin D Flashes an Exit Signal for IL-1.* Immunity, 2018. **48**(1): p. 1-3.
375. Shi, J., et al., *Cleavage of GSDMD by inflammatory caspases determines pyroptotic cell death.* Nature, 2015. **526**(7575): p. 660-5.
376. Ramos-Junior, E.S. and A.C. Morandini, *Gasdermin: A new player to the inflammasome game.* Biomed J, 2017. **40**(6): p. 313-316.
377. Kayagaki, N., et al., *NINJ1 mediates plasma membrane rupture during lytic cell death.* Nature, 2021. **591**(7848): p. 131-136.
378. Broz, P. and V.M. Dixit, *Inflammasomes: mechanism of assembly, regulation and signalling.* Nat Rev Immunol, 2016. **16**(7): p. 407-20.
379. Baroja-Mazo, A., et al., *The NLRP3 inflammasome is released as a particulate danger signal that amplifies the inflammatory response.* Nat Immunol, 2014. **15**(8): p. 738-48.
380. Franklin, B.S., et al., *The adaptor ASC has extracellular and 'prionoid' activities that propagate inflammation.* Nat Immunol, 2014. **15**(8): p. 727-37.
381. Weindel, C.G., et al., *Mitochondrial ROS promotes susceptibility to infection via gasdermin D-mediated necroptosis.* Cell, 2022. **185**(17): p. 3214-3231.e23.
382. Gaul, S., et al., *Extracellular NLRP3 inflammasome particles are internalized by human coronary artery smooth muscle cells and induce pro-atherogenic effects.* Sci Rep, 2021. **11**(1): p. 15156.

383. Miao, E.A., et al., *Caspase-1-induced pyroptosis is an innate immune effector mechanism against intracellular bacteria.* Nat Immunol, 2010. **11**(12): p. 1136-42.
384. Guarda, G., et al., *Differential expression of NLRP3 among hematopoietic cells.* J Immunol, 2011. **186**(4): p. 2529-34.
385. Hanamsagar, R., M.L. Hanke, and T. Kielian, *Toll-like receptor (TLR) and inflammasome actions in the central nervous system.* Trends Immunol, 2012. **33**(7): p. 333-42.
386. Hornung, V. and E. Latz, *Critical functions of priming and lysosomal damage for NLRP3 activation.* Eur J Immunol, 2010. **40**(3): p. 620-3.
387. Lundberg, I., et al., *Decreased expression of interleukin-1alpha, interleukin-1beta, and cell adhesion molecules in muscle tissue following corticosteroid treatment in patients with polymyositis and dermatomyositis.* Arthritis Rheum, 2000. **43**(2): p. 336-48.
388. Rawat, R., et al., *Inflammasome up-regulation and activation in dysferlin-deficient skeletal muscle.* Am J Pathol, 2010. **176**(6): p. 2891-900.
389. Elliott, E.I. and F.S. Sutterwala, *Initiation and perpetuation of NLRP3 inflammasome activation and assembly.* Immunol Rev, 2015. **265**(1): p. 35-52.
390. Franchi, L., R. Muñoz-Planillo, and G. Núñez, *Sensing and reacting to microbes through the inflammasomes.* Nat Immunol, 2012. **13**(4): p. 325-32.
391. Franchi, L., et al., *Cytosolic double-stranded RNA activates the NLRP3 inflammasome via MAVS-induced membrane permeabilization and K+ efflux.* J Immunol, 2014. **193**(8): p. 4214-4222.
392. Mariathasan, S., et al., *Cryopyrin activates the inflammasome in response to toxins and ATP.* Nature, 2006. **440**(7081): p. 228-32.
393. Yamasaki, K., et al., *NLRP3/cryopyrin is necessary for interleukin-1beta (IL-1beta) release in response to hyaluronan, an endogenous trigger of inflammation in response to injury.* J Biol Chem, 2009. **284**(19): p. 12762-71.
394. Halle, A., et al., *The NALP3 inflammasome is involved in the innate immune response to amyloid-beta.* Nat Immunol, 2008. **9**(8): p. 857-65.
395. Dostert, C., et al., *Innate immune activation through Nalp3 inflammasome sensing of asbestos and silica.* Science, 2008. **320**(5876): p. 674-7.
396. Martinon, F., et al., *Gout-associated uric acid crystals activate the NALP3 inflammasome.* Nature, 2006. **440**(7081): p. 237-41.
397. Feldmeyer, L., et al., *The inflammasome mediates UVB-induced activation and secretion of interleukin-1beta by keratinocytes.* Curr Biol, 2007. **17**(13): p. 1140-5.

398. Zhuang, Y., et al., *Albumin impairs renal tubular tight junctions via targeting the NLRP3 inflammasome.* Am J Physiol Renal Physiol, 2015. **308**(9): p. F1012-9.
399. Wen, H., et al., *Fatty acid-induced NLRP3-ASC inflammasome activation interferes with insulin signaling.* Nat Immunol, 2011. **12**(5): p. 408-15.
400. Koizumi, Y., et al., *Inflammasome activation via intracellular NLRs triggered by bacterial infection.* Cell Microbiol, 2012. **14**(2): p. 149-54.
401. Róg, J., et al., *Dystrophic mdx mouse myoblasts exhibit elevated ATP/UTP-evoked metabotropic purinergic responses and alterations in calcium signalling.* Biochim Biophys Acta Mol Basis Dis, 2019. **1865**(6): p. 1138-1151.
402. Young, C.N., et al., *P2X7 purinoceptor alterations in dystrophic mdx mouse muscles: relationship to pathology and potential target for treatment.* J Cell Mol Med, 2012. **16**(5): p. 1026-37.
403. Di, A., et al., *The TWIK2 Potassium Efflux Channel in Macrophages Mediates NLRP3 Inflammasome-Induced Inflammation.* Immunity, 2018. **49**(1): p. 56-65.e4.
404. Okada, M., et al., *The lysosome rupture-activated TAK1-JNK pathway regulates NLRP3 inflammasome activation.* J Biol Chem, 2014. **289**(47): p. 32926-36.
405. Heid, M.E., et al., *Mitochondrial reactive oxygen species induces NLRP3-dependent lysosomal damage and inflammasome activation.* J Immunol, 2013. **191**(10): p. 5230-8.
406. Gurung, P., J.R. Lukens, and T.D. Kanneganti, *Mitochondria: diversity in the regulation of the NLRP3 inflammasome.* Trends Mol Med, 2015. **21**(3): p. 193-201.
407. Zhou, R., et al., *Thioredoxin-interacting protein links oxidative stress to inflammasome activation.* Nat Immunol, 2010. **11**(2): p. 136-40.
408. Ramos-Tovar, E. and P. Muriel, *Molecular Mechanisms That Link Oxidative Stress, Inflammation, and Fibrosis in the Liver.* Antioxidants (Basel), 2020. **9**(12).
409. Kayagaki, N., et al., *Noncanonical inflammasome activation by intracellular LPS independent of TLR4.* Science, 2013. **341**(6151): p. 1246-9.
410. Hagar, J.A., et al., *Cytoplasmic LPS activates caspase-11: implications in TLR4-independent endotoxic shock.* Science, 2013. **341**(6151): p. 1250-3.
411. Wang, Z., et al., *NLRP3 Inflammasome and Inflammatory Diseases.* Oxid Med Cell Longev, 2020. **2020**: p. 4063562.
412. Blevins, H.M., et al., *The NLRP3 Inflammasome Pathway: A Review of Mechanisms and Inhibitors for the Treatment of Inflammatory Diseases.* Front Aging Neurosci, 2022. **14**: p. 879021.

413. Kelley, N., et al., *The NLRP3 Inflammasome: An Overview of Mechanisms of Activation and Regulation.* Int J Mol Sci, 2019. **20**(13).
414. Spalinger, M.R., et al., *NLRP3 tyrosine phosphorylation is controlled by protein tyrosine phosphatase PTPN22.* J Clin Invest, 2016. **126**(11): p. 4388.
415. Shenoy, A.R., et al., *GBP5 promotes NLRP3 inflammasome assembly and immunity in mammals.* Science, 2012. **336**(6080): p. 481-5.
416. Lu, B., et al., *Novel role of PKR in inflammasome activation and HMGB1 release.* Nature, 2012. **488**(7413): p. 670-4.
417. Yoshida, K., et al., *PKR induces the expression of NLRP3 by regulating the NF-κB pathway in Porphyromonas gingivalis-infected osteoblasts.* Exp Cell Res, 2017. **354**(1): p. 57-64.
418. Lang, T., et al., *Macrophage migration inhibitory factor is required for NLRP3 inflammasome activation.* Nat Commun, 2018. **9**(1): p. 2223.
419. Li, X., et al., *MARK4 regulates NLRP3 positioning and inflammasome activation through a microtubule-dependent mechanism.* Nat Commun, 2017. **8**: p. 15986.
420. Piippo, N., et al., *Hsp90 inhibition as a means to inhibit activation of the NLRP3 inflammasome.* Sci Rep, 2018. **8**(1): p. 6720.
421. de Almeida, L., et al., *The PYRIN Domain-only Protein POP1 Inhibits Inflammasome Assembly and Ameliorates Inflammatory Disease.* Immunity, 2015. **43**(2): p. 264-76.
422. Ratsimandresey, R.A., et al., *The PYRIN domain-only protein POP2 inhibits inflammasome priming and activation.* Nat Commun, 2017. **8**: p. 15556.
423. Lu, A., et al., *Molecular basis of caspase-1 polymerization and its inhibition by a new capping mechanism.* Nat Struct Mol Biol, 2016. **23**(5): p. 416-25.
424. Nalbandian, A., et al., *Activation of the NLRP3 Inflammasome Is Associated with Valosin-Containing Protein Myopathy.* Inflammation, 2017. **40**(1): p. 21-41.
425. Kummer, K., et al., *Inflammasome in Skeletal Muscle: NLRP3 Is an Inflammatory Cell Stress Component in Inclusion Body Myositis.* Int J Mol Sci, 2023. **24**(13).
426. Jiang, H., et al., *Identification of a selective and direct NLRP3 inhibitor to treat inflammatory disorders.* J Exp Med, 2017. **214**(11): p. 3219-3238.
427. Shen, K., et al., *Molecular Mechanism of a Specific NLRP3 Inhibitor to Alleviate Seizure Severity Induced by Pentylenetetrazole.* Curr Mol Pharmacol, 2021. **14**(4): p. 579-586.
428. Wang, X., et al., *NLRP3 inflammasome inhibitor CY-09 reduces hepatic steatosis in experimental NAFLD mice.* Biochem Biophys Res Commun, 2021. **534**: p. 734-739.

429. Han, S., et al., *Inhibiting NLRP3 Inflammasome Activation by CY-09 Helps to Restore Cerebral Glucose Metabolism in 3×Tg-AD Mice.* Antioxidants (Basel), 2023. **12**(3).
430. Messerschmitt, P.J., et al., *Osteosarcoma Phenotype Is Inhibited by 3,4-Methylenedioxy-β-nitrostyrene.* Sarcoma, 2012. **2012**: p. 479712.
431. Xiao, M., et al., *3,4-Methylenedioxy-β-Nitrostyrene Ameliorates Experimental Burn Wound Progression by Inhibiting the NLRP3 Inflammasome Activation.* Plast Reconstr Surg, 2016. **137**(3): p. 566e-575e.
432. Zheng, J., et al., *3,4-Methylenedioxy-β-Nitrostyrene Alleviates Dextran Sulfate Sodium-Induced Mouse Colitis by Inhibiting the NLRP3 Inflammasome.* Front Pharmacol, 2022. **13**: p. 866228.
433. Gao, R.F., et al., *The covalent NLRP3-inflammasome inhibitor Oridonin relieves myocardial infarction induced myocardial fibrosis and cardiac remodeling in mice.* Int Immunopharmacol, 2021. **90**: p. 107133.
434. Xu, J., et al., *Therapeutic Potential of Oridonin and Its Analogs: From Anticancer and Antiinflammation to Neuroprotection.* Molecules, 2018. **23**(2).
435. Kuwar, R., et al., *A Novel Inhibitor Targeting NLRP3 Inflammasome Reduces Neuropathology and Improves Cognitive Function in Alzheimer's Disease Transgenic Mice.* J Alzheimers Dis, 2021. **82**(4): p. 1769-1783.
436. Kuwar, R., et al., *A novel small molecular NLRP3 inflammasome inhibitor alleviates neuroinflammatory response following traumatic brain injury.* J Neuroinflammation, 2019. **16**(1): p. 81.
437. Pang, L., et al., *Development of novel oridonin analogs as specifically targeted NLRP3 inflammasome inhibitors for the treatment of dextran sulfate sodium-induced colitis.* Eur J Med Chem, 2023. **245**(Pt 2): p. 114919.
438. Pellegrini, C., et al., *A Comparative Study on the Efficacy of NLRP3 Inflammasome Signaling Inhibitors in a Pre-clinical Model of Bowel Inflammation.* Front Pharmacol, 2018. **9**: p. 1405.
439. Ambati, M., et al., *Identification of fluoxetine as a direct NLRP3 inhibitor to treat atrophic macular degeneration.* Proc Natl Acad Sci U S A, 2021. **118**(41).
440. Bakhshi, S. and S. Shamsi, *MCC950 in the treatment of NLRP3-mediated inflammatory diseases: Latest evidence and therapeutic outcomes.* Int Immunopharmacol, 2022. **106**: p. 108595.
441. Corcoran, S.E., R. Halai, and M.A. Cooper, *Pharmacological Inhibition of the Nod-Like Receptor Family Pyrin Domain Containing 3 Inflammasome with MCC950.* Pharmacol Rev, 2021. **73**(3): p. 968-1000.

442. Chen, Y., et al., *RRx-001 ameliorates inflammatory diseases by acting as a potent covalent NLRP3 inhibitor.* Cell Mol Immunol, 2021. **18**(6): p. 1425-1436.
443. Jayabalan, N., et al., *A Review of RRx-001: A Late-Stage Multi-Indication Inhibitor of NLRP3 Activation and Chronic Inflammation.* Drugs, 2023. **83**(5): p. 389-402.
444. Parmar, D.V., et al., *Safety, Tolerability, Pharmacokinetics, and Pharmacodynamics of the Oral NLRP3 Inflammasome Inhibitor ZYIL1: First-in-Human Phase 1 Studies (Single Ascending Dose and Multiple Ascending Dose).* Clin Pharmacol Drug Dev, 2023. **12**(2): p. 202-211.
445. Marchetti, C., et al., *OLT1177, a β-sulfonyl nitrile compound, safe in humans, inhibits the NLRP3 inflammasome and reverses the metabolic cost of inflammation.* Proc Natl Acad Sci U S A, 2018. **115**(7): p. E1530-e1539.
446. Klück, V., et al., *Dapansutrile, an oral selective NLRP3 inflammasome inhibitor, for treatment of gout flares: an open-label, dose-adaptive, proof-of-concept, phase 2a trial.* Lancet Rheumatol, 2020. **2**(5): p. e270-e280.
447. Wohlford, G.F., et al., *Phase 1B, Randomized, Double-Blinded, Dose Escalation, Single-Center, Repeat Dose Safety and Pharmacodynamics Study of the Oral NLRP3 Inhibitor Dapansutrile in Subjects With NYHA II-III Systolic Heart Failure.* J Cardiovasc Pharmacol, 2020. **77**(1): p. 49-60.
448. Paik, S., et al., *An update on the regulatory mechanisms of NLRP3 inflammasome activation.* Cell Mol Immunol, 2021. **18**(5): p. 1141-1160.
449. Chen, S., et al., *Novel Role for Tranilast in Regulating NLRP3 Ubiquitination, Vascular Inflammation, and Atherosclerosis.* J Am Heart Assoc, 2020. **9**(12): p. e015513.
450. Manzo, E., et al., *Medium-Chain Fatty Acids, Beta-Hydroxybutyric Acid and Genetic Modulation of the Carnitine Shuttle Are Protective in a Drosophila Model of ALS Based on TDP-43.* Front Mol Neurosci, 2018. **11**: p. 182.
451. Goldberg, E.L., et al., *β-Hydroxybutyrate Deactivates Neutrophil NLRP3 Inflammasome to Relieve Gout Flares.* Cell Rep, 2017. **18**(9): p. 2077-2087.
452. Yamanashi, T., et al., *Beta-hydroxybutyrate, an endogenic NLRP3 inflammasome inhibitor, attenuates stress-induced behavioral and inflammatory responses.* Sci Rep, 2017. **7**(1): p. 7677.
453. Chakraborty, S., et al., *Salt-Responsive Metabolite, β-Hydroxybutyrate, Attenuates Hypertension.* Cell Rep, 2018. **25**(3): p. 677-689.e4.
454. Rho, J.M., L.R. Shao, and C.E. Stafstrom, *2-Deoxyglucose and Beta-Hydroxybutyrate: Metabolic Agents for Seizure Control.* Front Cell Neurosci, 2019. **13**: p. 172.

455. Coll, R.C., et al., *MCC950 directly targets the NLRP3 ATP-hydrolysis motif for inflammasome inhibition.* Nat Chem Biol, 2019. **15**(6): p. 556-559.
456. Tapia-Abellán, A., et al., *MCC950 closes the active conformation of NLRP3 to an inactive state.* Nature chemical biology, 2019. **15**(6): p. 560-564.
457. Brydges, S.D., et al., *Inflammasome-mediated disease animal models reveal roles for innate but not adaptive immunity.* Immunity, 2009. **30**(6): p. 875-87.
458. Coll, R.C., et al., *A small-molecule inhibitor of the NLRP3 inflammasome for the treatment of inflammatory diseases.* Nat Med, 2015. **21**(3): p. 248-55.
459. Ma, Y., et al., *Heme Oxygenase-1 in Macrophages Impairs the Perfusion Recovery After Hindlimb Ischemia by Suppressing Autolysosome-Dependent Degradation of NLRP3.* Arterioscler Thromb Vasc Biol, 2021. **41**(5): p. 1710-1723.
460. Yan, X., et al., *MCC950 Ameliorates Diabetic Muscle Atrophy in Mice by Inhibition of Pyroptosis and Its Synergistic Effect with Aerobic Exercise.* Molecules, 2024. **29**(3).
461. Mangan, M.S.J., et al., *Targeting the NLRP3 inflammasome in inflammatory diseases.* Nat Rev Drug Discov, 2018. **17**(8): p. 588-606.
462. Kennedy, C.R., et al., *A Probe for NLRP3 Inflammasome Inhibitor MCC950 Identifies Carbonic Anhydrase 2 as a Novel Target.* ACS Chem Biol, 2021. **16**(6): p. 982-990.
463. *Carbonic Anhydrase Inhibitors*, in *LiverTox: Clinical and Research Information on Drug-Induced Liver Injury*. 2012, National Institute of Diabetes and Digestive and Kidney Diseases: Bethesda (MD).
464. Zhang, X., et al., *Inhibitors of the NLRP3 inflammasome pathway as promising therapeutic candidates for inflammatory diseases (Review).* Int J Mol Med, 2023. **51**(4).
465. Fang, W.Y., et al., *Triptolide prevents LPS-induced skeletal muscle atrophy via inhibiting NF-κB/TNF-α and regulating protein synthesis/degradation pathway.* Br J Pharmacol, 2021. **178**(15): p. 2998-3016.
466. Chen, Y., Q. Qian, and J. Yu, *Carbenoxolone ameliorates insulin sensitivity in obese mice induced by high fat diet via regulating the IκB-α/NF-κB pathway and NLRP3 inflammasome.* Biomed Pharmacother, 2019. **115**: p. 108868.
467. Nabavi, S.M., et al., *Anti-inflammatory effects of Melatonin: A mechanistic review.* Crit Rev Food Sci Nutr, 2019. **59**(sup1): p. S4-s16.
468. Sayed, R.K., et al., *The Impact of Melatonin and NLRP3 Inflammasome on the Expression of microRNAs in Aged Muscle.* Antioxidants (Basel), 2021. **10**(4).

469. Sayed, R.K.A., et al., *The Protective Effect of Melatonin Against Age-Associated, Sarcopenia-Dependent Tubular Aggregate Formation, Lactate Depletion, and Mitochondrial Changes.* J Gerontol A Biol Sci Med Sci, 2018. **73**(10): p. 1330-1338.
470. García, J.A., et al., *Disruption of the NF-κB/NLRP3 connection by melatonin requires retinoid-related orphan receptor-α and blocks the septic response in mice.* Faseb j, 2015. **29**(9): p. 3863-75.
471. Sadeghi, A., et al., *Curcumin ameliorates palmitate-induced inflammation in skeletal muscle cells by regulating JNK/NF-kB pathway and ROS production.* Inflammopharmacology, 2018. **26**(5): p. 1265-1272.
472. Pan, Y., et al., *Curcumin alleviates dystrophic muscle pathology in mdx mice.* Mol Cells, 2008. **25**(4): p. 531-7.
473. Dong, X., et al., *Metformin Increases Sarcolemma Integrity and Ameliorates Neuromuscular Deficits in a Murine Model of Duchenne Muscular Dystrophy.* Front Physiol, 2021. **12**: p. 642908.
474. Ljubicic, V., et al., *Resveratrol induces expression of the slow, oxidative phenotype in mdx mouse muscle together with enhanced activity of the SIRT1-PGC-1α axis.* Am J Physiol Cell Physiol, 2014. **307**(1): p. C66-82.
475. Bastin, J. and F. Djouadi, *Resveratrol and Myopathy.* Nutrients, 2016. **8**(5).
476. Dial, A.G., et al., *The Role of AMPK in Neuromuscular Biology and Disease.* Trends Endocrinol Metab, 2018. **29**(5): p. 300-312.
477. Cordero, M.D., M.R. Williams, and B. Ryffel, *AMP-Activated Protein Kinase Regulation of the NLRP3 Inflammasome during Aging.* Trends Endocrinol Metab, 2018. **29**(1): p. 8-17.
478. Chang, L., et al., *Ghrelin improves muscle function in dystrophin-deficient mdx mice by inhibiting NLRP3 inflammasome activation.* Life Sci, 2019. **232**: p. 116654.
479. Pradhan, G., S.L. Samson, and Y. Sun, *Ghrelin: much more than a hunger hormone.* Curr Opin Clin Nutr Metab Care, 2013. **16**(6): p. 619-24.
480. Lu, L., et al., *Shikonin extracted from medicinal Chinese herbs exerts anti-inflammatory effect via proteasome inhibition.* Eur J Pharmacol, 2011. **658**(2-3): p. 242-7.
481. Liu, D., et al., *PKM2-dependent glycolysis promotes skeletal muscle cell pyroptosis by activating the NLRP3 inflammasome in dermatomyositis/polymyositis.* Rheumatology (Oxford), 2021. **60**(5): p. 2177-2189.
482. Kien, C.L., et al., *Lipidomic evidence that lowering the typical dietary palmitate to oleate ratio in humans decreases the leukocyte production of proinflammatory cytokines and muscle expression of redox-sensitive genes.* J Nutr Biochem, 2015. **26**(12): p. 1599-606.

483. Wang, L., et al., *Trimetazidine attenuates dexamethasone-induced muscle atrophy via inhibiting NLRP3/GSDMD pathway-mediated pyroptosis.* Cell Death Discov, 2021. **7**(1): p. 251.
484. Ma, M., K. Chai, and R. Deng, *Study of the correlation between the noncanonical pathway of pyroptosis and idiopathic inflammatory myopathy.* Int Immunopharmacol, 2021. **98**: p. 107810.
485. Adinolfi, E., et al., *The P2X7 receptor: A main player in inflammation.* Biochem Pharmacol, 2018. **151**: p. 234-244.
486. Zhou, J., et al., *Inhibition of P2X7 Purinergic Receptor Ameliorates Cardiac Fibrosis by Suppressing NLRP3/IL-1β Pathway.* Oxid Med Cell Longev, 2020. **2020**: p. 7956274.
487. Lamkanfi, M., et al., *Glyburide inhibits the Cryopyrin/Nalp3 inflammasome.* J Cell Biol, 2009. **187**(1): p. 61-70.
488. Cao, D.Y., et al., *A small molecule inhibitor of caspase-1 inhibits NLRP3 inflammasome activation and pyroptosis to alleviate gouty inflammation.* Immunol Lett, 2022. **244**: p. 28-39.
489. Wannamaker, W., et al., *(S)-1-((S)-2-{[1-(4-amino-3-chloro-phenyl)-methanoyl]-amino}-3,3-dimethyl-butanoyl)-pyrrolidine-2-carboxylic acid ((2R,3S)-2-ethoxy-5-oxo-tetrahydro-furan-3-yl)-amide (VX-765), an orally available selective interleukin (IL)-converting enzyme/caspase-1 inhibitor, exhibits potent anti-inflammatory activities by inhibiting the release of IL-1beta and IL-18.* J Pharmacol Exp Ther, 2007. **321**(2): p. 509-16.
490. Amand, M., et al., *The anti-caspase 1 inhibitor VX-765 reduces immune activation, CD4(+) T cell depletion, viral load, and total HIV-1 DNA in HIV-1 infected humanized mice.* Elife, 2023. **12**.
491. Wu, S., et al., *VX765, a Specific Caspase-1 Inhibitor, Alleviates Lung Ischemia Reperfusion Injury by Suppressing Endothelial Pyroptosis and Barrier Dysfunction.* Biomed Res Int, 2021. **2021**: p. 4525988.
492. Jin, Y., et al., *Novel role for caspase 1 inhibitor VX765 in suppressing NLRP3 inflammasome assembly and atherosclerosis via promoting mitophagy and efferocytosis.* Cell Death Dis, 2022. **13**(5): p. 512.
493. Flores, J., et al., *Publisher Correction: Pre-symptomatic Caspase-1 inhibitor delays cognitive decline in a mouse model of Alzheimer disease and aging.* Nat Commun, 2021. **12**(1): p. 2271.
494. Calabrese, L.H., *Anakinra treatment of patients with rheumatoid arthritis.* Ann Pharmacother, 2002. **36**(7-8): p. 1204-9.
495. Jesus, A.A. and R. Goldbach-Mansky, *IL-1 blockade in autoinflammatory syndromes.* Annu Rev Med, 2014. **65**: p. 223-44.
496. Hoffman, H.M., *Rilonacept for the treatment of cryopyrin-associated periodic syndromes (CAPS).* Expert Opin Biol Ther, 2009. **9**(4): p. 519-31.

497. Fava, A.M., et al., *Rilonacept for the treatment of recurrent pericarditis.* Expert Opin Biol Ther, 2022. **22**(1): p. 7-16.
498. Curran, M.P., *Canakinumab: in patients with cryopyrin-associated periodic syndromes.* BioDrugs, 2012. **26**(1): p. 53-9.
499. Orrock, J.E. and N.T. Ilowite, *Canakinumab for the treatment of active systemic juvenile idiopathic arthritis.* Expert Rev Clin Pharmacol, 2016. **9**(8): p. 1015-24.
500. Malcova, H., et al., *IL-1 Inhibitors in the Treatment of Monogenic Periodic Fever Syndromes: From the Past to the Future Perspectives.* Front Immunol, 2020. **11**: p. 619257.
501. Sfriso, P., et al., *Canakinumab for the treatment of adult-onset Still's disease.* Expert Rev Clin Immunol, 2020. **16**(2): p. 129-138.
502. Choudhury, R.P., et al., *Arterial Effects of Canakinumab in Patients With Atherosclerosis and Type 2 Diabetes or Glucose Intolerance.* J Am Coll Cardiol, 2016. **68**(16): p. 1769-1780.
503. Russell, K.S., et al., *A randomized, placebo-controlled trial of canakinumab in patients with peripheral artery disease.* Vasc Med, 2019. **24**(5): p. 414-421.
504. Ertuglu, L.A., et al., *A randomized controlled pilot trial of anakinra and pioglitazone for protein metabolism in patients on maintenance haemodialysis.* J Cachexia Sarcopenia Muscle, 2024. **15**(1): p. 401-411.
505. Kosmidis, M.L., et al., *The effect of anakinra, an IL1 receptor antagonist, in patients with sporadic inclusion body myositis (sIBM): a small pilot study.* J Neurol Sci, 2013. **334**(1-2): p. 123-5.
506. Nicholls, M., *CANTOS: One year on: When the findings of the CANTOS trial were unveiled at ESC Congress 2017 in Barcelona, there was a sense of hope that a new era in preventive cardiology was set to begin. One year on, CANTOS Principle Investigator and study author Paul M. Ridker discusses whether that optimism is being realized.* Eur Heart J, 2018. **39**(45): p. 3989-3990.
507. Kiltz, U., et al., *Prolonged treatment with Tadekinig alfa in adult-onset Still's disease.* Ann Rheum Dis, 2020. **79**(1): p. e10.
508. Gabay, C., et al., *Open-label, multicentre, dose-escalating phase II clinical trial on the safety and efficacy of tadekinig alfa (IL-18BP) in adult-onset Still's disease.* Ann Rheum Dis, 2018. **77**(6): p. 840-847.
509. Canna, S.W., et al., *Life-threatening NLRC4-associated hyperinflammation successfully treated with IL-18 inhibition.* J Allergy Clin Immunol, 2017. **139**(5): p. 1698-1701.
510. Wlodek, E., et al., *A pilot study evaluating GSK1070806 inhibition of interleukin-18 in renal transplant delayed graft function.* PLoS One, 2021. **16**(3): p. e0247972.

511. Hu, J.J., et al., *FDA-approved disulfiram inhibits pyroptosis by blocking gasdermin D pore formation.* Nat Immunol, 2020. **21**(7): p. 736-745.
512. Rathkey, J.K., et al., *Chemical disruption of the pyroptotic pore-forming protein gasdermin D inhibits inflammatory cell death and sepsis.* Sci Immunol, 2018. **3**(26).
513. Humphries, F., et al., *Succination inactivates gasdermin D and blocks pyroptosis.* Science, 2020. **369**(6511): p. 1633-1637.
514. Xia, L., et al., *Inhibition of Gasdermin D-Mediated Pyroptosis Attenuates the Severity of Seizures and Astroglial Damage in Kainic Acid-Induced Epileptic Mice.* Front Pharmacol, 2021. **12**: p. 751644.
515. Lu, C., et al., *Disulfiram: a novel repurposed drug for cancer therapy.* Cancer Chemother Pharmacol, 2021. **87**(2): p. 159-172.
516. Sun, L., et al., *Mixed lineage kinase domain-like protein mediates necrosis signaling downstream of RIP3 kinase.* Cell, 2012. **148**(1-2): p. 213-27.
517. Kornberg, M.D., et al., *Dimethyl fumarate targets GAPDH and aerobic glycolysis to modulate immunity.* Science, 2018. **360**(6387): p. 449-453.
518. de Vasconcelos, N.M., et al., *An Apoptotic Caspase Network Safeguards Cell Death Induction in Pyroptotic Macrophages.* Cell Rep, 2020. **32**(4): p. 107959.
519. Vande Walle, L. and M. Lamkanfi, *Drugging the NLRP3 inflammasome: from signalling mechanisms to therapeutic targets.* Nature Reviews Drug Discovery, 2024. **23**(1): p. 43-66.
520. Desu, H.L., et al., *IC100: a novel anti-ASC monoclonal antibody improves functional outcomes in an animal model of multiple sclerosis.* J Neuroinflammation, 2020. **17**(1): p. 143.
521. Bertheloot, D., et al., *Nanobodies dismantle post-pyroptotic ASC specks and counteract inflammation in vivo.* EMBO Mol Med, 2022. **14**(6): p. e15415.
522. Kayagaki, N., et al., *Inhibiting membrane rupture with NINJ1 antibodies limits tissue injury.* Nature, 2023. **618**(7967): p. 1072-1077.

Chapter 2: Aims of the work

Chapter 2: Aims of the work

Context

Duchenne muscular dystrophy (DMD) is the most frequently inherited human myopathy and the most devastating type of muscular dystrophy. Although dystrophin mutations represent the primary cause of DMD, it is the secondary processes involving persistent inflammation and subsequent impaired regeneration that likely exacerbate disease progression [1].

Over the past decade, our team has focused on the anti-inflammatory effects of Adiponectin (ApN) on the muscle [2]. ApN is a hormone abundantly secreted by adipocytes; which exhibits insulin-sensitizing, fat-burning as well as modulatory effects on oxidative stress in the skeletal muscle [3]. Previously, we demonstrated that ApN can efficiently improve the dystrophic phenotype [4]. However, its practical therapeutic application is limited. As a result, several ApN mimics have been developed such as ALY688 and AdipoRon, which are the most promising. While ALY688, a small peptide, has never been tested on cardiac nor skeletal muscle yet, AdipoRon, a synthetic molecule, already showed interesting results on mdx skeletal muscle by mitigating inflammation and oxidative stress as well as promoting the myogenic programme [5].

More recently, our research unveiled the pivotal role of the NLRP3 inflammasome in driving the chronic and severe inflammation characteristic of DMD. Indeed, by crossing mdx mice, a murine model of DMD, with Nlrp3-knockout mice, we observed a significant reduction in the overactivation of all inflammasome components. Additionally, these mice exhibited enhanced global muscle force/endurance and reduced muscle damage compared to regular mdx mice. Finally, when crossed with mice overexpressing ApN, mdx mice displayed reduced NLRP3 inflammasome activation and an improved phenotype, thus confirming the rationale for targeting NLRP3 inflammasome as a therapeutic option for DMD [6].

Objectives

Besides gene therapy, which is limited to a small set of patients harboring specific mutations [7, 8], the only medication currently used to slow down the course of DMD is glucocorticoids (GCs). Their anti-inflammatory and immunosuppressive characteristics are beneficial in the evolution of the disease [9]. Unfortunately, their prolonged usage is responsible for several adverse effects such as cushingoid facies, weight gain, glucose intolerance, growth retardation, vertebral fractures and muscular atrophy [9]. As a result, therapeutic alternatives to GCs are importantly needed.

Based on our previous results obtained on mdx mice [5, 6], we hypothesized that either a specific NLRP3 inhibitor or an ApN mimics may play a beneficial role in the pathogenesis of DMD by attenuating inflammation/oxidative stress and by possibly carrying out additional anti-fibrotic and pro-myogenic properties. To investigate whether these new treatment options could be effective for the management of DMD, we proceeded as following:

Study 1

We first examined if a targeted approach by using a selective NLRP3 inhibitor called MCC950 could be effective in mdx mice. As such, four-week-old mdx mice were orally treated for 2 months with MCC950, and compared with untreated (mdx) and wild-type (WT) mice. *In vivo* functional tests were carried out to measure the global force and endurance of mice, while *ex vivo* biochemical and molecular analyses were performed to evaluate the pathophysiology of the skeletal muscle. Finally, *in vitro* tests were conducted on primary cultures of DMD human myotubes.

We undoubtedly demonstrate that MCC950, can greatly attenuate the dystrophic phenotype in mdx mice, due to its anti-inflammatory, anti-pyroptotic and anti-fibrotic properties. By studying its mechanism of action, we also highlight GSDMD-induced pyroptosis as a novel type of programmed necrotic cell death in DMD.

Article 1:

Dubuisson N, Davis-López de Carrizosa MA, Versele R, Selvais CM, Noel L, Van den Bergh PYK, Brichard SM, Abou-Samra M. Inhibiting the inflammasome with MCC950

counteracts muscle pyroptosis and improves Duchenne muscular dystrophy; Front Immunol. 2022; 13: 1049076.

Study 2

Next, we tested if the ApN mimic called ALY688 could be sufficient to counteract DMD. To this end, four-week-old mdx mice were subcutaneously treated for two months with ALY688 and then compared to untreated mdx and WT mice. In vivo and ex vivo tests were performed to assess muscle function and pathophysiology. Additionally, in vitro tests were conducted on human DMD myotubes.

We showed that ALY688 significantly improved the physical performance of mice and exerted potent anti-inflammatory, anti-oxidative and anti-fibrotic actions on the dystrophic muscle. Additionally, ALY688 hampered myonecrosis, partly mediated by necroptosis, and enhanced the myogenic program. Some of these effects were also recapitulated in human DMD myotubes. ALY688's protective and beneficial properties were mainly mediated by the AMPK-PGC-1α axis, which led to suppression of NF-κβ and TGF-β. Our results demonstrate that an ApN mimic may be a promising and effective therapeutic prospect for a better management of DMD.

Article 2:

Dubuisson N, Versele R, Davis-López de Carrizosa MA, Selvais CM, Noel L, Planchon C, Van den Bergh PYK, Brichard SM, Abou-Samra M. The Adiponectin Receptor Agonist, ALY688: A Promising Therapeutic for Fibrosis in the Dystrophic Muscle. Cells. 2023 Aug 19;12(16):2101.

Study 3

Finally, our aim was to assess the impact of AdipoRon, another ApN mimic, on cardiac muscle. Given that cardiomyopathy is the primary cause of mortality in individuals with DMD, we sought to extend the earlier findings obtained with AdipoRon to the cardiac muscle.

To this end, we treated mdx mice with AdipoRon at 14 months of age, as cardiomyopathy develops late in life in mdx mice, at a dose of 50 mg/kg/day for 8 weeks. At the end of the treatment, 16-month-old mice were sacrificed, after having undergone an echocardiography, *in vivo* functional tests as well as ex vivo biochemical and molecular testing.

This study clearly demonstrated that AdipoRon significantly reduced markers of cardiac inflammation, oxidative stress, hypertrophy and fibrosis, while increasing those of mitochondrial biogenesis. Cardiac dysfunction and ventricular hypertrophy were also reversed in the treated group as showed by echocardiography. These effects were mainly mediated by ApN receptor-1 (AdipoR1) and CAMKK2/AMPK pathways.

Article 3:

Abou-Samra M, **Dubuisson N**, Marino A, Selvais C, Romain V, Davis-López de Carrizosa M, Noel L, Beauloye C, Horman S, and Brichard S. Striking cardioprotective effects of an Adiponectin Receptor Agonist in an aged mouse model of Duchenne Muscular Dystrophy. Submitted.

References

1. Duan, D., et al., *Duchenne muscular dystrophy.* Nature Reviews Disease Primers, 2021. **7**(1): p. 13.
2. Abou-Samra, M., Sophie Lecompte, Olivier Schakman, Laurence Noel, Marie C. Many, Philippe Gailly, and Sonia M. Brichard, *Involvement of Adiponectin in the Pathogenesis of Dystrophinopathy.* Skeletal Muscle, 2015. **5**: p. 25.
3. Abou-Samra, M., et al., *Adiponectin and Its Mimics on Skeletal Muscle: Insulin Sensitizers, Fat Burners, Exercise Mimickers, Muscling Pills … or Everything Together?* Int J Mol Sci, 2020. **21**(7).
4. Abou-Samra, M., Raphaël Boursereau, Sophie Lecompte, Laurence Noel, and Sonia M. Brichard, *Potential Therapeutic Action of Adiponectin in Duchenne Muscular Dystrophy.* The American Journal of Pathology 2017. **187**(7): p. 1577–85.
5. Abou-Samra, M., et al., *AdipoRon, a new therapeutic prospect for Duchenne muscular dystrophy.* J Cachexia Sarcopenia Muscle, 2020. **11**(2): p. 518-533.
6. Boursereau, R., et al., *Downregulation of the NLRP3 inflammasome by adiponectin rescues Duchenne muscular dystrophy.* BMC Biol, 2018. **16**(1): p. 33.
7. Jones, D., *Duchenne muscular dystrophy awaits gene therapy.* Nat Biotechnol, 2019. **37**(4): p. 335-337.
8. Elangkovan, N. and G. Dickson, *Gene Therapy for Duchenne Muscular Dystrophy.* J Neuromuscul Dis, 2021. **8**(s2): p. S303-s316.
9. Matthews, E., et al., *Corticosteroids for the treatment of Duchenne muscular dystrophy.* Cochrane Database Syst Rev, 2016. **2016**(5): p. Cd003725.

Chapter 3: Results

Chapter 3: Results

Study 1

Inhibiting the inflammasome with MCC950 counteracts muscle pyroptosis and improves Duchenne muscular dystrophy

Nicolas Dubuisson[1,2*†], Maria A. Davis-López de Carrizosa[1,3†], Romain Versele[1], Camille M. Selvais[1], Laurence Noel[1], Peter van den Bergh[2], Sonia M. Brichard[1] and Michel Abou-Samra[1]

[1] Endocrinology, Diabetes and Nutrition Unit, Institute of Experimental and Clinical Research (IREC), Medical Sector, Université Catholique de Louvain (UCLouvain), Avenue Hippocrate 55, 1200 Brussels, Belgium;
[2] Neuromuscular Reference Center, Department of Neurology, Cliniques Universitaires Saint-Luc, Avenue Hippocrate 10, 1200 Brussels, Belgium
[3] Departamento de Fisiología, Facultad de Biología, Universidad de Sevilla, 41012 Seville, Spain

†: These authors contributed equally to this work and share first authorship

***Corresponding author:**
Nicolas Dubuisson
E-mail : nicolas.j.dubuisson@uclouvain.be

Keywords: Duchenne muscular dystrophy, NLRP3 Inflammasome, Gasdermin, N-GSDMD, Pyroptosis, Muscle inflammation, MCC950.

Abstract

Background

Duchenne muscular dystrophy (DMD) is the most common inherited human myopathy. Typically, the secondary process involving severe inflammation and necrosis exacerbate disease progression. Previously, we reported that the NLRP3 inflammasome complex plays a crucial role in this disorder. Moreover, pyroptosis, a form of programmed necrotic cell death, is triggered by NLRP3 via gasdermin D (GSDMD). So far, pyroptosis has never been described either in healthy muscle or in dystrophic muscle. The aim of this study was to unravel the role of NLRP3 inflammasome in DMD and explore a potentially promising treatment with MCC950 that selectively inhibits NLRP3.

Methods

Four-week-old mdx mice (*n*=6 per group) were orally treated for 2 months with MCC950 (mdx-T), a highly potent, specific, small-molecule inhibitor of NLRP3, and compared with untreated (mdx) and wild-type (WT) mice. *In vivo* functional tests were carried out to measure the global force and endurance of mice. *Ex vivo* biochemical and molecular analyses were performed to evaluate the pathophysiology of the skeletal muscle. Finally, *in vitro* tests were conducted on primary cultures of DMD human myotubes.

Results

After MCC950 treatment, mdx mice exhibited a significant reduction of inflammation, macrophage infiltration and oxidative stress (-20 to -65%, $P<0.05$ *vs* untreated mdx). Mdx-T mice displayed considerably less myonecrosis (-54%, $P<0.05$ *vs* mdx) and fibrosis (-75%, $P<0.01$ *vs* mdx). Moreover, a more mature myofibre phenotype, characterized by larger-sized fibres and higher expression of mature myosin heavy chains 1 and 7 was observed. Mdx-T also exhibited enhanced force and resistance to fatigue (+20 to 60%, $P<0.05$ or less). These beneficial effects resulted from MCC950 inhibition of both active Caspase-1 (-46%, $P=0.075$) and cleaved gasdermin D (N-GSDMD) (-42% in medium-sized-fibres, $P<0.001$). Finally, the anti-inflammatory action and the anti-pyroptotic effect of MCC950 were also recapitulated in DMD human myotubes.

Conclusion

Specific inhibition of the NLRP3 inflammasome can significantly attenuate the dystrophic phenotype. A novel finding of this study is the overactivation of GSDMD, which is hampered by MCC950. This ultimately leads to less inflammation and pyroptosis and to a better muscle maturation and function. Targeting NLRP3 might lead to an effective therapeutic approach for a better management of DMD.

Introduction

Duchenne muscular dystrophy (DMD) is the most common inherited myopathy and one of the most severe muscle-wasting diseases eventually leading to wheel chair, assisted ventilation and premature death [1]. DMD is caused by mutations in the gene encoding dystrophin, a key scaffolding protein that provides structural stability and integrity to muscle fibre membrane. Dystrophin-deficient fibres are highly susceptible to injury, resulting in endless cycles of muscle necrosis and repair that lead to fibrosis and weakness [2]. Although dystrophin mutations represent the primary cause of DMD, it is the secondary processes involving persistent inflammation and necrosis that likely exacerbate disease progression [3, 4].

The NLRP3 inflammasome plays a pivotal role in diseases resulting from sterile and excessive inflammatory responses [5, 6]. Upon activation, NLRP3, a sensor of the innate immune system that belongs to the NOD-Like receptor family (NLR), oligomerizes with an adaptor (ASC) forming intracellular signalling hubs that activate caspase-1. Caspase-1 then cleaves two pro-inflammatory cytokines into their mature forms (IL-1β and IL-18) and gasdermin D (GSDMD) into its active effector. Next, released GSDMD generates pores in the plasma membrane, thereby leading to pyroptosis, a necrotic cell death type [5, 7] and ultimately facilitating the release of mature inflammatory cytokines. We have shown that the inflammasome is overactivated in dystrophic mouse muscle as well as in myotubes from DMD patients. Moreover, genetic inactivation of Nlrp3 markedly attenuates the dystrophic phenotype in mdx mice, a murine model of DMD [3]. Targeting the inflammasome through highly potent, selective, small molecule inhibitors could thus be a promising approach for such a devastating disease.

The recently discovered molecule MCC950, is an extremely potent and selective inhibitor of NLRP3 [8-10]. It proved to be successful in animal models characterised by some degree of sterile inflammation like atherosclerosis, colitis, cerebral ischemia or cholestatic liver injury [11-14]. It also attenuated some biological and clinical features in a mouse model exhibiting a very rare syndrome due to an aberrant host Valosin-Containing Protein (VCP) and combining inclusion body myopathy with bone and cerebral lesions [15]. However, in this model, the improvement in some organs may have indirect repercussions on the others. As yet, pharmacological blockade of the inflammasome has not been investigated in DMD, although NLRP3 plays a key pathogenic role in this muscular disease.

The aim of this work was to explore whether inflammasome blockade by MCC950 may play a beneficial role in DMD. To this end, MCC950 was orally administered for a period of 2 months, very early in mdx mice because muscle degenerative-regenerative cycles begin as soon as 3–4 weeks of age [16]. We first examined whether treated mdx mice exhibited improved muscular function together with lower degree of skeletal muscle inflammation, oxidative stress, necrosis and fibrosis. We then unravelled the mechanisms underlying the potential beneficial effects brought about by MCC950. Finally, we examined whether some of these effects may be recapitulated in human by using primary cultures of DMD myotubes.

Materials and Methods

Animals

C57BL/10ScSn-*Dmd*^{mdx}J mdx mice (murine model of DMD) and C57BL/10ScSnJ mice [used as wild-type (WT) controls] were purchased from Jackson Laboratory (Maine, USA). Three groups of male mice (n = 6 per group) were compared. At 4 weeks of age, each group received solid drink, replacing the water bottles. The first group was WT mice, the second group consisted of untreated mdx mice (mdx), while the third group was composed by treated mdx mice (mdx-T). This last group received MCC950 (40 mg/kg/day for 4 weeks, then 80 mg/kg/day for another 4-week period) (Avistron chemistry, Cornwall, UK) added to a solid drink, which was replaced every day. The choice of MCC950 dosage and duration was based on current literature and our preliminary experiments [15, 17]. Animals were maintained under a standard laboratory chow and housed at a constant temperature (22°C) with a fixed 12 h light to 12 h dark cycle (lights on from 7 a.m. to 7 p.m.). 12-week-old mice were sacrificed between 09.00 and 11.00 h. Pairs of *tibialis anterior* (TA) and *quadriceps* (Q) muscles were weighed, frozen in liquid nitrogen, and stored at −80°C for subsequent analyses.

In vivo studies of global force and resistance

At week 11 (i.e., 1 week prior to sacrifice), mice were submitted to two widely used and reliable functional tests [2, 3, 18].

Wire test. Mice were suspended by their limbs from a wire and the time until they completely released their grasp and fell was recorded. Mice that reached a set limit of 600 seconds were allowed to stop the experiment, while others were directly retested, up to three times, and their maximum hanging time was recorded. The holding impulse (body mass x hang time), used to oppose the gravitational force, was then calculated [18][18][18][18][18][18].

Grip test. Limb strength was recorded using a grid connected to a sensor (Panlab-Bioseb, Vitrolles, France). Mice were gently laid on the top of a grid so that their front paws could grip the grid. Mice were then pulled back steadily until the grip was released down the complete length of the grid. Each test was repeated three times at an interval of 15 min. Results are presented as the mean of the three values of force recorded, related to body weight [2].

Bright-field histochemistry

Tibialis anterior muscles (TA) were fixed in 10% formalin for 24 h and embedded in paraffin. Immunohistochemistry was carried out as previously described [2] using antibodies directed against cluster of differentiation 68 (CD68), 4-hydroxy-2-nonenal (HNE), interleukin 1-beta detecting mature and precursor form (IL-1β), interleukin 18 detecting only mature form (IL-18), peroxiredoxin 3 (PRDX3), and tumor necrosis factor alpha (TNFα) (supplementary information, Table S1). Whole muscle sections were scanned, and then the optical density of diaminobenzidine (DAB, ThermoFisher-Scientific, Waltham, MA, USA) deposits (IL-1β, TNFα, HNE and PRDX3) or the percentage of stained areas (IL-18, CD68) was quantified using Fiji (NIH, Maryland, USA). TA sections were also stained with haematoxylin and eosin. In addition, *Quadriceps* (Q) sections (described below) were stained with Picro-Sirius red (Abcam, Cambridge, UK) to evaluate muscle fibrosis. Fibrotic tissue was scored setting a color balance threshold and data obtained were expressed as the percentage of total section area.

Immunofluorescence and morphometry

Quadriceps (Q) muscles were embedded in optimum cutting temperature medium (OCT; VWR International, Dublin, Ireland) and frozen in liquid nitrogen chilled isopentane (Sigma-Aldrich, St. Louis, MO, USA). 10 µm transversal cryosections were fixed with 4% paraformaldehyde and blocked with 10% goat serum. Antibodies directed against CD68, CD206, IL-1β, laminin, embryonic myosin heavy chain 3 (Myh3), and the cleaved form of gasdermin (N-GSDMD) [19], were used. Mouse IgG-AF488 was used for the detection of necrotic myofibres (Table S1). Secondary antibodies were AF488 and AF647-conjugated goat anti-rabbit or anti-rat (Sigma-Aldrich), respectively. Finally, nuclei were stained with DAPI (ThermoFisher-Scientific). Negative controls were performed by omission of the primary antibody. Images were acquired with an epifluorescence (AXIO-observerZ1, Zeiss, Germany) or a confocal microscope (LSM800, Zeiss) for N-GSDMD, and staining was quantified with Fiji.

Total number of macrophages was quantified as the number of CD68 stained particles per field. The proportion of M2 over the total number of macrophages was assessed calculating the ratio of CD68-CD206 double positive cells over CD68-only positive cells as described [20]. IL-1β was quantified as the mean grey value of muscle section after background subtraction, and IgG uptake as the percentage of stained area per field after applying a fixed detection threshold. Myh3^{+} fibres were counted and expressed as percentage of the total number of fibres per field. N-GSDMD density (number of N-Gasdermin^{+} particles per 100 µm^{2}) was quantified for each fibre and evaluated according to fibre size (see below). Totally 396, 1337 and 1378 fibres were analysed for WT, mdx and mdx-T groups respectively. Difference in fibres analysed between WT and the other two groups was explained by the higher number of small-sized fibres in dystrophic muscles (see later).

Fibre size assessed by cross-sectional area (CSA) and minimum Feret's diameter (MFD), and centrally nucleated fibres (CNF) were calculated using a personalized version of MuscleJ [21] based on the automatic detection of laminin and DAPI immunofluorescence. Approximately 6500 fibres per group were quantified. Fibres were then assigned to one of three categories based on their size [small (S), medium (M) or large (L)]. Middle-sized fibres were defined as ranging from the 10th to the 90th percentile (P) of WT fibre size distribution, whereas other fibres were categorized as small (below P10; <33µm) and large (above P90; >74µm), respectively.

Culture of human myotubes

Primary cultures of human skeletal muscle cells were initiated from myoblasts of DMD patients (n = 4; age range: 12–15 years), which were provided by the French Telethon Myobank-AFM. Myoblasts were grown in DMEM/F-12 supplemented with 20% fetal bovine serum (FBS), 1% L-Glutamine, 1% non-essential amino acids and 1% penicillin-streptomycin (all from ThermoFisher-Scientific) at 37 °C in 5% CO2. After reaching a density of 80-90%, the growth medium was replaced with a fusion medium, where 20% FBS was replaced by 2% horse serum, and differentiation was allowed to continue for 14 days (time required to obtain mature myotubes with characteristic elongated and multinucleated morphology). Medium was changed every other day. Cells were always used at passages between 4 and 10. At day 14, myotubes were pre-treated or not with MCC950 (10 µM) for 24 h, while being challenged or not with human recombinant TNFα (15 ng/mL) + human interferon gamma (IFNγ) (15 ng/mL) (both from PeproTech, New Jersey, USA) for the last 22 h and then stimulated with ATP (5mM) (Roche, Basel, Switzerland) for the last 2 h.

RNA extraction and real-time quantitative PCR

RNA was isolated from muscle tissues or from cultured cells with TriPure reagent (Sigma-Aldrich). RT-qPCR primers for mouse cyclophilin, NLRP3 and ASC were used as previously reported [3]. New mouse primer sequences were transforming growth factor beta (TGFβ) (Table S2). RT-qPCR primers for human TATA box-binding protein (TBP), TNFα, and IL-1β, were also similar to those previously reported [22]. New human primer sequences were IL-18 (Table S2). Threshold cycles (Ct) were measured in duplicate.

Protein extraction

Muscle samples and cultured cells were homogenized in a lysis buffer supplemented with 1% protease/phosphatase inhibitor cocktail (both from Cell Signaling Technology, Leiden, The Netherlands) and 10 mM NaF (Sigma-Aldrich). Proteins were quantified using the Bradford method and 10–150 µg of total protein extracts were used for each analysis.ELISA assays were used to specifically detect and quantify Utrophin A (UTRN) (Antibodies Online, Atlanta, USA), the active forms (phosphorylated form) of Smad2, of p65 subunit of nuclear factor-kappa B (NF-κB) (both from Cell Signaling Technology) and of N-GSDMD (MyBiosource, San Diego, USA). Kits were based on colorimetric methods and were carried out following manufacturer's instructions.Immunoblotting was performed, as reported [3], by using a rabbit polyclonal antibody directed against pro-caspase 1 (46 kDa) and cleaved caspase 1 (20 kDa) (Bio-connect, Huissen, The Nederlands). Signals were revealed by enhanced chemiluminescence, then quantified and normalized to total proteins of each corresponding lane detected with Ponceau staining (Figure S1) [23], using Fiji.

Statistical analysis

Results are means ± standard error of mean (SEM) for the indicated number of mice or human subjects. When the three groups of mice (WT, mdx, and mdx-T) were compared, the effects of MCC950 were assessed by one-way analysis of variance followed by Tukey's test. When four cell cultures conditions were compared, the effects of MCC950 and inflammation were assessed by two-way analysis of variance (raw paired data for each subject) followed by post hoc Sidak's multiple comparisons. In some cases, comparisons between the treated group and its respective control were carried out using two-tailed paired or unpaired Student's *t*-test. All statistical analyses were performed with Prism 9 (GraphPad Software, Inc., San Diego, CA). Differences were considered statistically significant at $P < 0.05$.

Results

MCC950 does not affect muscle mass while it improves muscle function

MCC950 was administered orally to mdx mice for 2 months, starting at 4 weeks of age. Mdx littermates were thus separated into two groups: those who received a daily dose of MCC950 (mdx-T) and those who were left untreated (mdx). Both groups were also compared with untreated wild-type (WT) control mice. MCC950 treatment did affect neither the total body weight of dystrophic mice, nor the weight of removed muscles (*Tibialis anterior* (TA) and *Quadriceps* (Q), data not shown).

In order to evaluate the effects of MCC950 on muscle function, mice were subjected to two functional tests *in vivo*: the wire test and the grip test. The wire test gives an indication on muscle force and resistance to fatigue. In this test, the time during which the mouse is suspended on a horizontal wire is measured. Mdx mice fell down faster than WT mice, while mdx-T ones showed intermediate resistance (+60% *vs* mdx) (Figure 1A). The grip test measures strength of limb muscles. The force developed by forelimbs was lower in mdx mice than in WT ones, while it was partially rescued by MCC950 treatment (+20% *vs* mdx) (Figure 1B). These data indicate enhanced force and resistance to fatigue in dystrophic muscle under MCC950 treatment.

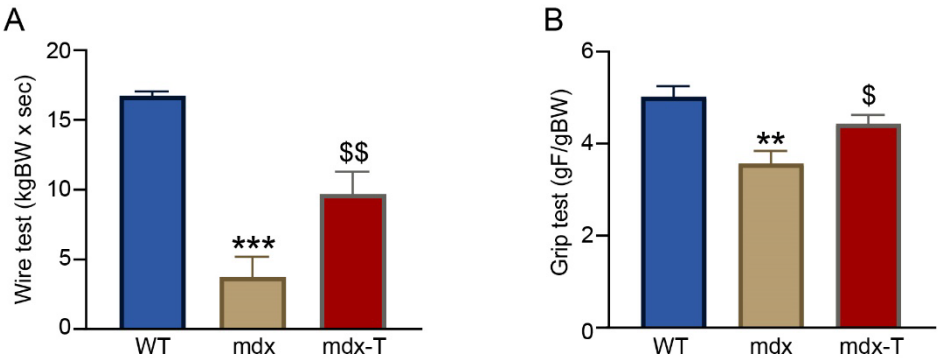

Figure 1. MCC950 treatment improves global force and resistance of mdx mice. *Three groups of mice were compared at the age of 11 weeks: WT, mdx (untreated) and mdx-T (mdx treated with MCC950) mice. Functional tests were carried out in vivo.* ***(A)*** *Mice were subjected to a wire test where they were suspended by their limbs and the time until they completely released the wire and fell was registered (seconds). This time was then normalized to body weight (kgBW x sec).* ***(B)*** *Mice were lowered on a grid connected to a sensor to measure the muscle force of their forelimbs; data were then expressed in gram-*

force relative to gram-body weight (gF/gBW). Data are means ± SEM; n = 6 mice per group for all experiments. Statistical analysis was performed using one-way ANOVA followed by Tukey's test. * *P < 0.05,* ** *P < 0.01,* *** *P < 0.001 vs WT mice.* $^{\$}P < 0.05$, $^{\$\$}P < 0.01$ *vs* mdx mice.

MCC950 effectively reduces muscle inflammation and oxidative stress

We tested the hypothesis that oral administration of MCC950 could slow down the progression of the dystrophic pathology by counteracting excessive inflammatory and oxidative reactions. When compared to WT mice, myofibres from TA muscles of mdx mice displayed a strong immunolabeling for the inflammatory cytokines, IL-1β and IL-18 (Figure 2A). Quantification of DAB staining confirmed that IL-1β and IL-18 immunolabeling was much higher in mdx than in WT mice (Figure 2B). Qualitatively, similar results were observed for TNFα, another main inflammatory cytokine and for CD68, a pan-macrophage marker. Accordingly, massive inflammatory infiltrates were observed within dystrophic muscle after haematoxylin and eosin staining (Figure S2). Like pro-inflammatory markers, two oxidative stress markers (HNE, a lipid peroxidation product and PRDX3, an antioxidant enzyme), were increased in mdx mice.

In mdx-T mice, all these markers of inflammation or oxidative stress were either significantly decreased compared to regular mdx (IL-1β: -25%; CD68: -64%; HNE: -18%) or were not (or less) significantly different from those of WT ones (Figure 2A,B).

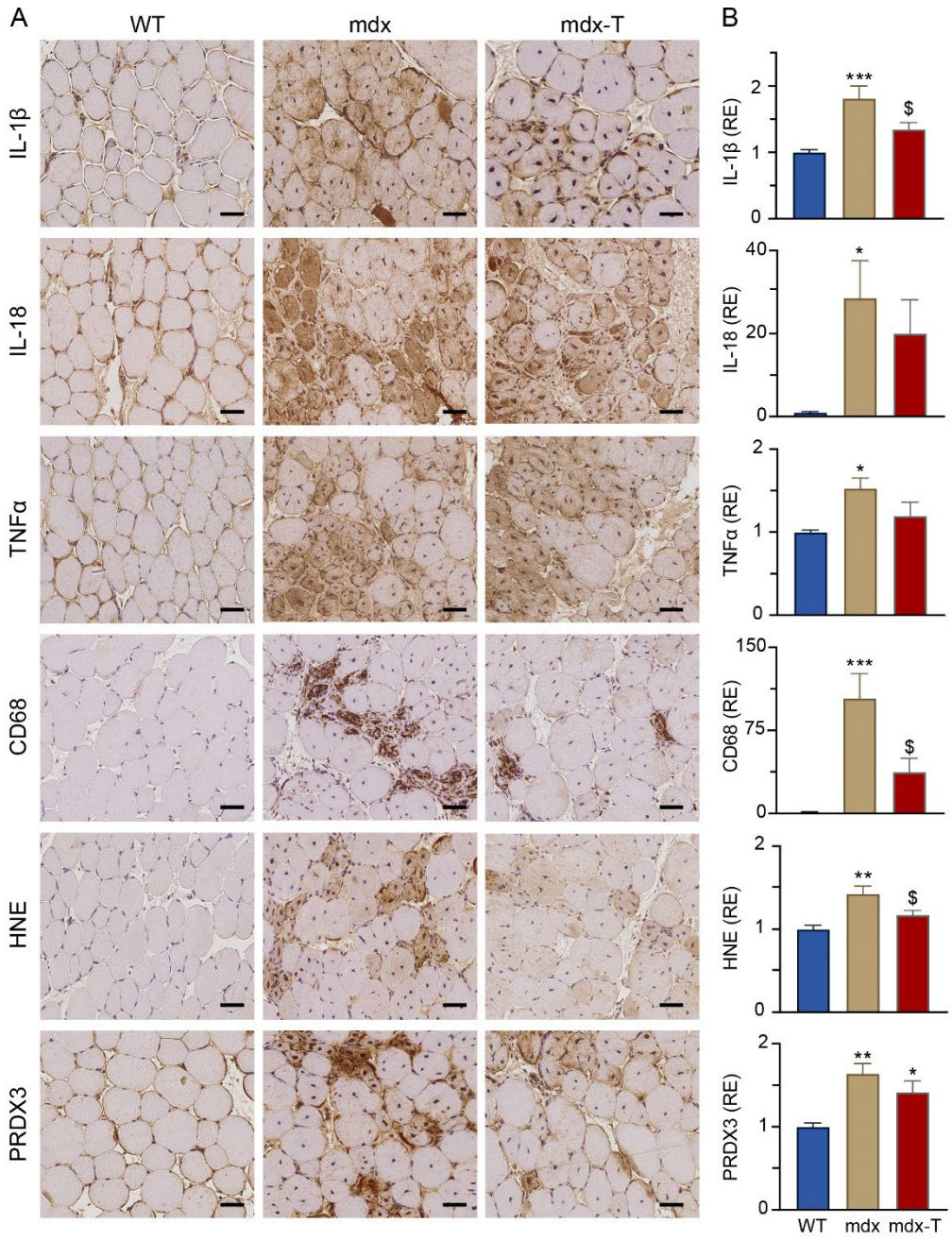

Fig.2 MCC950 treatment reduces muscle inflammation and oxidative stress in mdx mice. *Immunohistochemistry was performed on Tibialis anterior muscle (TA) of the 3 groups of mice.* ***(A)*** *Sections were stained with specific antibodies directed against three pro-*

inflammatory cytokines (IL-1β, IL-18 and TNFα), one pan-macrophage marker (CD68) and two oxidative stress markers (HNE and PRDX3). Representative sections for 6 mice per group are shown. Scale bars = 50 µm. ***(B)*** *Quantification of inflammation and oxidative stress markers. Data are presented as relative expression (RE) compared to WT values and are means ± SEM; n = 6 mice per group for all experiments. Statistical analysis was performed using a one-way ANOVA followed by Tukey's test.* $^{*}P < 0.05$, $^{**}P < 0.01$, $^{***}P < 0.001$ *vs WT mice.* $^{\$}P < 0.05$ *vs mdx mice.*

MCC950 slows down the necrosis-regeneration turnover in dystrophic muscle

We next tested the idea that MCC950 could curb the necrosis-regeneration turnover, which is otherwise accelerated in the dystrophic muscle. For these experiments, we performed immunofluorescence on serial Q sections for the three first labellings (Figure 3A). As in TA (see Figure 2), mdx mice showed a strong immunostaining for CD68 (detected as stained particles) and for IL-1β, both of which tended to decrease in mdx-T animals (Figure 3B). Likewise, the percentage of necrotic areas assessed by the uptake of mouse IgG, a well-known marker of membrane leakage [24], was markedly increased in mdx mice but was reduced to WT values in mdx-T ones (Figure 3B). Moreover, areas that were positive for CD68 and IL-1β were also positive for IgG, indicating an interplay between macrophage infiltration, IL-1β production and necrosis that clusters in the same muscle subareas.

In other Q sections, we also showed that among CD68 positive macrophages, the portion of CD206 positive cells, a specific marker of M2 macrophages [25], was significantly increased in mdx-T mice in comparison with untreated mice. This indicates a potential switch in macrophage polarisation towards an anti-inflammatory phenotype (Figure 3A).

We next quantified the expression of embryonic myosin heavy chain 3 (Myh3), a marker of early muscle regeneration [26]. This myosin type is usually expressed during development but can be transiently re-expressed in adult muscle upon injury [26]. As expected, there was almost no embryonic positive myofibres in WT mice, while mdx mice displayed approximately 25% of immuno-positive fibres, a percentage that decreased to <10% in treated animals (Figure 3A,B).

Taken together, these data indicate that mdx mice displayed large inflammatory and necrotic areas combined with early embryonic regenerating myofibres. All of which were markedly attenuated under treatment.

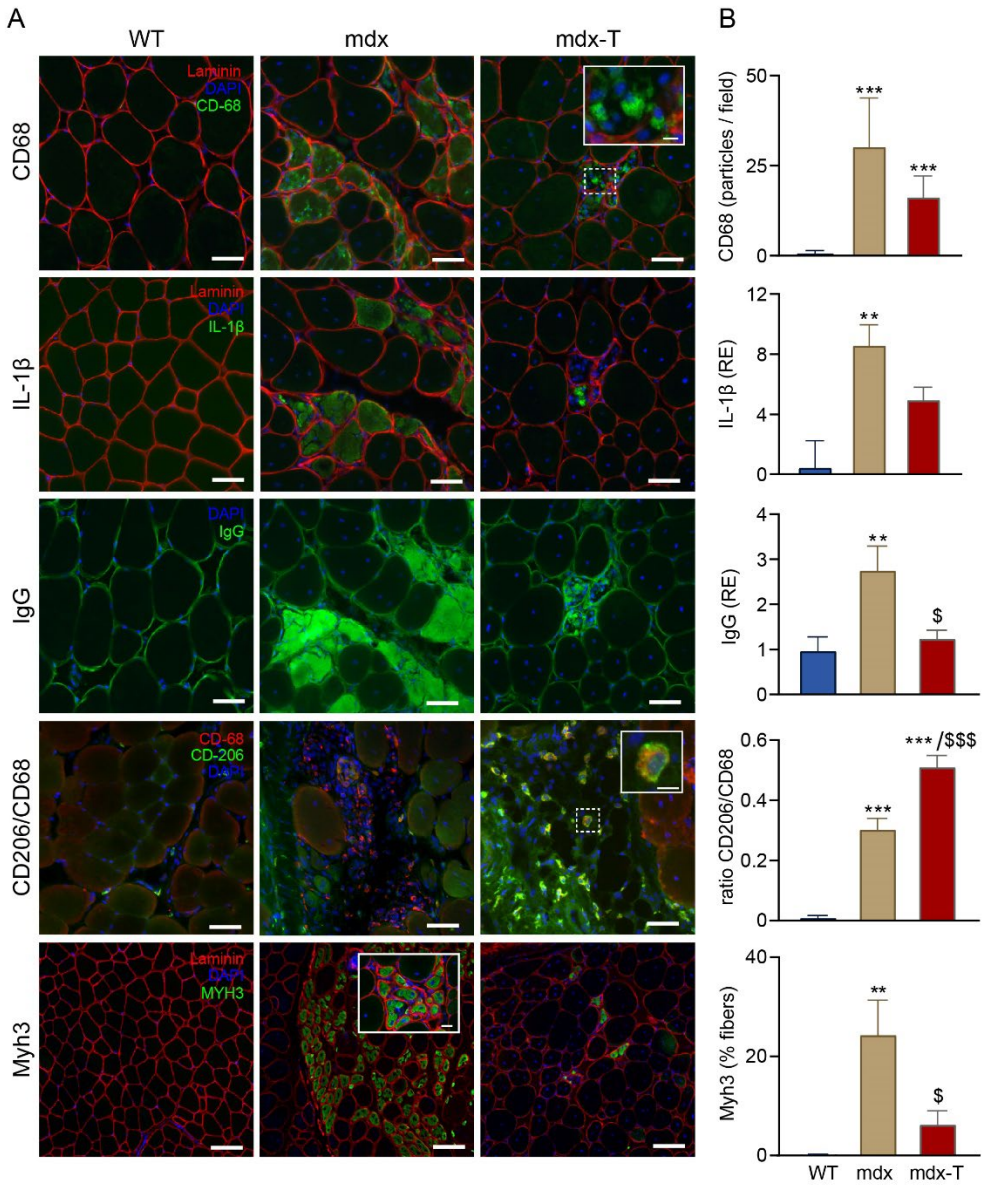

Fig.3 MCC950 treatment curbs the accelerated necrosis-regeneration turn-over of mdx mice. *Immunofluorescence staining was performed in Quadriceps muscle (Q) from the 3 groups of mice.* ***(A)*** *Sections were stained with specific antibodies directed against CD68, IL-1β, mouse IgG, CD206 and MyH3 (all in green). Laminin antibody was used to delineate basal membrane (red). Nuclei were counterstained with DAPI (blue). The first three immunolabellings (CD68, IL1-β and IgG) were performed on serial cross sections. Scale bars = 50 µm (CD68, IL-1β, IgG and CD206) and 100 µm (Myh3). Insets: higher magnification of*

$CD68^+$ and $CD206^+$ macrophages (scale bars = 10µm) and $Myh3^+$ fibres (scale bars = 20 µm). ***(B)*** *Quantification of CD68, IL-1β, mouse IgG, CD206 and MyH3. Results for CD68 and Myh3 are shown as number of positive particles and % of positive fibres, respectively. IL1-β and IgG uptake are presented as relative expression (RE) compared to WT values. CD206 is represented as the ratio of CD206+/CD68+. Data are means ± SEM; n = 6 mice per group for all experiments.* Statistical analysis was performed using one-way ANOVA followed by Tukey's test. $^{**}P < 0.01$, $^{***}P < 0.001$ *vs* WT mice. $^{\$}P < 0.05$, $^{\$\$\$}P < 0.001$ *vs* mdx mice.

MCC950 treatment enhances muscle fibre size and maturation in mdx mice.

In line with the observation that newly regenerating fibres are small in size [27], average myofibre size measured either CSA or MFD was decreased in mdx mice but was not different in mdx-T animals compared to WT ones (Figure 4A). Moreover, fibre distribution based on MFD indicates that the percentage of small (S) myofibres was higher in mdx than in WT mice (Figure 4B), with a significant reduction in mdx treated mice compared to regular mdx (Figure 4C, Pale red *vs* pale beige pie charts).

However, the proportion of fibres with central nuclei (CNF), a hallmark of fibres that have undergone regeneration, which was almost undetectable in WT mice, remained similarly elevated in mdx mice whether treated or not (Figure 4D). Yet, this marker does not discriminate between fibres at the early or late stage of regeneration [28]. Because mdx-T mice have globally larger fibres than regular mdx (Figure 4A), with less staining for Myh3, we speculated that the regeneration process was more complete under MCC950. We thus measured the expression of mature forms of myosin heavy chain such as Myh1 and Myh7. Accordingly, mRNA abundance of Myh1, a marker of fast-twitch glycolytic type II fibres, tended to be increased in mdx-T mice compared to untreated ones (+32%; Figure 4E). Likewise, Myh7, a marker of slow-twitch oxidative type I fibres, was augmented in mdx-T mice compared to control WT (3.5-fold), while there was no significant difference between regular mdx and WT mice (Figure 4F).

Taken together, these results indicate that mdx-T mice exhibited a significant reduction of necrotic areas requiring fewer regenerating fibres, which develop a more mature phenotype.

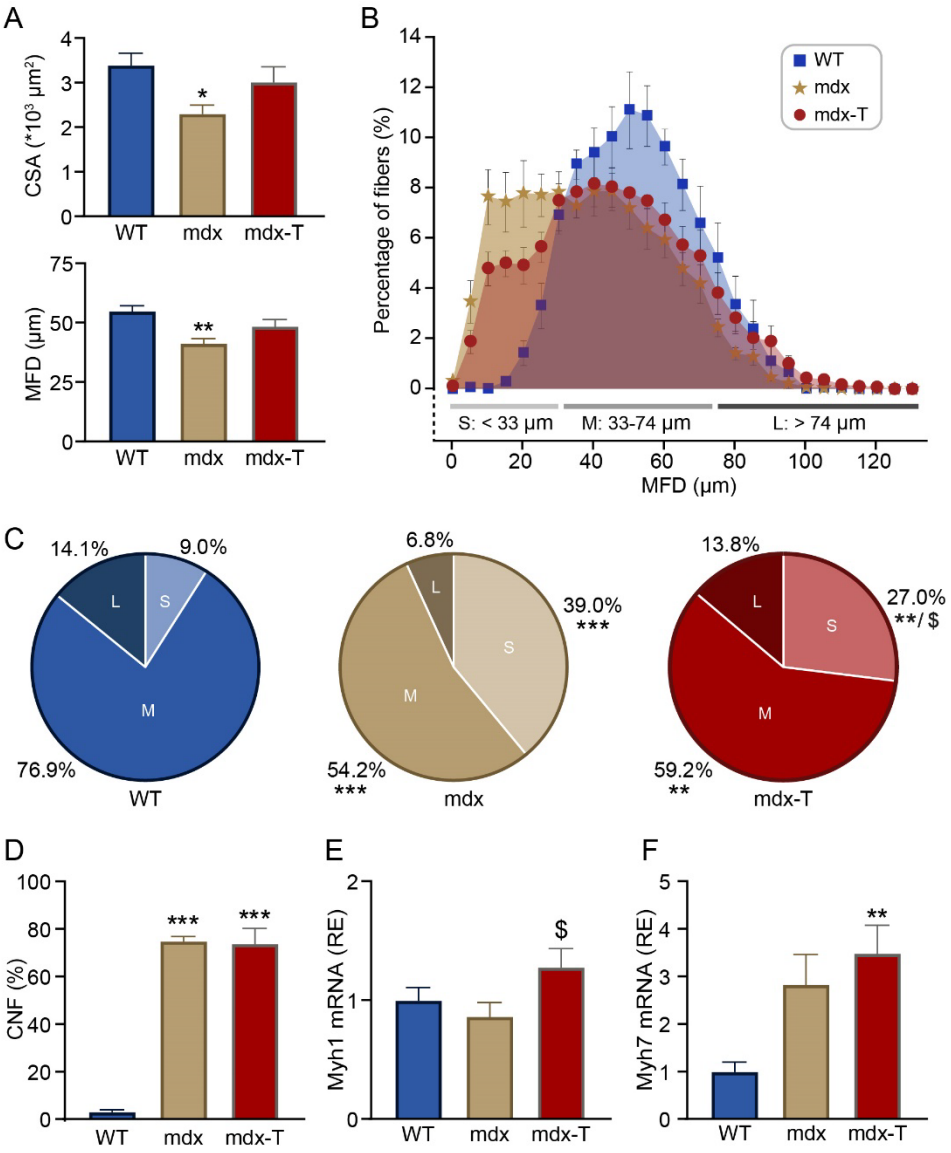

Fig.4 MCC950 treatment enhances muscle fibre size and maturation in mdx mice. (A) *Quantification of global fibre size based on cross-sectional area (CSA) or minimum Feret's diameter (MFD) in Q sections from the 3 groups of mice.* ***(B)*** *Overall distribution of fibre MFD. Data are expressed as percentage of myofibres in bins of 5 µm each. Fibres were classified into three categories based on their size [small (S), medium (M) or large (L)].* ***(C)*** *Pie chart representing the percentage of small (pale), middle-sized (regular) and large myofibres (dark) for each group.* ***(D)*** *Quantification of the percentage of central nucleated fibres (CNF) per field.* ***(E,F)*** *mRNA levels of Myh1 and Myh7, markers of glycolytic and oxidative muscle*

fibres, respectively. These levels were normalized to cyclophilin A, and subsequent ratios were presented as relative expression compared to WT values. Data are means ± SEM; n = 6 mice per group for all experiments. Statistical analysis was performed using one-way ANOVA followed by Tukey's test ***(A-D, F)*** *or unpaired two-tailed t-test* ***(E)****. *P < 0.05, **P < 0.01, ***P < 0.001, vs WT mice, $P < 0.05, vs mdx mice.*

MCC950 attenuates fibrosis in mdx mice

Because inflammation and fibrosis can be viewed as a continuum of events within the framework of tissue defence, repair and regeneration, we next tested whether oral administration of MCC950 could decrease fibrosis in dystrophic muscle. Mdx muscle displayed a strong staining for Picro-Sirius red, a marker of fibrosis labelling collagen I and III. Yet, the percentage of fibrotic areas was reduced by ~75% in mdx-T mice (Figure 5A,B).

In addition, mRNA levels of TGFβ, a highly pleiotropic cytokine playing an important role in wound healing and inducing the production of extracellular matrix, were increased in mdx mice, while these levels were decreased by ~35% in mdx-T ones (Figure 5B).

We then measured Phosphorylated-Smad2 (P-Smad2), an effector protein being part of the TGFβ pathway, which is also a marker of muscle fibrosis. Likewise, mdx mice showed higher P-Smad2 protein levels in comparison with WT mice. Conversely, these levels were significantly diminished in mdx-T mice (~25%) (Figure 5B).

Taken together, these results indicate that mdx-T mice displayed a significant reduction of factors responsible for the fibrotic transition of myofibres, suggesting an anti-fibrotic potential for MCC950.

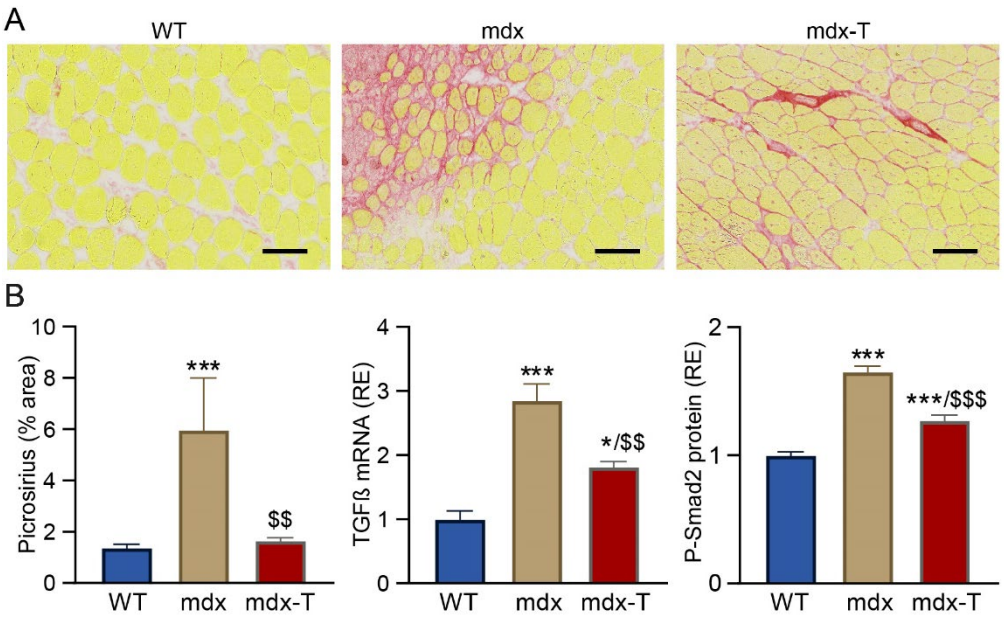

Fig.5 MCC950 treatment markedly reduces muscle fibrosis in mdx mice. *Experiments were performed on Q from the three groups of mice.* ***(A)*** *Picro-Sirius red staining.* ***(B)*** *Quantification of picro-Sirius red staining (expressed as % area). Scale bars = 200 µm. mRNA levels of TGFβ, a marker of extracellular matrix production. These levels were normalized to cyclophilin A. ELISA assay was used to quantify phosphorylated-Smad2 (P-Smad2). Results for TGFβ and P-Smad2 were then presented as relative expression compared to WT values. Data are means ± SEM; n = 6 mice per group for all experiments. Statistical analysis was performed using one-way ANOVA followed by Tukey's test. *P < 0.05, ***P < 0.001 vs WT mice. $^{\$\$}$P < 0.01, $^{\$\$\$}$P < 0.001 vs mdx mice.*

MCC950 exerts its effect by acting on key effectors of the inflammasome complex and on utrophin A, in mdx mice

On activation, NLRP3 oligomerizes with ASC, forming intracellular signalling hubs that activate caspase-1. Caspase-1 then generates the mature forms of pro-inflammatory cytokines (IL-1β and IL-18) and cleaves GSDMD, triggering pyroptosis. As MCC950 directly inactivates NLRP3 [9, 10], we explored its action on the two main effectors of the inflammasome complex: active Caspase-1 and N-GSDMD.

Firstly, we measured active Caspase-1 by Western blotting. The dominant subunit of active caspase-1 has recently been shown to be full-length p46 [29]. Our results confirm that p46 was strikingly elevated in mdx mice while it was reduced by ~45% in treated animals. Its cleaved product p20 follows a similar pattern with a rise in mdx mice and a ~45% decrease (though not significant) under MCC950 (Figure 6A).

Secondly, we studied the active form of gasdermin D (i.e. its cleaved N-GSDMD fragment), a gold standard marker to detect pyroptosis [19]. N-GSDMD was detected by immunofluorescence as stained green particles mainly located close to the sarcolemma. These particles were more abundant in mdx-mice (whether treated or not) than in WT ones (Figure 6B,C). N-GSDMD density was also inversely related to fibre size, being predominant in small and medium dystrophic myofibres while being almost absent in larger ones. Mdx-T mice exhibited a significant reduction of N-GSDMD density in medium sized-fibres compared to regular mdx, thereby suggesting a reduction of pyroptosis (Figure 6D).

As reduced action of caspase-1 and N-GSDMD should in turn reduce the activity of the transcription factor NF-κB, a master regulator of inflammation, we measured this parameter under MCC950 treatment. As expected, the active phosphorylated form of the p65 subunit of NF-κB was increased about two-fold in mdx mice, while it was reduced by 34% in mdx-T ones (Figure 6E). NF-κB serves as a priming signal that upregulates several inflammasome components. Accordingly, mRNA levels of NLRP3 were drastically increased in mdx mice and showed a tendency towards reduction in treated animals (Figure 6E). Likewise, mRNA levels of ASC were decreased after treatment (Figure 6E). Eventually, we measured Utrophin A (UTRN), an analogue of dystrophin that can help rescue the dystrophic phenotype [2, 30]. Accordingly, UTRN protein levels were slightly augmented in mdx mice, likely to compensate for the lack of dystrophin. These levels were further increased in mdx-T mice, possibly as a result of lower inflammation [31] (Figure 6E).

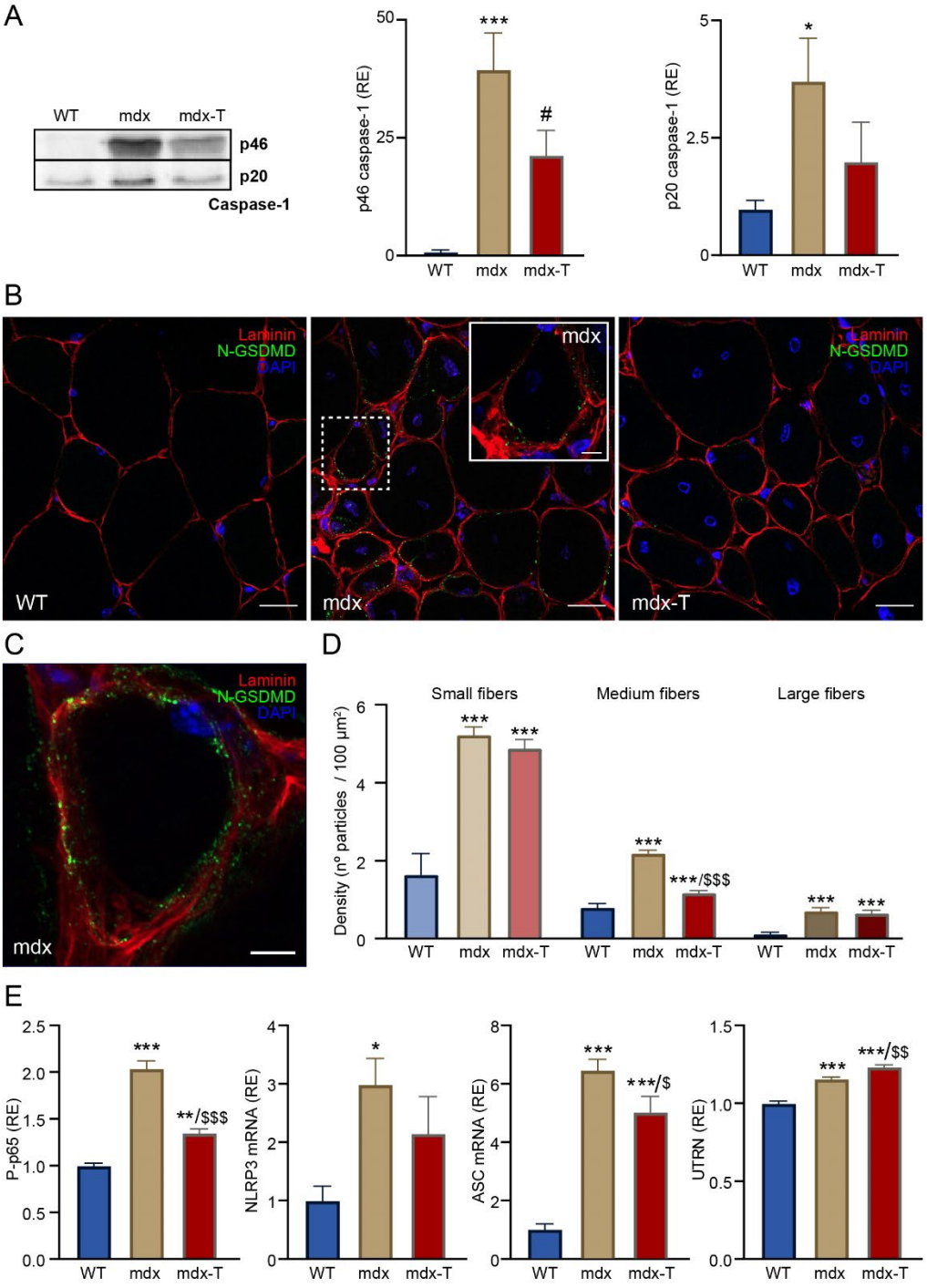
A
WT
mdx
mdx-T
p46
p20
Caspase-1
p46 caspase-1 (RE)
p20 caspase-1 (RE)
B
Laminin
N-GSDMD
DAPI
WT
mdx
mdx-T
C
D
Small fibers
Medium fibers
Large fibers
Density (nº particles / 100 µm²)
E
P-p65 (RE)
NLRP3 mRNA (RE)
ASC mRNA (RE)
UTRN (RE)

Fig.6 MCC950 treatment disrupts pyroptosis and increases the levels of a dystrophin analogue in mdx mice. *Experiments were performed on Q from the three groups of mice.* ***(A)*** *Caspase-1 analysis by Western blotting. Levels of each marker (full-length p46 and cleaved p20 subunit) were normalized to Rouge Ponceau (shown in Figure S1) and expressed relative to WT values.* ***(B)*** *Distribution of N-GSDMD density by immunofluorescence labelling. Sections were stained with specific antibodies directed against N-GSDMD (green) and laminin (red) and co-stained with DAPI (blue). The inset (dashed white square) shows the labelling of N-GSDMD in a small-sized fibre of a mdx untreated animal.* ***(C)*** *3D reconstruction of a small mdx fibre showing the distribution of N-GSDMD (green) close to the sarcolemma (laminin, red). Scale bars:* ***B*** *= 20 µm, inset on* ***B*** *= 5 µm,* ***C*** *= 5 µm.* ***(D)*** *N-GSDMD density (number of stained particles per 100 µm²) was quantified for each fibre and presented according to fibre size.* ***(E)*** *Levels of NF-κB activity, NLRP3 and ASC mRNAs, and UTRN protein. ELISAs were used to quantify the active phosphorylated form of the p65 subunit of NF-κB (P-p65) and UTRN. Absorbance data are presented as relative expression (RE) compared with WT values. mRNA levels were normalized to cyclophilin A, and the subsequent ratios presented as relative expression compared with WT. Data are expressed as means ± SEM; n = 6 mice per group for all experiments. Statistical analysis was performed using one-way ANOVA followed by Tukey's test.* $^{*}P < 0.05$, $^{**}P < 0.01$, $^{***}P < 0.001$ *vs WT mice.* $^{\$\$}P < 0.01$, $^{\$\$\$}P < 0.001$ *vs mdx mice. Comparisons between mdx-T and mdx were also carried out by unpaired two-tailed t-test (p46 caspase-1, ASC mRNA).* $^{\#}P = 0.075$ *vs mdx.*

MCC950 recapitulates its beneficial effect on human myotubes challenged by pro-inflammatory cytokines

Due to its convenience and cost-effectiveness, the mdx mouse remains the most widely used model for studying DMD [32]. However, since this model exhibits a milder phenotype than patients, it was important to validate our data in human myotubes. We thus examined the direct effects of MCC950 in primary cultures of DMD human myotubes. In order to mimic the inflammatory microenvironment of DMD, myotubes were challenged with an inflammatory stimulus (TNFα/IFNγ), along with ATP, a pyroptosis enhancer, while being pre-treated or not with MCC950.

We first tested the expression of the two pro-inflammatory cytokines, IL-1β and IL-18. mRNA levels for both cytokines were highly raised under inflammatory conditions, while MCC950 treatment reduced by ~50% their abundance (fourth *vs* third column) (Figure 7A,B). We also tested the expression of another inflammatory cytokine, TNFα, which is known to be significantly up-regulated in murine and human dystrophic muscles [2]. As expected, the pattern of TNFα mRNA was very similar to that of IL-1β and IL-18 (Figure 7 C). In addition, UTRN gene expression was decreased under inflammatory conditions, while MCC950 was capable of increasing its abundance by ~20% (fourth *vs* third column) (Figure 7D).

Moreover, the phosphorylated and active form of the p65 subunit of NF-κB (P-p65) was 5-fold higher in inflammatory conditions when compared to untreated ones (third *vs* first column), but was then down-regulated by ~40% under MCC950 treatment (fourth *vs* third column) (Figure 7E). Similarly, IL-1β protein levels were increased by 3-fold in inflammatory conditions while being halved after treatment (Figure 7F). Finally, DMD myotubes challenged with inflammation displayed high levels of activated N-GSDMD (>3-fold increase) (third *vs* first column). Again, treatment with MCC950 was able to halve those levels (Figure 7G).

Taken together, these results indicate a strong anti-inflammatory and anti-pyroptotic effects of MCC950 in human myotubes.

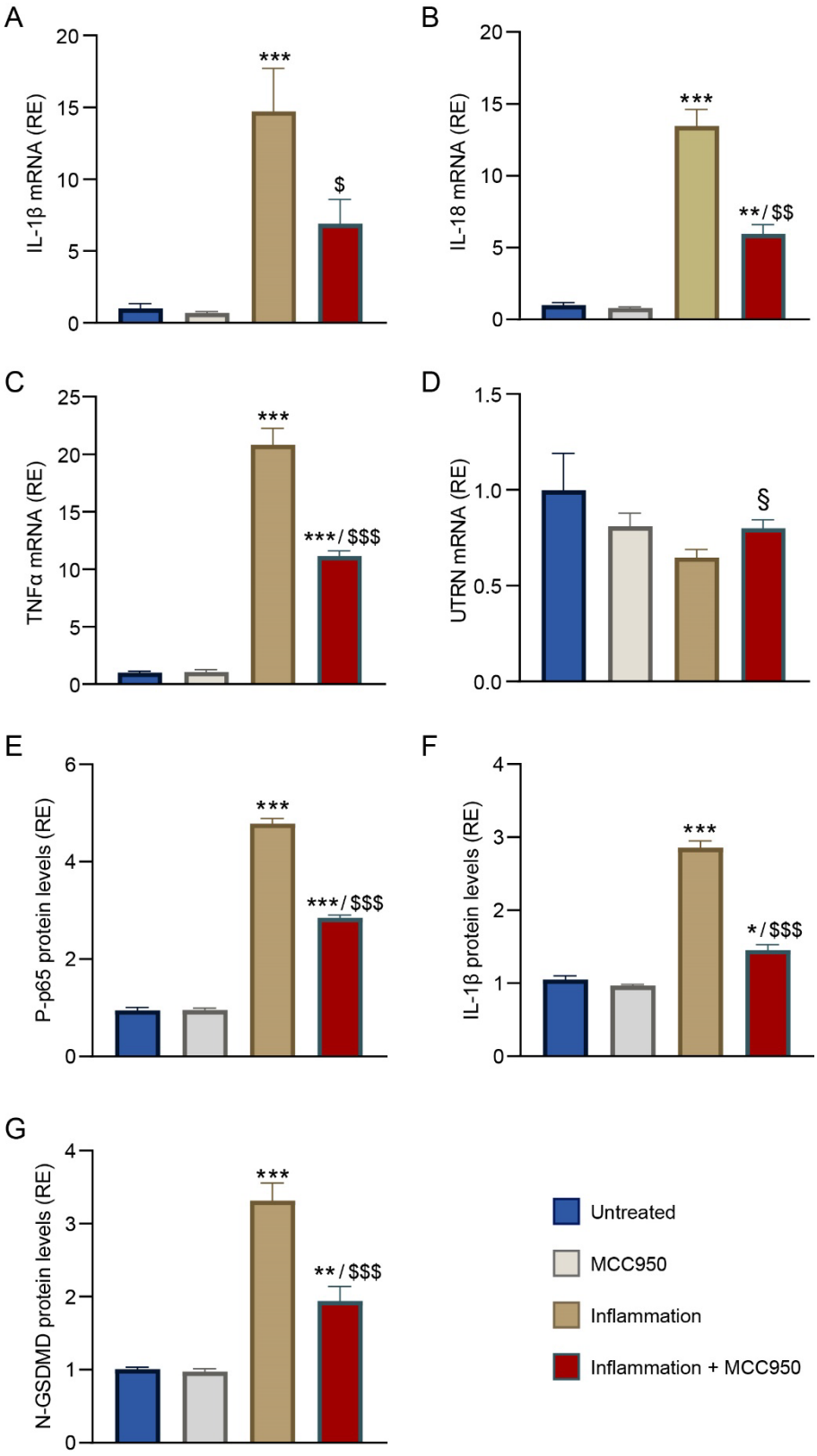
A
IL-1β mRNA (RE)
20
15
10
5
0
***
$
B
IL-18 mRNA (RE)
20
15
10
5
0
***
**/$$
C
TNFα mRNA (RE)
25
20
15
10
5
0
***
***/$$$
D
UTRN mRNA (RE)
1.5
1.0
0.5
0.0
§
E
P-p65 protein levels (RE)
6
4
2
0
***
***/$$$
F
IL-1β protein levels (RE)
4
3
2
1
0
***
*/$$$
G
N-GSDMD protein levels (RE)
4
3
2
1
0
***
**/$$$
Untreated
MCC950
Inflammation
Inflammation + MCC950

Fig.7 MCC950 treatment lessens inflammation and pyroptosis in challenged myotubes from DMD patients. (A-D) *mRNA levels of IL-1β, IL-18, TNFα, and UTRN in primary cultures of myotubes obtained from DMD patients. mRNA levels were normalized to human TATA box-binding protein.* ***(E-G)*** *ELISAs were used to quantify the active phosphorylated form of the p65 subunit of NF-κB (P-p65), IL-1β and N-GSDMD. Absorbance data are presented as relative expression (RE) compared with WT values. Cells were pre-treated or not with MCC950 (10 µM) for 24 h, while being challenged or not with human recombinant TNFα (15 ng/mL) + human interferon gamma (IFNγ) (15 ng/mL) for the last 22 h and then stimulated with ATP (5mM) for the last 2 h. The subsequent ratios are presented as relative expression compared with basal conditions (i.e. no ATP, no inflammation and no MCC950, represented by blue columns). Data are means ± SEM for 4 cultures, each obtained from a different donor (i.e., 4 DMD subjects). Statistical analysis was performed on paired data using two-way analysis of variance followed by Sidak's multiple comparison test.* $^{**}P < 0.01$, $^{***}P < 0.001$ *vs control (untreated).* $^{\$}P < 0.05$, $^{\$\$}P < 0.01$, $^{\$\$\$}P < 0.001$ *vs inflammatory condition. Comparison between MCC950 + inflammation and inflammation alone was also carried out by paired two-tailed t-test (UTRN).* $^{\S}P = 0.017$ *for the effect of the treatment.*

Discussion

The inflammasome is involved in the initiation or progression of diseases with a high impact on public health, such as metabolic disorders and neurodegenerative diseases [3]. It is also involved in some muscle diseases like dysferlin-deficiency [33] or aberrant host VCP [15]. Over-expression and activation of the NLRP3 inflammasome also plays a crucial pathogenic role in DMD. Conversely, genetic disruption of Nlrp3 [3], but oddly not of ASC [34], alleviates the dystrophic phenotype of mdx mice. Herein, we found that therapeutic inhibition of the inflammasome exerts potent protective effects on the dystrophic skeletal muscle, thereby offering a new and exciting prospect for managing DMD.

Oral administration of MCC950 to mdx mice for 2 months decreased muscle inflammation as shown by the reduction of pro-inflammatory cytokines such as IL-1β and IL-18 (Figure 8). The total number of macrophages infiltrates (CD68+) was also reduced. Interestingly, the treatment seems to promote a shift towards a M2 oriented population attested by the increased CD206/CD68 ratio, which is relevant as M2 macrophages play a major role in anti-inflammatory responses [25]. Accordingly, MCC950 treated animals also exhibited a reduction of necrosis and fibrosis (Figure 8) [24, 28]. Less necrosis was then associated with less need for very early regenerating myofibres [26]. Moreover, fibre maturation was more complete under MCC950, as attested by enhanced expression of mature forms of myosin heavy chain such as Myh1 and Myh7 and larger fibre size (Figure 8). In addition, MCC950 treatment potently attenuated muscle fibrosis, by reducing TGFβ levels and curbing its signaling pathway involving Smad2 protein [25]. All these beneficial

effects, together with a slight rise in utrophin may improve muscle function and attenuate the dystrophic phenotype.

We next explored the main mechanisms underlying the protective action brought about by MCC950 on dystrophic muscle. To this end, we investigated two key effectors of the inflammasome complex: Caspase-1 and GSDMD. Active Caspase-1 generates the mature forms of pro-inflammatory cytokines (IL-1β and IL-18) and cleaves GSDMD, triggering pyroptosis (Figure 8). Both full-length Caspase-1 (p46), which could be the dominant species of active caspase-1 [29] and its cleavage product (p20) were strongly increased in mdx mice but tended to be reduced under MCC950. The second effector, GSDMD is the executioner of pyroptosis via its cleaved N-terminal fragment (N-GSDMD). Pyroptosis is a form of programmed necrotic cell death caused by plasma membrane pore formation, resulting in cell swelling and eventually lysis. The pores can also serve as a gate for extracellular release of mature interleukins, resulting in an amplification of the inflammatory response [5, 7] (Figure 8). To the best of our knowledge, GSDMD has not yet been studied *in vivo* or *ex vivo* in skeletal muscle, and certainly not in dystrophic muscle. Herein, we show by immunofluorescence the location and density of N-GSDMD in dystrophic muscle and the effect exerted by MCC950. As expected, N-GSDMD was predominantly located in close contact to the fibre sarcolemma, where it forms the pyroptotic pores [5, 7, 19]. Moreover, N-GSDMD particles were rarely detectable in healthy muscle, while being abundant in dystrophic one. These findings indicate that pyroptosis could be a novel programmed cell death type in DMD. Furthermore, density of the active form of GSDMD was inversely related to fibre size, suggesting that small and medium size myofibre are more prone to pyroptosis. This is in line with the recent hypothesis stating that branched dystrophic fibres, which are smaller in size, are very sensitive to rupture during muscle activity, leading to fibre death [35-37]. Remarkably, mdx mice treated with MCC950 showed a significant reduction of N-GSDMD density in medium-sized myofibres compared to regular mdx. Although there were no significant differences in small-sized fibres between both groups, it should be stressed that the proportion of small fibres was lower in mdx-T than in regular mdx (27 *vs* 39%, Figure 4C pale red *vs* beige S marked pie charts). Taken together, these results indicate that the overall density of N-GSDMD is actually decreased in treated animals, thereby demonstrating an important effect of MCC950 on pyroptosis in the dystrophic muscle. Blockade of both main effectors of NLRP3 ultimately led to decreased activity of NF-κB, which in turn reduced the priming of NLRP3 (i.e., reduced transcription of several inflammasome components and lowered the expression of other pro-inflammatory actors like TNFα; see Figures 2 and 7) [38].

We next transposed our mouse data in human, by using primary cultures of myotubes derived from DMD subjects. As expected, we recapitulated the protective anti-inflammatory and anti-pyroptotic effects obtained in mice, strongly confirming the potential value of MCC950 in DMD patients.

DMD still awaits efficient gene therapy [39, 40]. Meanwhile, glucocorticoids (GCs) remain the only option commonly used in this disease [1, 41]. Their beneficial effects have mostly been ascribed to reduced inflammation [42]. However, such a treatment is hampered by several adverse effects: weight gain, growth retardation, Cushingoid appearance as well as bone demineralization, glucose intolerance and hypertension. NLRP3 inhibitors could well be a strong alternative to GCs due to their powerful anti-inflammatory, anti-necrotic and anti-fibrotic action on the skeletal muscle. They also appear to be more selective than GCs, by only affecting the NLRP3 inflammasome pathway, thus implying less adverse events.

In addition, by targeting the NLRP3 inflammasome, MCC950 remains highly potent in comparison to specific inhibitors downstream of NLRP3 pathway. For instance, MCC950 was able to rescue neonatal lethality in a genetic mouse model of Cryopyrin-Associated Autoinflammatory Syndromes (CAPS) caused by NLRP3 activating mutation while targeted blockade of IL-1β alone was unable to do so [8, 43]. This was ascribed to additional inhibition of IL-18 and pyroptosis afforded by MCC950. Moreover, specific targeting of NLRP3 (and not of other types of inflammasome) may explain why MCC950 is less immunosuppressive than biologic compounds (e.g., Canakinumab [8, 17]).

Pharmaceutical companies are investing in specific inhibitors of NLRP3. Some of them are under investigation for inflammatory diseases such as Inzomelid for CAPS (phase I) (ClinicalTrials.gov Identifier: NCT04015076), OLT1177 for treatment of gout flares (phase II) [44], and ZYIL1 for viral inflammatory diseases characterised by cytokine IL-1β flare. (phase I) (ClinicalTrials.gov Identifier: NCT04972188). We feel that MCC950 and other specific inflammasome inhibitors exhibiting potent pleiotropic effects have a crucial role to play in managing DMD treatment.

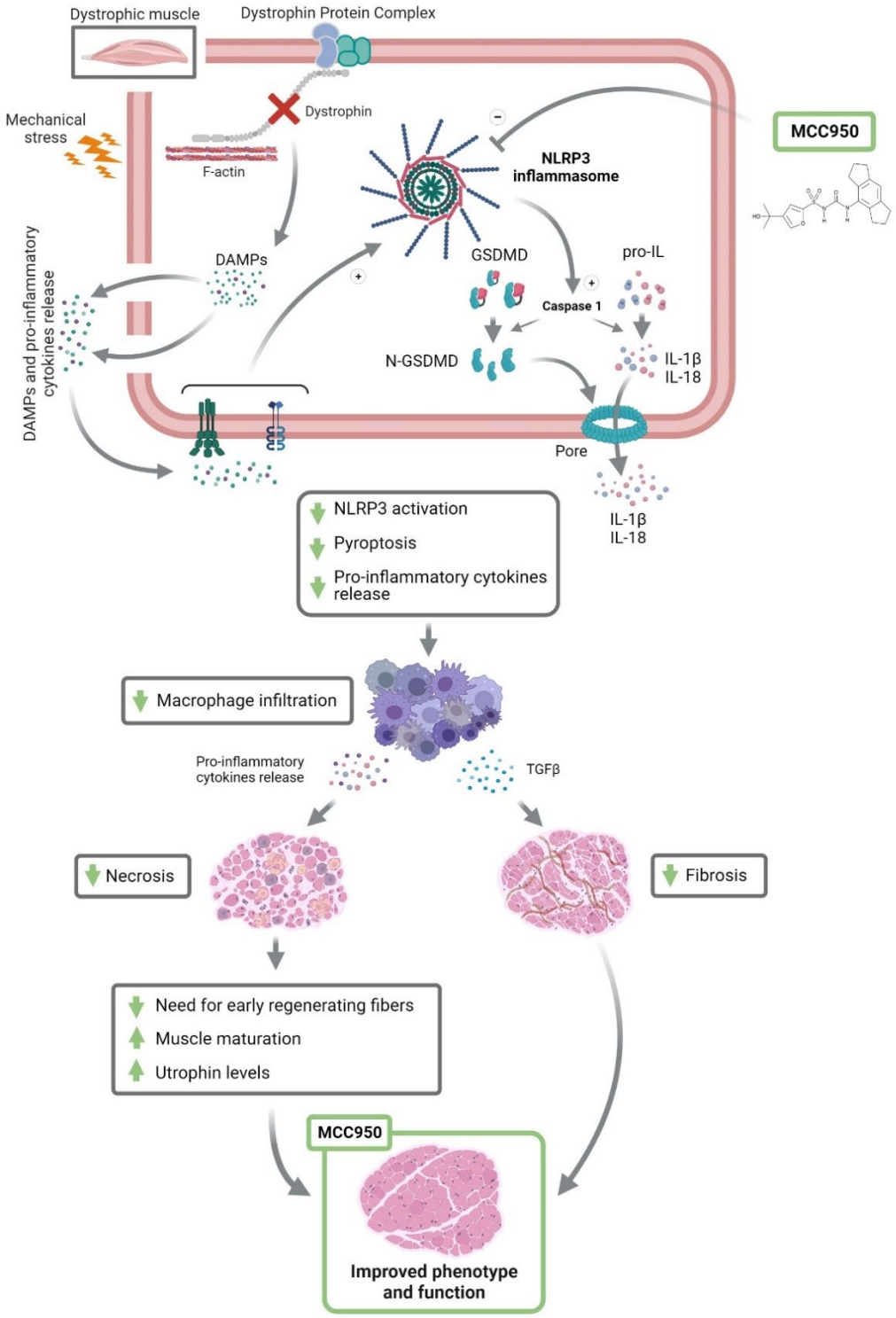
Dystrophic muscle
Dystrophin Protein Complex
Dystrophin
Mechanical stress
F-actin
MCC950
NLRP3 inflammasome
DAMPs
GSDMD
pro-IL
Caspase 1
N-GSDMD
IL-1β
IL-18
DAMPs and pro-inflammatory cytokines release
Pore
IL-1β
IL-18
NLRP3 activation
Pyroptosis
Pro-inflammatory cytokines release
Macrophage infiltration
Pro-inflammatory cytokines release
TGFβ
Necrosis
Fibrosis
Need for early regenerating fibers
Muscle maturation
Utrophin levels
MCC950
Improved phenotype and function

Fig.8 Inhibiting the inflammasome helps rescue the dystrophic phenotype. *DMD gene mutations cause the absence of the dystrophin protein, which weakens the fibre membrane making it more sensitive to mechanical stress. This leads to microtears and the release of damage-associated molecular patterns (DAMPs) and pro-inflammatory cytokines. The latter will activate NLRP3 inflammasome and consequently caspase-1, which in turn cleaves and activates N-GSDMD, IL-1β and IL-18, leading to pyroptotic channel formation and the release of mature pro-inflammatory cytokines. By blocking NLRP3, MCC950 could markedly attenuate this process. This beneficial action will decrease macrophage (M1 and M2) infiltration and shift the macrophage polarization towards an anti-inflammatory phenotype (M2), leading to anti-necrotic and anti-fibrotic properties. Finally, MCC950 will allow for a better myofibre maturation and increase utrophin expression, therefore leading to an improved muscle function and phenotype. +, stimulation; -, inhibition; GSDMD, gasdermin D. This figure was created with Biorender.*

Conclusion

In summary, the innate immune system and the NLRP3 complex play a central role in the pathogenesis of DMD. We highlight GSDMD-induced pyroptosis as a novel type of programmed necrotic cell death in this disease. We undoubtedly demonstrate that MCC950, a small molecule inhibiting selectively NLRP3, can greatly attenuate the dystrophic phenotype in mdx mice, due to its anti-inflammatory, anti-pyroptotic and anti-fibrotic properties. Inflammasome inhibitors could open new therapeutic prospects for the management of DMD or other muscle and inflammatory disorders.

Conflict of Interest

The authors declare that the research was conducted in the absence of any commercial or financial relationships that could be construed as a potential conflict of interest.

Author Contributions

Conceptualization: SMB and PVDB; MAS conducted pilot studies with AdipoRon and initiated this work; methodology: ND, MAS, SMB and LN; formal analysis: ND, MAD-LdC, MAS, CMS, RV and LN; investigation: ND, MAD-LdC and MAS; writing original draft: ND, MAD-LdC, MAS and SMB; writing review and editing: ND, MAD-LdC, MAS, CMS, RV, LN, PVDB and SMB; supervision: SMB and PVDB; funding acquisition: ND, MAS, PVDB and SMB.

Funding

This work was supported by grants from the Belgian Telethon (ABMM) to ND, the French Association against Myopathies (AFM Téléthon), and the Fund for Scientific Research FNRS (PDR/T.0026.21) to SB. MAS is Chargé de Recherches and ND Spécialiste Doctorant from the FNRS. CMS has received a fellowship from the FRIA. MAD-LdC received a fellowship from the Wallonie-Bruxelles International Excellence Program.

Acknowledgments

We are grateful to the IREC imaging platform for the use of the equipment and their aid, to Pr. Philippe Gailly and Dr. Olivier Schakman for providing the necessary equipment and the know-how for the *in vivo* functional tests.

References

1. Duan, D., et al., *Duchenne muscular dystrophy.* Nature Reviews Disease Primers, 2021. **7**(1): p. 13.
2. Abou-Samra, M., et al., *AdipoRon, a new therapeutic prospect for Duchenne muscular dystrophy.* J Cachexia Sarcopenia Muscle, 2020. **11**(2): p. 518-533.
3. Boursereau, R., et al., *Downregulation of the NLRP3 inflammasome by adiponectin rescues Duchenne muscular dystrophy.* BMC Biol, 2018. **16**(1): p. 33.
4. Acharyya, S., et al., *Interplay of IKK/NF-kappaB signaling in macrophages and myofibers promotes muscle degeneration in Duchenne muscular dystrophy.* J Clin Invest, 2007. **117**(4): p. 889-901.
5. Dubuisson, N., et al., *Walking down Skeletal Muscle Lane: From Inflammasome to Disease.* Cells, 2021. **10**(11).
6. Mangan, M.S.J., et al., *Targeting the NLRP3 inflammasome in inflammatory diseases.* Nat Rev Drug Discov, 2018. **17**(8): p. 588-606.
7. Shi, J., W. Gao, and F. Shao, *Pyroptosis: Gasdermin-Mediated Programmed Necrotic Cell Death.* Trends Biochem Sci, 2017. **42**(4): p. 245-254.
8. Coll, R.C., et al., *A small-molecule inhibitor of the NLRP3 inflammasome for the treatment of inflammatory diseases.* Nat Med, 2015. **21**(3): p. 248-55.
9. Tapia-Abellán, A., et al., *MCC950 closes the active conformation of NLRP3 to an inactive state.* Nature chemical biology, 2019. **15**(6): p. 560-564.
10. Coll, R.C., et al., *MCC950 directly targets the NLRP3 ATP-hydrolysis motif for inflammasome inhibition.* Nat Chem Biol, 2019. **15**(6): p. 556-559.
11. van der Heijden, T., et al., *NLRP3 Inflammasome Inhibition by MCC950 Reduces Atherosclerotic Lesion Development in Apolipoprotein E-Deficient Mice-Brief Report.* Arterioscler Thromb Vasc Biol, 2017. **37**(8): p. 1457-1461.
12. Perera, A.P., et al., *MCC950, a specific small molecule inhibitor of NLRP3 inflammasome attenuates colonic inflammation in spontaneous colitis mice.* Sci Rep, 2018. **8**(1): p. 8618.
13. Ward, R., et al., *NLRP3 inflammasome inhibition with MCC950 improves diabetes-mediated cognitive impairment and vasoneuronal remodeling after ischemia.* Pharmacol Res, 2019. **142**: p. 237-250.
14. Qu, J., et al., *The selective NLRP3 inflammasome inhibitor MCC950 alleviates cholestatic liver injury and fibrosis in mice.* Int Immunopharmacol, 2019. **70**: p. 147-155.
15. Nalbandian, A., et al., *Activation of the NLRP3 Inflammasome Is Associated with Valosin-Containing Protein Myopathy.* Inflammation, 2017. **40**(1): p. 21-41.

16. Gillis, J.M., *Understanding dystrophinopathies: an inventory of the structural and functional consequences of the absence of dystrophin in muscles of the mdx mouse.* J Muscle Res Cell Motil, 1999. **20**(7): p. 605-25.
17. Ludwig-Portugall, I., et al., *An NLRP3-specific inflammasome inhibitor attenuates crystal-induced kidney fibrosis in mice.* Kidney Int, 2016. **90**(3): p. 525-39.
18. *<van Putten M. The use of hanging wire tests to monitor muscle strength and condition over time. In DMDM.2.1.004. 2011. httpstreat-nmd.orgwp-contentuploads202106uncategorized-Wire-test.pdf. Accessed 23 Feb 2022..pdf>.*
19. Karmakar, M., et al., *N-GSDMD trafficking to neutrophil organelles facilitates IL-1β release independently of plasma membrane pores and pyroptosis.* Nat Commun, 2020. **11**(1): p. 2212.
20. Svendsen, P., et al., *Mouse CD163 deficiency strongly enhances experimental collagen-induced arthritis.* Sci Rep, 2020. **10**(1): p. 12447.
21. Mayeuf-Louchart, A., et al., *MuscleJ: a high-content analysis method to study skeletal muscle with a new Fiji tool.* Skelet Muscle, 2018. **8**(1): p. 25.
22. Abou-Samra, M., Sophie Lecompte, Olivier Schakman, Laurence Noel, Marie C. Many, Philippe Gailly, and Sonia M. Brichard, *Involvement of Adiponectin in the Pathogenesis of Dystrophinopathy.* Skeletal Muscle, 2015. **5**: p. 25.
23. Sander, H., et al., *Ponceau S waste: Ponceau S staining for total protein normalization.* Anal Biochem, 2019. **575**: p. 44-53.
24. Morgan, J.E., et al., *Necroptosis mediates myofibre death in dystrophin-deficient mice.* Nat Commun, 2018. **9**(1): p. 3655.
25. Tidball, J.G., *Regulation of muscle growth and regeneration by the immune system.* Nat Rev Immunol, 2017. **17**(3): p. 165-178.
26. Schiaffino, S., et al., *Developmental myosins: expression patterns and functional significance.* Skelet Muscle, 2015. **5**: p. 22.
27. Schiaffino, S., et al., *Fetal myosin immunoreactivity in human dystrophic muscle.* Muscle Nerve, 1986. **9**(1): p. 51-8.
28. Forcina, L., M. Cosentino, and A. Musarò, *Mechanisms Regulating Muscle Regeneration: Insights into the Interrelated and Time-Dependent Phases of Tissue Healing.* Cells, 2020. **9**(5).
29. Boucher, D., et al., *Caspase-1 self-cleavage is an intrinsic mechanism to terminate inflammasome activity.* J Exp Med, 2018. **215**(3): p. 827-840.
30. Al-Rewashdy, H., et al., *Utrophin A is essential in mediating the functional adaptations of mdx mouse muscle following chronic AMPK activation.* Hum Mol Genet, 2015. **24**(5): p. 1243-55.
31. Gordon, B.S.D.D., Diana C. Kostek, Matthew C. , *Resveratrol decreases inflammation and increases utrophin gene expression in the mdx mouse*

model of duchenne muscular dystrophy. . Clinical Nutrition, 2013. **1**(32): p. 104–111.
32. McGreevy, J.W., et al., *Animal models of Duchenne muscular dystrophy: from basic mechanisms to gene therapy.* Dis Model Mech, 2015. **8**(3): p. 195-213.
33. Rawat, R., et al., *Inflammasome up-regulation and activation in dysferlin-deficient skeletal muscle.* Am J Pathol, 2010. **176**(6): p. 2891-900.
34. Lau, Y.S., et al., *Genetic disruption of the inflammasome adaptor ASC has minimal impact on the pathogenesis of Duchenne muscular dystrophy in mdx mice.* Life Sci, 2020. **257**: p. 118069.
35. Carlson, C.G., *Does the Pathogenic Sequence of Skeletal Muscle Degeneration in Duchenne Muscular Dystrophy Begin and End with Unrestrained Satellite Cell Activation?* Muscles, 2022. **1**(1): p. 75-81.
36. Chan, S. and S.I. Head, *The role of branched fibres in the pathogenesis of Duchenne muscular dystrophy.* Exp Physiol, 2011. **96**(6): p. 564-71.
37. Head, S.I., *Branched fibres in old dystrophic mdx muscle are associated with mechanical weakening of the sarcolemma, abnormal Ca2+ transients and a breakdown of Ca2+ homeostasis during fatigue.* Exp Physiol, 2010. **95**(5): p. 641-56.
38. Bauernfeind, F.G., et al., *Cutting edge: NF-kappaB activating pattern recognition and cytokine receptors license NLRP3 inflammasome activation by regulating NLRP3 expression.* J Immunol, 2009. **183**(2): p. 787-91.
39. Jones, D., *Duchenne muscular dystrophy awaits gene therapy.* Nat Biotechnol, 2019. **37**: p. 335–337.
40. Walter, M.C. and P. Reilich, *Recent developments in Duchenne muscular dystrophy: facts and numbers.* J Cachexia Sarcopenia Muscle, 2017. **8**(5): p. 681-685.
41. Matthews, E., et al., *Corticosteroids for the treatment of Duchenne muscular dystrophy.* Cochrane Database Syst Rev, 2016. **2016**(5): p. Cd003725.
42. Reeves, E.K., et al., *Glucocorticoid analogues: potential therapeutic alternatives for treating inflammatory muscle diseases.* Endocr Metab Immune Disord Drug Targets, 2012. **12**(1): p. 95-103.
43. Jiang, H., et al., *Identification of a selective and direct NLRP3 inhibitor to treat inflammatory disorders.* J Exp Med, 2017. **214**(11): p. 3219-3238.
44. Klück, V., et al., *Dapansutrile, an oral selective NLRP3 inflammasome inhibitor, for treatment of gout flares: an open-label, dose-adaptive, proof-of-concept, phase 2a trial.* Lancet Rheumatol, 2020. **2**(5): p. e270-e280.

Supplementary Material

Table S1. Antibody Information Chart

Antibody	Species raised	Dilution	Incubation time	Temp.	Product code	Source
Immunohistochemistry						
CD68	rabbit polyclonal	1/500	2h30	RT	ab125212	Abcam, Cambridge, UK
HNE	rabbit polyclonal	1/200	Overnight	4°C	ab46545	Abcam, Cambridge, UK
IL-1β	rabbit polyclonal	1/200	2h30	RT	ab2105	Abcam, Cambridge, UK
IL-18	rabbit polyclonal	1/100	Overnight	4°C	ab71495	Abcam, Cambridge, UK
PRDX3	rabbit polyclonal	1/1000	Overnight	4°C	/	Gift from Bernard Knoops, UCL, Belgium[a]
TNFα	rabbit polyclonal	1/100	2h30	RT	ab6671	Abcam, Cambridge, UK
Immunofluorescence						
CD68	rabbit polyclonal	1/500	Overnight	4°C	ab125212	Abcam, Cambridge, UK
IL-1β	rabbit polyclonal	1/500	Overnight	4°C	ab2105	Abcam, Cambridge, UK
IgG	goat polyclonal	1/500	1h	RT	A-11001	Invitrogen, Carlsbad, US
Laminin-2 (α-2 chain)	rat monoclonal	1/1000	Overnight	4°C	L0663	Sigma Aldrich, Missouri, USA
Myh3	rabbit polyclonal	1/200	Overnight	4°C	LS-C336252	LS Bio, Seattle, USA
N-GSDMD	rabbit monoclonal	1/50	Overnight	4°C	ab2015203	Abcam, Cambridge, UK
Western Blotting						
Caspase-1	rabbit monoclonal	1/5000	Overnight	4°C	LS-C138140-100	Bio-connect, Toronto, Canada

[a]*Leyens G, Donnay I, Knoops B. Cloning of Bovine Peroxiredoxins-Gene Expression in Bovine Tissues and Amino Acid Sequence Comparison with Rat, Mouse and Primate Peroxiredoxins. Comp Biochem Physiol B Biochem Mol Biol (2003) 136(4):943-55. Epub 2003/12/10. doi: 10.1016/s1096-4959(03)00290-2. RT: Room temperature; N-GSDMD: N-Gasdermin D.*

Table S2. Primer sequence table

Gene			Sequence (5'-3')	Annealling temperature
TGFβ	mouse	Forward	TTGCTTCAGCTCCACAGAGA	62
		Reverse	TGGTTGTAGAGGGCAAGGAC	62
IL-18	human	Forward	TGCAGTCTACACAGCTTCGG	62
		Reverse	GCAGCCATCTTTATTCCTGCG	62

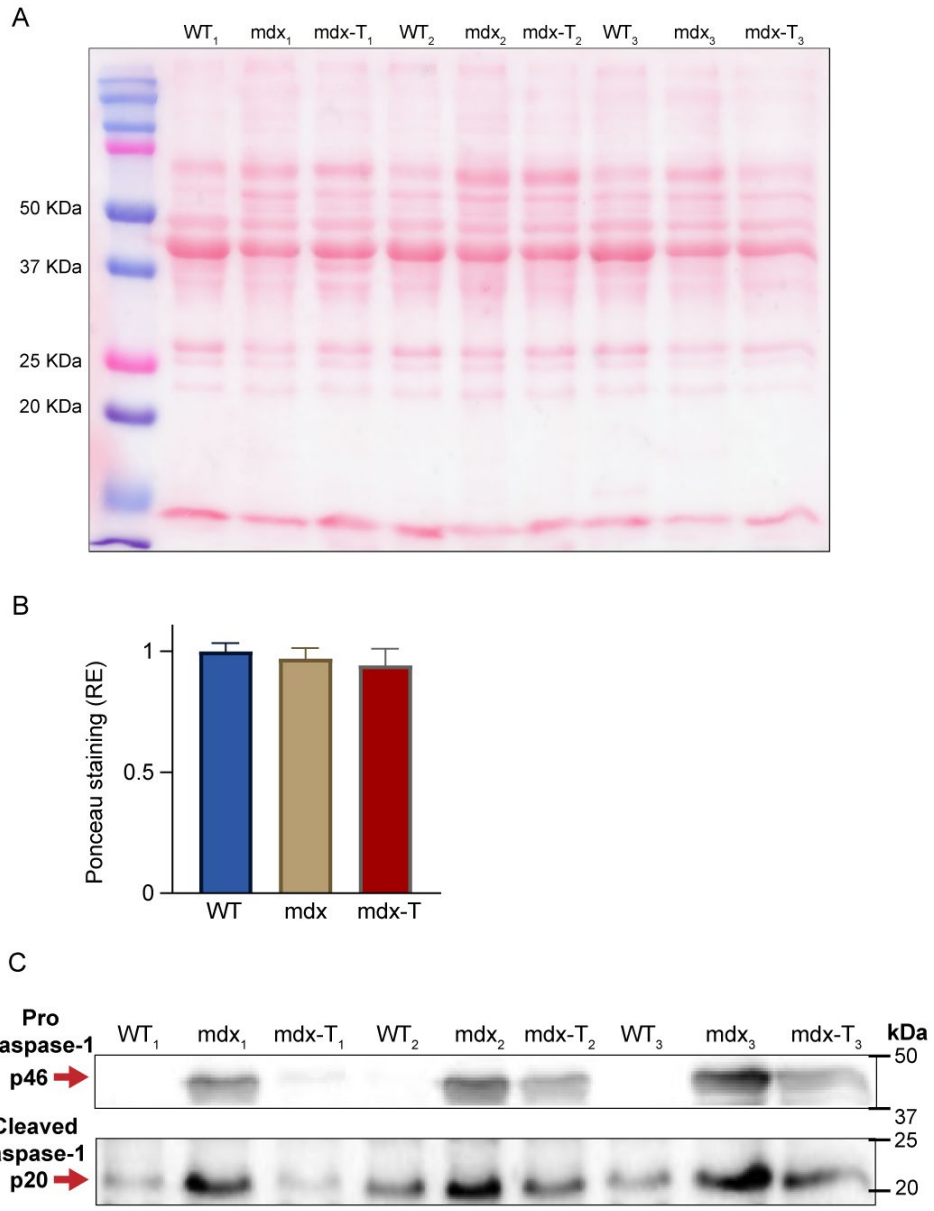

Fig S1. *Representative Western blotting of pro-caspase-1 (p46) and cleaved caspase-1 (p20).* ***(A)*** *The full ponceau-staining membrane from Western blotting of pro-caspase-1 (p46) and cleaved caspase-1 (p20) with WT, mdx and mdx-T mice (three animals for each condition but representative for all the animals studied).* ***(B)*** *Quantification of ponceau-staining expressed as relative expression compared to WT. RE: relative expression.* ***(C)*** *Western blotting of pro-caspase-1 (p46) and cleaved caspase-1 (p20) after low and high exposure times respectively.*

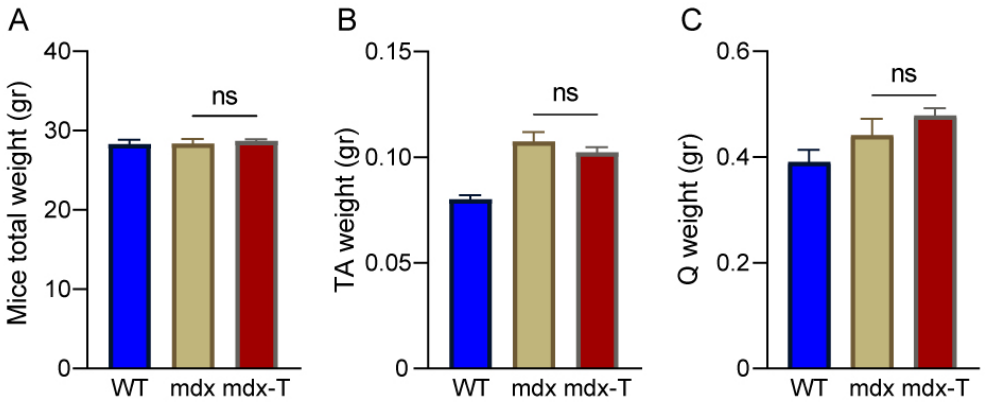

Fig S2. *Comparison of animal and muscle weight from the three groups of mice.Three groups of mice were compared at the age of 12 wks: wild-type (WT) mice, mdx-T mice (mdx mice treated with MCC950), and their mdx littermates (true controls). The total weight of the mice (A), the tibialis anterior (B) and the quadriceps (C) muscle were recorded at sacrifice. No difference was observed between mdx and mdx-T animals. Results are expressed in grams (gr). Data are means ± SEM for six mice per group. TA = tibialis anterior, Q = quadriceps, ns = non significant.*

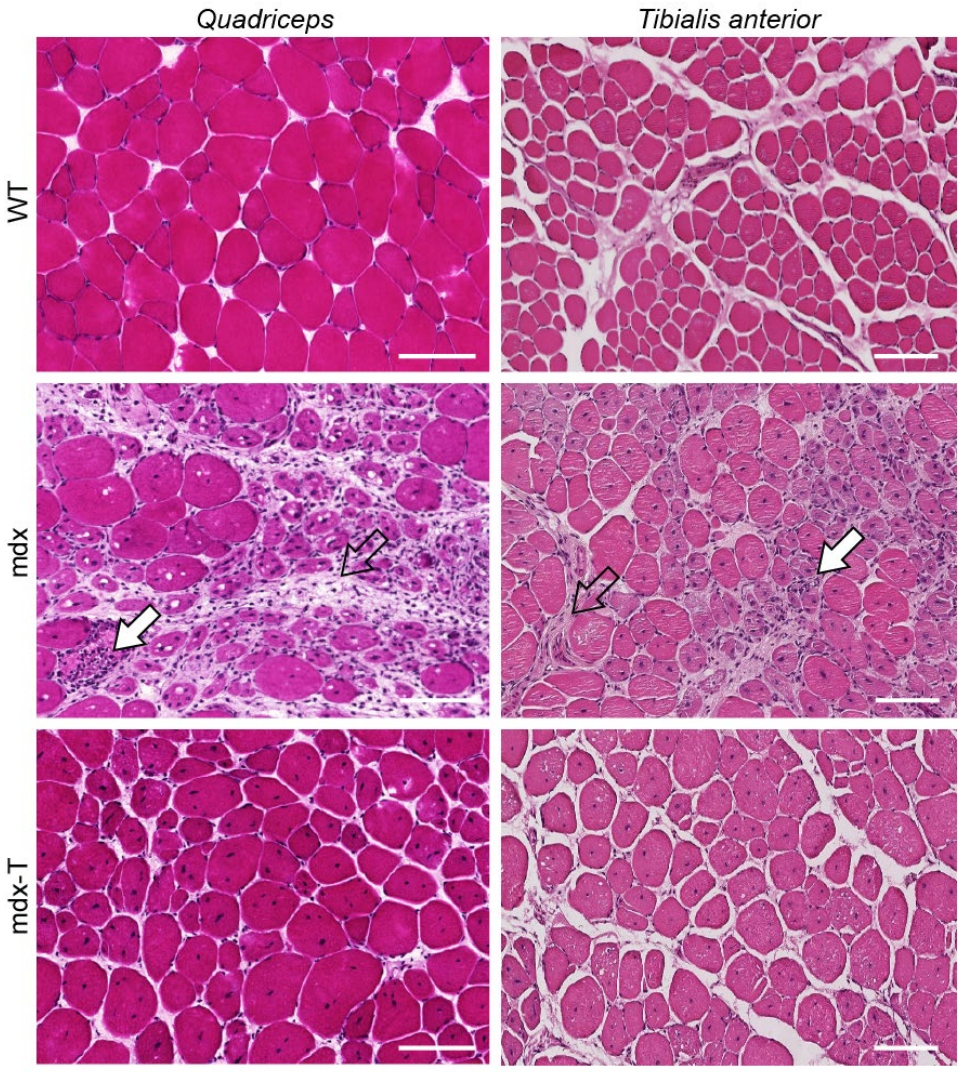

Fig S3. *Haematoxylin & Eosin staining of Quadriceps and Tibialis anterior sections from the three groups of mice. The effects of MCC950 were already observed after H&E staining of TA and Q muscle cross sections. Indeed, while WT muscle cross-section displayed normal morphology, mdx Q and TA showed a dystrophic pattern, witnessed by central nuclei, the presence of fibrotic tissue (empty arrow) and higher degree of inflammatory cell infiltration (white arrow). This phenotype was partially rescued in mdx-T mice. Scale bar = 100 µm.*

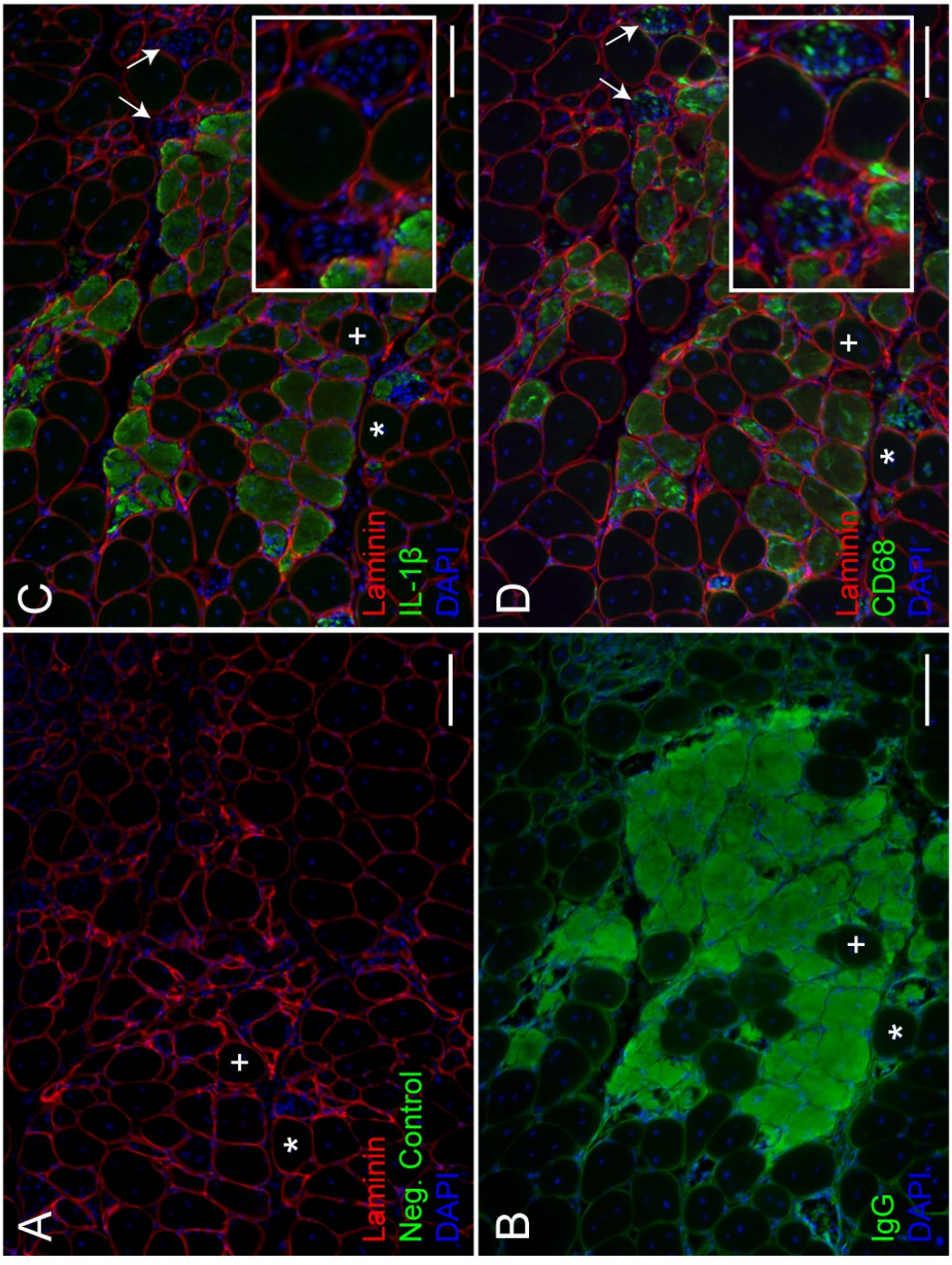
A
Laminin
Neg. Control
DAPI
B
IgG
DAPI
C
Laminin
IL-1β
DAPI
D
Laminin
CD68
DAPI

Fig S4. *Negative control of the antibodies to IL-1β and to CD68. Representative fluorescent images from four parallel mdx quadriceps cross sections showing the negative control for the anti-rabbit primary antibodies (A), the necrotic fibres stained with a goat anti-mouse IgG-AF488 (B), cytokine IL-1β positive areas stained with an anti-rabbit IL-1β antibody (C) and macrophages stained with an anti-rabbit CD68 antibody (D). To facilitate the recognition of myofibres, the negative control and the sections incubated with the primary antibody to IL-1β or to CD68 were co-stained with a rat anti-laminin antibody combined with a goat anti-rat-AF647 secondary antibody. After applying the same exposure time for the green channel on all four sections, no green signal could be detected on the section that was not incubated with any of the anti-rabbit primary antibodies (A), demonstrating that the goat anti-rabbit-AF488 secondary antibody itself did not yield any unspecific staining on necrotic myofibers. The asterisk (*) and plus sign (+) in the images show the same fibers in all the sections. Insets shown in C and D correspond to the same two myofibers with the white arrows on the same images. Note that not all the areas positive for CD68 (macrophages) were immuno-positive for IL-1β. Scale bar: 100 µm.*

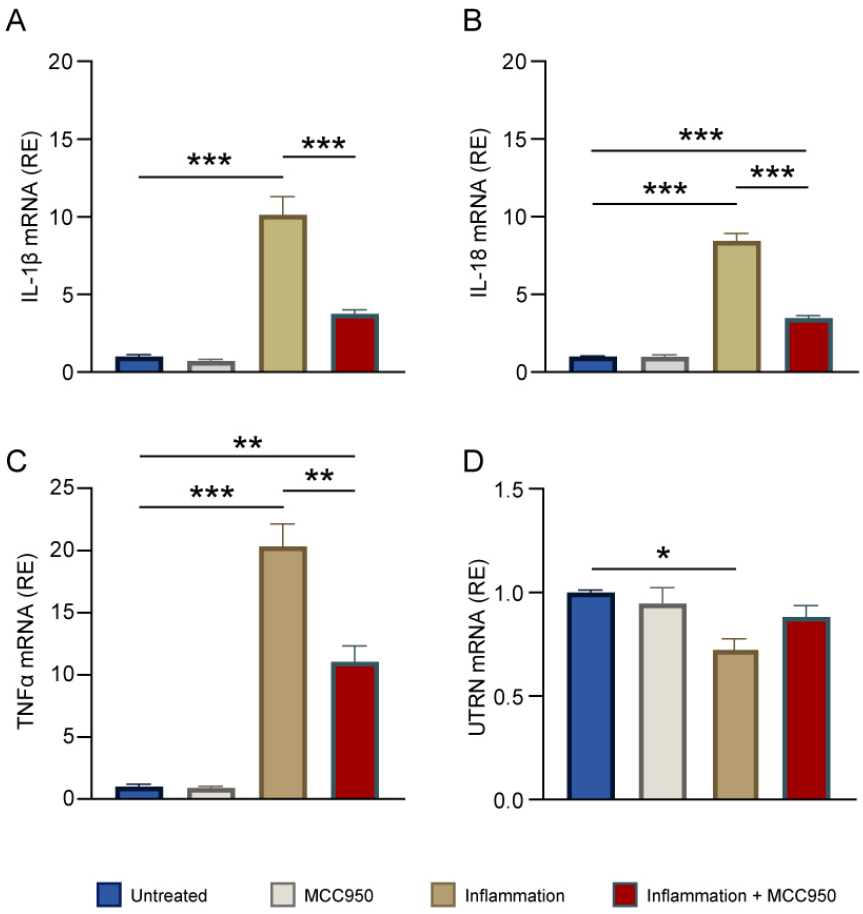

Fig S5. *Effects of MCC950 treatment on healthy human myotubes challenged by pro-inflammatory cytokines. mRNA levels of IL-1β (A), IL-18 (B), TNFα (C), and utrophin A (D) in primary culture of human healthy myotubes. Cells were treated with or without MCC950 (10 µM), while being challenged or not with TNFα (15 ng/mL) and IFNγ (15 ng/mL) for 24 h. mRNA levels were normalized to human TATA box-binding protein. The subsequent ratios are presented as relative expression compared with basal conditions (i.e. no inflammation and no MCC950, represented by blue columns). Data are means ± SEM for 4 cultures per group, each obtained from a different donor (i.e., 4 healthy subjects). Statistical analysis was performed on paired data using two-way analysis of variance followed by Sidak's multiple comparison test. *P < 0.05, **P < 0.01, ***P < 0.001, vs. control (basal) and inflammatory condition.*

Study 2

The adiponectin receptor agonist, ALY688: a promising therapeutic for fibrosis in the dystrophic muscle

Nicolas Dubuisson[1,2†], Romain Versele[1†], Maria A. Davis-López de Carrizosa[1,3], Camille M. Selvais[1], Laurence Noel[1], Chloé Planchon[1], Peter Y.K. Van den Bergh[2], Sonia M. Brichard[1] and Michel Abou-Samra[1*]

[1] Endocrinology, Diabetes and Nutrition Unit, Institute of Experimental and Clinical Research (IREC), Medical Sector, Université Catholique de Louvain (UCLouvain), Avenue Hippocrate 55, 1200 Brussels, Belgium;

[2] Neuromuscular Reference Center, Department of Neurology, Cliniques Universitaires Saint-Luc, Avenue Hippocrate 10, 1200 Brussels, Belgium

[3] Departamento de Fisiología, Facultad de Biología, Universidad de Sevilla, 41012 Seville, Spain

†: These authors contributed equally to this work and share first authorship

*** Correspondance:**

Nicolas Dubuisson

E-mail : nicolas.j.dubuisson@uclouvain.be

Keywords: Duchenne muscular dystrophy, Adiponectin, ALY688, Skeletal Muscle, AMPK, Inflammation, Regeneration, Fibrosis, Myonecrosis, Necroptosis.

Abstract

Duchenne muscular dystrophy (DMD) is one of the most devastating myopathies, where severe inflammation exacerbates disease progression. Previously, we demonstrated that adiponectin (ApN), a hormone with powerful pleiotropic effects, can efficiently improve the dystrophic phenotype. However, its practical therapeutic application is limited. In this study, we investigated ALY688, a small peptide ApN receptor agonist, as a potential novel treatment for DMD. Four-week-old mdx mice were subcutaneously treated for two months with ALY688 and then compared to untreated mdx and wild-type mice. *In vivo* & *ex vivo* tests were performed to assess muscle function and pathophysiology. Additionally, *in vitro* tests were conducted on human DMD myotubes. Our results showed that ALY688 significantly improved the physical performance of mice and exerted potent anti-inflammatory, anti-oxidative and anti-fibrotic actions on the dystrophic muscle. Additionally, ALY688 hampered myonecrosis, partly mediated by necroptosis, and enhanced the myogenic program. Some of these effects were also recapitulated in human DMD myotubes. ALY688's protective and beneficial properties were mainly mediated by the AMPK-PGC-1α (proliferator-activated receptor γ coactivator-1α) axis, which led to suppression of NF-κβ and TGF-β. Our results demonstrate that an ApN mimic may be a promising and effective therapeutic prospect for a better management of DMD.

Introduction

Duchenne muscular dystrophy (DMD) is one of the most prevalent inherited myopathies, affecting 1/3.500 boys [1]. DMD remains a rapidly progressive and lethal disorder, where patients are typically wheelchair bound by 8–14 years of age and die from cardiac or respiratory failure during their third decade [2]. This myopathy is caused by mutations in the gene encoding dystrophin, a protein that provides structural stability and integrity to myofibre membrane [1]. Mutations in dystrophin result in membrane damage, allowing severe inflammation/oxidative stress and necrosis [1, 3]. Ongoing cycles of muscle necrosis and repair cause exhaustion of satellite cells and impaired regeneration capacity. Eventually, muscle fibres are gradually replaced by fibrosis, leading to muscle wasting and weakness [1, 4]. Although dystrophin mutation is the primary cause of DMD, it is the secondary processes involving persistent inflammation, impaired regeneration and prolific fibrosis that actually worsen the course of the disease [3, 4].

Adiponectin (ApN) is a hormone abundantly secreted by adipocytes. It promotes insulin-sensitizing, fat-burning, and anti-inflammatory/oxidative actions, thereby effectively counteracting several metabolic disorders, including type 2 diabetes, obesity, and cardiovascular disease [5]. ApN exerts its pleiotropic effects in a variety of cell types through binding to its main receptors, AdipoR1 and AdipoR2 [6]. AdipoR1, which has a high-affinity for both full-length and the cleaved globular fragment of ApN (gApN), is mainly expressed in skeletal muscle, whereas AdipoR2 is predominantly expressed in the liver [7]. As skeletal muscle is a main target tissue of ApN, we tested this hormone in mdx mice, a mouse model of DMD. When we crossed mdx mice with transgenic mice overexpressing ApN, this hormone delays disease progression by reducing muscle inflammation/injury and improving force/myogenesis [8]. Conversely, when we crossed mdx mice with ApN-knockout mice, the resulting mdx mice displayed a reverse picture, which was corrected by muscular electro-transfer of the ApN gene. Thus, ApN may be a powerful protector of the skeletal muscle [9]. However, there are some limitations in using ApN directly as a therapeutic agent. Its complex quaternary structure and rapid turnover impede its production in sustained amounts [5]. As a result, the search for novel compounds with AdipoRs agonist activity, which may further be easily produced, has been developing over the last decade.

ALY688 (formerly known as ADP355), is a decapeptide AdipoRs agonist, which is derived from the active site of human gApN and acts preferentially through AdipoR1. This first-in-class small peptide agonist was discovered as an inhibitor of cancer cell growth that was more potent than gApN [10, 11]. Later on, several other beneficial metabolic effects were observed both *in vitro* and *in vivo*. More specifically, when administered to mice, ALY688 reduced inflammation and fibrosis after toxic liver or heart injury [12-14]; it also attenuated insulin resistance induced by high-fat/high-sucrose-diet [15], and inhibited atherosclerosis in apoE-deficient

mice [16]. As yet, its potential anti-inflammatory, pro-myogenic and anti-fibrotic properties have not been tested in skeletal muscle and *a fortiori* not in the dystrophic muscle.

The aim of this study was to explore whether ALY688 may play a beneficial role in DMD. To this end, ALY688 was administered subcutaneously (sc) for a period of 2 months, starting early in mdx mice since muscle degenerative-regenerative cycles begin as soon as 3–4 weeks of age [17]. We first examined whether treated mice showed reduced skeletal muscle inflammation, oxidative stress, and fibrosis as well as enhanced muscular function. Then, we uncovered the potential mechanisms of action underlying the effects of ALY688. Finally, we also evaluated some of these effects in primary cultures of human myotubes originating from healthy subjects and DMD patients.

Materials and Methods

Animals

C57BL/10ScSn-DmdmdxJ mdx mice (murine model of DMD) and C57BL/10ScSnJ mice [used as wild-type (WT) controls] were purchased from Jackson Laboratory (Maine, USA). The cohort was divided into four groups of male mice. Each group comprised 10 mice. The first group was composed of WT mice, the second one of untreated mdx mice (mdx), while the third and fourth groups were composed of mdx mice treated with an extended release (ER) form of ALY688 at either 3 mg/kg/day or 15 mg/kg/day (mdx-T3 or mdx-T15). Compound dosage and treatment duration were based on Allysta pharmaceuticals' preliminary experiments. ALY688 (ER formulation) was administered daily by subcutaneously (sc) injection for 2 months. Regular mdx mice were injected with saline. Animals were maintained under a standard laboratory chow and housed at a constant temperature (22°C) with a fixed 12 h light to 12 h dark cycle (lights on from 7 a.m. to 7 p.m.). 12-week-old mice were sacrificed between 09.00 and 11.00 h. Pairs of muscles [*Quadriceps* (Q) and *Gastrocnemius* (G), *Tibialis anterior* (TA)] were weighed, frozen in liquid nitrogen, and stored at −80°C for subsequent analyses. These are mixed muscles with similar fibre type composition [18, 19].

In vivo studies of muscle function

At week 11 (i.e., 1 week prior to sacrifice), mice were submitted to three widely used and reliable functional tests [20-22]. These tests were performed successively, one test per day over a 5-day period.

Wire test. Mice were suspended by their limbs from a wire and the time until they completely released their grasp and fell was recorded. Mice that reached a set limit of 600 seconds were allowed to stop the experiment, while others were directly retested, up to three times, and their maximum hanging time was recorded. The

holding impulse (body mass x hang time), used to oppose the gravitational force, was then calculated [22].

Grip test. Limb strength was recorded using a grid connected to a sensor (Panlab-Bioseb, Vitrolles, France). Mice were gently laid on the top of a grid so that their front paws could grip the grid. Mice were then pulled back steadily until the grip was released down the complete length of the grid. Each test was repeated three times at an interval of 15 minutes. Results are presented as the mean of the three values of force recorded, related to body weight [21].

Treadmill exhaustion test. After two consecutive days of acclimation to the moving belt (Panlab-Bioseb), mice were submitted to a treadmill exhaustion test with an upward inclination of 5° and increasing speed rate over 4 steps. The mice started by running 10 minutes at a pace of 20 cm/sec (step 1), then 5 minutes at 25 cm/sec (step 2), followed by 5 minutes at 30 cm/sec (step 3) and finally 5 minutes at a maximum speed of 35 cm/sec (step 4). Exhaustion was defined as the inability of the animal to run on the treadmill for 5 sec despite laying on top of the shock grid and receiving repeated aversive stimuli [23-25]. The distance covered in meters (m) during the test was recorded either after exhaustion or at the end of the test. If the mouse was able to complete all steps, the total test duration was 25 minutes for a maximal distance covered of 390 meters.

Bright-field histochemistry

G muscles were fixed in 10% formalin for 24 h and embedded in paraffin. Immunohistochemistry was carried out as previously described [20, 21]. Briefly, 5 µm sections were processed using antibodies directed against interleukin 1-beta (IL-1β), tumor necrosis factor alpha (TNFα), peroxiredoxin 3 (PRDX3), 4-hydroxy-2-nonenal (HNE) and cluster of differentiation 68 (CD68) (supplementary information, Table S1). Before immunostaining, sections were submitted to heat-mediated antigen retrieval using a microwave oven and Tris-citrate buffer (pH 6.5). Binding of antibodies was detected by applying for 30 min at room temperature a secondary antibody, which was a biotinylated goat anti-rabbit IgG (H + L). For each marker, all slides were treated simultaneously for immunohistochemistry analysis and diaminobenzidine revelation (DAB, Thermo Fisher Scientific, Waltham, MA, USA) and then analysed together. Whole muscle sections were scanned, and then the percentage of areas stained with DAB was quantified using QuPath (opensource, https://qupath.github.io, Belfast, UK). TA sections were also stained with haematoxylin and eosin to evaluate myonecrosis. Quantification of myonecrosis is shown as the proportion (%) of whole muscle section area occupied by fibres with fragmented sarcoplasm and inflammatory cells [26]. In addition, Q sections (described below) were stained with Picrosirius red (Abcam, Cambridge, UK) to evaluate muscle fibrosis. Fibrotic tissue was scored setting a colour balance threshold and data obtained were expressed as the percentage of total section area.

Immunofluorescence

Q muscles were embedded in optimum cutting temperature medium (OCT; VWR International, Dublin, Ireland) and frozen in liquid nitrogen chilled isopentane (VWR International). 10 µm transversal cryosections were fixed with 4% paraformaldehyde and blocked with 10% goat serum. Antibodies directed against dystrophin and laminin were used (Table S1). Secondary antibodies were AF488 and AF647-conjugated goat anti-rabbit or anti-rat (Sigma-Aldrich, St-Louis, MO, USA), respectively. Finally, nuclei were stained with DAPI (Thermo Fisher Scientific). Whole-slides were scanned with a fluorescence microscope (Axio Scan.Z1, Zeiss, Oberkochen, Germany). Dystrophin-positive fibres were counted and expressed as the percentage of the total number of fibres per muscle (ZEN 3.4 blue edition, Zeiss). A dystrophin-positive revertant fibre (RF) was scored when more than half of its membrane circumference expressed a green positive signal [27]. The number of clusters (with at least two adjacent RFs) and the maximal number of RFs in a cluster were counted on whole sections as well [27]. Centrally nucleated fibres (CNF) were also calculated using a personalized version of MuscleJ [28] based on the automatic detection of laminin and DAPI immunofluorescence.

Culture of murine C2C12 cell lines

Murine C2C12 myoblasts were cultured in Dulbecco's modified Eagle's medium (DMEM), 10% Foetal bovine serum (FBS), 1% non-essential amino acids, 1% L-glutamine and 1% antibiotic-antimycotic (all from Thermo Fisher Scientific) at 37 °C in 5% CO2. Briefly, after reaching 80-90% confluence, the growth medium was substituted by a fusion medium, where 10% FBS was replaced by 2% heat-inactivated horse serum (HS; Thermo Fisher Scientific), for 6 days to induce myogenic differentiation. The differentiation medium was changed every other day. Then, myotubes were treated or not with mouse recombinant TNFα (10 ng/mL) + mouse interferon gamma (IFNγ) (10 ng/mL) (TNFα and IFNγ from PeproTech, Hamburg, Germany) and/or ALY688 (100nM) for 24 h. The ALY688 concentration was chosen based on a previous study [15] and on our preliminary experiments (data not shown). ALY688 used in all *in vitro* experiments was the conventional form of the compound (i.e. not the extended-release one). At the end of the experiments, myotubes were rinsed twice in cold PBS before RNA extraction.

Culture of human myotubes

Primary cultures of human skeletal muscle cells were initiated from myoblasts of DMD patients (n = 4; age range: 12–15 years) and healthy subjects (n = 3; age range: 15–17 years), which were provided by the French Telethon Myobank-AFM. Myoblasts were grown in DMEM/F-12 supplemented with 20% FBS, 1% non-essential amino acids, 1% L-glutamine, and 1% antibiotic-antimycotic (all from Thermo Fisher Scientific) at 37 °C in 5% CO2. After reaching a density of 80-90%, the growth medium was substituted by a fusion medium, where 20% FBS was

replaced by 2% HS, and differentiation was allowed to continue for 14 days (time required to obtain mature myotubes with characteristic elongated and multinucleated morphology). Medium was changed every other day. Cells were always used at passages between 4 and 10. At day 14, myotubes were either left untreated, or treated with AdipoRon (25 µM) or ALY688 (conventional formulation) at different concentrations (from 10 pM up to 300 nM) for 24 h, while being challenged or not with TNFα (15 ng/mL) + IFNγ (15 ng/mL) (both from PeproTech) for 24 h.
In some experiments, cells were first transfected before inflammatory challenge and ALY688 (100 nM) treatment. Briefly, cells were transfected with either the On-Targetplus non-targeting pool siRNAs (negative control, NT siRNAs) or a specific On-Targetplus siRNA SMARTpool against human AdipoR1 (50 nM) (from Dharmacon, Thermo Fisher Scientific) using 7 µL of Lipofectamine RNAiMAX reagent (Thermo Fisher Scientific) for 24 h. RNA silencing was effective, ranging around 95 % in all experiments. Next, the medium was renewed and cells were treated with ALY688 (100nM) and with TNFα + IFNγ (15 ng/mL each) for an additional 24 h.
At the end of the experiments, cells were rinsed twice in cold PBS before RNA or protein extraction.

RNA extraction and real-time quantitative PCR

RNA was isolated from muscle tissues or cultured cells with TriPure reagent (Sigma-Aldrich). RT-qPCR primers for mouse cyclophilin, Collagen Type I Alpha 1 Chain (COL1A1), Collagen Type III Alpha 1 Chain (COL3A1), estrogen receptor-related alpha (ERRα), Myogenic regulatory factors 4 (Mrf4) and Myh1 are provided in Table S2. RT-qPCR primers for human TATA box-binding protein (TBP), AdipoR1, IL-1β, TNFα and Utrophin (UTRN) are also indicated in Table S2. Threshold cycles (Ct) were always measured in duplicate.

Protein extraction and ELISAs

Muscle samples and cultured cells were homogenized in a lysis buffer supplemented with 1% protease/phosphatase inhibitor cocktail (both from Cell Signaling Technology, Leiden, The Netherlands) and 10 mM NaF (Sigma-Aldrich). Protein levels were quantified using the Bradford method and 10–150 µg of total protein extracts were used for ELISAs.
ELISA assays allowed to specifically detect and quantify HNE (Abcam), Myogenin, Myh7, UTRN (all from Antibodies Online, Atlanta, USA), the active and phosphorylated forms of AMP-activated protein kinase (AMPK), receptor-interacting protein (RIP) family of serine-threonine kinases, Smad2, p65 subunit of nuclear factor-kappa B (NF-κB) (all from Cell Signaling Technology) as well as TNFα, peroxisome proliferator-activated receptor γ coactivator-1α (PGC-1α) and active transforming growth factor-β (TGF-β) (all from MyBiosource, San Diego, USA)(Table

S3; [20, 21, 29, 30]). Kits were based on colorimetric methods and were carried out following manufacturer's instructions.

Statistical analysis

Results are means ± standard error of mean (SEM) for the indicated number of mice, C2C12 cells or human subjects. When the four groups of mice (WT, mdx, mdx-T3 and mdx-T15) were compared, the differences between groups were assessed by one-way analysis of variance (ANOVA) followed by Tukey's test. In one experiment (RFs), as WT values were undetectable, the 3 groups of dystrophic mice were compared by one-way ANOVA followed by Dunnett's test (treated mdx vs untreated ones). When comparisons between two myotube conditions from a given subject were made, a two-tailed paired Student's *t* test was used. *In vitro* dose-response curves were generated using nonlinear regression. The analysis provided the median inhibitory (IC_{50}) or activating concentration (EC_{50}). Comparisons between data points were then carried out by repeated measures ANOVA followed by post hoc Dunnett's test, where every mean was compared to the condition without ALY688, which was arbitrary set up to a very low concentration of the compound (i.e. 10^{-12} M). All statistical analyses and graph fitting were achieved with Prism 9 (GraphPad Software, Inc., San Diego, CA). Differences were considered statistically significant at $P < 0.05$.

Results

ALY688 enhances force and endurance of mdx mice

Two different doses of ALY688ER were injected sc to mdx mice for 2 months, starting at 4 weeks of age. Mdx littermates were separated into three groups: those which were treated with a daily dose of ALY688 at 3 or 15 mg/kg/day (mdx-T3 and mdx-T15) and those who were left untreated (mdx). These three groups were also compared with untreated wild-type (WT) control mice. ALY688 treatment did not affect the total body weight of dystrophic mice, nor the weight of the different removed muscles (Figure S1 and Table S4). Macroscopic evaluation of liver and kidney after treatment was also unremarkable, thus indicating that the treatment was well tolerated.

To evaluate the effects of ALY688 on muscle function, mice were subjected to three functional tests: the wire test, the grip test and the treadmill exhaustion test. The wire test gives an indication on muscle fatigue and coordination. In this test, the time during which the mouse is suspended on a horizontal wire is measured. Mdx mice fell down much faster than WT mice, mdx-T3 mice showed intermediate laps of time (+34% *vs* mdx), while mdx-T15 showed remarkable improvement (+67% *vs* mdx) and reached normal values (Figure 1A).

The grip test measures strength of limb muscles. The force developed by four limbs was decreased in mdx mice, while being rescued by ALY688 (+20% and +13% in mdx-T3 and mdx-T15, respectively) (Figure 1B).

The uphill treadmill exhaustion test provides valuable data on muscle endurance. The speed rate was gradually increased over four consecutive steps. The distance covered by mdx mice was significantly reduced, while that of treated mice was not different from controls (Figure 1C). More specifically, a higher number of treated mice were able to succeed in the last step despite the incremental speed, thereby confirming improved muscle endurance compared to regular mdx. (Figure 1D)

Taken together, these data indicate enhanced force and resistance to fatigue in dystrophic muscle under ALY688 treatment.

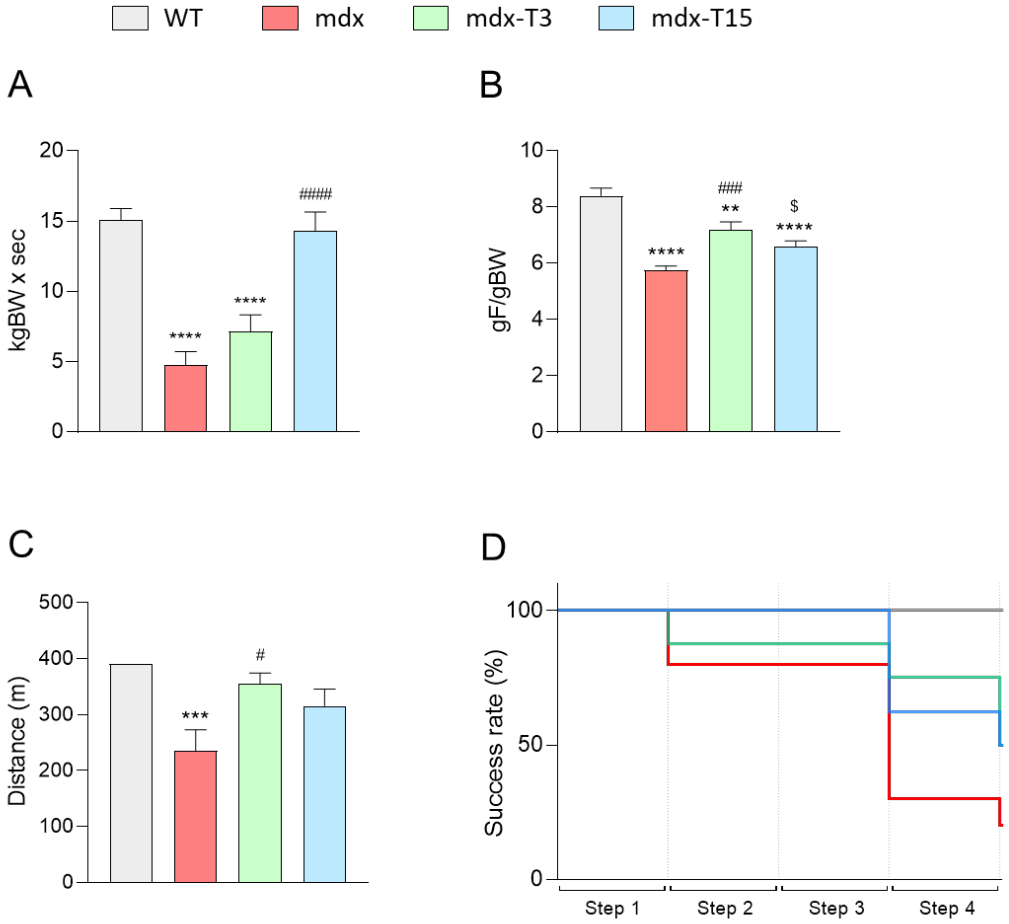

Figure 1. ALY688 treatment improves muscle function and endurance of mdx mice. *Four groups of mice were compared at the age of 11 weeks: WT, mdx (untreated), mdx treated with ALY688 3 mg/kg (mdx-T3) and mdx treated with ALY688 15 mg/kg (mdx-T15) mice. Functional tests were carried out in vivo.* ***(A)*** *Mice were subjected to a wire test where they were suspended by their limbs and the time until they completely released the wire and fell was registered (seconds). This time was then normalised to body weight (kgBW x sec).* ***(B)*** *Mice were lowered on a grid connected to a sensor to measure the muscle force of their four limbs; data were then expressed in gram-force relative to gram-body weight (gF/gBW).* ***(C)*** *Mice were placed on a moving belt and encouraged to run to exhaustion with an uphill inclination of 5° and a gradually increasing speed. The mice started by running 10 minutes at a pace of 20cm/sec (step 1), then 5 minutes at 25cm/sec (step 2), followed by 5 minutes at 30cm/sec (step 3) and finally 5 minutes at a maximum speed set up at 35cm/sec (step 4). The distance covered in meters (m) was recorded either after exhaustion or at the end of the test.* ***(D)*** *Treadmill exhaustion test's success rate. Data are means ± SEM; n = 8-10 mice for*

all experiments. Statistical analysis was performed using one-way ANOVA followed by Tukey's test. ** P < 0.01, ***P < 0.001, ****P < 0.0001 vs WT mice. $^{\$}$P = 0.08, $^{\#}$P < 0.05, $^{\#\#\#}$P < 0.001, $^{\#\#\#\#}$P < 0.001 vs mdx mice.

ALY688 effectively reduces muscle inflammation and oxidative stress

We next studied inflammation and oxidative stress in dystrophic muscle and tested the hypothesis that ALY688 could slow down the progression of these events (Figure 2).

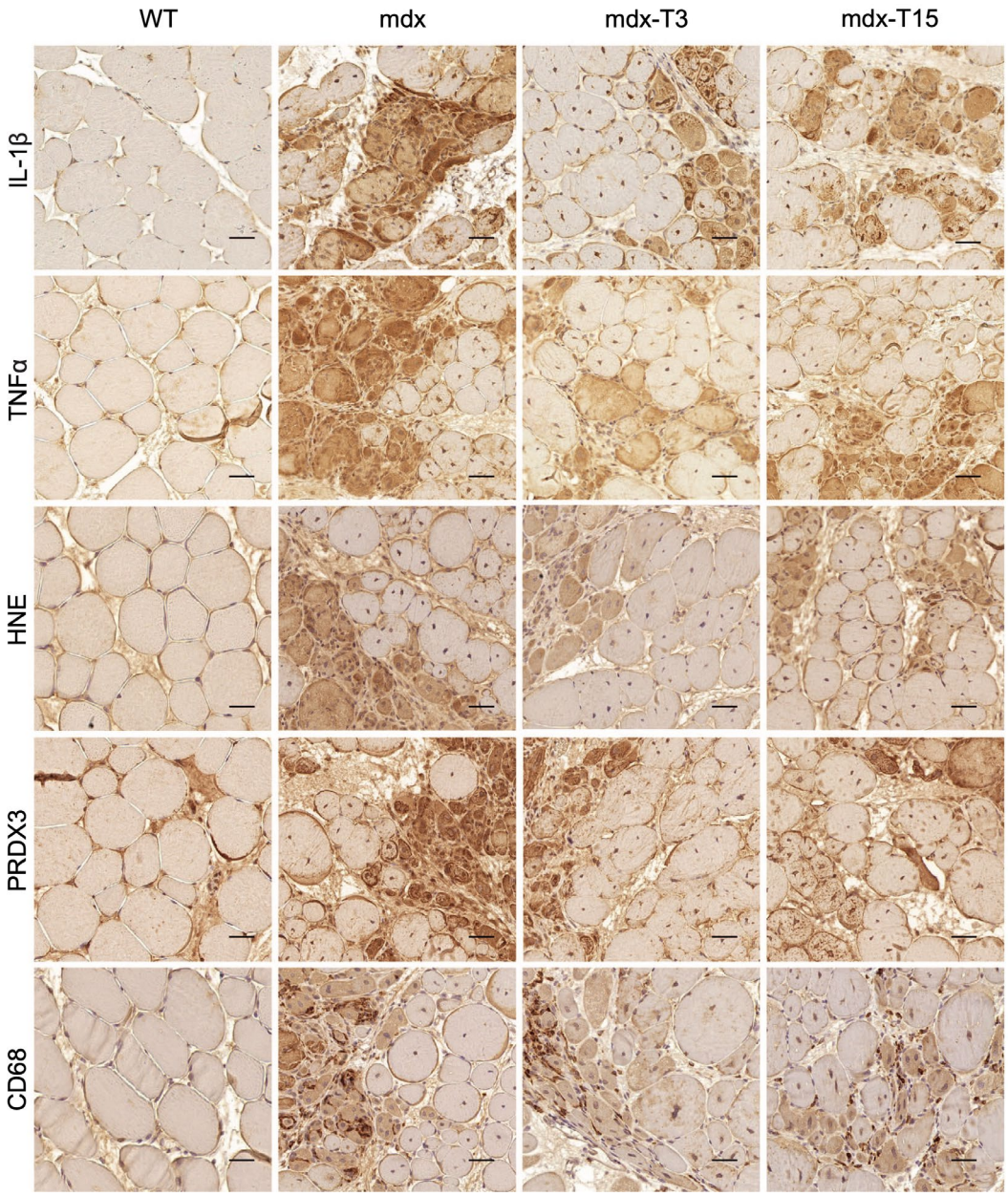

Figure 2. ALY688 treatment reduces muscle inflammation and oxidative stress in mdx mice. *Immunohistochemistry was performed on G muscle of the 4 groups of mice. Sections were stained with specific antibodies directed against two pro-inflammatory cytokines (IL-1ß and TNFα), two oxidative stress markers (HNE and PRDX3) and one pan-macrophage marker (CD68). Representative sections for 6 mice per group is shown. Scale bars = 50 µm.*

When compared to WT mice, myofibres from G muscles of mdx mice displayed a strong immunolabeling for inflammatory cytokines (IL-1β and TNFα), oxidative stress markers (a lipid peroxidation product, HNE and an antioxidant enzyme, PRDX3) as well as for the macrophage marker, CD68. Immunolabelling for all these markers of inflammation or oxidative stress was attenuated in treated mice (Figure 2).

Quantification of DAB staining confirmed that these parameters in mdx-treated mice were either significantly decreased compared to regular mdx (IL-1β: -54% and -40%; PRDX3: -49% and -43%; CD68: -47% and -44% in mdx-T3 and mdx-T15, respectively) or less significantly different from those of WT (Figure 3, A-E). In addition, TNFα and HNE protein levels measured by ELISAs were also significantly decreased (-40%) in whole Q muscle homogenates from treated *vs* untreated mdx animals, thereby strengthening the anti-inflammatory and anti-oxidative effect of the compound (Figure 3, F-G).

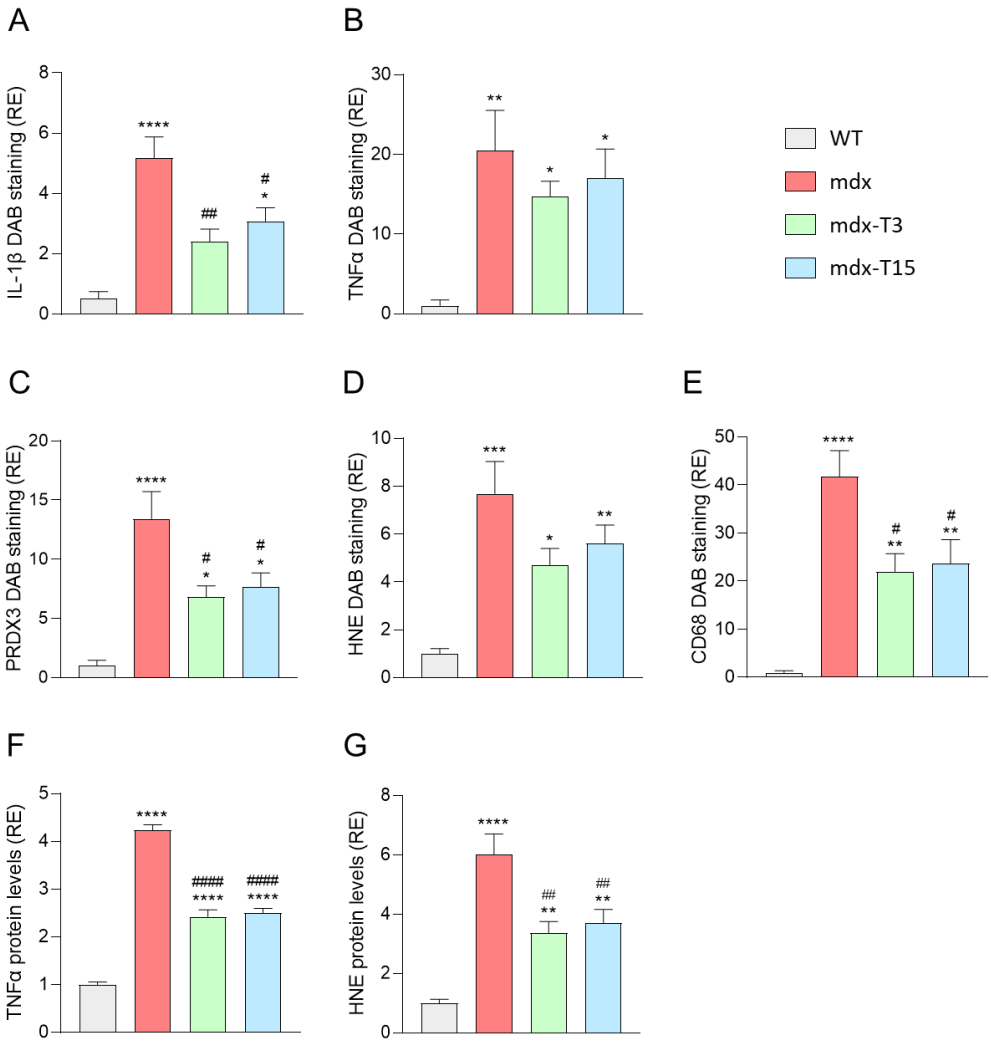

Figure 3. ALY688 treatment reduces muscle inflammation and oxidative stress in mdx mice. (A-E) *Immunohistochemistry quantification of IL-1β, TNFα, HNE, PRDX3 and CD68 on G muscle in the 4 groups of mice. Data are calculated as the percentage area stained by DAB, then presented as relative expression compared to WT mice (RE).* ***(F-G)*** *ELISA quantification of TNFα and HNE protein levels in whole Q muscle homogenates; data are then presented as RE. Results are means ± SEM; n = 6 mice per group for all experiments. Statistical analysis was performed using a one-way ANOVA followed by Tukey's test.* $^{*}P < 0.05$, $^{**}P < 0.01$, $^{***}P < 0.001$, $^{****}P < 0.0001$ *vs WT mice.* $^{\#}P < 0.05$, $^{\#\#}P < 0.01$, $^{\#\#\#\#}P < 0.0001$ *vs mdx mice.*

In conclusion, ALY688 reduced inflammation, oxidative stress and infiltration of $CD68^+$ macrophages in treated mdx mice.

ALY688 counteracts myonecrosis in mdx mice

Because inflammation may subsequently lead to muscle damage and necrosis, we hypothesized that ALY688 could also reduce myonecrosis. This parameter was assessed by inflammatory infiltrates and fragmented myofibres and quantified on H&E-stained TA sections. Myonecrosis was significantly reduced in both treated groups (~-60%) compared to regular mdx. (Figure 4A, B). In addition, protein levels of P-RIP, a novel marker a necroptosis in DMD [31] was also significantly decreased in treated mice (-25%; Figure 4C). There was no significant difference in the percentage of central nucleated fibres (CNF) in Q muscles from 3 groups of dystrophic mice (data not shown). However, this parameter is of limited use in identifying any striking reduction in recent active myonecrosis and subsequent regeneration in adult mdx mice [32].

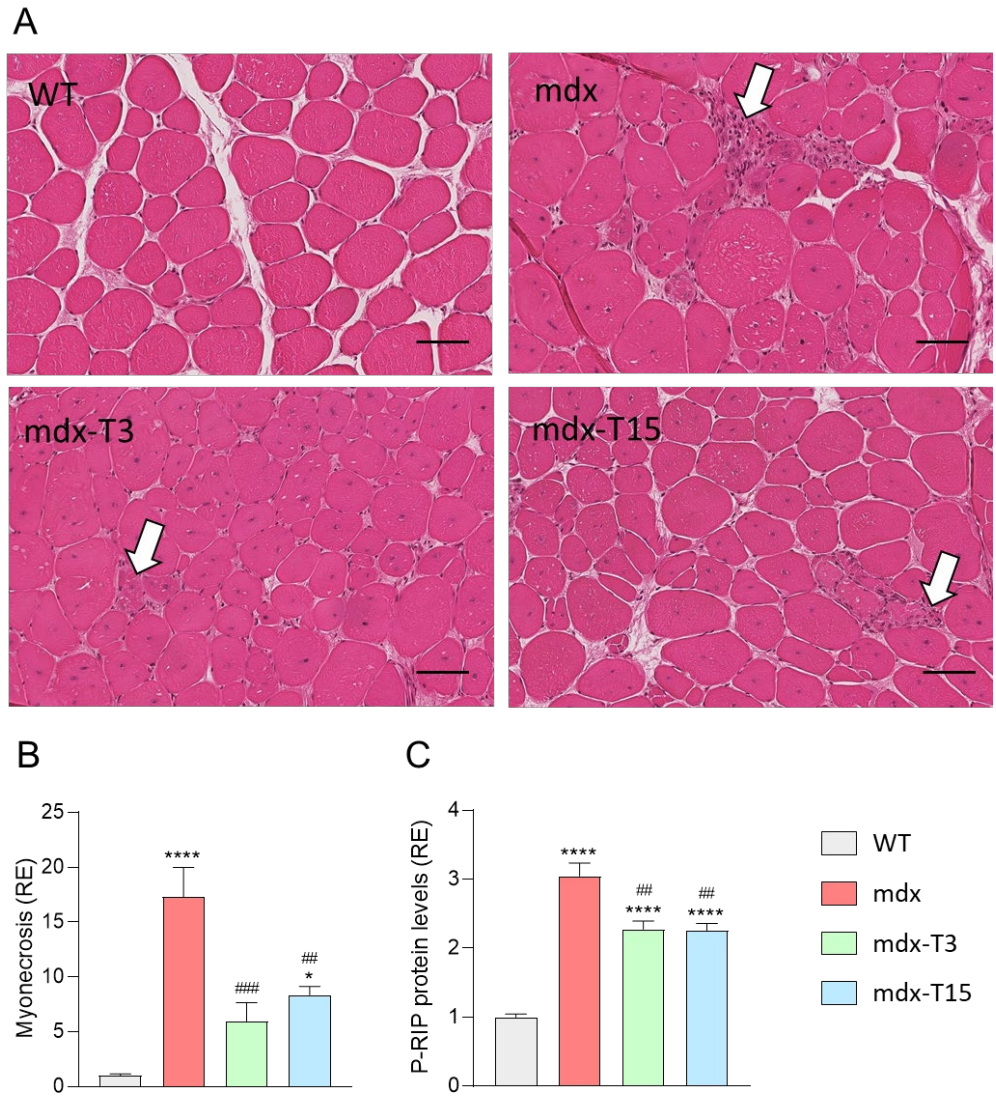

Figure 4. Quantification of myonecrosis in muscle sections of mdx mice. (A) *H&E-stained transverse sections of paraffin-embedded tibialis anterior (TA) muscles. Areas of myonecrosis encompass both muscle fibres with fragmented sarcoplasm and inflammatory cells.* ***(B)*** *Quantification is calculated as the proportion (%) of whole muscle section area occupied by myonecrosis, then presented as relative expression compared to WT mice (RE).* ***(C)*** *ELISA assays were used to quantify P-RIP, a marker of necroptosis on Q muscle; data are then presented as RE. Results are means ± SEM; n = 6 mice per group for all experiments.*

Statistical analysis was performed using a one-way ANOVA followed by Tukey's test. $^{*}P < 0.05$, $^{****}P < 0.0001$ vs WT mice. $^{\#\#}P < 0.05$, $^{\#\#\#}P < 0.01$ vs mdx mice. Scale bars: 100 µm.

Taken together, these results indicate that ALY688 markedly attenuates myonecrosis by inhibiting, at least in part, the necroptosis pathway in dystrophic mice.

ALY688 increases the number of revertant myofibres and enhances the myogenic program in mdx mice

Because inflammation and cell damage may subsequently lead to muscle regeneration, we hypothesised that ALY688 could promote a muscle healing process. Studies were performed in Q muscles.

First, we studied the presence of revertant fibres (RFs), which serves as an index of muscle regeneration capacity [27]. RFs are dystrophin-positive myofibres expressed at low percentages both in DMD patients and mdx mice [27]. We thus detected by immunofluorescence the expression of dystrophin, which is located near the sarcolemma. There were almost no RFs in Q sections of mdx mice, while mdx-T3 and -T15 mice displayed 4 to 5 times more immuno-positive fibres, respectively (Figure 5A, B). Likewise, the number of clusters (with at least two adjacent RFs) and the maximal number of RFs within a cluster were or tended to be higher in treated mdx than in untreated ones (Figure 5B, C).

In addition, mRNA levels of Mrf4, a muscle marker of late differentiation was more than halved in mdx mice, while these levels tended to re-increase in treated animals (Figure 5E). Protein levels of Myogenin were decreased in mdx mice, as described [33] and restored by the treatment, while protein abundance of Myosin heavy chain, Myh7, a marker of slow-twitch oxidative type I fibres, found in mature muscle was overexpressed by ALY688 (Figure 5F, G).-In vitro experiments in murine C2C12 myotubes cultured in an inflammatory context to mimic the dystrophic microenvironment unambiguously confirmed those data. ALY688 induced a strong restoration of both Mrf4 and Myh7. In agreement with improved oxidative phenotype, gene expression of ERRα, a marker of mitochondrial biogenesis, was also normalized (Figure S2). Myh1 mRNAs, a marker of fast-twitch glycolytic type II fibres was not or quasi not modified both ex vivo and in vitro (not shown).

Taken together, these results indicate that ALY688 may enhance the myogenic program in dystrophic muscle and its oxidative capacity.

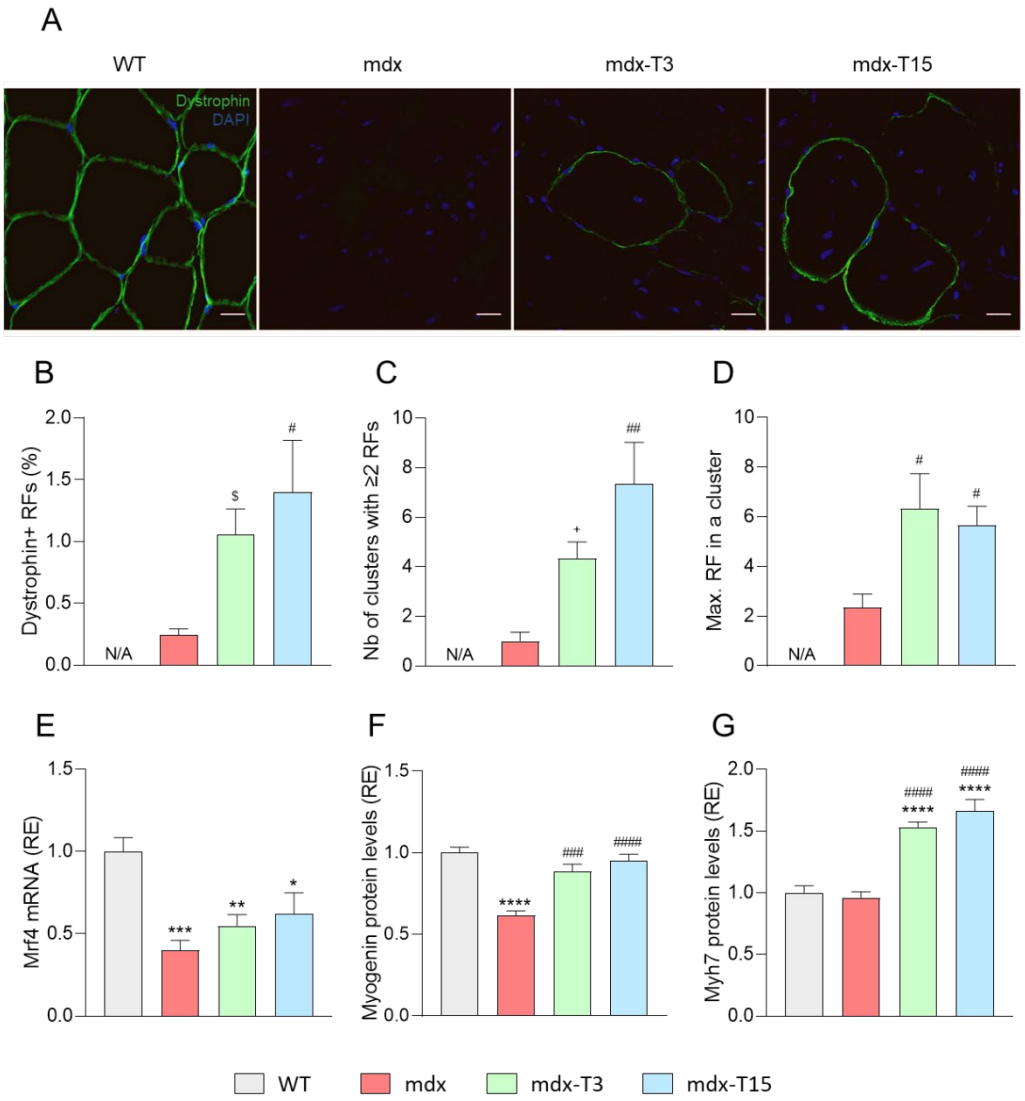

Figure 5. ALY688 treatment increases the number of revertant myofibres and enhances the myogenic program in mdx mice. *Immunofluorescence staining, mRNA and protein abundance measurements were performed on Q muscle in the 4 groups of mice.* ***(A)*** *Sections were stained with specific antibodies directed against dystrophin (in green). Nuclei were counterstained with DAPI (blue). Scale bars = 20 µm.* ***(B-D)*** *Quantification of dystrophin-positive revertant fibres (RF). The number of RFs per section was counted according to the following categories: (**B**) the % of RFs, (**C**) the number of RF clusters, and (**D**) the maximum number of RFs in a single cluster.* ***(E)*** *mRNA levels of Mrf4, a marker of late muscle differentiation was quantified,–normalised to Cyclophilin and then presented as relative expression (RE) compared to WT values.* ***(F-G)*** *Protein levels of Myogenin, a differentiation*

marker and Myh7, a marker of slow-twitch oxidative type I fibres were measured by ELISA; data are then presented as RE. Results are means ± SEM n=6 mice per group for all experiments. Statistical analysis was performed one-way ANOVA followed by Tukey's test (or Dunnett's test for B-D). $^{*}P < 0.05$, $^{**}P < 0.01$, $^{***}P < 0.001$, $^{****}P < 0.0001$ vs WT mice. $^{\$}P = 0.09$, $^{+}P = 0.07$, $^{\#}P < 0.05$, $^{\#\#}P < 0.01$, $^{\#\#\#}P < 0.001$, $^{\#\#\#\#}P < 0.0001$ vs mdx mice.

ALY688 attenuates fibrosis in mdx mice

We next investigated whether administration of ALY688 could reduce fibrosis, a hallmark of muscular dystrophies and a major cause of muscle weakness [34]. Q mdx muscle displayed a strong staining for Picrosirius red, a marker of fibrosis labelling collagen types I and III. In contrast, the percentage of fibrotic areas was reduced by ∼50-60 % in mdx treated mice (Figures 6A and 5B). In addition, protein levels of TGF-β, a highly pleiotropic cytokine playing an important role in wound healing and inducing the production of extracellular matrix, were increased in mdx mice, but returned back to normal in mice treated with the peptide (Figure 6C). The active form of Smad2 (P-Smad2), an effector protein of the TGF-β pathway, was also higher in mdx mice than in WT ones, while being diminished in mdx mice treated with ALY688 (∼45%) (Figure 6D). Additionally, gene expression of Collagen type I alpha 1 (COL1A1) and Collagen type III alpha 1 (COL3A1) was also quantified (Figure 6E and 6F). Treatment with ALY688 reduced the expression of Col1A1 by half, while Col3A1 was diminished by ∼40%.

Taken together, these results indicate that muscle accumulation of fibrosis-related factors and subsequent fibrosis is strongly reduced by ALY688 treatment in mdx mice.

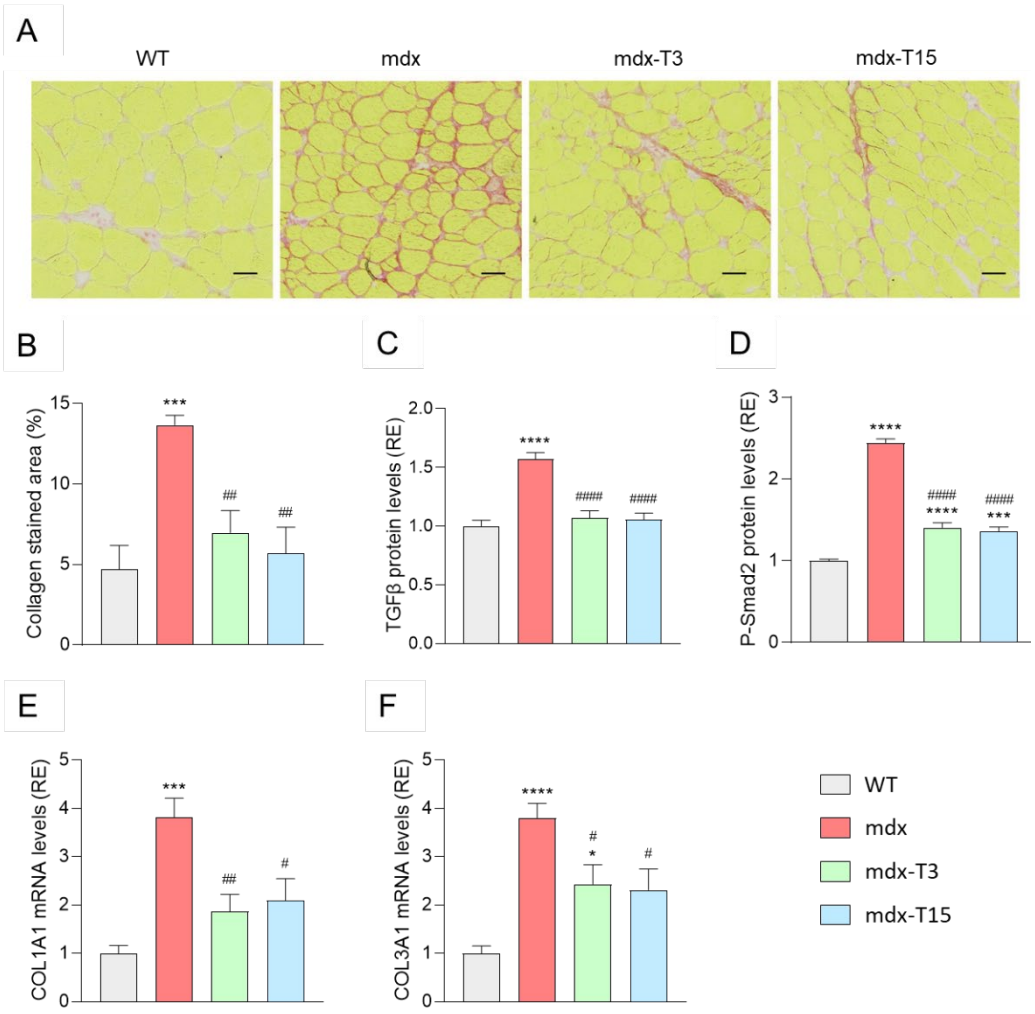

Figure 6. ALY688 treatment markedly reduces muscle fibrosis in mdx mice. Experiments were performed on Q muscle from the four groups of mice. (A) *Picrosirius red staining. Scale bars = 100 µm.* ***(B)*** *Quantification of Picrosirius red (expressed as % of collagen stained area).* ***(C-D)*** *ELISA assays were used to quantify TGF-β, a marker of extracellular matrix production, and phosphorylated-Smad2 (P-Smad2), an effector of the TGF-β pathway.* ***(E-F)*** *mRNA levels of COL1A1 and COL3A1. These levels were normalised to Cyclophilin. Results for TGF-β, P-Smad2, COL1A1 and COL3A1 were presented as relative expression (RE) compared to WT values. Data are means ± SEM; n = 6 mice per group for all experiments. Statistical analysis was performed using one-way ANOVA followed by Tukey's test. $^{***}P < 0.001$, $^{****}P < 0.001$ vs WT mice. $^{\#}P < 0.05$, $^{\#\#}P < 0.01$, $^{\#\#\#\#}P < 0.0001$ vs mdx mice.*

ALY688 enhances key effectors of the AMPK pathway in mdx mice

We examined on TA muscles whether ALY688 could, like ApN, stimulate the AMPK-PGC-1α axis. AMPK activity (P-AMPK) was actually increased by ALY688 (+55% vs other untreated groups; Figure 7A). PGC-1α protein levels were decreased in mdx mice (-25%) and rescued by ALY688 (Figure 7B). As AMPK-PGC-1α axis is known to repress the activity of NF-κB, a master regulator of inflammation [20], we measured this parameter. As expected, NF-κB activity (P-p65 subunit) was ∼3-fold higher in mdx than in WT mice, but was then reduced by ∼35% under ALY688 treatment (Figure 7C). Lastly, the protein levels of Utrophin (UTRN), an analogue of dystrophin and a target of PGC-1α [8, 35], were quantified in dystrophic muscle. Accordingly, UTRN protein levels were slightly augmented in mdx mice, likely to compensate for the lack of dystrophin [8]. These levels were further slightly but significantly increased (∼10%) in treated mice, possibly as a result of lower inflammation [36] (Figure 7D).

These results indicate that ALY688 potently activates the AMPK-PGC-1α axis in mdx mice, thereby decreasing NF-κB activity and upregulating UTRN.

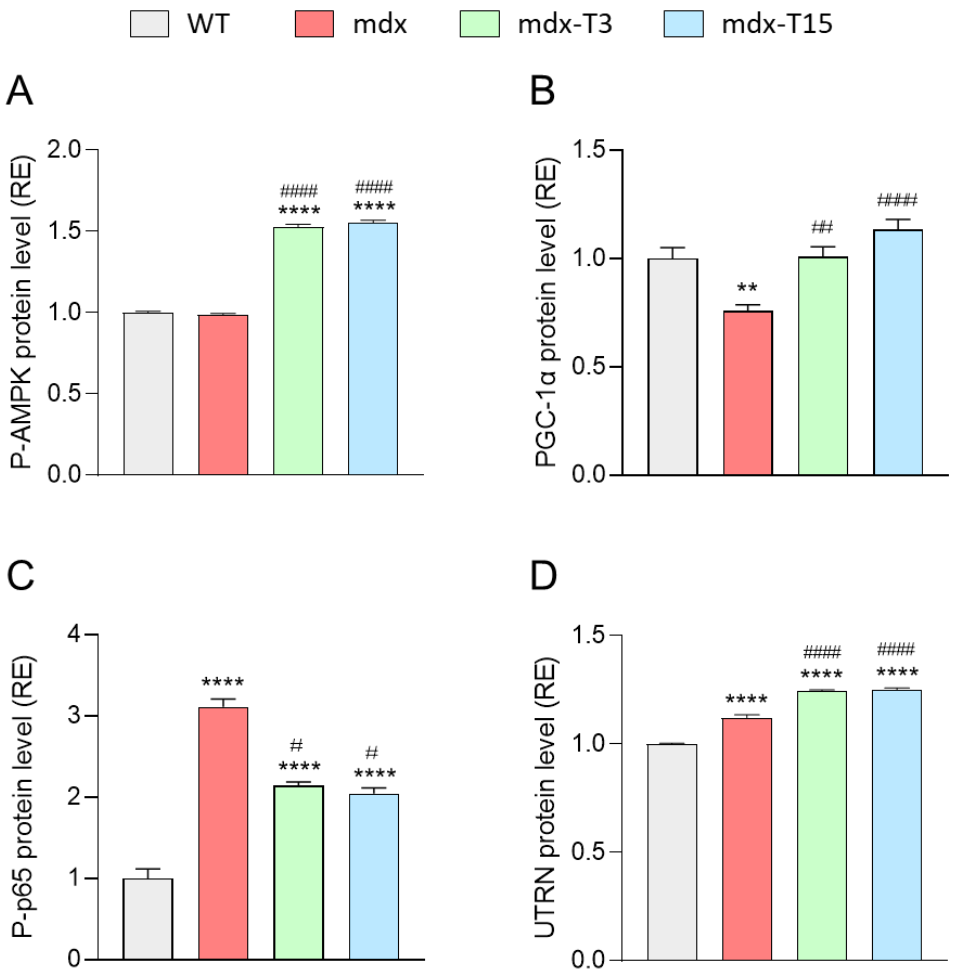

Figure 7. ALY688 treatment activates key effectors of the AMPK-PGC-1α axis in mdx mice. *Experiments were performed on TA from the four groups of mice.* ***(A)*** *Levels of AMPK activity,* ***(B)*** *PGC-1α protein,* ***(C)*** *NF-κB activity (P-p65 subunit), and* ***(D)*** *UTRN protein quantified by ELISAs. Absorbance data are presented as relative expression (RE) compared with WT values. Data are means ± SEM; n = 6 mice per group for all experiments. Statistical analysis was performed using one-way ANOVA followed by Tukey's test.* $^{**}P < 0.01$, $^{****}P < 0.0001$ *vs WT mice.* $^{\#}P < 0.05$, $^{\#\#}P < 0.01$, $^{\#\#\#\#}P < 0.0001$ *vs mdx mice.*

ALY688 recapitulates its beneficial effects on human myotubes challenged by pro-inflammatory cytokines

Due to its convenience and cost-effectiveness, the mdx mouse remains the most widely used model for studying DMD [37]. However, since this model exhibits a milder phenotype than patients, it was important to validate our data in human myotubes. We thus examined the direct effects of ALY688 in primary cultures of DMD and healthy myotubes. In order to mimic the inflammatory microenvironment of DMD, we challenged the myotubes with an inflammatory stimulus (TNFα/IFNγ) for 24 h, while ALY688 was added at different concentrations (from 10 pM to 300 nM).

Firstly, we confirmed the reproducibility of the ALY688 anti-inflammatory and pro-UTRN effects in human tissue, via its action on AdipoR1 (Figure 8). Gene expression levels of IL-1β, TNFα and UTRN were quantified over a range of ALY688 concentrations and dose-response curves were generated. A significant reduction of IL-1β and TNFα was detected starting from 10 pM ALY688 ($p < 0.01$ or less; Figure 8A, B) and an increase in UTRN from 10 nM onwards ($p < 0.01$; Figure 8C). The maximal effect for each parameter was obtained at about 100-300 nM ALY688. The median inhibitory concentrations (IC_{50}) for IL-1 β and TNFα were achieved around ∼100 and ∼35 pM, respectively, while the median activating concentration (EC_{50}) for UTRN was a bit higher (Figure 8A-C). Similar effects of ALY688 treatment were observed on challenged myotubes derived from healthy subjects (Figure S4).

To establish the central role of AdipoR1 in ALY688 effects, human myotubes were transfected with either a non-targeting pool siRNAs (siNT as negative control) or a specific siRNA against human AdipoR1 and were then exposed to 100 nM ALY688 and the inflammatory cocktail. First, we verified the effectiveness of the siRNA against AdipoR1 (siAR1) by demonstrating that its presence almost completely abolished AdipoR1 mRNA levels (Figure S3). Then, gene expression of the pro-inflammatory cytokines IL-1β and TNFα was quantified. The results showed a significant ∼2.5 and ∼3.5-fold increase, respectively under the effect of siAR1 compared to the siNT control group (Figure 7D, E). UTRN gene expression level was slightly but significantly decreased by ∼16% after AdipoR1 inhibition compared to the control group (Figure 8F). Taken together, these results demonstrate the AdipoR1-dependent effects of ALY688.

Secondly, we tested the effects of ALY688 on the AdipoR1-AMPK signalling pathway. Dose-response curves were also established for the activities of P-AMPK, P-p65 and for protein levels of UTRN (Figure 9A-C). The results show positive correlations between the concentration of ALY688 and the activation of AMPK or UTRN protein abundance, while a negative correlation was found with P-p65. ALY688 was already effective on the 3 parameters from 100 pM onwards ($p < 0.05$ or less) with a maximal response around 100-300 nM. EC_{50}/IC_{50} were within a nanomolar range. Once again, silencing AdipoR1 reversed all the effects of ALY688

(Figure 9D-F). Likewise, ALY688 was effective on challenged myotubes derived from healthy subjects (Figure S5).
Finally, we compared the effects of an optimal concentration of ALY688 (100 nM) with an optimal concentration of AdipoRon (25 µM) [20] on all these parameters. ALY688 was usually as affective as AdipoRon, but at much lower concentrations (100 nM vs 25 µM) (Figure 10).
Taken together, these results show that ALY688 potently activates the AMPK signalling pathway in human DMD myotubes, leading to downregulated NF-κB activity and pro-inflammatory cytokine abundance, and upregulated UTRN levels, in an AdipoR1-dependent manner.

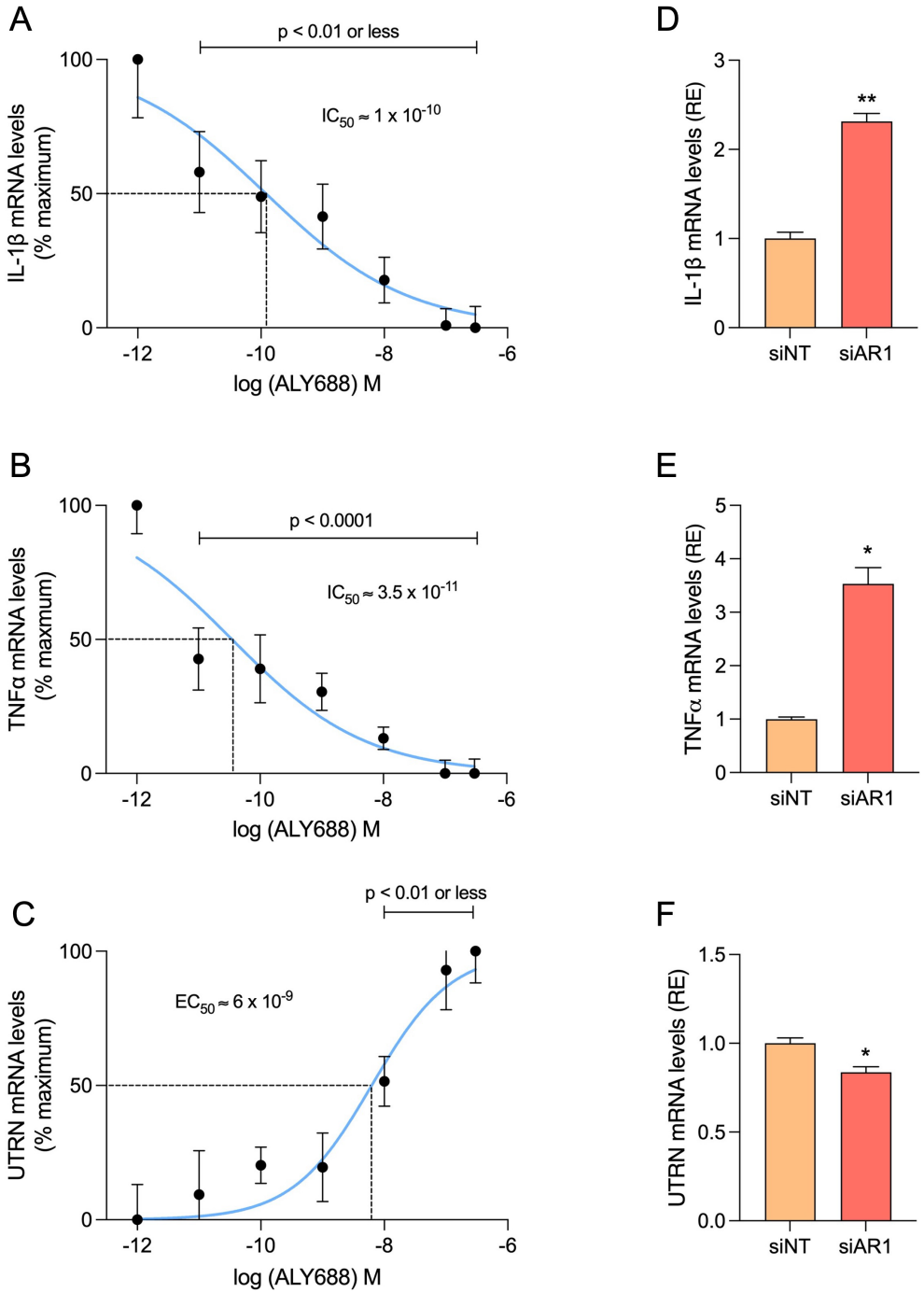
A
p < 0.01 or less
IC50 ≈ 1 x 10-10
IL-1β mRNA levels (% maximum)
log (ALY688) M
D
IL-1β mRNA levels (RE)
siNT
siAR1
B
p < 0.0001
IC50 ≈ 3.5 x 10-11
TNFα mRNA levels (% maxmum)
log (ALY688) M
E
TNFα mRNA levels (RE)
siNT
siAR1
C
p < 0.01 or less
EC50 ≈ 6 x 10-9
UTRN mRNA levels (% maximum)
log (ALY688) M
F
UTRN mRNA levels (RE)
siNT
siAR1

Figure 8. ALY688 recapitulates its anti-inflammatory and pro-UTRN effects in human DMD myotubes, via its action on AdipoR1. (A-C) *Dose-response curves illustrating the effects of ALY688 on IL-1β, TNFα, and UTRN mRNA levels in primary cultures of myotubes obtained from DMD patients. Cells were treated or not with several concentrations of ALY688 (from 10 pM to 300 nM) for 24 h, while being challenged with an inflammatory cocktail (human recombinant TNFα/INFγ, each at 15 ng/mL). mRNA levels were normalised to human TATA box-binding protein. Data were then presented as % of the maximal levels obtained either without (A, B) or with 300 nM ALY688 (C).* ***(D-F)*** *In some experiments, cells were first transfected (24 h) with siRNA against AdipoR1 (50 nM) or a negative [non-targeting, siNT (50 nM)] control and then treated with ALY688 (100 nM) combined to inflammation (TNFα/IFNγ) for an additional 24h. After normalisation, mRNA levels were presented as relative expression (RE) to siNT conditions (D-F). Data are means ± SEM for 4 cultures, each obtained from a different donor (i.e., 4 DMD subjects). Statistical analysis was performed using repeated measures of ANOVA followed by Dunnett's test (A-C) or two-tailed paired Student's t-test (D-F).* $^{*}P < 0.05$, $^{**}P < 0.01$ *vs siNT.*

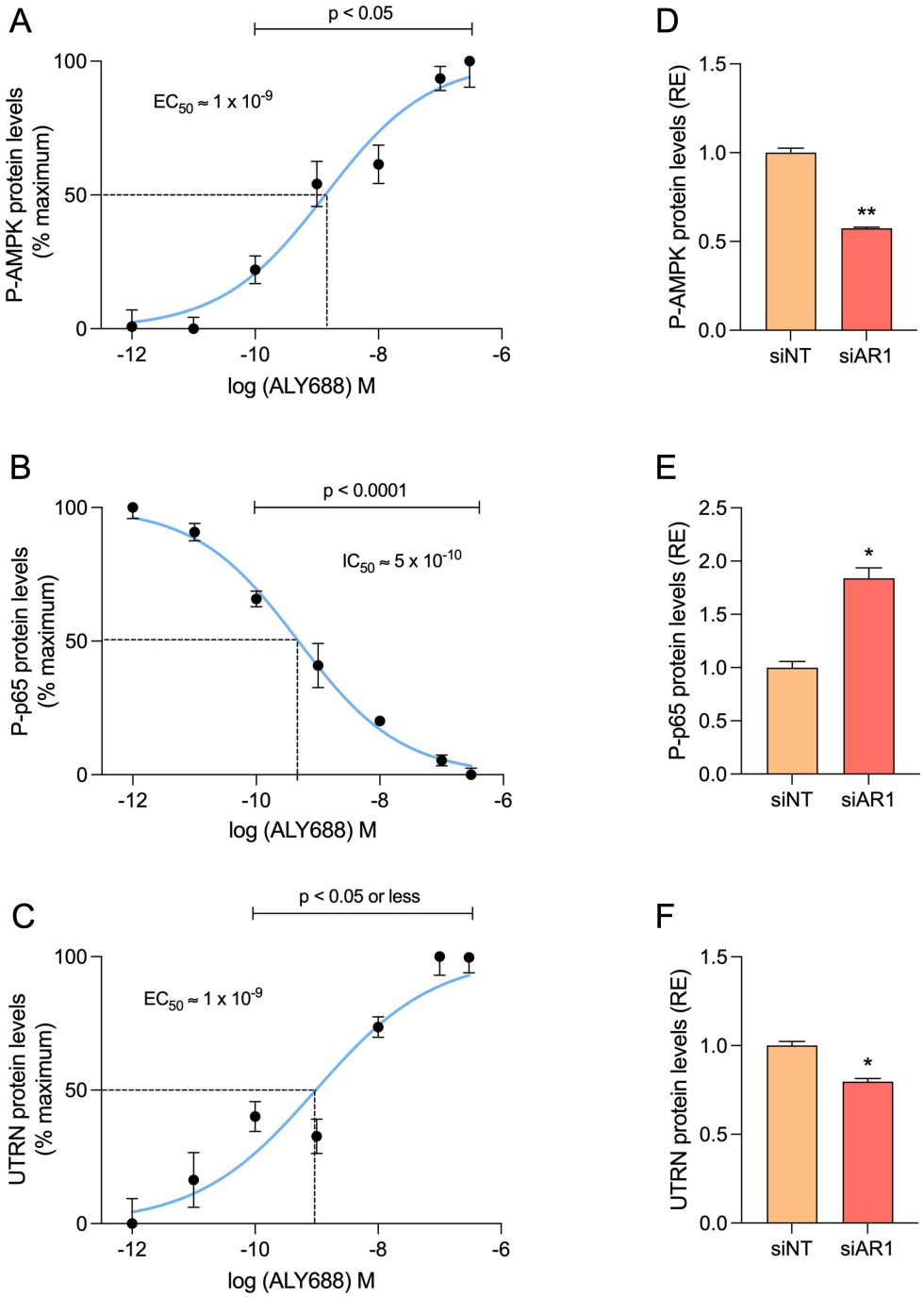
A
p < 0.05
EC50 ≈ 1 x 10-9
P-AMPK protein levels (% maximum)
log (ALY688) M
D
P-AMPK protein levels (RE)
**
siNT
siAR1
B
p < 0.0001
IC50 ≈ 5 x 10-10
P-p65 protein levels (% maximum)
log (ALY688) M
E
P-p65 protein levels (RE)
*
siNT
siAR1
C
p < 0.05 or less
EC50 ≈ 1 x 10-9
UTRN protein levels (% maximum)
log (ALY688) M
F
UTRN protein levels (RE)
*
siNT
siAR1

Figure 9. ALY688 treatment recapitulates its effects on key effectors of the AMPK signalling in human DMD myotubes, via its action on AdipoR1. (A-C) *Dose-response curves illustrating the effects of ALY688 on AMPK and NF-κB activity (P-p65 subunit), and UTRN protein levels in primary cultures of myotubes obtained from DMD patients. Cells were treated or not with several concentrations of ALY688 (from 10 pM to 300 nM) for 24 h, while being challenged with an inflammatory cocktail (human recombinant TNFα/INFγ, each at 15 ng/mL). Levels of each protein were measured by ELISAs and then presented as % of the maximum achieved either without (B) or with 300 nM ALY688 (A-C).* ***(D-F)*** *In some experiments, cells were first transfected (24 h) with siRNA against AdipoR1 (50 nM) or a negative [non-targeting, siNT (50 nM)] control and then treated with ALY688 (100 nM) combined to inflammation (TNFα/IFNγ) for an additional 24h. For each protein, levels were presented as relative expression (RE) compared with siNT conditions. Data are means ± SEM for 4 cultures, each obtained from a different donor (i.e., 4 DMD subjects). Statistical analysis was performed using repeated measures of ANOVA followed by Dunnett's test or using two-tailed paired Student's t-test. $^{*}P < 0.05$, $^{**}P < 0.01$ vs siNT.*

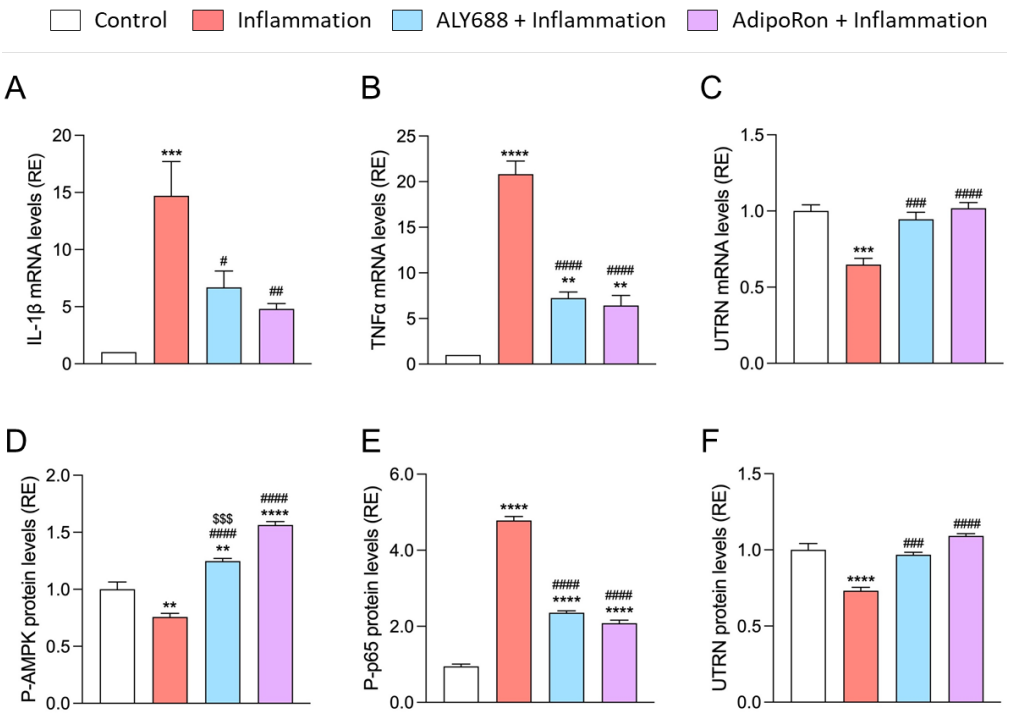

Figure 10. Comparison of two adiponectin receptor agonists (ALY688 and AdipoRon) in challenged myotubes from DMD patients. *Myotubes were either left untreated or treated with AdipoRon (25 µM) or ALY688 (100 nM) for 24 h, while being challenged or not with and inflammatory cocktail [TNFα (15 ng/mL) + (IFNγ) (15 ng/mL)].* ***(A-C)*** *mRNA levels of pro-inflammatory cytokines (IL-1ß and TNFα) and UTRN. mRNA levels were normalised to human TATA box-binding protein and the subsequent ratios were presented as relative*

expression (RE) compared with the control condition (i.e. no compound, no inflammation). ***(D-F)*** *Levels of AMPK and NF-κB activity (P-p65 subunit), and UTRN protein were quantified by ELISAs and presented as relative expression (RE) compared with control. Data are means ± SEM for 4 cultures, each obtained from a different donor (i.e., 4 DMD subjects). Statistical analysis was performed using one-way ANOVA followed by Tukey's test.* $^{**}P < 0.01$, $^{***}P < 0.001$, $^{****}P < 0.0001$ *vs Control.* $^{\#}P < 0.05$, $^{\#\#}P < 0.01$, $^{\#\#\#}P < 0.001$, $^{\#\#\#\#}P < 0.0001$ *vs Inflammation.* $^{\$\$\$}P < 0.001$ *vs AdipoRon*

Discussion

Due to its interesting properties, we have been studying Adiponectin (ApN) for almost two decades, with a special focus on its beneficial and protective properties on muscle, as a main target tissue [5]. More recently, we started investigating its effects in Duchenne muscular dystrophy (DMD). We and others have shown low circulating levels of ApN in mdx mice [8, 38], and in human patients [39], while ApN supplementation was able to counteract the progression of the disease in the mouse model [8, 9]. Therefore, there is a rationale to therapeutically correcting the low levels of ApN in DMD patients.

However, the direct use of ApN as a therapeutic agent is very limited. Several small molecules and short peptides have been recently identified that target ApN receptors (AdipoRs) and mimic some of ApN effects. Today, two of these have been extensively characterised, AdipoRon and ALY688 (formerly known as ADP355) [5]. AdipoRon is an ApN receptor small-molecule agonist, first discovered by Okada-Iwabu [40], and is now being studied in a large range of preclinical disease models [5]. We have recently shown that daily administration of AdipoRon for two months was able to rescue the dystrophic phenotype by attenuating muscle inflammation and injury, while enhancing muscle regeneration and function [20]. However, even though AdipoRon has been commercially available for a decade, it has only been used for research purposes and no human clinical trials have been conducted. ALY688 is also an ApN receptor agonist. This decapeptide has been developed by Otvos et al., 2011 [10], and now exists in two different formulations. First, a conventional formulation, used either for *in vitro* studies or as an ophthalmic solution, which has been recently tested in a Phase 1/2a clinical study to evaluate the safety and efficacy in subjects with xerophthalmia (dry eyes) (NCT04201574). Second, an extended release formulation of ALY688 (ALY688ER), administered subcutaneously, recently developed to target inflammatory and fibrotic diseases. Thus, ALY688 is a strong candidate for clinical evaluation in the near future as a promising therapeutic. One novel interest of this study was to investigate the full effect of ALY688 on the dystrophic skeletal muscle, and to potentially offer a new and promising therapeutic prospect for better management of DMD.

We showed that a daily sc administration over an eight-week period could protect the dystrophic muscle from excessive inflammatory responses and oxidative stress (Figure 11). Indeed, pro-inflammatory cytokine expression, oxidative stress

markers, $CD68^+$ macrophages infiltrates, were reduced in mdx treated animals. Likewise, the extension of myonecrosis was decreased in treated mdx mice. The abundance P-RIP protein, a necroptosis factor that contributes to myofibre death in DMD muscle [31], was also reduced, suggesting that this protein could at least in part play a role in the anti-myonecrotic effect of ALY688. Taken together, our findings are consistent with other studies showing that administration of ALY688 significantly reduced hepatic macrophage activation [13] as well as inflammation, oxidative stress and tissue damage after toxic heart injury [14].

ALY688 also positively modulated the muscle regeneration process (Figure 11). Indeed, mdx mice, as well as challenged C2C12 muscle cells, treated with ALY688 displayed increased expression of muscle differentiation and maturation factors. Similarly, other studies demonstrated the tissue regenerating process, where treatment with ALY688 prevented cardiac atrophy and promoted liver regeneration [13, 14]. Moreover, treated mice displayed more revertant fibres (RFs) than untreated mdx mice. RFs are sporadic dystrophin-positive myofibres observed in both DMD patients and mdx mice [41]. They arise from alternative splicing in satellite cells and their expansion reflects the activity of these precursor cells, and thus serves as an index of muscle regeneration capacity [27, 42]. This result highlights for the first time the effect of an ApN mimic on the presence and expansion of RFs in DMD, thus strengthening the protective and regenerative effects of ALY688 on the dystrophic muscle.

Fibrosis is thought to be one prominent pathological mechanism in DMD, leading to impaired muscle function and ultimately death [4, 34]. It is well known that the chronic muscle injury and inflammation, seen in DMD, leads to the recruitment of fibro-adipogenic progenitors (FAPs), which in turn differentiate into fibroblasts by TGF-β thereby increasing the deposition of connective tissues [43, 44]. TGF-β is a major mediator of the fibrotic response and acts via its effector, the phosphorylated and active form of Smad2, which can then promote the formation of collagen type I and III. To date, DMD still awaits a prominent anti-fibrotic treatment [45]. In the present study, we highlight the potent anti-fibrotic properties of ALY688 (Figure 11), as demonstrated by normalised Picrosirius Red staining. In addition, the quantification of major profibrotic actors such as TGF-β and P-Smad2, as well as the end products such as collagen types I and III, were also either markedly reduced or normalised after ALY688 treatment. These results correlate with the effects of ALY688 observed previously on fibrotic heart [14] and liver [12, 13].

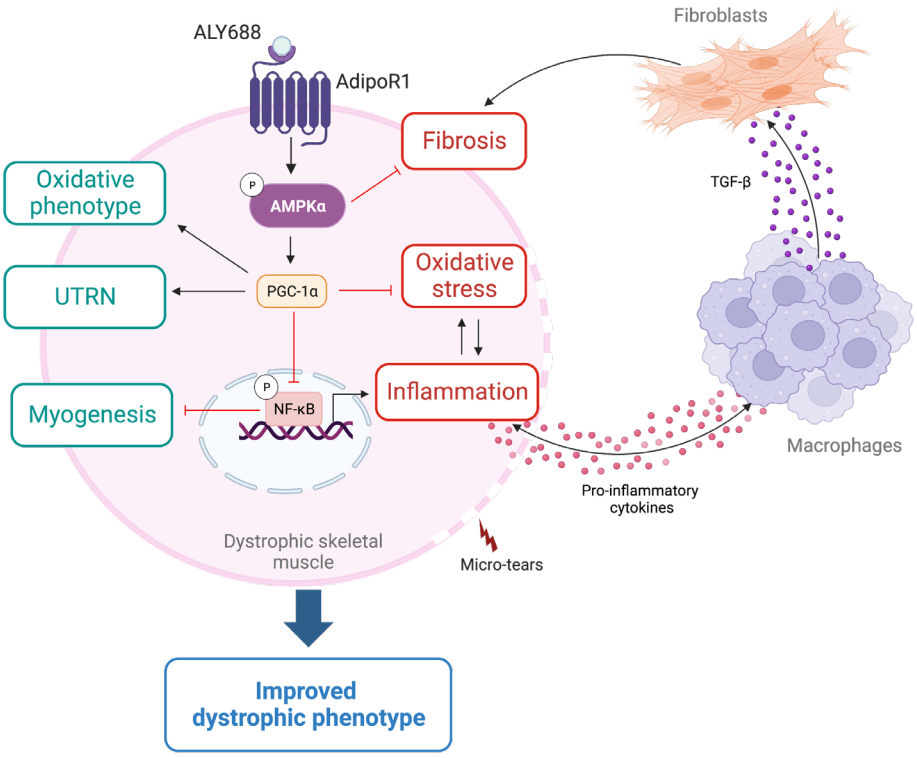

Figure 11. Proposed model for the effects of ALY688 in DMD. *This figure summarises the effects and the mechanism of action of ALY688 on the dystrophic skeletal muscle, which is characterised by micro-tears in the sarcolemma due to lack of dystrophin protein. Briefly, binding of ALY688 to AdipoR1 will activate AMPK-PGC-1α pathway. Then, PGC-1α represses NF-κB activity resultinin reduction of inflammation and necrosis, and in improved myogenic program. In addition, activation AMPK-PGC-1α axis will help mediate several effects of ALY688. First, increased muscle oxidative capacity and function. Second, increased expression and production of utrophin (UTRN) and reduced oxidative stress, which would protect the dystrophic muscle. Third, marked decrease in TGF-β levels and signalling pathway, either directly or indirectly by reducing inflammation, and subsequently blunted muscle fibrosis. These beneficial and protective properties will thus lead to an improved dystrophic phenotype. All these effects have been demonstrated on skeletal muscle from mdx mice and/or confirmed in human DMD myotubes. Pointed head black arrows indicate activation or induction, while blunt head red arrows indicate inhibition. Boxes with processes in green represent net beneficial effects of ALY688, while boxes with processes in red represent deleterious factors inhibited by ALY688. Created with BioRender.com.*

By exploring the mechanisms of action of ALY688, we found that AMPK was activated in ALY688-treated mice, as demonstrated by the increased phosphorylated form of AMPK and the subsequent increased levels of PGC-1α (Figure 11). This activation helps to rescue the dystrophic phenotype by four fundamental mechanisms. First, AMPK-PGC-1α axis is a powerful suppressor of NF-κB signalling and of inflammation [46], which in turn improves the dystrophic muscle, as already demonstrated in other studies [3, 8, 47, 48]. Second, PGC-1α, via mitochondrial biogenesis and function that are impaired in DMD [49], can contribute to the change of muscle fibre type towards an oxidative phenotype, which is more resistant to the absence of dystrophin [50]. A similar switch has been observed with AdipoRon [20]. Likewise, overactivation of PGC-1α by histone deacetylase inhibitors also mitigated the dystrophic phenotype by reverting mitochondrial biogenesis deficit [49]. Third, expression and protein levels of utrophin, a dystrophin analogue, are increased by AMPK-PGC-1α. Up-regulation of utrophin may restore sarcolemmal integrity and confer morphological and functional improvements in mdx mice [35, 51]. Fourth, AMPK can be a powerful suppressor of TGF-β/Smad signalling [52, 53]. *A contrario*, specific AMPK inhibition in mice FAPs has been shown to enhance TGF-β signalling and promote fibrosis in regenerated muscles [54]. Moreover, macrophages also promote fibrosis in dystrophic muscles, while AMPK activation might reduce their TGF-β production and subsequently their pro-fibrotic effect [55]. Our findings demonstrate that ALY688 can be a potent AMPK signalling activator, suppressing NF-κB and TGF-β activities and upregulating utrophin. This in turn may lessen muscle inflammation, stress and fibrosis, protect muscle against injury, and enhance muscle state and function, thus strikingly alleviating the dystrophic phenotype (figure 11). Beside AMPK signalling, ALY688 could activate, similar to ApN, other cascades and effectors, such as Ca2+/ calmodulin-dependent protein kinase kinase, p38 mitogen-activated protein kinase, peroxisome proliferator activated receptor alpha, ceramidase activity and others, to exert a plethora of metabolic and protective actions in several target tissues and organs [5, 56-58].

A puzzling lack of a clear dose-dependent effect of ALY688-ER was observed *in vivo*. We cannot exclude an incomplete or uneven distribution of the active compound. Alternatively, activation of some metabolic pathways/functions may follow a “bell-shaped” curve, with the 3 mg/kg/day dose already being optimal, while the beneficial effects could be limited at highest doses, as has been reported for some AdipoR agonists [59].

The mdx mouse remains one of the best-known animal models for DMD research due to its practicality and affordability [60]. Although mice express a non-functional dystrophin due to a point mutation in the DMD gene, they display a milder phenotype than DMD patients [61]. Therefore, it was crucial to confirm our findings using human myotubes from DMD patients. Hence, we showed that primary cultures of either healthy or DMD myotubes produced effects similar to those shown in mdx mice, and support earlier findings from our studies with ApN [8, 62].

Indeed, the conventional solution of ALY688 used *in vitro* was extremely effective at counteracting inflammation in challenged myotubes, even at extremely low concentrations. The central role of the AdipoR1-AMPK-PGC-1α pathway was also confirmed in human myotubes, as the effects of ALY688 were totally dependent on the presence of AdipoR1.

We next assessed the effectiveness of ALY688 with that of AdipoRon both *in vivo/ex vivo* and *in vitro*. Firstly, when we compared the effects of ALY688 found in mdx mice, to those previously described with AdipoRon [20], both ApN mimics effectively reduced muscle inflammation and improved muscle performance, but AdipoRon had a slightly better pro-myogenic effect while ALY688 displayed very potent anti-fibrotic properties. The anti-fibrotic potential of AdipoRon has not been explored in DMD yet, but some studies reported it could mitigate cutaneous, liver and renal fibrosis [63-65]. Secondly, when we directly compared the *in vitro* effects of ALY688 to those of AdipoRon on human DMD myotubes, both ApN mimics exhibited similar protective effects, but this was reached at much lower (200-fold) concentrations with ALY688 (optimal concentrations: 25µM for AdipoRon [20] vs 100 nM for ALY688). More interestingly, ALY688 was already effective on most parameters at a very low concentration of 100 pM, giving ALY688 a clear advantage over AdipoRon for the *in vitro* study.

Besides gene therapy, which is limited to a small set of patients [66, 67], the only medication currently used to slow the course of DMD is glucocorticoids (GCs). Their anti-inflammatory and immunosuppressive characteristics are beneficial in the treatment of this disease [68]. Unfortunately, their prolonged usage is responsible for several adverse effects such as cushingoid facies, weight gain, glucose intolerance, growth retardation, vertebral fractures, and muscular atrophy [68]. As a result, ALY688's anti-inflammatory, pro-myogenic and potent anti-fibrotic effects on skeletal muscle make it a potentially attractive alternative to GCs. ALY688 also has the benefit of protecting liver and cardiac functions in mice, and seems to be safe in our study and in other murine models, as well as in formal toxicology studies [12-14, 16]. Moreover, unlike GCs, ALY688 could enhance insulin sensitivity and regulate adiposity, thereby improving metabolic condition [15, 69].

Conclusions

In conclusion, our data show that ALY688, an ApN mimetic, could strongly induce AMPK signalling and exert potent protective effects on the dystrophic muscle. More specifically, ALY688 proved to be a powerful anti-fibrotic agent that could prevent or mitigate fibrosis in the skeletal muscle, thus providing a high priority treatment option for patients. ALY688 could also be highly impactful for the treatment of other muscles including the heart, or inflammatory and fibrotic diseases.

Supplementary Materials: The following supporting information can be downloaded at: www.mdpi.com/xxx/s1, Tables S1, S2, S3 & S4, Figures S1, S2, S3, S4 & S5.

Author Contributions: Conceptualization: MA-S and SMB. Methodology: ND, RV, and MA-S. Formal analysis: ND, CP, MD-LC, LN, CMS, RV and MA-S. Investigation: ND, CP, RV, MD-LC and MA-S. Writing original draft: ND, RV, SMB and MA-S. Writing review and editing: ND, CP, MD-LC, CMS, RV, LN, PV, MA-S, and SMB. Supervision: MA-S and SMB. Funding acquisition: ND, MA-S, PV and SMB. All authors contributed to the article and approved the submitted version.

Funding: This study was funded by a research contract agreement with Allysta Pharmaceuticals Inc. This work was also supported by grants from the Belgian Telethon (ABMM), the French Association against Myopathies (AFM Téléthon), and the Fund for Scientific Research– FNRS (PDR/T.0026.21). MAS is Chargé de Recherches and ND Spécialiste Doctorant at the FNRS. CMS has received a fellowship from the FRIA.

Institutional Review Board Statement: All procedures conducted on mice were approved by the Ethical Committee for Animal Experimentation from the Medical Sector at Université Catholique de Louvain (no. LA1230396). Primary cultures of human myotubes from DMD or healthy subjects were obtained via Myobank-AFM (Association Française contre les Myopathies) in accordance with approved guidelines and regulations of the bioethics department of the Direction Générale de la Recherche et de l'Innovation, France (DGRI no. AC-2013-1868).

Informed Consent Statement: Written informed consent to participate in this study was provided by the participants' legal guardian/next of kin.

Data Availability Statement: The raw data supporting the conclusions of this article will be made available by the authors, without undue reservation.

Acknowledgments: We are grateful to the IREC imaging platform for the use of the equipment and their aid. This work is generated within the European Reference Network for Neuromuscular Diseases.

Conflicts of Interest: The authors declare no conflict of interest. The funders had no role in the design of the study; in the collection, analyses, or interpretation of data; in the writing of the manuscript; or in the decision to publish the results.

References

1. Blake, D.J., et al., *Function and genetics of dystrophin and dystrophin-related proteins in muscle.* Physiol Rev, 2002. **82**(2): p. 291-329.
2. Ryder, S., et al., *The burden, epidemiology, costs and treatment for Duchenne muscular dystrophy: an evidence review.* Orphanet J Rare Dis, 2017. **12**(1): p. 79.
3. Acharyya, S., et al., *Interplay of IKK/NF-kappaB signaling in macrophages and myofibers promotes muscle degeneration in Duchenne muscular dystrophy.* J Clin Invest, 2007. **117**(4): p. 889-901.
4. Klingler, W., et al., *The role of fibrosis in Duchenne muscular dystrophy.* Acta Myol, 2012. **31**(3): p. 184-95.
5. Abou-Samra, M., et al., *Adiponectin and Its Mimics on Skeletal Muscle: Insulin Sensitizers, Fat Burners, Exercise Mimickers, Muscling Pills … or Everything Together?* Int J Mol Sci, 2020. **21**(7).
6. Yamauchi, T., et al., *Targeted disruption of AdipoR1 and AdipoR2 causes abrogation of adiponectin binding and metabolic actions.* Nat Med, 2007. **13**(3): p. 332-9.
7. Yamauchi, T., et al., *Cloning of adiponectin receptors that mediate antidiabetic metabolic effects.* Nature, 2003. **423**(6941): p. 762-9.
8. Abou-Samra, M., et al., *Involvement of adiponectin in the pathogenesis of dystrophinopathy.* Skelet Muscle, 2015. **5**: p. 25.
9. Abou-Samra, M., et al., *Potential Therapeutic Action of Adiponectin in Duchenne Muscular Dystrophy.* Am J Pathol, 2017. **187**(7): p. 1577-1585.
10. Otvos, L., Jr., et al., *Design and development of a peptide-based adiponectin receptor agonist for cancer treatment.* BMC Biotechnol, 2011. **11**: p. 90.
11. Otvos, L., Jr., *Potential Adiponectin Receptor Response Modifier Therapeutics.* Front Endocrinol (Lausanne), 2019. **10**: p. 539.
12. Kumar, P., et al., *Adiponectin agonist ADP355 attenuates CCl4-induced liver fibrosis in mice.* PLoS One, 2014. **9**(10): p. e110405.
13. Wang, H., et al., *Adiponectin-derived active peptide ADP355 exerts anti-inflammatory and anti-fibrotic activities in thioacetamide-induced liver injury.* Sci Rep, 2016. **6**: p. 19445.
14. Zhao, D., et al., *Adiponectin agonist ADP355 ameliorates doxorubicin-induced cardiotoxicity by decreasing cardiomyocyte apoptosis and oxidative stress.* Biochem Biophys Res Commun, 2020. **533**(3): p. 304-312.
15. Sung, H.K., et al., *ALY688 elicits adiponectin-mimetic signaling and improves insulin action in skeletal muscle cells.* Am J Physiol Cell Physiol, 2022. **322**(2): p. C151-c163.

16. Sun, L., et al., *Activation of Adiponectin Receptor Regulates Proprotein Convertase Subtilisin/Kexin Type 9 Expression and Inhibits Lesions in ApoE-Deficient Mice.* Arterioscler Thromb Vasc Biol, 2017. **37**(7): p. 1290-1300.
17. Porter, J.D., et al., *A chronic inflammatory response dominates the skeletal muscle molecular signature in dystrophin-deficient mdx mice.* Hum Mol Genet, 2002. **11**(3): p. 263-72.
18. Kastenschmidt, J.M., et al., *QuantiMus: A Machine Learning-Based Approach for High Precision Analysis of Skeletal Muscle Morphology.* Front Physiol, 2019. **10**: p. 1416.
19. Augusto, V., et al., *Skeletal muscle fiber types in C57BL6J mice.* J. morphol. Sci, 2004. **21**: p. 89-94.
20. Abou-Samra, M., et al., *AdipoRon, a new therapeutic prospect for Duchenne muscular dystrophy.* J Cachexia Sarcopenia Muscle, 2020. **11**(2): p. 518-533.
21. Dubuisson, N., et al., *Inhibiting the inflammasome with MCC950 counteracts muscle pyroptosis and improves Duchenne muscular dystrophy.* Front Immunol, 2022. **13**: p. 1049076.
22. *<van Putten M. The use of hanging wire tests to monitor muscle strength and condition over time. In DMDM.2.1.004. 2011. httpstreat-nmd.orgwp-contentuploads202106uncategorized-Wire-test.pdf. Accessed 23 Feb 2022..pdf>.*
23. Bi, P., et al., *Stage-specific effects of Notch activation during skeletal myogenesis.* Elife, 2016. **5**.
24. Yue, F., et al., *Conditional Loss of Pten in Myogenic Progenitors Leads to Postnatal Skeletal Muscle Hypertrophy but Age-Dependent Exhaustion of Satellite Cells.* Cell Rep, 2016. **17**(9): p. 2340-2353.
25. Castro, B. and S. Kuang, *Evaluation of Muscle Performance in Mice by Treadmill Exhaustion Test and Whole-limb Grip Strength Assay.* Bio Protoc, 2017. **7**(8).
26. Grounds, M., *Quantification of histopathology in Haemotoxylin and Eosin stained muscle sections. In DMD_M.1.2.007. 2014. https://treat-nmd.org/wp-content/uploads/2016/08/MDX-DMD_M.1.2.007-28.pdf p-7/13. Accessed 26.07.23. pdf.*
27. Rodrigues, M., et al., *Impaired regenerative capacity and lower revertant fibre expansion in dystrophin-deficient mdx muscles on DBA/2 background.* Sci Rep, 2016. **6**: p. 38371.
28. Mayeuf-Louchart, A., et al., *MuscleJ: a high-content analysis method to study skeletal muscle with a new Fiji tool.* Skelet Muscle, 2018. **8**(1): p. 25.
29. Selvais, C.M., et al., *AdipoRon enhances healthspan in middle-aged obese mice: striking alleviation of myosteatosis and muscle degenerative markers.* J Cachexia Sarcopenia Muscle, 2023. **14**(1): p. 464-478.

30. Narola, J., et al., *Conditional expression of TGF-β1 in skeletal muscles causes endomysial fibrosis and myofibers atrophy.* PLoS One, 2013. **8**(11): p. e79356.
31. Morgan, J.E., et al., *Necroptosis mediates myofibre death in dystrophin-deficient mice.* Nat Commun, 2018. **9**(1): p. 3655.
32. Grounds, M.D., et al., *Biomarkers for Duchenne muscular dystrophy: myonecrosis, inflammation and oxidative stress.* Dis Model Mech, 2020. **13**(2).
33. Lazzarin, M., et al., *Lack of dystrophin influences muscle inflammation but not myogenic regulatory factors after eccentric exercise in mdx mice.* Motriz. Revista de Educação Física, 2020. **26**.
34. Mahdy, M.A.A., *Skeletal muscle fibrosis: an overview.* Cell Tissue Res, 2019. **375**(3): p. 575-588.
35. Al-Rewashdy, H., et al., *Utrophin A is essential in mediating the functional adaptations of mdx mouse muscle following chronic AMPK activation.* Hum Mol Genet, 2015. **24**(5): p. 1243-55.
36. Gordon, B.S., D.C. Delgado Diaz, and M.C. Kostek, *Resveratrol decreases inflammation and increases utrophin gene expression in the mdx mouse model of Duchenne muscular dystrophy.* Clin Nutr, 2013. **32**(1): p. 104-11.
37. McGreevy, J.W., et al., *Animal models of Duchenne muscular dystrophy: from basic mechanisms to gene therapy.* Dis Model Mech, 2015. **8**(3): p. 195-213.
38. Hathout, Y., et al., *Discovery of serum protein biomarkers in the mdx mouse model and cross-species comparison to Duchenne muscular dystrophy patients.* Hum Mol Genet, 2014. **23**(24): p. 6458-69.
39. Hathout, Y., et al., *Disease-specific and glucocorticoid-responsive serum biomarkers for Duchenne Muscular Dystrophy.* Sci Rep, 2019. **9**(1): p. 12167.
40. Okada-Iwabu, M., et al., *A small-molecule AdipoR agonist for type 2 diabetes and short life in obesity.* Nature, 2013. **503**(7477): p. 493-9.
41. Lu, Q.L., et al., *Massive idiosyncratic exon skipping corrects the nonsense mutation in dystrophic mouse muscle and produces functional revertant fibers by clonal expansion.* J Cell Biol, 2000. **148**(5): p. 985-96.
42. Yokota, T., et al., *Expansion of revertant fibers in dystrophic mdx muscles reflects activity of muscle precursor cells and serves as an index of muscle regeneration.* J Cell Sci, 2006. **119**(Pt 13): p. 2679-87.
43. Biferali, B., et al., *Fibro-Adipogenic Progenitors Cross-Talk in Skeletal Muscle: The Social Network.* Front Physiol, 2019. **10**: p. 1074.
44. Tidball, J.G. and M. Wehling-Henricks, *Shifts in macrophage cytokine production drive muscle fibrosis.* Nat Med, 2015. **21**(7): p. 665-6.

45. Yao, S., et al., *Current Pharmacological Strategies for Duchenne Muscular Dystrophy.* Front Cell Dev Biol, 2021. **9**: p. 689533.
46. Salminen, A., J.M. Hyttinen, and K. Kaarniranta, *AMP-activated protein kinase inhibits NF-κB signaling and inflammation: impact on healthspan and lifespan.* J Mol Med (Berl), 2011. **89**(7): p. 667-76.
47. Heier, C.R., et al., *VBP15, a novel anti-inflammatory and membrane-stabilizer, improves muscular dystrophy without side effects.* EMBO Mol Med, 2013. **5**(10): p. 1569-85.
48. Siegel, A.L., et al., *Treatment with inhibitors of the NF-kappaB pathway improves whole body tension development in the mdx mouse.* Neuromuscul Disord, 2009. **19**(2): p. 131-9.
49. Giovarelli, M., et al., *Givinostat as metabolic enhancer reverting mitochondrial biogenesis deficit in Duchenne Muscular Dystrophy.* Pharmacol Res, 2021. **170**: p. 105751.
50. Selsby, J.T., et al., *Rescue of dystrophic skeletal muscle by PGC-1α involves a fast to slow fiber type shift in the mdx mouse.* PLoS One, 2012. **7**(1): p. e30063.
51. Squire, S., et al., *Prevention of pathology in mdx mice by expression of utrophin: analysis using an inducible transgenic expression system.* Hum Mol Genet, 2002. **11**(26): p. 3333-44.
52. Marangoni, R.G., et al., *Adiponectin is an endogenous anti-fibrotic mediator and therapeutic target.* Sci Rep, 2017. **7**(1): p. 4397.
53. Darmawan, C.C., et al., *Adiponectin-Based Peptide (ADP355) Inhibits Transforming Growth Factor-β1-Induced Fibrosis in Keloids.* Int J Mol Sci, 2020. **21**(8).
54. Liu, X., et al., *AMP-activated protein kinase inhibition in fibro-adipogenic progenitors impairs muscle regeneration and increases fibrosis.* J Cachexia Sarcopenia Muscle, 2023. **14**(1): p. 479-492.
55. Juban, G., et al., *AMPK Activation Regulates LTBP4-Dependent TGF-β1 Secretion by Pro-inflammatory Macrophages and Controls Fibrosis in Duchenne Muscular Dystrophy.* Cell Rep, 2018. **25**(8): p. 2163-2176.e6.
56. Ruan, H. and L.Q. Dong, *Adiponectin signaling and function in insulin target tissues.* J Mol Cell Biol, 2016. **8**(2): p. 101-9.
57. Gamberi, T., et al., *Adiponectin Signaling Pathways in Liver Diseases.* Biomedicines, 2018. **6**(2).
58. Iwabu, M., et al., *Adiponectin and AdipoR1 regulate PGC-1alpha and mitochondria by Ca(2+) and AMPK/SIRT1.* Nature, 2010. **464**(7293): p. 1313-9.
59. Wang, Y., et al., *AdipoRon exerts opposing effects on insulin sensitivity via fibroblast growth factor 21-mediated time-dependent mechanisms.* J Biol Chem, 2022. **298**(3): p. 101641.

60. Rodrigues, M., et al., *Current Translational Research and Murine Models For Duchenne Muscular Dystrophy.* J Neuromuscul Dis, 2016. **3**(1): p. 29-48.
61. Chamberlain, J.S., et al., *Dystrophin-deficient mdx mice display a reduced life span and are susceptible to spontaneous rhabdomyosarcoma.* Faseb j, 2007. **21**(9): p. 2195-204.
62. Lecompte, S., et al., *Skeletal muscle secretome in Duchenne muscular dystrophy: a pivotal anti-inflammatory role of adiponectin.* Cell Mol Life Sci, 2017. **74**(13): p. 2487-2501.
63. Yamashita, T., et al., *An orally-active adiponectin receptor agonist mitigates cutaneous fibrosis, inflammation and microvascular pathology in a murine model of systemic sclerosis.* Sci Rep, 2018. **8**(1): p. 11843.
64. Sha, M., et al., *Therapeutic effects of AdipoRon on liver inflammation and fibrosis induced by CCl(4) in mice.* Int Immunopharmacol, 2020. **79**: p. 106157.
65. Li, Y., et al., *AdipoRon Attenuates Hypertension-Induced Epithelial-Mesenchymal Transition and Renal Fibrosis via Promoting Epithelial Autophagy.* J Cardiovasc Transl Res, 2021. **14**(3): p. 538-545.
66. Jones, D., *Duchenne muscular dystrophy awaits gene therapy.* Nat Biotechnol, 2019. **37**: p. 335–337.
67. Elangkovan, N. and G. Dickson, *Gene Therapy for Duchenne Muscular Dystrophy.* J Neuromuscul Dis, 2021. **8**(s2): p. S303-s316.
68. Matthews, E., et al., *Corticosteroids for the treatment of Duchenne muscular dystrophy.* Cochrane Database Syst Rev, 2016(5): p. CD003725.
69. Da Eira, D., et al., *Effects of the adiponectin mimetic compound ALY688 on glucose and fat metabolism in visceral and subcutaneous rat adipocytes.* Adipocyte, 2020. **9**(1): p. 550-562.

Supplementary materials

Table S1. Antibody Information Chart for Immunohistochemistry and Immunofluorescence

Antibody	Species raised	Dilution	Incubation time	T°	Product code	Source
Immunohistochemistry						
IL-1β	rabbit polyclonal	1/200	2h30	RT	ab2105	Abcam, Cambridge, UK
TNFα	rabbit polyclonal	1/100	2h30	RT	ab6671	Abcam, Cambridge, UK
HNE	rabbit polyclonal	1/200	Overnight	4°C	ab46545	Abcam, Cambridge, UK
PRDX3	rabbit polyclonal	1/1000	Overnight	4°C	/	Gift from Bernard Knoops, UCL, Belgium[a]
CD68	rabbit polyclonal	1/500	2h30	RT	ab125212	Abcam, Cambridge, UK
Immunofluorescence						
Dystrophin	rabbit polyclonal	1/200	Overnight	4°C	ab15277	Abcam, Cambridge, UK
Laminin-2 (α-2 chain)	rat monoclonal	1/1000	Overnight	4°C	L0663	Sigma Aldrich, Missouri, USA

[a]*Leyens G, Donnay I, Knoops B. Cloning of Bovine Peroxiredoxins-Gene Expression in Bovine Tissues and Amino Acid Sequence Comparison with Rat, Mouse and Primate Peroxiredoxins. Comp Biochem Physiol B Biochem Mol Biol (2003) 136(4):943-55. Epub 2003/12/10. doi: 10.1016/s1096-4959(03)00290-2.* *RT: Room temperature*

Table S2. Sequences of real-time PCR primers

Gene	Forward primer (5'-3')	Reverse primer (5'-3')	Melting T°
Mouse			
COL1A1	CCGATGGATTCCCGTTCGAGT	GGTGGACATTAGGCGCAGGA	62°C
COL3A1	AAGAGGATCTGAGGGCTCGC	AGGGTGAAAAGCCACCAGACT	62°C
Cyclophilin	AACCCCACCGTGTTCTTC	TGCCTTCTTTCACCTTCCC	62°C
Cyclophilin	TGCAAACAGCTCGAAGGAGACGC	ACGCCACTGTCGCTTTTCGCC	67°C
ERRα	GCCTCTGGCTACCACTACGG	CAGACGCACACCCTCCTTGA	62°C
Mrf4	TGCGGATTTCCTGCGCACCT	GCATCCACGTTTGCTCCTCCTTCC	67°C
Myh7	GGTGCCAAGGGCCTGAATGAGGAG	GGTCTGAGGGCTTCACGGGCAC	67°C
Human			
AdipoR1	ACTCCTAAGCACCGGCAGAC	CAAGCCAAGTCCCAGGAACA	62°C
IL1-β	GAATCTCCGACCACCACTACA	TGCACATAAGCCTCGTTATCCC	62°C
TBP	CCCCATGACTCCCATGACCC	ACGAAGTGCAATGGTCTTTAGGT	62°C
TNFα	CTCTTCTGCCTGCTGCACTTT	GATGATCTGACTGCCTGGGC	62°C
UTRN	ATTGTAAGGCCCTGAGACGGG	TTCAGGGGCCTCAATTGGCT	62°C

Cyclophilin and TBP were used as reference gene in mice and humans, respectively.

Table S3. ELISA kit references

Antibody	ELISA kit number	Source	Previous work using the cited kit in muscle
HNE	ab238538	Abcam	Abou Samra et al, JCSM, 2020
Myh7B	ABIN6968750	Antibodies-online	No citation available
Myogenin	ABIN6957954	Antibodies-online	No citation available
P-AMPK	#7959	Cell Signaling Technology	Abou Samra et al, JCSM, 2020
PGC-1α	MBS707053	MyBioSource	Selvais et al, JCSM, 2023
P-p65	#7173	Cell Signaling Technology	Abou Samra et al, JCSM, 2020
P-RIP	#88918	Cell Signaling Technology	No citation available
P-SMAD2	#7348	Cell Signaling Technology	Dubuisson et al, Front Immunol, 2022
TGF-β	MBS824944	MyBioSource	Narola et al, PLoS One, 2013
TNFα	MBS2884132	MyBioSource	Abou Samra et al, JCSM, 2020
UTRN	ABIN6960407	Antibodies-online	Abou Samra et al, JCSM, 2020

Table S4. Skeletal muscle weight at the end of the study

Muscle	Weight	WT (mean+/-SEM)	mdx (mean+/-SEM)	mdx-T3 (mean+/-SEM)	mdx-T15 (mean+/-SEM)
Tibialis anterior (TA)	Weight (mg)	83.6 ± 1.5	147.8 ± 3.1***	153.5 ± 4.0***	145.7 ± 4.1***
	Relative weight (mg/gBW)	2.9 ± 0.1	4.4 ± 0.1***	4.5 ± 0.1***	4.4 ± 0.1***
Gastrocnemius (G)	Weight (mg)	313.6 ± 2.8	378.5 ± 7.2***	388.9 ± 9.1***	386.6 ± 8.1***
	Relative weight (mg/gBW)	10.8 ± 0.2	11.4 ± 0.1	11.4 ± 0.2	11.6 ± 0.2
Quadriceps (Q)	Weight (mg)	376.2 ± 5.9	568.9 ± 18.3***	569.6 ± 16.2***	563.6 ± 15.2***
	Relative weight (mg/gBW)	13.0 ± 0.3	17.1 ± 0.4***	16.7 ± 0.4***	16.9 ± 0.4***

Table S4. Effects of ALY688 treatment on muscle weight. *The total (mg) and relative (corrected by body weight (mg/gBW)) weight of TA, G and Q from the four groups of mice were compared at the age of 12 weeks (sacrifice). Data are means ± SEM; n = 8-10 mice per group. Statistical analysis was performed using one-way ANOVA followed by Tukey's test.* ***$P < 0.001$ vs WT.*

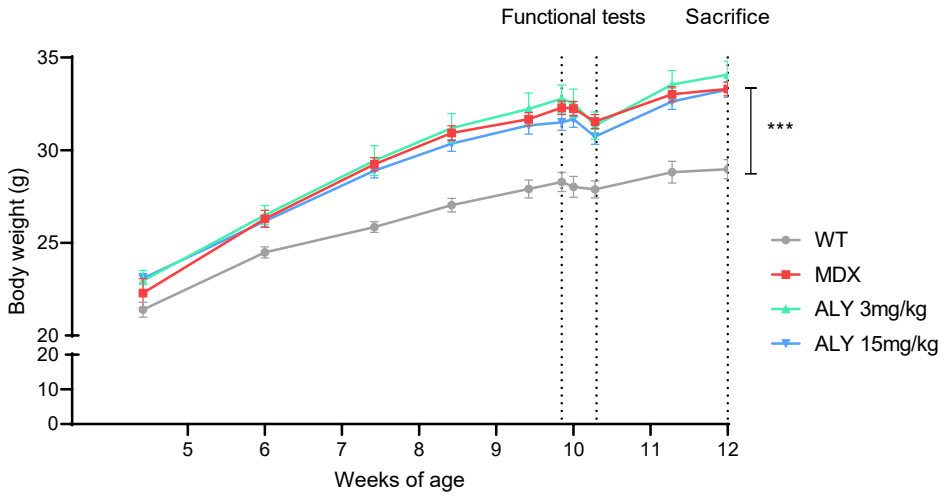

Figure S1. Effects of ALY688 treatment on body weight. *The body weight of the four groups of mice were compared throughout the study period (from the age of 4 weeks to the age of 12 weeks): WT, mdx (untreated), mdx treated with ALY688 3 mg/kg (mdx-T3) and mdx treated with ALY688 15 mg/kg (mdx-T15) mice. Data are means ± SEM; n = 8-10 mice per group. Statistical analysis was performed using one-way ANOVA followed by Tukey's test.* $^{***}P < 0.001$ *vs WT. As already described (Coley et al. Hum. Mol. Gen., 2016), mdx mice were bigger than WT ones and their skeletal muscles were heavier, reflecting the well-documented muscle hypertrophy of this model. Most importantly, all the mice displayed harmonious weight growth during the study and no difference was observed between untreated and treated mdx mice, thereby confirming the absence of deleterious effect caused by ALY688*

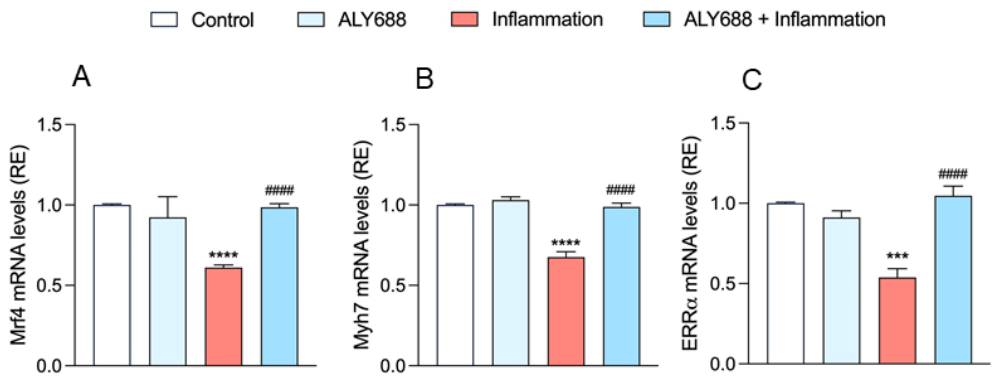

Figure S2. Effects of ALY688 treatment on muscle markers of differentiation and fibre phenotype in C2C12. *Experiments were performed on murine C2C12 myotubes. Cells were treated or not with ALY688 (100 nM) for 24 h, while being challenged or not with an inflammatory cocktail [TNFα (10 ng/mL) and IFNγ (10 ng/ml)].* ***(A-C)*** *mRNA levels of markers of muscle differentiation (Mrf4), oxidative (Myh7) fibres as well as of mitochondrial biogenesis (ERRα) were quantified. These levels were normalised to Cyclophilin A. Results were then presented as relative expression compared to control condition (i.e no inflammation, no ALY688). Data are means ± SEM; n = 4 independent cultures for all experiments. Statistical analysis was performed using one-way ANOVA followed by Tukey's test.* $^{***}P < 0.001$, $^{****}P < 0.0001$ *vs controls.* $^{\#\#\#\#}P < 0.0001$ *vs inflammatory condition.*

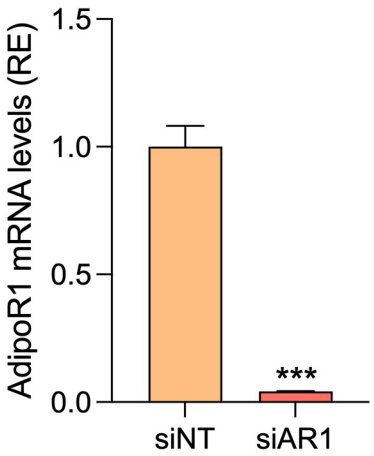

Figure S3. Effectiveness of siRNA against AdipoR1. *Human myotubes were transfected with siRNA against AdipoR1 (50 nM) or a negative control [non-targeting, siNT (50 nM)] for 24h. AdipoR1 mRNA levels were normalised to human TATA box-binding protein. The subsequent ratios are presented as relative expression (RE) compared with siNT conditions. Data are means ± SEM for 4 cultures, each obtained from a different donor (i.e., 4 DMD subjects). Statistical analysis was performed using two-tailed paired Student's t-test.* $^{***}P < 0.001$ *for indicated conditions.*

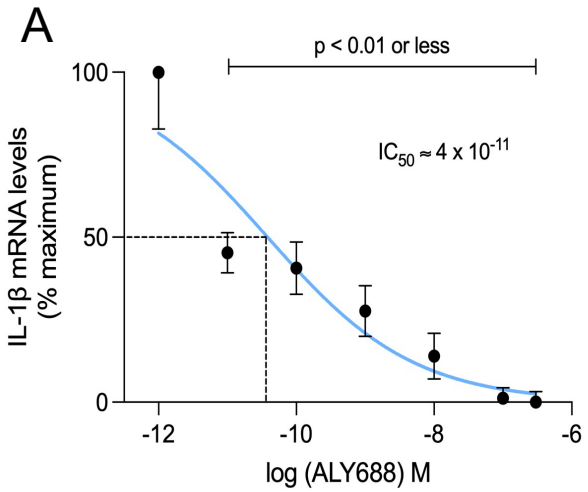
A
p < 0.01 or less
IC50 ≈ 4 x 10-11
IL-1β mRNA levels (% maximum)
100
50
0
-12
-10
-8
-6
log (ALY688) M

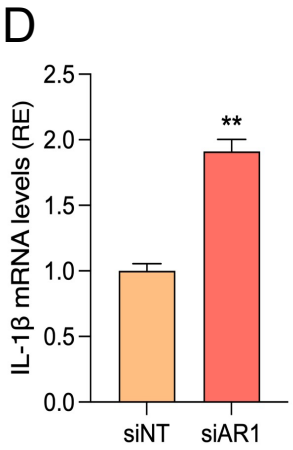
D
IL-1β mRNA levels (RE)
2.5
2.0
1.5
1.0
0.5
0.0
**
siNT
siAR1

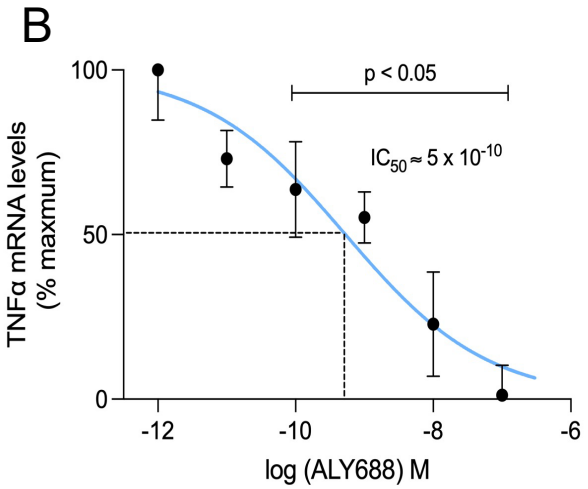
B
p < 0.05
IC50 ≈ 5 x 10-10
TNFα mRNA levels (% maxmum)
100
50
0
-12
-10
-8
-6
log (ALY688) M

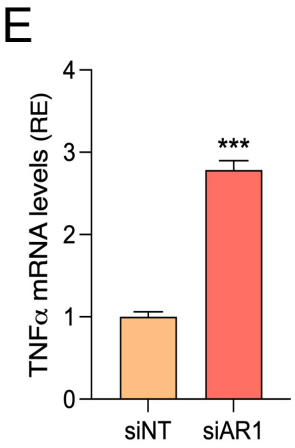
E
TNFα mRNA levels (RE)
4
3
2
1
0
***
siNT
siAR1

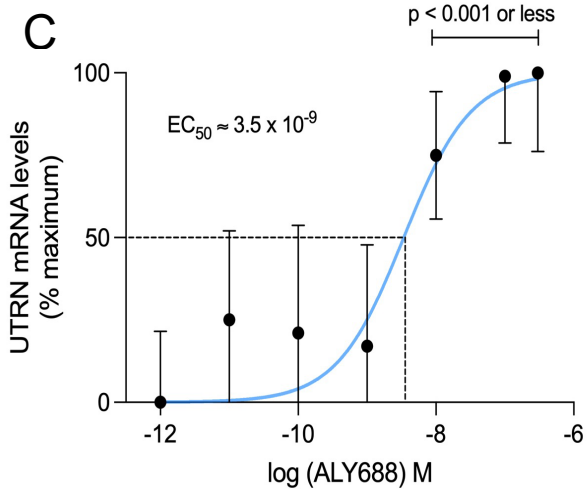
C
p < 0.001 or less
EC50 ≈ 3.5 x 10-9
UTRN mRNA levels (% maximum)
100
50
0
-12
-10
-8
-6
log (ALY688) M

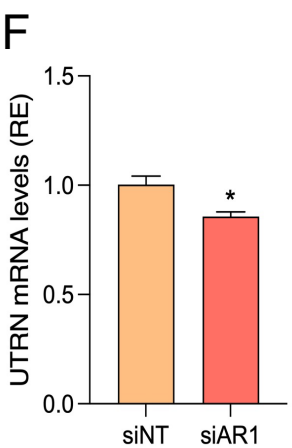
F
UTRN mRNA levels (RE)
1.5
1.0
0.5
0.0
*
siNT
siAR1

Figure S4. ALY688 recapitulates its anti-inflammatory and pro-UTRN effects in human healthy myotubes, via its action on AdipoR1. (A-C) *Dose-response curves illustrating the effects of ALY688 on IL-1β, TNFα, and UTRN mRNA levels in primary cultures of myotubes obtained from healthy subjects. Cells were treated or not with several concentrations of ALY688 (from 10 pM to 300 nM) for 24 h, while being challenged with an inflammatory cocktail (human recombinant TNFα/INFγ, each at 15 ng/mL). mRNA levels were normalised to human TATA box-binding protein. Data were then presented as % of the maximal levels obtained either without (A, B) or with 300 nM ALY688 (C).* ***(D-F)*** *In some experiments, cells were first transfected with siRNA against AdipoR1 (50 nM) or a negative control [non-targeting, siNT (50 nM)] for 24h and then treated with ALY688 (100 nM) combined to inflammation (TNFα/IFNγ) for an additional 24h. After normalisation, mRNA levels were presented as relative expression (RE) to siNT conditions (D-F). Data are means ± SEM for 4 cultures, each obtained from a different donor (i.e., 4 healthy subjects). Statistical analysis was performed using repeated measures of ANOVA followed by Dunnett's test (A-C) or two-tailed paired Student's t-test (D-F).* $^{*}P < 0.05$, $^{**}P < 0.01$, $^{***}P < 0.001$ *vs siNT.*

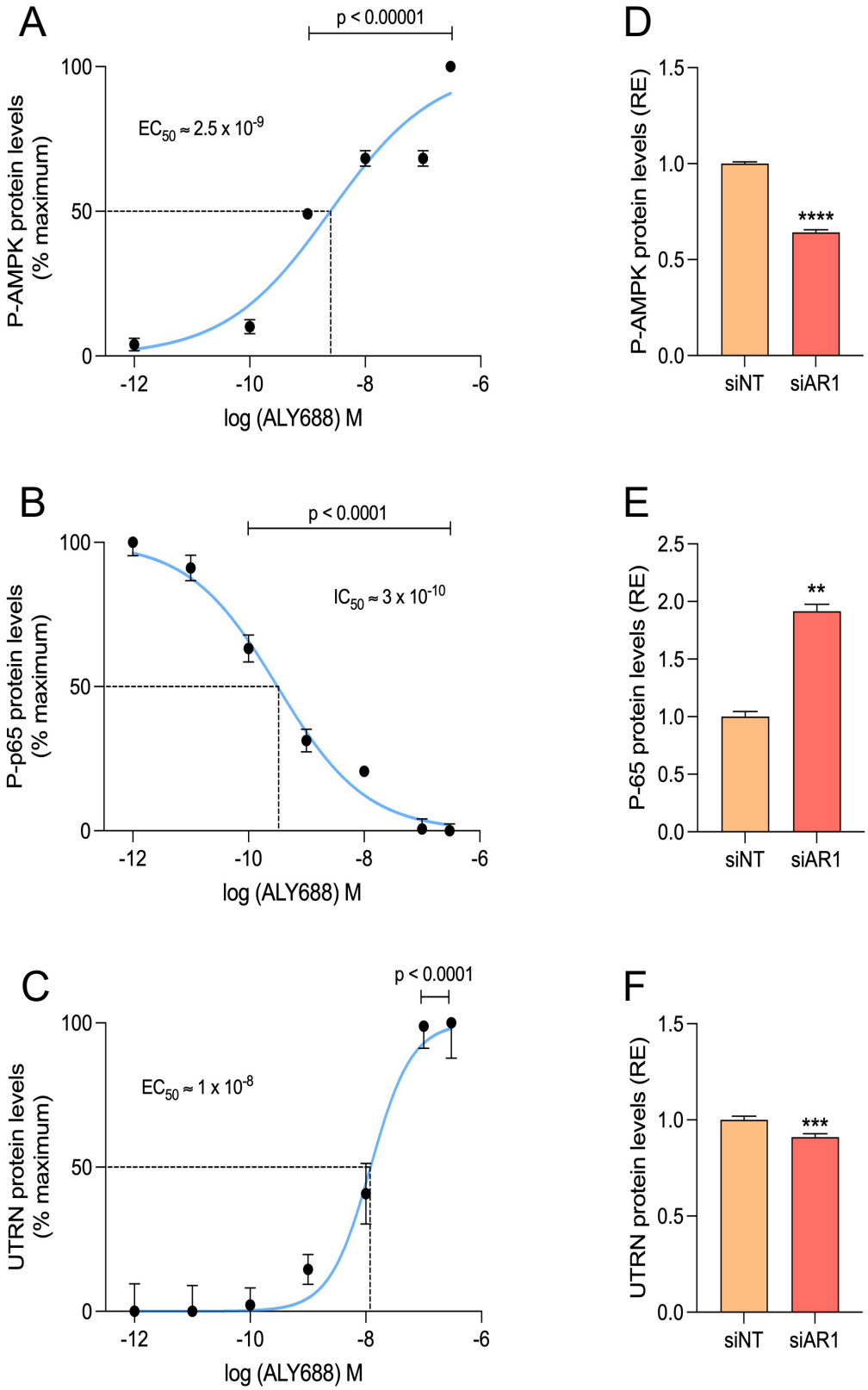
A
p < 0.00001
P-AMPK protein levels (% maximum)
EC50 ≈ 2.5 x 10-9
log (ALY688) M
D
P-AMPK protein levels (RE)
****
siNT
siAR1
B
p < 0.0001
P-p65 protein levels (% maximum)
IC50 ≈ 3 x 10-10
log (ALY688) M
E
P-65 protein levels (RE)
**
siNT
siAR1
C
p < 0.0001
UTRN protein levels (% maximum)
EC50 ≈ 1 x 10-8
log (ALY688) M
F
UTRN protein levels (RE)
***
siNT
siAR1

Figure S5. ALY688 treatment recapitulates its effects on key effectors of the AMPK signalling in human healthy myotubes, via its action on AdipoR1. (A-C) *Dose-response curves illustrating the effects of ALY688 on AMPK and NF-κB activity (P-p65 subunit), and UTRN protein levels in primary cultures of myotubes obtained from healthy subjects. Cells were treated or not with several concentrations of ALY688 (from10 pM to 300 nM) for 24 h, while being challenged with an inflammatory cocktail (human recombinant TNFα/INFγ, each at 15 ng/mL). Levels of each protein were measured by ELISAs and then presented as % of the maximum achieved either without (B) or with 300 nM ALY688 (A, C).* ***(D-F)*** *In some experiments, cells were first transfected with siRNA against AdipoR1 (50 nM) or a negative control [non-targeting, siNT (50 nM)] for 24h and then treated with ALY688 (100 nM) combined to inflammation (TNFα/IFNγ) for an additional 24h. For each protein, levels were presented as relative expression (RE) compared with siNT conditions. Data are means ± SEM for 4 cultures, each obtained from a different donor (i.e., 4 healthy subjects). Statistical analysis was performed using repeated measures of ANOVA followed by Dunnett's test (A-C) or using two-tailed paired Student's t-test (D-F).* $^{**}P < 0.01$, $^{***}P < 0.001$, $^{****}P < 0.0001$ *vs siNT.*

Study 3

Striking cardioprotective effects of an Adiponectin Receptor Agonist in an aged mouse model of Duchenne Muscular Dystrophy

Michel Abou-Samra[1], Nicolas Dubuisson[1, 2], Alice Marino[3], Camille M. Selvais[1], Versele Romain[1], Maria A. Davis-López de Carrizosa[1,4], Laurence Noel[1], Christophe Beauloye[3], Sandrine Horman[3], and Sonia M. Brichard[1]

[1] Endocrinology, Diabetes and Nutrition Unit. Institute of Experimental and Clinical Research (IREC), Medical Sector, Université Catholique de Louvain (UCLouvain), Avenue Hippocrate 55, 1200 Brussels, Belgium.
[2] Cardiovascular Research Unit. Institute of Experimental and Clinical Research. Medical Sector, Université Catholique de Louvain (UCLouvain), Avenue Hippocrate 55, 1200 Brussels, Belgium.
[2] Neuromuscular Reference Center, Department of Neurology, Cliniques Universitaires Saint-Luc, Avenue Hippocrate 10, 1200 Brussels, Belgium
[4] Departamento de Fisiología, Facultad de Biología, Universidad de Sevilla, 41012 Seville, Spain.

***Corresponding author:**
Michel Abou-Samra
E-mail: michel.abousamra@uclouvain.be

Keywords: Adiponectin, Duchenne Muscular Dystrophy, cardiomyopathy, inflammation, fibrosis, mitochondria, AMPK.

Abstract

Adiponectin (ApN) is a hormone with powerful pleiotropic effects on various tissues and organs. We previously showed that ApN is able to counteract a devastating muscle disease, Duchenne muscular dystrophy (DMD). However, its therapeutic use is limited. Today, an ApN mimic stands out: AdipoRon, an orally active small-molecule that can be easily produced and administered. Although cardiomyopathy is the leading cause of death in DMD, the effects of ApN/AdipoRon on the dystrophic heart have not yet been tested. Our recent work originally unveiled the potent protective effects of AdipoRon on dystrophic skeletal muscle. In this study, we investigated whether these effects could be extended to dystrophic heart.
As cardiomyopathy develops late in life in mdx mice (DMD mouse model), 14-month-old mdx mice were treated orally for 2 months with AdipoRon (mdx-AR) at a dose of 50mg/kg/day and then compared to untreated (mdx) and age-matched wild-type (WT) mice. *In vivo* echocardiography revealed cardiac dysfunction and ventricular hypertrophy in mdx mice compared to WT mice. Both abnormalities were completely reversed in mdx-AR mice. In addition, mdx-AR mice showed marked increase in muscle strength and endurance, compared to untreated mdx mice. *Ex vivo* analyses revealed that AdipoRon treatment significantly reduced markers of cardiac inflammation, oxidative stress, hypertrophy and fibrosis, while increasing those of mitochondrial biogenesis. These effects were mainly mediated by ApN receptor-1 and CAMKK2/AMPK pathways.

Therefore, by exerting striking protective and beneficial effects on both dystrophic skeletal and cardiac muscles, AdipoRon may offer new therapeutic perspectives for a global and better management of DMD.

Introduction

Duchenne muscular dystrophy (DMD) is a devastating condition characterized by the progressive wasting of skeletal muscles, respiratory insufficiency, and cardiomyopathy [1]. Historically, respiratory failure has been the primary factor contributing to mortality in patients with DMD. However, advancements in the management of respiratory symptoms have led to an increase in the life expectancy of DMD patients. This improved longevity, increased the clinical relevance of heart disease in DMD, as nearly all patients aged 18 and above will exhibit signs of cardiomyopathy [2]. In the last decade, heart failure has even emerged as the primary cause of death in DMD [3].

To address the cardiac impairments associated with DMD, timely intervention and early identification of cardiomyopathy are crucial. Unfortunately, existing treatments for dilated cardiomyopathy remain insufficient due to a limited comprehension of the precise mechanisms contributing to heart failure in DMD. Conventional methods typically involve the use of glucocorticoids, angiotensin-converting enzyme inhibitors and β-adrenoceptor antagonists. Presently, these therapies are only able to slow down the processes of cardiac remodeling and the onset of heart failure without reversing it [4]. Therefore, new medications are highly needed.

Over nearly two decades, we have dedicated our research to exploring the intriguing properties of Adiponectin (ApN), placing a particular emphasis on its beneficial and protective effects on muscle, a primary target tissue [5]. Adiponectin (ApN) is a hormone released by adipocytes. Its actions include promoting insulin sensitivity, facilitating fat burning, and exerting anti-inflammatory and antioxidative effects. These properties make it a potent agent in mitigating several metabolic disorders, such as type 2 diabetes, obesity, and cardiovascular diseases [5]. The pleiotropic effects of ApN are mediated through its interaction with two primary receptors, AdipoR1 and AdipoR2 [6]. AdipoR1 is predominantly expressed in skeletal and cardiac muscles, while AdipoR2 exhibits higher expression levels in the liver. This distribution of receptors allows ApN to elicit its beneficial effects across various tissues, contributing to its role in maintaining metabolic balance and combating associated disorders [5].

More recently, our focus has extended to investigating ApN impacts in the context of Duchenne muscular dystrophy (DMD). Both our research and that of others have revealed diminished circulating levels of ApN in mdx mice [7, 8] and human patients [9]. Notably, supplementation with ApN has demonstrated the capability to counteract the disease progression in the best studied animal model of DMD, namely the mdx mouse model [7, 10]. This establishes a rationale for

therapeutically addressing the low ApN levels in individuals with DMD. However, the direct utilization of ApN as a therapeutic agent is severely limited. Recently, a number of small molecules and short peptides have been identified, targeting ApN receptors (AdipoRs) and replicating some of the effects attributed to ApN. This opens up avenues for therapeutic interventions that harness ApN's beneficial properties through alternative agents with improved applicability and effectiveness.

AdipoRon, identified as an adiponectin receptor small-molecule agonist [11], has demonstrated compelling outcomes in addressing dystrophic alterations. Indeed, it exhibited the ability to alleviate muscle inflammation and injury, concurrently promoting muscle regeneration and function [12]. Additionally, AdipoRon has already exhibited promising effects on the heart, showcasing cardioprotective properties in cases of cardiovascular complications originating from obesity-related disorders [13]. It has also mitigated cardiac inflammation, oxidative stress, and apoptosis by enhancing cardiac lipid metabolism in type 2 diabetic mice models [14, 15]. Yet, there remains a significant gap in our understanding of AdipoRon's impact on Duchenne cardiomyopathy. Exploration of its effects in this specific context is therefore of interest.

To this end, AdipoRon was administered orally, at an optimal dose of 50 mg/kg/day [12] for a period of 8 weeks, starting at the age of 14 months, while dilated cardiomyopathy and contractile deviances start to be evident after 12 months of age in *mdx* mice [16, 17]. We first examined whether treated mice showed reduced cardiac dysfunction, decreased inflammation, oxidative stress and fibrosis as well as enhanced mitochondrial function, thereby contributing to an improved dystrophic phenotype. Then, we uncovered the potential mechanisms of action underlying the effects of AdipoRon.

Materials and Methods

Animals

C57BL/10ScSn-*Dmd*^{mdx}J mdx mice (murine model of Duchenne muscular dystrophy) and C57BL/10ScSnJ mice (used as wild-type (WT) controls) were purchased from Jackson Laboratory (Maine, USA). Three groups of male mice (*n* = 6-8/group) were compared in our experiments. At 14 months of age, each group of mice received solid drinks, replacing the water bottles. The first group was WT mice, the second group consisted of untreated mdx mice (mdx), while the third group consisted of treated mdx mice (mdx-AR). For this last group, a dose of 50 mg/kg/day of AdipoRon (Bio-Techne, Minnesota, U.S.) was incorporated into a solidified water (Solid Drink, Triple A Trading, Tiel, Netherlands) that replaced the water bottles. Solid drinks were replaced every day over a period of 8 weeks. Animals were maintained under a standard laboratory chow and housed at a constant temperature (22°) with a fixed 12h light – 12h dark cycle (lights on from 7 a.m. to 7 p.m.). At the end of the treatment, 16-month-old mice were sacrificed, as described [12], 1 week after echocardiography and *in vivo* functional tests.

Echocardiographic analyses

Cardiac dimensions and function were analysed by transthoracic echocardiography using a Vevo 3100 Imaging System (FUJIFILM VisualSonics, Toronto, Canada) as described [18]. Mice were lightly anesthetized with inhaled isoflurane (1%, in 100% O2). Left ventricle (LV) volumes were measured using B-mode parasternal long-axis view, at end-systole and end-diastole, from which ejection fraction (EF %) was deduced. LV mass was calculated from LV long-axis measurements. Left ventricle end-diastolic (LVDd) and end-systolic (LVDs) dimensions were measured from the M-mode traces, and fractional shortening (FS %) was calculated as follows: [(LVDd − LVDs)/LVDd*100]. All measurements and analysis were performed by the same experienced operator who was blinded to the experimental groups.

In vivo studies of global force or resistance

Mice were submitted to 3 main tests [12]:
Wire test. Mice were suspended by their limbs from a 1.5 mm-thick, 60 cm-long metallic wire at 45 cm above soft ground. The time (sec) until they completely released their grasp and fell was recorded. Mice that reached a set limit of 180 seconds were allowed to stop the experiment, while others were directly retested, up to three times, and their maximum hanging time was recorded. For each mouse,

three trials were performed at an interval of 15 min and the scores of the three trials were then averaged.

*Grip test. M*ice were gently laid on the top of the grid connected to a sensor (Panlab-Bioseb, Vitrolles, France), so that their front paws (forelimb test) or both fore and hind paws (combined test) can grip the grid. Mice were then pulled back steadily until their grip was released down the length of the grid. Each test was repeated three times at an interval of 15 min. Results are presented as the mean of the 3 values of force recorded, related to body weight.

Eccentric exercise. Mice were subjected to a downhill running exercise on a treadmill (Panlab-Bioseb) with a downward inclination of 15°, and at a speed of 10 m/min for 10 min. This training was repeated daily for 3 days. Results represent the distance (meters) covered by each mouse on the 3rd day, with a maximum distance of 100 m.

Quantification of muscle damage markers in plasma

Plasma Creatine Kinase (CK) and Lactate Dehydrogenase (LDH) activities were quantified to evaluate skeletal muscle damage as injured muscles release CK and LDH into the bloodstream at high levels. Kits were based on colorimetric methods and were used following the manufacturer's instructions (BioAssay Systems – GENTAUR BVBA, Kampenhout, Belgium). CK and LDH activities were expressed as IU/L.

RNA extraction and real-time quantitative PCR (RT-qPCR)

RNA was isolated from mouse cardiac muscles with TriPure reagent (Sigma-Aldrich). 1 µg of total RNA were reverse transcribed, and 40 ng total RNA equivalents were amplified using an iCycler iQ real-time PCR detection system (Bio-Rad Laboratories, Nazareth, Belgium) as described [12]. RT-qPCR primers for mouse cyclophilin, tumour necrosis factor alpha (TNFα), interleukin 1 beta (IL-1β), interleukin 10 (IL-10), peroxiredoxin 3 (PRDX3), adiponectin receptors 1 & 2 (AdipoR1/2), and mitochondrial transcription factor A (mtTFA) were used as reported [10, 19-21]. New mouse primer sequences for transforming growth factor beta 1 (TGF-β1), smooth muscle alpha-actin (αSMA), B-type natriuretic peptide (BNP), atrial natriuretic peptide (ANP), peroxisome proliferator-activated receptor-gamma coactivator (PGC-1α), and estrogen-related receptor alpha (ERRα), can be found in supplementary material and data, table 1. The threshold cycles (Ct) were measured in separate tubes and in duplicate. The identity and purity of the amplified product were checked by electrophoresis on agarose minigels, and

analysis of the melting curve was carried out at the end of the amplification. Additionally, each plate included a negative control for each set of primers.

Protein extraction and ELISAs

Mouse cardiac muscles were homogenized in a lysis buffer supplemented with 1% protease/phosphatase inhibitor cocktail (Cell Signaling Technology, BIOKE, Leiden, The Netherlands) and 10mM NaF. Proteins were quantified using the Bradford method and were stored at -80°C. 25-150 µg of total protein extracts were used for each analysis. ELISA assays were used to specifically detect and quantify the active phosphorylated form of AMP-activated protein kinase alpha (P-AMPK), the active phosphorylated form of the p65 subunit of nuclear factor kappa B (NF-κB) (P-P65), and the active phosphorylated form of SMAD2 (P-SMAD2) (all from Cell Signaling Technology). ELISA assays were also used to quantify the levels of ANP, 4-Hydroxynonenal (HNE), TNFα, IL-1β, IL-10 (all from Abcam, Cambridge, UK), utrophin A (UTRN) (from Antibodies Online, Atlanta, USA), TGF-β, AdipoR1, AdipoR2, the active phosphorylated form of Calcium/Calmodulin Dependent Protein Kinase Kinase 2 (CAMKK2), peroxisome proliferator-activated receptor α (PPARα), PPAR gamma coactivator 1 alpha (PGC-1α), Translocase of Outer Mitochondrial Membrane 20 (TOMM20), and the active phosphorylated form of Ribosome-inactivating protein (P-RIP) (all from MyBiosource – Bio-Connect Diagnostics B.V., Huissen, The Netherlands). Kits were based on colorimetric methods and were carried out following manufacturer's instructions.

Bright-field histochemistry and morphometry

Heart muscle samples were fixed in 10% formalin for 24 h and then embedded in paraffin. 5 µm sections were processed as previously described [12], using rabbit polyclonal antibodies directed against TNFα (dilution 1:100, incubation 2 h 30 min), IL-1β (1:200, 2 h 30 min), PRDX3 (1:500, 2 h 30 min), and HNE, (1:100, 2 h 30 min) (PRDX3 is a gift from Bernard Knoops [22], University of Louvain, Brussels, Belgium, rest are from Abcam). Before immunostaining, sections were submitted to heat-mediated antigen retrieval using a microwave oven and Tris-citrate buffer (pH 6.5). Binding of antibodies was detected by applying for 30 min at room temperature a secondary antibody, which was a biotinylated goat anti-rabbit IgG (H + L) (Labconsult, Brussels, Belgium). Peroxidase activity was revealed with 3,3'-diaminobenzidine (DAB) (Thermo Fisher Scientific, Aalst, Belgium), which produces a brown staining. For each marker, all slides were treated simultaneously for immunohistochemistry analysis and DAB revelation and then analysed together. Immunohistochemical controls were performed by omission of the first antibody

or of the first and second antibodies or by using preimmunize serum. In addition, Picro-Sirius red (Abcam) staining was used to evaluate muscle fibrosis. Whole muscle sections were scanned using the Leica SCN400 slide scanner (Leica microsystems, Diegem, Belgium), and then the percentage of DAB deposit areas or Red stained areas, within muscle fibres, was quantified using ImageJ (NIH, Maryland, USA).

Statistical analysis

Results are means ± SD for the indicated number of mice. The effects of AdipoRon in the three groups of mice (WT, mdx and mdx-AR) were assessed by one-way ANOVA followed by Tukey's test (Prism 9; GraphPad Software, California, USA). Differences were considered statistically significant at $p < 0.05$.

Study approval

All procedures conducted on mice were approved by the Ethical Committee for Animal Experimentation from the Medical Sector at Université Catholique de Louvain (n° LA1230396).

Results

Effects of AdipoRon treatment on dystrophic cardiac dysfunction

Since mdx mice display significant cardiac histological abnormalities later on in life, and since cardiac dysfunction is only detectable by echocardiogram starting 12 months of age ([16, 17], our own pilot study), AdipoRon was administered orally to mdx mice at 14 months of age for a period of 2 months. Mdx littermates were thus separated into two groups: those who received a daily dose of AdipoRon at 50 mg/kg (mdx-AR) and those who were left untreated (mdx). Both groups were also compared to untreated wild-type (WT) control mice. Echocardiographic analyses for the three groups of mice revealed no changes in the end-systolic and diastolic volumes, and the fractional shortening (Fig. 1A-C). However, the heart rate and the ejection fraction were decreased in mdx mice compared to WT mice, while they were normalised after AdipoRon treatment (Fig. 1D, E). Moreover, body weight was slightly decreased in mdx mice compared to WT mice and was unchanged in mdx-AR mice (Fig.1F). LVmass tended to increase in mdx mice but was corrected by the treatment (Fig.1G). Finally, LVmass/BW was increased in mdx mice compared to WT mice, while it was again normalised after AdipoRon treatment (Fig. 1H). These data suggest an improved cardiac hypertrophy and function under AdipoRon treatment in aged mdx mice.

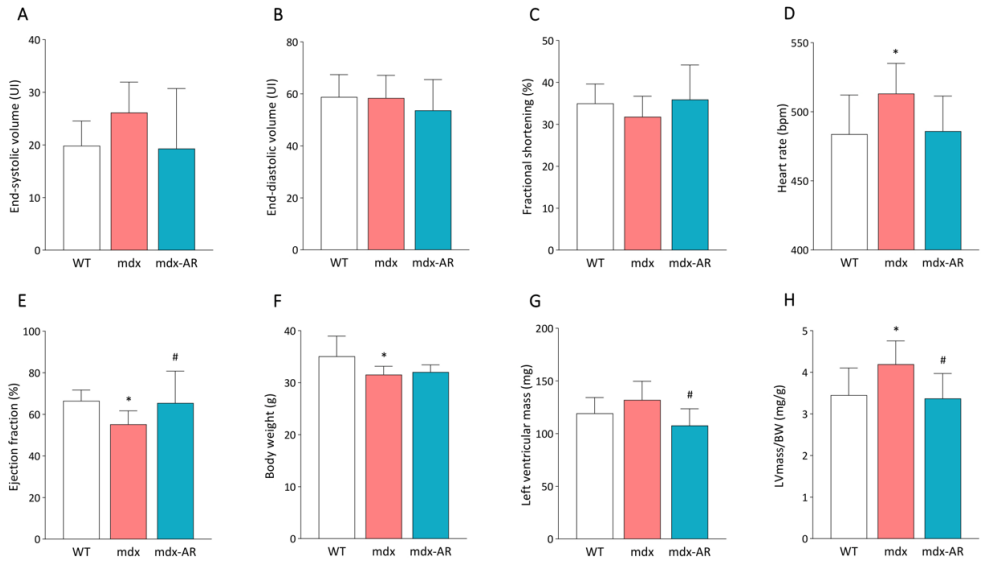

Fig.1. Effects of AdipoRon treatment on cardiac dysfunction in adult mdx mice. *Cardiac dimensions and function were analyzed in vivo by transthoracic echocardiography in mice*

from the three groups. ***(A)*** *End-systolic volume (UI).* ***(B)*** *End-diastolic volume (UI).* ***(C)*** *Fractional shortening (%).* ***(D)*** *Heart rate (bpm).* ***(E)*** *Ejection fraction (%).* ***(F)*** *Body weight (g).* ***(G)*** *Left ventricular mass (mg).* ***(H)*** *Left ventricular mass over body weight (LVmass/BW) (mg/g). Data are means ± SD; n = 7-8 mice per group for all tests. Statistical analysis was performed using one-way ANOVA followed by Tukey's test.* $p < 0.05$ *vs. WT mice. #* $p < 0.05$ *vs. mdx mice.*

Effects of AdipoRon treatment on dystrophic cardiac inflammation and oxidative stress

We next tested *ex vivo* whether oral administration of AdipoRon to aged mdx mice could reverse the dystrophic pathology by counteracting deleterious inflammatory and stress responses in cardiac muscle, as previously seen in the dystrophic skeletal muscle [12]. When compared to WT mice, cardiac muscle fibres of aged untreated mdx mice displayed high gene expression for TNFα and for IL-1β, which encode for two major inflammatory cytokines [23], while their expression was normalized under AdipoRon treatment (Fig. 2A, B). These results were then validated by ELISA where both TNFα and IL-1β were found to be highly produced in dystrophic cardiac muscles (2-fold increase vs. WT mice), while their levels were decreased by ~ 40 % under AdipoRon treatment (Fig. 2E, F). Moreover, AdipoRon almost doubled the gene expression and protein levels of IL-10, a gene encoding for a key anti-inflammatory cytokine [24], when compared to both WT and mdx mice (Fig. 2C, G). Lastly, dystrophic cardiac muscle fibres had a ~ 40 % increase in the expression of peroxiredoxin 3 (PRDX3), a marker of oxidative stress (Fig. 2D), and a 2.5-fold increase in the protein levels of 4-hydroxy-2-nonenal (HNE), a lipid peroxidation product (Fig. 2H) [7, 10, 12]. In addition, immunolabelling revealed that these markers of inflammation and stress were highly produced within cardiac muscle fibres of mdx mice, when compared with WT and mdx-AR mice (Fig. 3A). Quantification of the immunolabelling showed that the extent of DAB staining for all markers within cardiac muscle fibres strongly correlated with the ones obtained for mRNA and proteins levels (Fig. 3B-E). Therefore, AdipoRon can strongly defend

the dystrophic cardiac muscle against excessive inflammatory responses and oxidative stress.

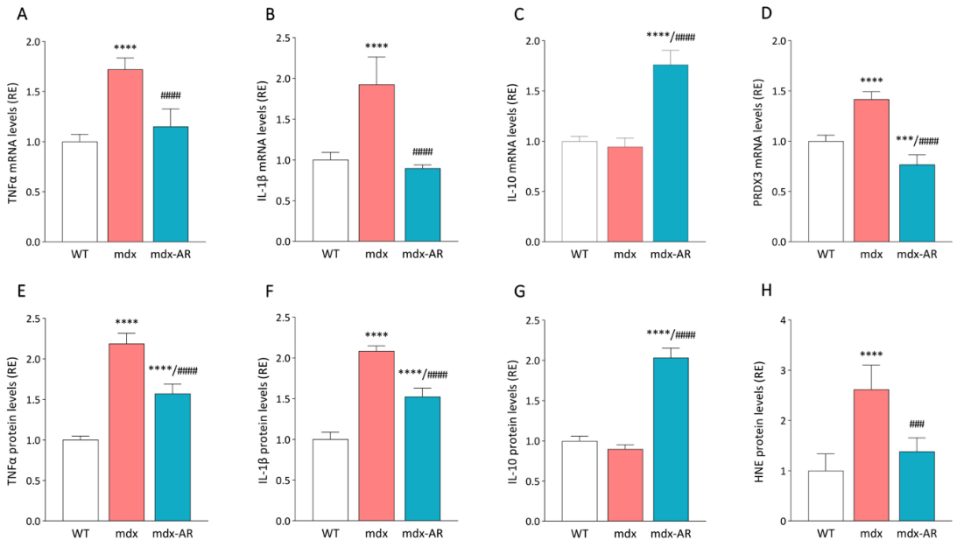

Fig.2. Effects of AdipoRon treatment on cardiac muscle inflammation and stress. *mRNA levels of* ***(A)*** *TNFα and* ***(B)*** *IL-1β, two major inflammatory genes.* ***(C)*** *mRNA levels of IL-10, an anti-inflammatory gene.* ***(D)*** *mRNA levels of PRDX3, a marker of oxidative stress. mRNA levels were normalized to cyclophilin, and the subsequent ratios were presented as relative expression compared to WT values. ELISA assays were used to quantify the levels of* ***(E)*** *TNFα and* ***(F)*** *IL-1β, two major inflammatory cytokines,* ***(G)*** *IL-10, a strong anti-inflammatory cytokine and* ***(H)*** *HNE, a lipid peroxidation product. Absorbance data were presented as relative expression compared to WT values. Data are means ± SD; n = 6 mice per group for all experiments. Statistical analysis was performed using one-way ANOVA followed by Tukey's test. *** p < 0.001, **** p < 0.0001 vs. WT mice. ### p < 0.001, #### p < 0.0001 vs. mdx mice.*

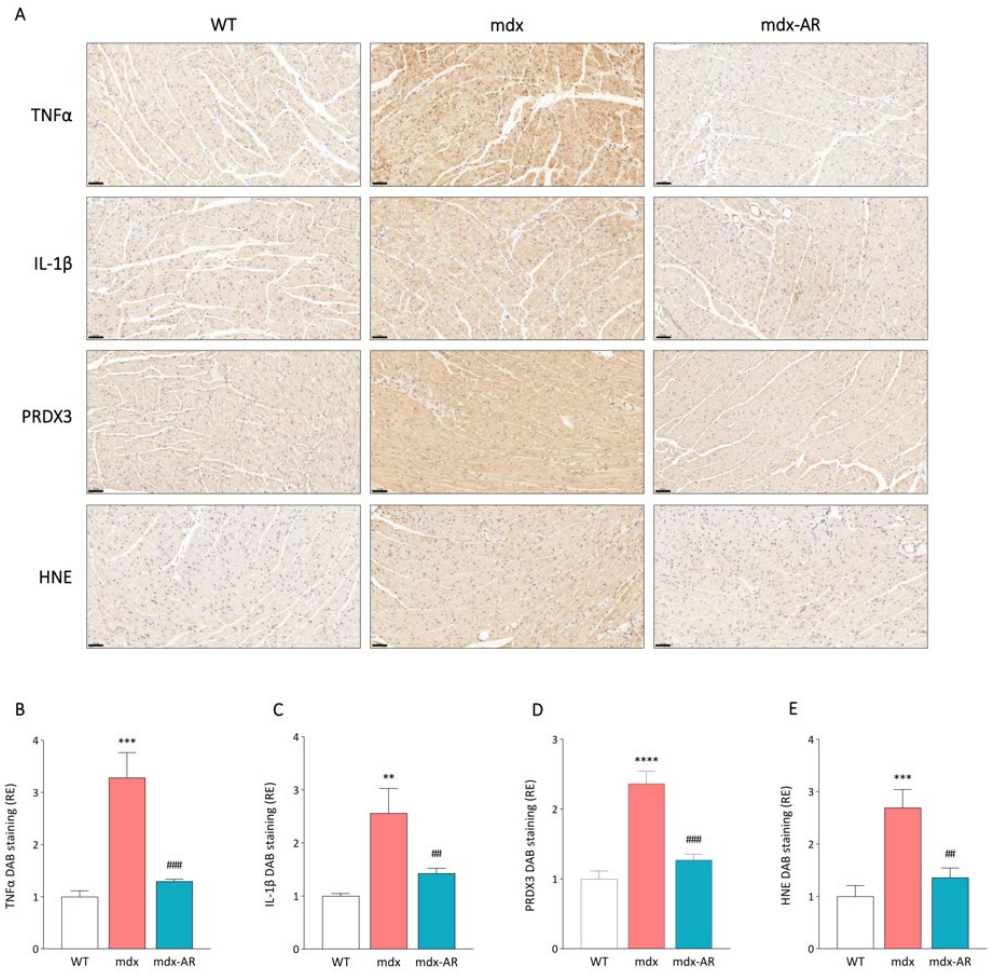

Fig.3. Effects of AdipoRon treatment on cardiac muscle inflammation and stress. (A) *Immunohistochemistry was performed on cardiac muscle sections with specific antibodies directed against two pro-inflammatory cytokines (TNFα and IL-1β) and two oxidative stress markers (PRDX3 and HNE). Scale bar = 50 µm. Quantification of* ***(B)*** *TNFα,* ***(C)*** *IL-1β,* ***(D)*** *PRDX3 and* ***(E)*** *HNE. For each immunolabelling of* ***(A)****, the percentage of DAB deposit areas was calculated within cardiac muscle sections. The subsequent ratios were presented as relative expression compared with WT values. Data are means ± SD; n = 6 mice per group for all experiments. Statistical analysis was performed using one-way ANOVA followed by Tukey's test. ** p < 0.01, *** p < 0.001, **** p < 0.0001 vs. WT mice. ## p < 0.001, ### p < 0.001 vs. mdx mice.*

Effects of AdipoRon treatment on dystrophic cardiac fibrosis and hypertrophy

We also investigated the effects of AdipoRon treatment on markers of fibrosis and hypertrophy in the dystrophic cardiac muscle. First, mdx muscle displayed a strong staining for Picrosirius red, a marker of fibrosis labelling collagen types I and III. By contrast, the percentage of fibrotic areas was reduced by half in mdx-AR mice (Fig. 4A, B). Moreover, and as expected, gene expression for αSMA and TGF-β1, two markers of cardiac fibrosis, was significantly increased by ~ 2- and 2.5-fold in mdx mice compared to WT mice, respectively while being reduced by 30-50% under AdipoRon treatment (Fig. 4C, D). Similarly, protein levels of active TGF-β and the active phosphorylated form of SMAD2 (P-SMAD2), an effector protein of the TGF-β pathway, were also increased by ~ 2- and 2.5-fold in mdx mice compared to WT mice, respectively, but were diminished by 25-50% in treated mdx-AR mice (Fig. 4E, F). Next, gene expression for both BNP and ANP, two markers of hypertrophy, significantly increased, 2.8- and 1.7-fold respectively, in mdx cardiac muscles compared to normal ones, with ANP protein levels almost doubling (Fig. 4G-I). This was then corrected and all mRNA/protein levels were normalized under AdipoRon

treatment (Fig. 4G-I). These data indicate a strong protective effect for AdipoRon against cardiac fibrosis and hypertrophy.

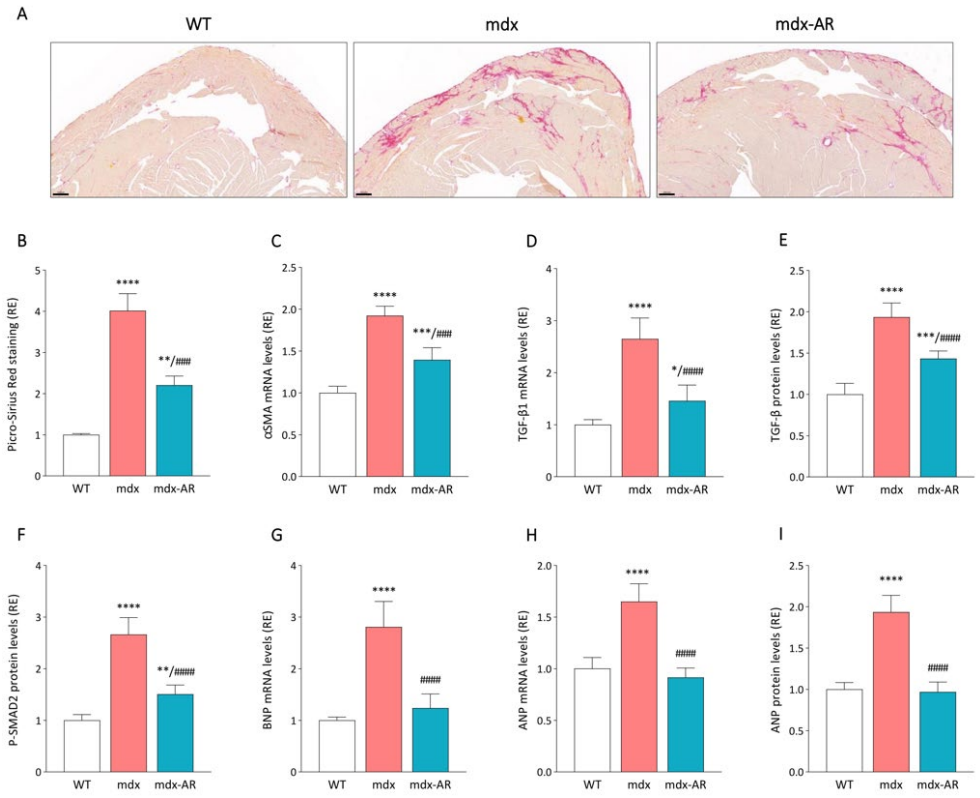

Fig.4. Effects of AdipoRon treatment on cardiac muscle fibrosis and hypertrophy. (A) *Picro-Sirius Red staining. Scale bar = 200 µm.* ***(B)*** *Quantification of Picro-Sirius Red staining. mRNA levels of* ***(C)*** *αSMA and* ***(D)*** *TGF-ß1, two markers of fibrosis. ELISA assays were used to quantify* ***(E)*** *TGF-ß and* ***(F)*** *the active phosphorylated form of SMAD2 (PSMAD2), a transcription factor mainly involved in TGF-ß signalling. mRNA levels of* ***(G)*** *BNP and* ***(H)*** *ANP, two markers of hypertrophy.* ***(I)*** *ELISA assay was also used to quantify the levels of ANP. The percentage of stained areas was calculated within cardiac muscle sections and the subsequent ratios were presented as relative expression compared with WT values. mRNA levels were normalized to cyclophilin, and the subsequent ratios were presented as relative expression compared to WT values. Absorbance data were presented as relative expression compared to WT values. Data are means ± SD; n = 6 mice per group for all experiments. Statistical analysis was performed using one-way ANOVA followed by Tukey's test. * p < 0.05, ** p < 0.01, *** p < 0.001, **** p < 0.0001 vs. WT mice. ## p < 0.01, ### p < 0.001, #### p < 0.0001 vs. mdx mice.*

Effects of AdipoRon treatment on dystrophic cardiac signalling pathways

AdipoRon, like ApN, specifically binds to AdipoRs thereby triggering a plethora of beneficial and protective effects [5]. More specifically, AdipoRon can bind to AdipoR1 and to AdipoR2 and activate mainly AMPK and PPARα signalling pathways, respectively [5, 6]. We first explored the expression and production of both ApN receptors 1 & 2 in the cardiac muscles. We detected a ~ 30-50% decrease in the gene expression and protein levels of AdipoR1 and AdipoR2 in mdx mice compared to WT, which were then corrected under AdipoRon treatment (Fig. 5A-D). However, when comparing the ct values, we revealed that AdipoR1 expression was 1000-fold higher than those of AdipoR2 in the cardiac muscle (Fig. 5 E), making AdipoR1 the primary ApN receptor in the heart. Next, we investigated the main signalling pathways possibly involved in the mechanisms of action of AdipoRon on the dystrophic cardiac muscle. First, no changes were detected in the activity of AMPK between WT and mdx mice, but in mdx-AR mice the active phosphorylated form of AMPK was drastically increased by ~ 2.5-fold (Fig. 5F). In addition, AdipoRon treatment significantly increased the activation of CAMKK2 (Fig. 5G), and slightly improved that of PPARα (Fig. 5H). Consequently, though activation of both AMPK and CAMKK2 signalling, AdipoRon helped rescue the gene expression and protein levels of PGC-1α, which were found to be blunted in untreated mdx mice (Fig. 5I, J). Finally, as previously seen in the dystrophic skeletal muscle [12], activation of AMPK pathway by AdipoRon have led to significant 40 % decrease in the activity of

NF-κB (Fig. 5K) and 15% increase in the levels of utrophin A, a dystrophin analogue and a target gene of PGC-1α (Fig. 5L), in the dystrophic heart.

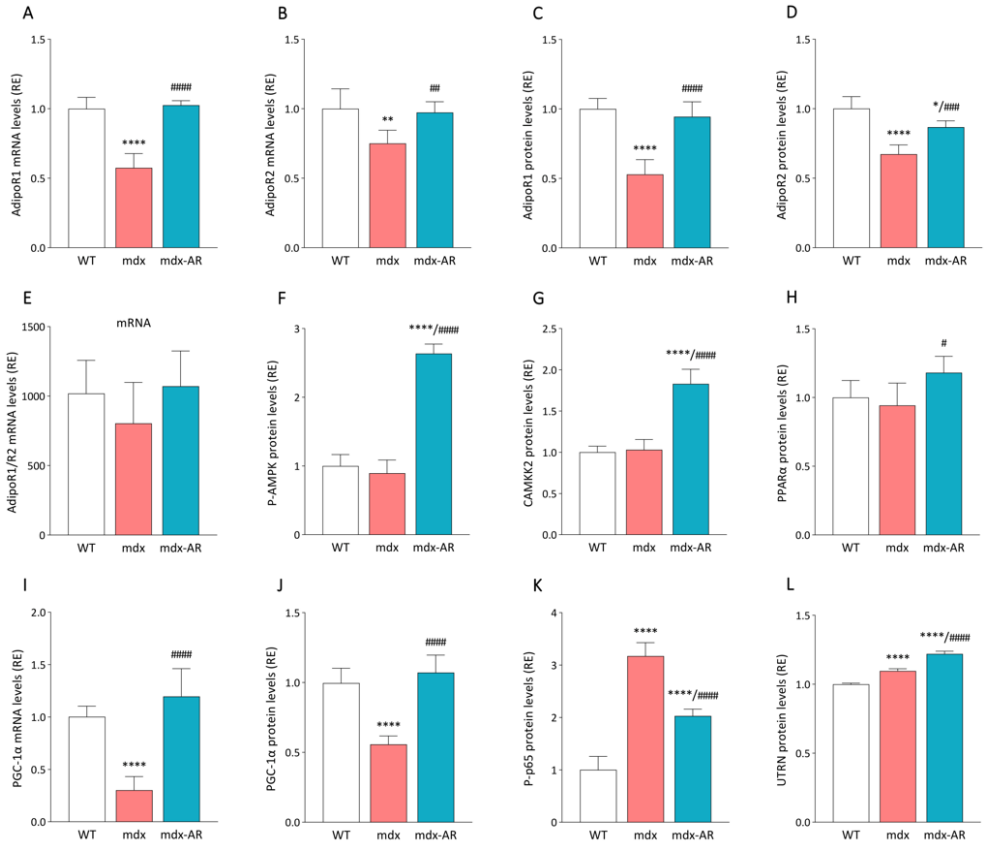

Fig.5. Effects of AdipoRon treatment on ApN receptors and signalling in the dystrophic cardiac muscle. *mRNA levels of* ***(A)*** *AdipoR1 and* ***(B)*** *AdipoR2, adiponectin main receptors. ELIISA assays were used to quantify* ***(C)*** *AdipoR1 and* ***(D)*** *AdipoR2.* ***(E)*** *The ratio of AdpoR1 over AdipoR2 mRNA levels was calculated within the cardiac muscle. ELIISA assays were used to quantify* ***(F)*** *the active phosphorylated form of AMPKα (P-AMPK),* ***(G)*** *calcium/calmodulin dependent protein kinase kinase 2 (CAMKK2), and* ***(H)*** *peroxisome proliferator-activated receptor alpha (PPARα), ApN/AdipoRon main signalling pathways in muscle.* ***(I)*** *mRNA levels of PGC-1α. ELISA assays were used to quantify* ***(J)*** *PGC-1α,* ***(K)*** *the active phosphorylated form of the p65 subunit of NF-κB (P-p65), a transcription factor mainly involved in inflammation, and* ***(L)*** *utrophin A (UTRN), a dystrophin analogue. mRNA levels were normalized to cyclophilin, and the subsequent ratios were presented as relative expression compared to WT values. Absorbance data were presented as relative expression compared to WT values. Data are means ± SD; n = 6 mice per group for all experiments.*

*Statistical analysis was performed using one-way ANOVA followed by Tukey's test. ** p < 0.01, **** p < 0.0001 vs. WT mice. ## p < 0.01, #### p < 0.0001 vs. mdx mice.*

Effects of AdipoRon treatment on dystrophic cardiac mitochondria, death, and overall function

Finally, we tested the expression of ERRα and mtTFA, two key markers of mitochondrial biogenesis and targets of PGC-1α. We found that AdipoRon treatment significantly increased their expression of, as well as the protein levels of TOMM20, a marker of mitochondrial content, which followed the same expression profile (Fig. 6 A-C). These data suggest that by mainly binding to AdipoR1 and activating CAMKK2-AMPK signalling, AdipoRon could potently enhance mitochondrial content. This was ultimately translated by an improved overall force and endurance of treated old mdx mice. Indeed, three *in vivo* functional tests were carried out: the wire test, the grip test and a treadmill exercise [12, 25]. The wire test gives an indication on muscle fatigue and coordination. In this test, the time during which the mouse is suspended on a horizontal wire is measured. Mdx mice fell down much quicker than WT mice (31 vs 97 sec, respectively), while mdx-AR mice showed intermediate resistance (55 sec) (Fig. 6E). The grip test measures strength of limb muscles. The force developed by forelimbs of mdx mice was 40% lower than that of WT mice, while it was partially rescued by AdipoRon treatment (over 20 %) (Fig. 6F). Similar results were observed for the combined fore- and hind-limb force (Fig. 6G). Finally, resistance to fatigue was further evaluated by an eccentric treadmill. On the last day (3rd) of exercise, both WT and mdx-AR mice covered the maximum distance (100 m), while the running distance of mdx mice markedly fell to ~ 75 m (Fig. 6H). These data indicate enhanced dystrophic muscle force, coordination and resistance under AdipoRon treatment in aged mdx mice. Accordingly, AdipoRon treatment protected the dystrophic muscle from injury, as seen with plasma activities for creatine kinase (CK) and lactate dehydrogenase (LDH). CK and LDH are sarcoplasmic enzymes that are released in circulation after sarcolemmal breach or tear following injury [7, 12, 26]. Plasma activities for both CK and LDH, measured herein, were ~ 4-fold higher in mdx than in WT mice, while they declined by over 40% in treated mdx-AR mice (Fig. 6I, J). Moreover, the phosphorylated and of RIP protein (P-RIP) was almost 3.5-fold higher in dystrophic cardiac muscles than in normal ones, but were reduced by 35% after treatment (Fig. 6K). P-RIP is a main factor of necroptosis, a programmed form of necrosis or inflammatory cell death, which contributes to myofibre degeneration in DMD

muscles [25, 27]. Hence, late AdipoRon treatment is likely to significantly blunt sarcolemmal injury and death in aged dystrophic skeletal and cardiac muscles.

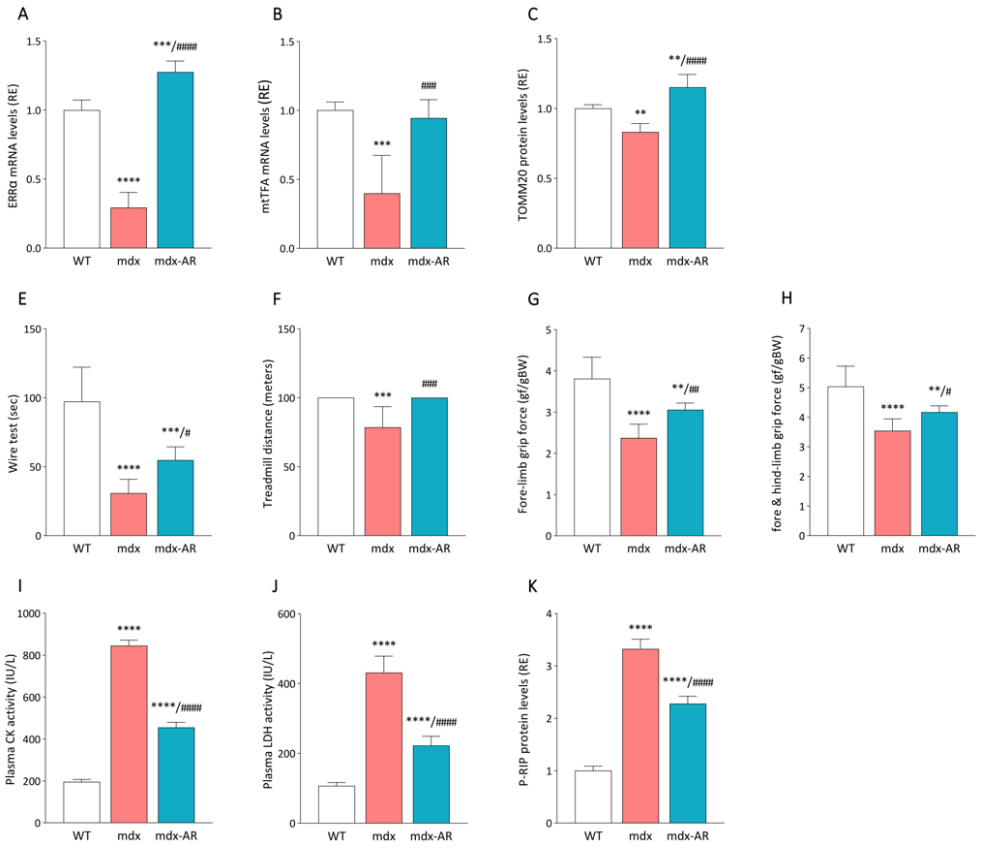

Fig.6. Effects of AdipoRon treatment on cardiac muscle oxidative capacity, function and injury. *mRNA levels of* ***(A)*** *ERRα, and* ***(B)*** *mtTFA, two markers of mitochondrial biogenesis. ELISA assay was used to quantify* ***(C)*** *TOMM20, a marker of mitochondrial content. Functional in vivo studies were carried out in mice from the three groups.* ***(E)*** *Mice were subjected to a wire test where they were suspended by their limbs and the time until they completely released the wire and fell was recorded (sec).* ***(F)*** *Mice were submitted to a downhill treadmill exercise for 10 min during 3 consecutive days. On the 3rd session, the covered distance (meters) was measured for each mouse, 100 m being the maximal distance. Mice were lowered on a grid connected to a sensor to measure the muscle force* ***(G)*** *of their forelimbs or* ***(H)*** *of both their fore- and hind-limbs; data were then expressed in gram-force relative to body weight (gf/gBW). Muscle injury was assessed, in non-exercised mice, by plasma activity of CK* ***(I)*** *and LDH* ***(J)*** *expressed as IU/L. ELISA assay was used to quantify* ***(K)*** *the active phosphorylated form of RIP (P-RIP), an important regulator of cellular stress that triggers a regulated pathway for necrotic cell death called necroptosis.*

*mRNA levels were normalized to cyclophilin, and the subsequent ratios were presented as relative expression compared to WT values. Absorbance data were presented as relative expression compared to WT values. Data are means ± SD; n = 6 mice per group for all ex vivo experiments. Data are means ± SD; n = 7-8 mice per group for all in vivo functional tests. Statistical analysis was performed using one-way ANOVA followed by Tukey's test. ** p < 0.01, *** p < 0.001, **** p < 0.0001 vs. WT mice. # p < 0.05, ## p < 0.01, ### p < 0.001, #### p < 0.0001 vs. mdx mice.*

Discussion

The findings of this study unveiled that a late eight-week oral administration of AdipoRon exerted a protective impact on the dystrophic cardiac muscle of 14-month-old mdx mice. This intervention demonstrated efficacy in alleviating injuries, reducing exaggerated inflammatory responses and fibrosis, while enhancing mitochondrial biogenesis and overall muscle function. These favorable outcomes collectively contributed to the amelioration of the dystrophic phenotype.

There is evidence that Duchenne dilated cardiomyopathy (DMD-DCM) initially starts with sarcolemmal damage combined with alterations of mechanisms of repair, which are later worsened by inflammatory cells and cytokines, thus resulting in necrosis and fibrosis [28, 29]. In mdx mice, DCM is marked by accumulation of connective tissue and alterations in contractility which already develops around 10-12 months of age in *mdx* mice [16, 30, 31]. Our pivotal study (not published) didn't show any cardiac echography alteration before 12 months of age. Based on these data, we decided to test 14 months old mice for the current study. At this old age, the contractile dysfunction the left ventricular myocardium is present, thereby decreasing the left ventricular ejection fraction [16, 32]. These abnormalities were confirmed in our mdx untreated mice, but were normalised after AdipoRon treatment. Morphologically, mdx DCM is characterized by hypertrophy of the left ventricle (LV), including an increase in the size of individual cardiomyocytes. This can be a compensatory response to the increased workload on the heart [33, 34]. In our study, LV mass corrected by mice body weight was higher in mdx mice compared to controls. We did not however find a difference in the LV shortening fraction between both treated and untreated mdx mice, but as already observed in another study [35]. Additionally, *ex vivo* testing revealed that markers of hypertrophy were only present in the dystrophic cardiac muscles of untreated animals. Indeed, levels of BNP and ANP, 2 key genes whose expressions are significantly up-regulated in pathological cardiac hypertrophy [36], were markedly increased in hearts of mdx mice when compared to WT. All these abnormalities were again normalised after AdipoRon treatment, indicating a potent protective role against cardiac hypertrophy and dysfunction.

Furthermore, mdx mice treated with AdipoRon showed an elevation in anti-inflammatory cytokines, combined with a reduction in the expression of pro-inflammatory cytokines and oxidative stress markers. The extension of muscle injury and myonecrosis was also diminished. More specifically, levels of CK and LDH, both indicative of muscle membrane breach [12], were reduced, along with P-RIP protein, a necroptosis factor contributing to myofiber death in DMD muscle [25]. This suggests that suppression of RIP activity might, at least partially, contribute to

the anti-myonecrotic effect of AdipoRon. Overall, our findings align with other research demonstrating that the administration of AdipoRon significantly diminishes inflammation, oxidative stress, and tissue damage following heart injury [15].

Fibrosis emerges as one of the initial clinical manifestations in dystrophic cardiac pathology, manifesting in patients before the age of 10 [37], and as early as 2 months of age in mice [38]. It is widely acknowledged that cardiac injury and inflammation in DMD prompt the recruitment of fibro-adipogenic progenitors (FAPs), which subsequently differentiate into fibroblasts under the influence of TGF-β, thereby augmenting the deposition of connective tissues [39, 40]. TGF-β serves as a pivotal mediator of the fibrotic response, acting through its effector, the phosphorylated and active form of Smad2 [25]. In this study, we highlight the robust anti-fibrotic properties of AdipoRon, as evidenced by significant diminution of Picrosirius Red staining. Moreover, the quantification of active TGF-β and P-Smad2, demonstrated marked reductions following treatment. These findings align with the beneficial effects of AdipoRon observed both on myocardial fibrosis in heart failure with preserved ejection fraction (HFpEF) [41] and on intracardial fibrosis in diabetic mice [15].

We and others have shown that mdx mice display low circulating levels of ApN [7, 8]. In this study, we highlight a significant downregulation of both ApN receptors in the dystrophic cardiac muscles. These data align with those found life-threatening conditions associated with muscle wasting, such as chronic heart failure, where an ApN resistance was described due to AdipoR1 downregulation and inactivation of AMPK signaling [42]. Herein, treatment with AdipoRon restored AdipoRs levels and activated subsequent signaling pathways. Indeed, by exploring the mechanisms of action of AdipoRon in the heart, we found that the AMPK signaling pathway was activated in treated mice, as demonstrated by the increased phosphorylated form of AMPK combined with the subsequent increased levels of CAMKK2 and PGC-1α, as previously seen in the dystrophic skeletal muscle [7, 12]. Treatment even increased levels of AdipoR2-PPARα pathway. This is consistent with observations reported in diabetic mice, where AdipoRon was able to increase CAMKK2, AMPK and PPARα pathways and downstream signaling, thereby decreasing oxidative stress and apoptosis and exerting cardioprotective effects [43].

The AMPK pathway is also recognized for its role in conferring anti-inflammatory and anti-fibrotic properties, along with promoting mitochondrial biogenesis. Firstly, its anti-inflammatory effects are orchestrated primarily through potent suppression of NF-κB signaling [5, 44]. In our study, there was a notable reduction of over 40% in NF-κB activation. This repression of NF-κB is expected to contribute

to the restoration of cardiac function in mdx mice, as demonstrated by another group [17]. Secondly, its anti-fibrotic properties are mediated by the inhibition of TGF-β/Smad signaling [18, 45, 46]. The activation of the AMPK pathway has also demonstrated the ability to restrain dysfunctional vascular growth, a significant contributor to cardiovascular disease, by inhibiting TGF-β [47]. This mechanism partially elucidates the observed normalized ejection fraction and LV mass in our treated mice, affirming both enhanced cardiac function and diminished cardiac hypertrophy. Another study has previously demonstrated that activation of AMPK signaling counteracts the development of cardiac hypertrophy induced by isoproterenol [48]. Moreover, macrophages also promote fibrosis in DMD, while AMPK activation might reduce their TGF-β production and subsequently their pro-fibrotic effect [49]. Thirdly, the enhancement of mitochondrial biogenesis has been shown to be mediated by AMPK-PGC-1α [21, 50, 51]. PGC-1α was even found to stimulate the generation of mitochondria that are geared towards ATP production and exhibit high-level coupled respiration in cardiac myocytes [52]. In the present study, the administration of AdipoRon significantly increased the expression of ERRα and mtTFA, both recognized markers of mitochondrial biogenesis, as well as protein levels of TOMM20, a marker indicative of mitochondrial content. Our findings thus align with outcomes observed with AdipoRon showing a positive regulation of the myocardial mitochondrial energy metabolism pathways, in an induced cardiac hypertrophy mouse model [53]. In addition, Metformin, which by activating PGC-1α through AMPK induction, has demonstrated the restoration of the mitochondrial network and reduction of ROS generation in heart fibroblasts with chromosome 21 trisomy [54]. Comparable outcomes were also observed with the overactivation of PGC-1α through histone deacetylase inhibitors, demonstrating a mitigation of the dystrophic phenotype by addressing the deficit in mitochondrial biogenesis [55]. Lastly, activation of AMPK-CAMKK2-PGC-1α pathways also resulted in an elevation in utrophin, an analogue of dystrophin, with a noteworthy 15% increase in protein levels. The upregulation of utrophin holds the potential to reinstate sarcolemmal integrity, contributing to both morphological and functional enhancements in mdx mice [56, 57]. Our findings demonstrate that AdipoRon can be a potent AdipoR agonist, suppressing NF-κB and TGF-β activities, while enhancing mitochondrial biogenesis and upregulating utrophin. This in turn may lessen muscle inflammation, oxidative stress and fibrosis, protect the heart against injury and enhance mouse overall function, thus strikingly alleviating the dystrophic phenotype. This was demonstrated not only by positive echocardiographic results, but also by greatly enhanced performance in several *in vivo* functional tests.

Despite significant advancements and extensive research during the past three decades, an effective treatment for DMD is not available yet [58]. Various

pharmacological approaches, including glucocorticoids, Angiotensin-converting enzyme (ACE) inhibitors, Angiotensin receptor blockers (ARBs), mineralocorticoid receptor antagonists, and even simvastatin, have exhibited the potential to curtail fibrosis accumulation in dystrophic mouse and patient hearts. However a prominent anti-fibrotic treatment for DMD remains elusive [59]. Additionally, some of these treatments demonstrate relatively poor efficacy in addressing the specific challenges presented by the dystrophic heart. Hence, there is a crucial need for the development of treatments that strategically address both skeletal and cardiac muscle, and AdipoRon, an ApN receptor agonist, unquestionably emerges as a noteworthy candidate for consideration. Such interventions are crucial not only for enhancing the quality of life but also for extending the longevity of individuals with DMD.

This study unequivocally demonstrated the potent anti-inflammatory and anti-fibrotic effects of AdipoRon on the dystrophic cardiac muscle. Combined with its beneficial and protective effects on the dystrophic skeletal muscle [12], AdipoRon emerges as a potentially appealing therapeutic option. Furthermore, not only the safety profile of AdipoRon has been corroborated in various murine models and toxicology studies, but it has also been demonstrated that AdipoRon even exhibits the added advantage of safeguarding the liver, the kidneys, and enhancing metabolic functions in mice [5, 11, 21, 43]. It could even prolong the lifespan of obese treated mice [21], and exert various pleiotropic on a variety of tissues and organs [5].

References

1. Duan, D., et al., *Duchenne muscular dystrophy.* Nature Reviews Disease Primers, 2021. **7**(1): p. 13.
2. Rafael-Fortney, J.A., J.A. Chadwick, and S.V. Raman, *Duchenne Muscular Dystrophy Mice and Men: Can Understanding a Genetic Cardiomyopathy Inform Treatment of Other Myocardial Diseases?* Circ Res, 2016. **118**(7): p. 1059-61.
3. Schultz, T.I., F.J. Raucci, Jr., and F.N. Salloum, *Cardiovascular Disease in Duchenne Muscular Dystrophy: Overview and Insight Into Novel Therapeutic Targets.* JACC Basic Transl Sci, 2022. **7**(6): p. 608-625.
4. Buddhe, S., et al., *Cardiac Management of the Patient With Duchenne Muscular Dystrophy.* Pediatrics, 2018. **142**(Suppl 2): p. S72-s81.
5. Abou-Samra, M., et al., *Adiponectin and Its Mimics on Skeletal Muscle: Insulin Sensitizers, Fat Burners, Exercise Mimickers, Muscling Pills … or Everything Together?* Int J Mol Sci, 2020. **21**(7).
6. Yamauchi, T., et al., *Targeted disruption of AdipoR1 and AdipoR2 causes abrogation of adiponectin binding and metabolic actions.* Nat Med, 2007. **13**(3): p. 332-9.
7. Abou-Samra, M., et al., *Involvement of adiponectin in the pathogenesis of dystrophinopathy.* Skelet Muscle, 2015. **5**: p. 25.
8. Hathout, Y., et al., *Discovery of serum protein biomarkers in the mdx mouse model and cross-species comparison to Duchenne muscular dystrophy patients.* Hum Mol Genet, 2014. **23**(24): p. 6458-69.
9. Hathout, Y., et al., *Disease-specific and glucocorticoid-responsive serum biomarkers for Duchenne Muscular Dystrophy.* Sci Rep, 2019. **9**(1): p. 12167.
10. Abou-Samra, M., et al., *Potential Therapeutic Action of Adiponectin in Duchenne Muscular Dystrophy.* Am J Pathol, 2017. **187**(7): p. 1577-1585.
11. Okada-Iwabu, M., et al., *A small-molecule AdipoR agonist for type 2 diabetes and short life in obesity.* Nature, 2013. **503**(7477): p. 493-9.
12. Abou-Samra, M., et al., *AdipoRon, a new therapeutic prospect for Duchenne muscular dystrophy.* J Cachexia Sarcopenia Muscle, 2020. **11**(2): p. 518-533.
13. Zhang, Y., et al., *AdipoRon, the first orally active adiponectin receptor activator, attenuates postischemic myocardial apoptosis through both AMPK-mediated and AMPK-independent signalings.* Am J Physiol Endocrinol Metab, 2015. **309**(3): p. E275-82.
14. Jenke, A., et al., *AdipoRon Attenuates Inflammation and Impairment of Cardiac Function Associated With Cardiopulmonary Bypass-Induced*

Systemic Inflammatory Response Syndrome. J Am Heart Assoc, 2021. **10**(6): p. e018097.
15. Kim, Y., et al., *Adiponectin receptor agonist ameliorates cardiac lipotoxicity via enhancing ceramide metabolism in type 2 diabetic mice.* Cell Death & Disease, 2022. **13**(3): p. 282.
16. Quinlan, J.G., et al., *Evolution of the mdx mouse cardiomyopathy: physiological and morphological findings.* Neuromuscul Disord, 2004. **14**(8-9): p. 491-6.
17. Peterson, J.M., et al., *NF-kappaB inhibition rescues cardiac function by remodeling calcium genes in a Duchenne muscular dystrophy model.* Nat Commun, 2018. **9**(1): p. 3431.
18. Dufeys, C., et al., *AMPKα1 deletion in myofibroblasts exacerbates post-myocardial infarction fibrosis by a connexin 43 mechanism.* Basic Res Cardiol, 2021. **116**(1): p. 10.
19. Boursereau, R., et al., *Downregulation of the NLRP3 inflammasome by adiponectin rescues Duchenne muscular dystrophy.* BMC Biol, 2018. **16**(1): p. 33.
20. Delaigle, A.M., et al., *Induction of adiponectin in skeletal muscle of type 2 diabetic mice: In vivo and in vitro studies.* Diabetologia, 2006. **49**(6): p. 1311-23.
21. Selvais, C.M., et al., *AdipoRon enhances healthspan in middle-aged obese mice: striking alleviation of myosteatosis and muscle degenerative markers.* J Cachexia Sarcopenia Muscle, 2023. **14**(1): p. 464-478.
22. Leyens, G., I. Donnay, and B. Knoops, *Cloning of bovine peroxiredoxins-gene expression in bovine tissues and amino acid sequence comparison with rat, mouse and primate peroxiredoxins.* Comp Biochem Physiol B Biochem Mol Biol, 2003. **136**(4): p. 943-55.
23. De Paepe, B. and J.L. De Bleecker, *Cytokines and chemokines as regulators of skeletal muscle inflammation: presenting the case of Duchenne muscular dystrophy.* Mediators Inflamm, 2013. **2013**: p. 540370.
24. Tidball, J.G. and S.A. Villalta, *Regulatory interactions between muscle and the immune system during muscle regeneration.* Am J Physiol Regul Integr Comp Physiol, 2010. **298**(5): p. R1173-87.
25. Dubuisson, N., et al., *The Adiponectin Receptor Agonist, ALY688: A Promising Therapeutic for Fibrosis in the Dystrophic Muscle.* Cells, 2023. **12**(16).
26. Kristjansson, R.P., et al., *Common and rare variants associating with serum levels of creatine kinase and lactate dehydrogenase.* Nat Commun, 2016. **7**: p. 10572.

27. Morgan, J.E., et al., *Necroptosis mediates myofibre death in dystrophin-deficient mice.* Nat Commun, 2018. **9**(1): p. 3655.
28. Wallace, G.Q. and E.M. McNally, *Mechanisms of muscle degeneration, regeneration, and repair in the muscular dystrophies.* Annu Rev Physiol, 2009. **71**: p. 37-57.
29. Van Erp, C., et al., *Timeline of cardiac dystrophy in 3-18-month-old MDX mice.* Muscle Nerve, 2010. **42**(4): p. 504-13.
30. Spurney, C.F., et al., *Dystrophin-deficient cardiomyopathy in mouse: expression of Nox4 and Lox are associated with fibrosis and altered functional parameters in the heart.* Neuromuscul Disord, 2008. **18**(5): p. 371-81.
31. Farini, A., et al., *Fibrosis Rescue Improves Cardiac Function in Dystrophin-Deficient Mice and Duchenne Patient-Specific Cardiomyocytes by Immunoproteasome Modulation.* Am J Pathol, 2019. **189**(2): p. 339-353.
32. Zhang, W., et al., *Abnormal cardiac morphology, function and energy metabolism in the dystrophic mdx mouse: an MRI and MRS study.* J Mol Cell Cardiol, 2008. **45**(6): p. 754-60.
33. Marcadet, L., et al., *RANKL Inhibition Reduces Cardiac Hypertrophy in mdx Mice and Possibly in Children with Duchenne Muscular Dystrophy.* Cells, 2023. **12**(11).
34. Kamdar, F. and D.J. Garry, *Dystrophin-Deficient Cardiomyopathy.* J Am Coll Cardiol, 2016. **67**(21): p. 2533-46.
35. Fayssoil, A., et al., *Cardiac characterization of mdx mice using high-resolution doppler echocardiography.* J Ultrasound Med, 2013. **32**(5): p. 757-61.
36. Sheehy, S.P., S. Huang, and K.K. Parker, *Time-warped comparison of gene expression in adaptive and maladaptive cardiac hypertrophy.* Circ Cardiovasc Genet, 2009. **2**(2): p. 116-24.
37. Tandon, A., et al., *Myocardial fibrosis burden predicts left ventricular ejection fraction and is associated with age and steroid treatment duration in duchenne muscular dystrophy.* J Am Heart Assoc, 2015. **4**(4).
38. Li, Y., et al., *Blunted cardiac beta-adrenergic response as an early indication of cardiac dysfunction in Duchenne muscular dystrophy.* Cardiovasc Res, 2014. **103**(1): p. 60-71.
39. Biferali, B., et al., *Fibro-Adipogenic Progenitors Cross-Talk in Skeletal Muscle: The Social Network.* Front Physiol, 2019. **10**: p. 1074.
40. Tidball, J.G. and M. Wehling-Henricks, *Shifts in macrophage cytokine production drive muscle fibrosis.* Nat Med, 2015. **21**(7): p. 665-6.

41. Tan, W., et al., *AdipoRon ameliorates the progression of heart failure with preserved ejection fraction via mitigating lipid accumulation and fibrosis.* J Adv Res, 2024.
42. Van Berendoncks, A.M., et al., *Functional adiponectin resistance at the level of the skeletal muscle in mild to moderate chronic heart failure.* Circ Heart Fail, 2010. **3**(2): p. 185-94.
43. Kim, Y., et al., *The Adiponectin Receptor Agonist AdipoRon Ameliorates Diabetic Nephropathy in a Model of Type 2 Diabetes.* J Am Soc Nephrol, 2018. **29**(4): p. 1108-1127.
44. Salminen, A., J.M. Hyttinen, and K. Kaarniranta, *AMP-activated protein kinase inhibits NF-κB signaling and inflammation: impact on healthspan and lifespan.* J Mol Med (Berl), 2011. **89**(7): p. 667-76.
45. Marangoni, R.G., et al., *Adiponectin is an endogenous anti-fibrotic mediator and therapeutic target.* Sci Rep, 2017. **7**(1): p. 4397.
46. Lin, H., et al., *AMPK Inhibits the Stimulatory Effects of TGF-β on Smad2/3 Activity, Cell Migration, and Epithelial-to-Mesenchymal Transition.* Mol Pharmacol, 2015. **88**(6): p. 1062-71.
47. Stone, J.D., et al., *AMP-activated protein kinase inhibits transforming growth factor-β-mediated vascular smooth muscle cell growth: implications for a Smad-3-dependent mechanism.* Am J Physiol Heart Circ Physiol, 2015. **309**(8): p. H1251-9.
48. Zarrinpashneh, E., et al., *AMPKalpha2 counteracts the development of cardiac hypertrophy induced by isoproterenol.* Biochem Biophys Res Commun, 2008. **376**(4): p. 677-81.
49. Juban, G., et al., *AMPK Activation Regulates LTBP4-Dependent TGF-β1 Secretion by Pro-inflammatory Macrophages and Controls Fibrosis in Duchenne Muscular Dystrophy.* Cell Rep, 2018. **25**(8): p. 2163-2176.e6.
50. Austin, S. and J. St-Pierre, *PGC1α and mitochondrial metabolism--emerging concepts and relevance in ageing and neurodegenerative disorders.* J Cell Sci, 2012. **125**(Pt 21): p. 4963-71.
51. Marino, A., et al., *AMP-activated protein kinase: A remarkable contributor to preserve a healthy heart against ROS injury.* Free Radic Biol Med, 2021. **166**: p. 238-254.
52. Finck, B.N. and D.P. Kelly, *Peroxisome proliferator-activated receptor gamma coactivator-1 (PGC-1) regulatory cascade in cardiac physiology and disease.* Circulation, 2007. **115**(19): p. 2540-8.
53. Hu, X., et al., *AdipoRon prevents l-thyroxine or isoproterenol-induced cardiac hypertrophy through regulating the AMPK-related pathway.* Acta Biochim Biophys Sin (Shanghai), 2019. **51**(1): p. 20-30.

54. Izzo, A., et al., *Metformin restores the mitochondrial network and reverses mitochondrial dysfunction in Down syndrome cells.* Hum Mol Genet, 2017. **26**(6): p. 1056-1069.
55. Giovarelli, M., et al., *Givinostat as metabolic enhancer reverting mitochondrial biogenesis deficit in Duchenne Muscular Dystrophy.* Pharmacol Res, 2021. **170**: p. 105751.
56. Al-Rewashdy, H., et al., *Utrophin A is essential in mediating the functional adaptations of mdx mouse muscle following chronic AMPK activation.* Hum Mol Genet, 2015. **24**(5): p. 1243-55.
57. Squire, S., et al., *Prevention of pathology in mdx mice by expression of utrophin: analysis using an inducible transgenic expression system.* Hum Mol Genet, 2002. **11**(26): p. 3333-44.
58. Elangkovan, N. and G. Dickson, *Gene Therapy for Duchenne Muscular Dystrophy.* J Neuromuscul Dis, 2021. **8**(s2): p. S303-s316.
59. Yao, S., et al., *Current Pharmacological Strategies for Duchenne Muscular Dystrophy.* Front Cell Dev Biol, 2021. **9**: p. 689533.

Chapter 4: General discussion and perspectives

Chapter 4: General discussion and perspectives

Discussion

Effects of ApN mimics and inflammasome inhibitors in DMD

Duchenne muscular dystrophy (DMD) is a devastating myopathy characterized by muscle weakness and degenerative progressive evolution. Typically, the secondary process involving severe inflammation and necrosis exacerbate disease progression [1]. Despite advances in understanding and management, with a total of 390 clinical trials conducted as of January 2024 [2], DMD remains incurable, highlighting the ongoing need for research and therapeutic interventions [3]. Some therapies targeting the genetic cause of the disease are already available, such as exon skipping therapies. However, their use is limited to a subset of patient harboring specific mutations [4]. Another strategy focuses on combating the severe inflammation of the disease by using glucocorticosteroids (GCs) like prednisone and deflazacort. GCs exhibit efficacy in slowing muscle weakness progression and delaying ambulation loss in some patients. However, their utility is compromised by a broad spectrum of adverse effects, including weight gain, growth retardation, a cushingoid appearance, as well as bone demineralization, glucose intolerance, and hypertension [5].

This project was undertaken with the aim of exploring two innovative therapeutic avenues to improve the management of DMD. In the initial study, we pursued a targeted approach by focusing specifically on the inhibition of NLRP3 inflammasome. This complex molecular structure is implicated in the initiation or progression of various diseases, including certain muscle disorders like valosin containing protein (VCP) myopathy, dysferlinopathy, and DMD [6-8]. However, NLRP3 inflammasome inhibitors have never been tested on the dystrophic muscle yet. To successfully carry out our project, we administered an 8-week oral treatment of MCC950, a specific NLRP3 inhibitor, to 4 weeks old mdx mice. This treatment led to a notable decrease in muscle inflammation, evidenced by reduced macrophage infiltration, lower levels of pro-inflammatory cytokines such as IL-1β and IL-18, and diminished markers of oxidative stress. Additionally, animals treated with MCC950 exhibited reduced levels of necrosis and fibrosis in comparison with

untreated mdx mice. Importantly, we were the first to show that pyroptosis could be a novel programmed cell death type in DMD and was efficiently hampered by MCC950. These favorable outcomes, coupled with a modest increase in utrophin expression, were shown to enhance muscle function and mitigate the dystrophic phenotype [9].

The second approach employed a different method by investigating molecules having a much broader spectrum of action. Indeed, ApN has been shown to exert pleiotropic effects on several organs including the potential of ameliorating the dystrophic phenotype in mdx mice [10]. However, the direct application of ApN as a therapeutic agent remains limited due to its complex three-dimensional structure and its high molecular weight necessary for its metabolic properties [11]. Recent advancements have identified several small molecules and short peptides that target AdipoRs, seeking to replicate ApN's beneficial effects. Among these candidates, ALY688, a peptide which is derived from the globular region of ApN, and AdipoRon a small synthetic molecule, emerge as particularly promising. ALY688 was tested subcutaneously in 4 weeks old mdx mice for a two-month period at a dose of either 3 or 15mg/kg/day and confirmed its beneficial effect by mitigating excessive inflammatory responses in dystrophic muscle by reducing the expression of pro-inflammatory cytokines, oxidative stress markers, and CD68+ macrophage infiltrates. Additionally, it led to a decrease in the extension of myonecrosis and positively influenced the muscle regeneration process, while also demonstrating potent anti-fibrotic properties [12]. Importantly, while no safety issue was observed in mice, the effects of MCC950 and ALY688 compounds were recapitulated in human myotubes challenged with inflammatory stimuli mimicking the DMD microenvironment, thus encouraging potential translation towards human clinical trials.

Finally, we decided to expand our approach by evaluating a different aspect of the disease. Recognizing that cardiovascular disease is one of the leading causes of death in DMD patients [13], we tested AdipoRon on the cardiac muscle of mdx mice starting at the age of 60 weeks, as dilated cardiomyopathy and contractile deviations usually begin to manifest in 36- to 40-week-old mdx mice [14]. These mice were orally treated with a dose of 50 mg/kg/day for a period of 8 weeks, revealing unequivocally the potent anti-inflammatory and anti-fibrotic effects of

AdipoRon on cardiac muscle, along with improved cardiac function observed on echocardiography.

Comparison between ApN mimics and inflammasome inhibitors

As previously noted, both approaches diverge significantly. MCC950 is a molecule characterized by a distinct scaffold, meticulously crafted to selectively target NLRP3 and modulate the inflammation pathway [15]. In contrast, ALY688 and AdipoRon, a peptide and a small synthetic molecule respectively, exert a broad spectrum of favorable effects, ranging from anti-inflammatory properties to anti-fibrotic potency, along with pro-metabolic actions [12, 16, 17].

Their respective mechanisms of action explain these differences. MCC950 specifically binds the NLRP3 protein, preventing its oligomerization and activation. By inhibiting the activation of the NLRP3 inflammasome, MCC950 prevent the cleavage and release of pro-inflammatory cytokines such as IL-1β and IL-18, as well as the pyroptotic process, thereby specifically reducing the downstream inflammatory response [9]. On the other hand, ApN mimics acts upstream of the NLRP3 inflammasome by activating the AdipoR1-AMPK-SIRT1-PGC-1α pathway [18]. AMPK has been shown to repress NF-κB, a master regulator of inflammation, via PGC-1α and SIRT1 [19]. Additionally, AMPK promotes fatty acid oxidation through the transcription factor PPARα [20], exerts insulin-sensitizing actions via the phosphorylation of insulin receptor substrate-1 (IRS-1) [21], facilitates the translocation of GLUT-4 to the plasma membrane [22] and displays pro-myogenic effects by increasing the expression of proliferation and differentiation markers in skeletal muscle [23]. In summary, ApN mimics effects extend beyond inflammation to include metabolic regulation and cardiometabolic protection, making it a broader therapeutic target in conditions associated with inflammation and metabolic dysfunction.

When considering mode of administration, MCC950 and AdipoRon are taken orally, whereas ALY688 is administered subcutaneously. Although the oral route is typically regarded as the safest, least expensive, and often preferred method of administration by patients, it does present some limitations. Orally administered drugs must traverse the gastrointestinal tract to reach the small intestine for absorption, then pass through the intestinal wall and undergo metabolism in the liver before entering the bloodstream and reaching their target site. This metabolic

process can decrease the amount of drug that ultimately reaches the bloodstream contributing to a lower bioavailability [24]. In contrast, the subcutaneous route used for ALY688 involves the injection into the fatty tissue just beneath the skin. Following injection, the drug enters capillaries and is subsequently carried away by the bloodstream, or it may enter the bloodstream via the lymphatic vessels thus bypassing the gastrointestinal system and the liver's first-pass metabolism. The subcutaneous route is commonly used for administering protein and peptide drugs, as these molecules would be degraded in the digestive tract if taken orally [25].

The most effective dosage for our products was investigated through various dose tests either on C2C12 or on human myotubes. Ultimately, we selected a concentration of 10 μM as the optimal dose for MCC950, while the dose-response curve done for ALY688 and AdipoRon confirmed that a concentration of 100 nM and 25 μM yielded the best outcome, respectively [9, 12]. Moreover, AdipoRon and ALY688 were directly compared showing that ALY688 was usually as effective as AdipoRon, but at much lower concentrations (100 nM vs. 25 μM). We did not compare directly ApN mimics with MCC950 on the same myotube culture. However, we can attempt to provide some comparisons. While, a MCC950 concentration of 10 μM, successfully halved NF-κB expression and pro-inflammatory cytokines, the same effect was obtained with ALY688 at approximately ~100, ~35 pM, and 1 nM for IL-1 β, TNFα, and NF-κB, respectively [9, 12]. Based on these findings, we can therefore posit a 100-fold difference between ALY688 and MCC950, while MCC950 would be 2.5x more potent than AdipoRon. Further pharmacokinetic and pharmacodynamic studies in humans will be necessary to ascertain the appropriate dosage based on drug exposure and response. `

In terms of safety profile, MCC950 has undergone extensive preclinical studies and showed no alarming signals, with doses typically ranging from 10 to 200 mg/kg [26]. However, during evaluation in a phase II clinical trial for the treatment of rheumatoid arthritis, an elevation of serum liver enzyme levels, indicative of potential liver toxicity, was observed [27]. New generation NLRP3 inhibitors based on the structure of MCC950 are currently under development with hopefully a better safety profile.

On the other hand, AdipoRon did not raise any concerns while being used for more than one decade in research settings [28]. Lastly, ALY688 exists in two formulations: the initial formulation, which was utilized for in vitro experimentation and for topical use, and the extended-release (ER) formulation, which has been recently developed. The phase I/II clinical trial using the topical form for dry eye disease demonstrated a good safety profile for participants [29]. The ER formulation safety profile has been assessed by Allysta Pharmaceuticals on different preclinical models, but has not been publicly disclosed yet. Studies on this matter are scarce in the literature, but doses between 3 to 15 mg/kg in mice seem to be well tolerated [12].

The role of ApN mimics and inflammasome inhibitors in the current therapeutic arsenal for DMD.

Today's therapeutic arsenal for DMD includes diverse approaches aimed at managing symptoms, enhancing quality of life, and addressing the underlying genetic cause. However, GCs and gene therapies have their limitations in terms of adverse events, availability for patients, or efficacy concerns. These limitations underscore the scarcity of effective therapies for DMD [30].

Three molecules, namely MCC950, AdipoRon and ALY688, emerge as potential candidates for DMD management. Like GCs, all these molecules primarily exert anti-inflammatory and anti-fibrotic actions [9, 12, 31]. However, ApN mimics also elicit additional pro-myogenic and cardiac beneficial effects [16, 32].

In practical terms, MCC950 or other new generation NLRP3 inhibitors would likely be utilized as a monotherapy to replace GCs. MCC950 appears to exhibit greater selectivity than GCs, affecting only the NLRP3 inflammasome pathway, thus suggesting a lower incidence of adverse events. Furthermore, compared to other direct or indirect inhibitors of the NLRP3 pathway, MCC950 retains high potency. For example, MCC950 demonstrated the ability to rescue neonatal lethality in a genetic mouse model of Cryopyrin-Associated Autoinflammatory Syndromes (CAPS) caused by an activating mutation in NLRP3, whereas targeted blockade of IL-1β alone was insufficient for such rescue. This efficacy was attributed to the additional inhibition of IL-18 and pyroptosis provided by MCC950. Moreover, the specific targeting of NLRP3 (without affecting the major anti-microbial inflammasomes NLRC4 and NLRP1) may explain why MCC950 exhibits lower immunosuppressive effects compared to biologic compounds such as canakinumab, which have been associated with an increased risk of serious infections [15].

ApN mimics, on the other hand, would ideally complement GCs treatment or gene therapy. Indeed, AdipoRon, has been shown to normalizes glucose metabolism and prevents obesity but not growth retardation induced by GCs in mice [33]. Furthermore, ApN mimics could also benefit viral vector-based DMD gene therapy such as exon-skipping or micro-dystrophin cDNA transfer [3, 34]. By mitigating the dystrophic micro-environment (strengthening leaky membranes and reducing inflammation and oxidative stress), pre-treatment with ApN mimics could avoid the

subsequent loss of virus-mediated genomes occurring in diseased muscle early after vector injection [34]. ALY688 or AdipoRon and DMD gene therapy could thus exert synergistic effects. Presently, we are engaged in a study where we combine micro-dystrophin vector injection with concurrent ALY688 treatment. This combined treatment approach is being compared with vector alone to evaluate potential synergistic effects. Finally, in comparison with several other AMPK activators, including AICAR, metformin, and resveratrol, which also alleviated certain pathological features of DMD in cell cultures and animal models, [35-39], ApN mimics have also the advantage to activate, other cascades and effectors, such as Ca^{2+}/calmodulin-dependent protein kinase kinase, p38 mitogen-activated protein kinase, PPARα, ceramidase activity and others, responsible for a plethora of additional metabolic and protective actions in several target tissues and organs [18, 40, 41].

Limitations

While we used standardized approaches developed by TREAT-NMD for our *in vivo* testing and stratified mdx animals according to their litter and weight to limit confounders, our tests were not blinded, which may introduce a risk of operator-related bias. Indeed, a single operator was responsible for the mice's care and the *in vivo* experiments. This design was preferred to avoid errors while shifting the mice between blinded and unblinded statuses. In a larger review, blinded studies using mdx mice were only achieved in 7.4% of the 200 papers published between 2001 and 2011 [42], indicating methodological challenges in setting up blinded studies with mdx mice.

The proportion of fibres with central nuclei (CNF), a hallmark of fibres that have undergone regeneration, was almost undetectable in WT mice, but remained similarly elevated in mdx mice regardless of treatment. Although initially perceived as disappointing, this result can be partly explained by the fact that CNF cannot distinguish between fibres at the early or late stages of regeneration. Newly regenerated myofibres in mdx mice retain a central location for about 50–100 days, and only 3–4% of myonuclei move to a peripheral subsarcolemmal position later [43]. Alternatively, we managed to confirm the promyogenic effects of the compound, by demonstrating the elevated expression of mature myosin heavy chains compared in treated animals confirming an enhanced regeneration process.

The mdx mouse is the most widely used and best-known animal model of DMD. However, this model shows significant differences from the human disease in terms of severity. The milder phenotype present in mdx mice is primarily due to their

highly efficient muscle regeneration capacity compared to humans. To address these discrepancies, we decided to directly test our drugs on human myotubes. The replication of our results in human cells confirmed the translatability of mdx mice as a useful animal model for DMD.

General conclusion

The three molecules tested in this study have shown very interesting effects on the skeletal and cardiac dystrophic muscles. By comparing them, it appears that ALY688 is active at a concentration approximately 100 and 250 times lower than MCC950 and AdipoRon respectively. Moreover, ApN mimics exert a broader effect, allowing them to be used both as a replacement for GCs or even in combination with them. This treatment could also facilitate exon-skipping or micro-dystrophin cDNA transfer treatments. Finally, being already used in human clinical trials, ALY688 seems poised to be tested for DMD in very short time, making our work quite valuable in the DMD therapeutic landscape.

Perspectives

Further explorations of inflammasome inhibitors and ApN mimics in pre-clinical research

We started investigating the beneficial effects of MCC950 and ApN mimics on the dystrophic muscle, however further experiments are needed to complete this study. Firstly, given that respiratory insufficiency is one the most common cause of premature death in DMD patients [44], we would like to extend our molecular and biochemical tests to the diaphragm, which is heavily affected by the disease. This muscle seems prone to early accumulation of adipose and connective tissue, the extent of which has been evident as early as 12 weeks of age in mdx mice. This muscle is most closely linked to human disease, where it weakens from adolescence, leading to hypoventilation and hypercapnia [45]. We thus would explore whether the three compounds retain their protective effects in this tissue. Secondly, it would be interesting to replicate the cardioprotective effect of AdipoRon, in mdx mice treated with ALY688. To explore this, we initiated a study where 56-weeks old mdx mice were treated with ALY688-ER at the optimal dose of 8 mg/kg (data from Allysta Inc.) for 12 weeks. In the second part of the study, we would like to translate our data to human iPSC derived cardiomyocytes. Preliminary results are shown in the annexes section.

Thirdly, we will further study in vitro the direct anti-inflammatory properties of the treatment in human DMD myotubes. We have already shown that the three molecules were powerful enough to significantly reduce the expression of two major proinflammatory cytokines, TNFα and IL-1β, in both human control and DMD myotubes, following an inflammatory stimulus. We now wish to perform further transcriptome and secretome analysis in order to detect a possible shift in myokine expression and secretion towards a less inflammatory profile, as seen after ApN treatment [46].

Lastly, the available data regarding the effects of ALY688 on the dystrophic muscle are currently limited to this study. In order to bolster the preclinical data and thus facilitate the transition of ALY688 into phase I clinical trials, it seems imperative to

conduct additional studies involving ALY688 in other animal models such as the DBA/2-mdx mice.

Translate our results to clinical trials

The goal of all the preclinical data showed across this work, is the translation towards human clinical trials. Regarding their stage of development, MCC950 has experienced a sudden halt in its development due to concerns about liver toxicity. This setback forced Pfizer to halt further clinical translation of MCC950 [47]. However, MCC950-derived analogues with improved potency and pharmacological profiles are currently being developed and clinically evaluated. Among them, RRx-101 is currently used in a phase III trial, while many others are already involved in phase II trials. Pharmaceutical companies are heavily investing in specific inhibitors of NLRP3, primarily exploring them in inflammatory and autoimmune disorders. Although these inhibitors have not yet been tested in clinical trials for muscle conditions, we believe that safe and successful inflammasome inhibitors will play a crucial role in managing DMD treatment. Our research may hopefully pave the way for expanding their indications to encompass muscle diseases with inflammatory components.

Despite being commercially available for a decade, AdipoRon has solely been utilized for research endeavors, and as of yet, no human clinical trials have been undertaken, thus constraining its translational prospects. ALY688, on the other hand, is already undergoing phase III clinical trials in patients with dry eye disease [29]. Its beneficial effect on mdx mice and his promising safety profile are encouraging and will prompt additional validation in other DMD animal models. We will continue collaborating with Allysta Pharmaceuticals to accumulate more evidence regarding the efficacy of the drug, with the aim of expediting the launch of a phase I/II study in Duchenne muscular dystrophy at the earliest opportunity.

Extend these treatments to other muscle disorders.

It would be interesting to extend this work to other myopathies where inflammation plays a pathogenic role such as limb girdle muscular dystrophy type 2 (LGMD2) caused by mutations in the dysferlin gene with resulting myofibre

plasma membrane abnormalities, or idiopathic inflammatory myopathies, a category of 206 autoimmune muscle disorders including polymyositis, dermatomyositis and inclusion body myositis. We will use the SJL/J mouse model of Dysferlin Deficiency (available from Jackson laboratories) as a model for LGMD2B [48]. The appropriate animal model for idiopathic inflammatory myopathies is still debated but as a first approach, we will induce experimental autoimmune myositis by vaccination twice with high dose of myosin and Pertussis Toxin [49]. All these animal models will be treated and muscle inflammation, damage and function will be analysed as described before [9, 12]. The use of these molecules could also be theoretically beneficial in any other disease, where NF-κB is over-active and leads to excessive inflammation.

References

1. Duan, D., et al., *Duchenne muscular dystrophy.* Nature Reviews Disease Primers, 2021. **7**(1): p. 13.
2. Tang, A. and T. Yokota, *Duchenne muscular dystrophy: promising early-stage clinical trials to watch.* Expert Opin Investig Drugs, 2024. **33**(3): p. 201-217.
3. Jones, D., *Duchenne muscular dystrophy awaits gene therapy.* Nat Biotechnol, 2019. **37**: p. 335–337.
4. Niks, E.H. and A. Aartsma-Rus, *Exon skipping: a first in class strategy for Duchenne muscular dystrophy.* Expert Opin Biol Ther, 2017. **17**(2): p. 225-236.
5. Guglieri, M., et al., *Effect of Different Corticosteroid Dosing Regimens on Clinical Outcomes in Boys With Duchenne Muscular Dystrophy: A Randomized Clinical Trial.* Jama, 2022. **327**(15): p. 1456-1468.
6. Rawat, R., et al., *Inflammasome up-regulation and activation in dysferlin-deficient skeletal muscle.* Am J Pathol, 2010. **176**(6): p. 2891-900.
7. Nalbandian, A., et al., *Activation of the NLRP3 Inflammasome Is Associated with Valosin-Containing Protein Myopathy.* Inflammation, 2017. **40**(1): p. 21-41.
8. Boursereau, R., et al., *Downregulation of the NLRP3 inflammasome by adiponectin rescues Duchenne muscular dystrophy.* BMC Biol, 2018. **16**(1): p. 33.
9. Dubuisson, N., et al., *Inhibiting the inflammasome with MCC950 counteracts muscle pyroptosis and improves Duchenne muscular dystrophy.* Front Immunol, 2022. **13**: p. 1049076.
10. Abou-Samra, M., Raphaël Boursereau, Sophie Lecompte, Laurence Noel, and Sonia M. Brichard, *Potential Therapeutic Action of Adiponectin in Duchenne Muscular Dystrophy.* The American Journal of Pathology 2017. **187**(7): p. 1577–85.
11. Maury, E. and S.M. Brichard, *Adipokine dysregulation, adipose tissue inflammation and metabolic syndrome.* Mol Cell Endocrinol, 2010. **314**(1): p. 1-16.
12. Dubuisson, N., et al., *The Adiponectin Receptor Agonist, ALY688: A Promising Therapeutic for Fibrosis in the Dystrophic Muscle.* Cells, 2023. **12**(16).
13. Cheeran, D., et al., *Predictors of Death in Adults With Duchenne Muscular Dystrophy-Associated Cardiomyopathy.* J Am Heart Assoc, 2017. **6**(10).

14. Farini, A., et al., *Fibrosis Rescue Improves Cardiac Function in Dystrophin-Deficient Mice and Duchenne Patient-Specific Cardiomyocytes by Immunoproteasome Modulation.* Am J Pathol, 2019. **189**(2): p. 339-353.
15. Coll, R.C., et al., *A small-molecule inhibitor of the NLRP3 inflammasome for the treatment of inflammatory diseases.* Nat Med, 2015. **21**(3): p. 248-55.
16. Abou-Samra, M., et al., *AdipoRon, a new therapeutic prospect for Duchenne muscular dystrophy.* J Cachexia Sarcopenia Muscle, 2020. **11**(2): p. 518-533.
17. Da Eira, D., et al., *Effects of the adiponectin mimetic compound ALY688 on glucose and fat metabolism in visceral and subcutaneous rat adipocytes.* Adipocyte, 2020. **9**(1): p. 550-562.
18. Abou-Samra, M., et al., *Adiponectin and Its Mimics on Skeletal Muscle: Insulin Sensitizers, Fat Burners, Exercise Mimickers, Muscling Pills … or Everything Together?* Int J Mol Sci, 2020. **21**(7).
19. Eisele, P.S., et al., *The peroxisome proliferator-activated receptor γ coactivator 1α/β (PGC-1) coactivators repress the transcriptional activity of NF-κB in skeletal muscle cells.* J Biol Chem, 2013. **288**(4): p. 2246-60.
20. Yoon, M.J., et al., *Adiponectin increases fatty acid oxidation in skeletal muscle cells by sequential activation of AMP-activated protein kinase, p38 mitogen-activated protein kinase, and peroxisome proliferator-activated receptor alpha.* Diabetes, 2006. **55**(9): p. 2562-70.
21. Wang, C., et al., *Adiponectin sensitizes insulin signaling by reducing p70 S6 kinase-mediated serine phosphorylation of IRS-1.* J Biol Chem, 2007. **282**(11): p. 7991-6.
22. Yamauchi, T., et al., *Globular adiponectin protected ob/ob mice from diabetes and ApoE-deficient mice from atherosclerosis.* J Biol Chem, 2003. **278**(4): p. 2461-8.
23. Fiaschi, T., et al., *Globular adiponectin activates motility and regenerative traits of muscle satellite cells.* PLoS One, 2012. **7**(5): p. e34782.
24. Lin, L. and H. Wong, *Predicting Oral Drug Absorption: Mini Review on Physiologically-Based Pharmacokinetic Models.* Pharmaceutics, 2017. **9**(4).
25. Wang, L., et al., *Therapeutic peptides: current applications and future directions.* Signal Transduction and Targeted Therapy, 2022. **7**(1): p. 48.
26. Ludwig-Portugall, I., et al., *An NLRP3-specific inflammasome inhibitor attenuates crystal-induced kidney fibrosis in mice.* Kidney Int, 2016. **90**(3): p. 525-39.
27. Mangan, M.S.J., et al., *Targeting the NLRP3 inflammasome in inflammatory diseases.* Nat Rev Drug Discov, 2018. **17**(8): p. 588-606.
28. Salmons, H.I., et al., *The Safety of Adiponectin Receptor Agonist AdipoRon in a Rabbit Model of Arthrofibrosis.* Tissue Eng Part C Methods, 2023. **29**(4): p. 154-159.

29. Lee, I.K., et al., *Enhanced Immunomodulation, Anti-Apoptosis, and Improved Tear Dynamics of (PEG)-BHD1028, a Novel Adiponectin Receptor Agonist Peptide, for Treating Dry Eye Disease.* Pharmaceutics, 2022. **15**(1).
30. Heydemann, A. and M. Siemionow, *A Brief Review of Duchenne Muscular Dystrophy Treatment Options, with an Emphasis on Two Novel Strategies.* Biomedicines, 2023. **11**(3).
31. Quattrocelli, M., et al., *Intermittent Glucocorticoid Dosing Improves Muscle Repair and Function in Mice with Limb-Girdle Muscular Dystrophy.* Am J Pathol, 2017. **187**(11): p. 2520-2535.
32. Jenke, A., et al., *AdipoRon Attenuates Inflammation and Impairment of Cardiac Function Associated With Cardiopulmonary Bypass-Induced Systemic Inflammatory Response Syndrome.* J Am Heart Assoc, 2021. **10**(6): p. e018097.
33. Nicolas, S., et al., *The adiponectin receptor agonist AdipoRon normalizes glucose metabolism and prevents obesity but not growth retardation induced by glucocorticoids in young mice.* Metabolism, 2020. **103**: p. 154027.
34. Duan, D., *Systemic AAV micro-dystrophin gene therapy for Duchenne muscular dystrophy.* Mol Ther 2018. **26**: p. 2337–2356.
35. Abou-Samra, M., Sophie Lecompte, Olivier Schakman, Laurence Noel, Marie C. Many, Philippe Gailly, and Sonia M. Brichard, *Involvement of Adiponectin in the Pathogenesis of Dystrophinopathy.* Skeletal Muscle, 2015. **5**: p. 25.
36. Dong, X., et al., *Metformin Increases Sarcolemma Integrity and Ameliorates Neuromuscular Deficits in a Murine Model of Duchenne Muscular Dystrophy.* Front Physiol, 2021. **12**: p. 642908.
37. Ljubicic, V., et al., *Resveratrol induces expression of the slow, oxidative phenotype in mdx mouse muscle together with enhanced activity of the SIRT1-PGC-1α axis.* Am J Physiol Cell Physiol, 2014. **307**(1): p. C66-82.
38. Bastin, J. and F. Djouadi, *Resveratrol and Myopathy.* Nutrients, 2016. **8**(5).
39. Dial, A.G., et al., *The Role of AMPK in Neuromuscular Biology and Disease.* Trends Endocrinol Metab, 2018. **29**(5): p. 300-312.
40. Iwabu, M., et al., *Adiponectin and AdipoR1 regulate PGC-1alpha and mitochondria by Ca(2+) and AMPK/SIRT1.* Nature, 2010. **464**(7293): p. 1313-9.
41. Gamberi, T., et al., *Adiponectin Signaling Pathways in Liver Diseases.* Biomedicines, 2018. **6**(2).
42. Willmann, R., et al., *Best Practices and Standard Protocols as a Tool to Enhance Translation for Neuromuscular Disorders.* J Neuromuscul Dis, 2015. **2**(2): p. 113-117.

43. McGeachie, J.K., et al., *Age-related changes in replication of myogenic cells in mdx mice: quantitative autoradiographic studies.* J Neurol Sci, 1993. **119**(2): p. 169-79.
44. Van Ruiten, H.J., et al., *Why are some patients with Duchenne muscular dystrophy dying young: An analysis of causes of death in North East England.* Eur J Paediatr Neurol, 2016. **20**(6): p. 904-909.
45. Manning, J. and D. O'Malley, *What has the mdx mouse model of Duchenne muscular dystrophy contributed to our understanding of this disease?* J Muscle Res Cell Motil, 2015. **36**(2): p. 155-67.
46. Lecompte, S., et al., *Skeletal muscle secretome in Duchenne muscular dystrophy: a pivotal anti-inflammatory role of adiponectin.* Cell Mol Life Sci, 2017. **74**(13): p. 2487-2501.
47. Corcoran, S.E., R. Halai, and M.A. Cooper, *Pharmacological Inhibition of the Nod-Like Receptor Family Pyrin Domain Containing 3 Inflammasome with MCC950.* Pharmacol Rev, 2021. **73**(3): p. 968-1000.
48. Kobayashi, K., et al., *Dysferlin and animal models for dysferlinopathy.* J Toxicol Pathol, 2012. **25**(2): p. 135-47.
49. Afzali, A.M., et al., *Animal models in idiopathic inflammatory myopathies: How to overcome a translational roadblock?* Autoimmun Rev, 2017. **16**(5): p. 478-494.

Annexes

Part I: ALY688 and its action on the cardiac muscle: Preliminary results

Introduction

Adiponectin (ApN) is a hormone known for its beneficial effects on various tissues and organs. Previously, we demonstrated ApN's ability to mitigate Duchenne muscular dystrophy (DMD), a debilitating muscle disease. However, the therapeutic application of ApN is hindered by its intricate structure. To address this challenge, ApN mimics such as AdipoRon and ALY688 have been developed. Our recent research has highlighted the robust protective properties of AdipoRon on both cardiac and skeletal muscle [1, 2]. While ALY688 has shown promising anti-inflammatory and anti-fibrotic effects in skeletal muscle when administered to mdx mice (a DMD mouse model) [3], its impact on cardiac muscle remains unexplored. Given that cardiomyopathy is the primary cause of mortality in DMD, we aimed to investigate the potential benefits of ALY688 on the dystrophic heart.

Methods

Animals

C57BL/10ScSn-*Dmd*^{mdx}J mdx mice (murine model of Duchenne muscular dystrophy) and C57BL/10ScSnJ mice (used as wild-type (WT) controls) were purchased from Jackson Laboratory (Maine, USA). Three groups of male mice (*n* = 6/group) were compared in our experiments. The first group was WT mice, the second group was composed of untreated mdx mice (mdx), while the third group consisted of treated mdx mice (mdx-ALY). For the final group, a dosage of 8 mg/kg/day of ALY688-ER (Allysta Pharmaceuticals) was delivered subcutaneously (sc) five days a week, commencing at 13 months of age and continuing for a duration of 12 weeks, while WT and Regular mdx mice were injected with saline. Animals were maintained under a standard laboratory chow and housed at a constant temperature (22°) with a fixed 12h light – 12h dark cycle (lights on from 7 a.m. to 7 p.m.). At the end of the treatment, 16-month-old mice were sacrificed, as described [3], 1 week after echocardiography and *in vivo* functional tests.

Echocardiographic analyses

Cardiac dimensions and function were analysed by transthoracic echocardiography using a Vevo 3100 Imaging System (FUJIFILM VisualSonics, Toronto, Canada) as

described [4]. Mice were lightly anesthetized with inhaled isoflurane (1%, in 100% O2). Left ventricle (LV) volumes were measured using B-mode parasternal long-axis view, at end-systole and end-diastole, from which ejection fraction (EF %) was deduced. LV mass was calculated from LV long-axis measurements. Left ventricle end-diastolic (LVDd) and end-systolic (LVDs) dimensions were measured from the M-mode traces, and fractional shortening (FS %) was calculated as follows: [(LVDd − LVDs)/LVDd*100]. All measurements and analysis were performed by the same experienced operator who was blinded to the experimental groups.

In vivo studies of global force or resistance

Throughout the study, we conducted three well-established and reliable functional tests [3, 5] at four specific time points to monitor the progression of performance over time. These assessments were conducted at week 56, before the initiation of treatment, at week 60 (intermediary assessment 1), week 64 (intermediary assessment 2), and week 67, one week before sacrifice. In every test session the three tests were carried out consecutively, spanning a 5-day period.

Wire test: mice were suspended by their limbs from a wire and the time until they completely released their grasp and fell was recorded. Mice that reached a set limit of 600 seconds were allowed to stop the experiment, while others were directly retested, up to three times, and their maximum hanging time was recorded. The holding impulse (body mass × hang time), used to oppose the gravitational force, was then calculated [5].

Grip test: limb strength was recorded using a grid connected to a sensor (Panlab-Bioseb, Vitrolles, France). Mice were gently laid on the top of a grid so that their front paws could grip the grid. Mice were then pulled back steadily until the grip was released down the complete length of the grid. Each test was repeated three times at an interval of 15 min. Results are presented as the mean of the three values of force recorded, related to body weight [3].

Treadmill exhaustion test: after two consecutive days of acclimation to the moving belt (Panlab-Bioseb), mice were submitted to a treadmill exhaustion test with an upward inclination of 5° and progressive increasing speed rate. The mice started by running 10 min at a pace of 20 cm/s, then the velocity was increased by 1cm/sec every minute to finally reach a maximum speed of 35cm/sec for an additional 10 minutes. Exhaustion was defined as the inability of the animal to run on the

treadmill for 5 seconds despite laying on top of the shock grid and receiving repeated aversive stimuli [3, 6]. The distance covered in meters (m) during the test was recorded either after exhaustion or at the end of the test. If the mouse was able to complete all steps, the total test duration was 35 min for a maximal distance covered of 756 m.

Statistical analysis

Results are means ± SD for the indicated number of mice. The effects of ALY688 in the three groups of mice (WT, mdx and mdx-ALY) were assessed by one-way ANOVA followed by Tukey's test (Prism 9; GraphPad Software, California, USA). Differences were considered statistically significant at $p < 0.05$.

Study approval

All procedures conducted on mice were approved by the Ethical Committee for Animal Experimentation from the Medical Sector at Université Catholique de Louvain (n° LA1230396).

Results

ALY688 improves force and muscle fatigue in mdx Mice

8mg/kg/day of ALY688ER were injected sc to mdx mice for 3 months, starting at 13 months of age. Mdx littermates were separated into two groups: those which were treated with a daily dose of ALY688ER (mdx-ALY) and those who were left untreated (mdx). These two groups were also compared with untreated wild-type (WT) control mice. ALY688 treatment did not affect the total body weight of dystrophic mice (Figure 1), nor the weight of the different removed muscles (figure 2). However, heart weights were significantly increased in the untreated mdx group compared to WT, indicating a severe hypertrophy, while ALY688 reduced and tended to normalize heart weights in treated mdx mice (figure 2). Macroscopic evaluation of the liver and kidney after treatment was also unremarkable, thus indicating that the treatment was well tolerated.

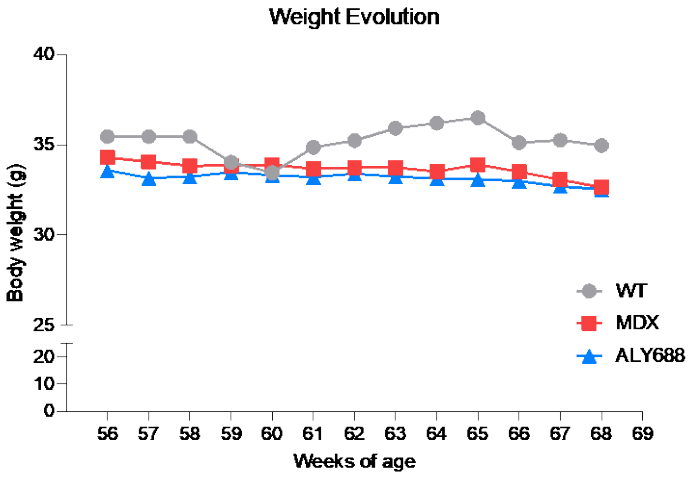

Figure 1. Mice's weight evolution throughout the study

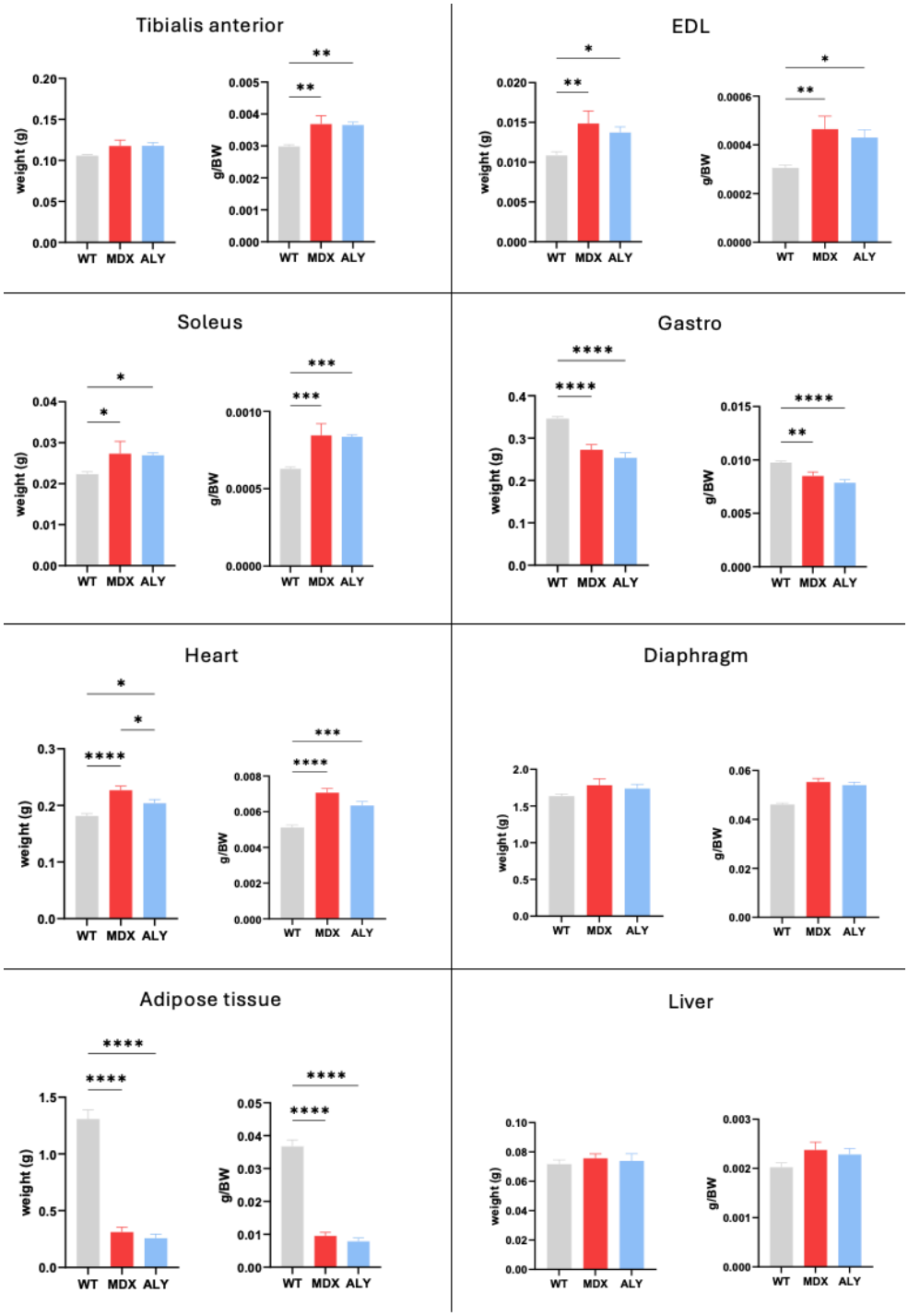
Tibialis anterior
weight (g)
g/BW
WT MDX ALY
EDL
Soleus
Gastro
Heart
Diaphragm
Adipose tissue
Liver

Figure 2. Tissues' weight. *Expressed in gram (g) or corrected by the total body weight (gBW). EDL: Extensor digitorum longus. *p < 0.05, **p < 0,01, ***p < 0,001, ****p < 0,0001. EDL: extensor digitorum longus, Gastro: gastrocnemius.*

To assess the impact of ALY688 on muscle function, mice underwent three functional tests: the wire test, grip test, and treadmill exhaustion test, at four distinct time points. The initial assessment was conducted at 56 weeks of age before treatment initiation (baseline), followed by evaluations at 60 and 64 weeks (intermediary assessment 1 and 2), respectively. The final assessment was performed at 68 weeks of age, one week before sacrifice. The wire test gives an indication of muscle fatigue and coordination. In this test, the time during which the mouse is suspended on a horizontal wire is measured. Mdx mice felt much faster than WT mice, while mdx-ALY showed a constant progression in their performances with time, punctuated by a final remarkable improvement (+45% vs. mdx) (Figure 3A-C).

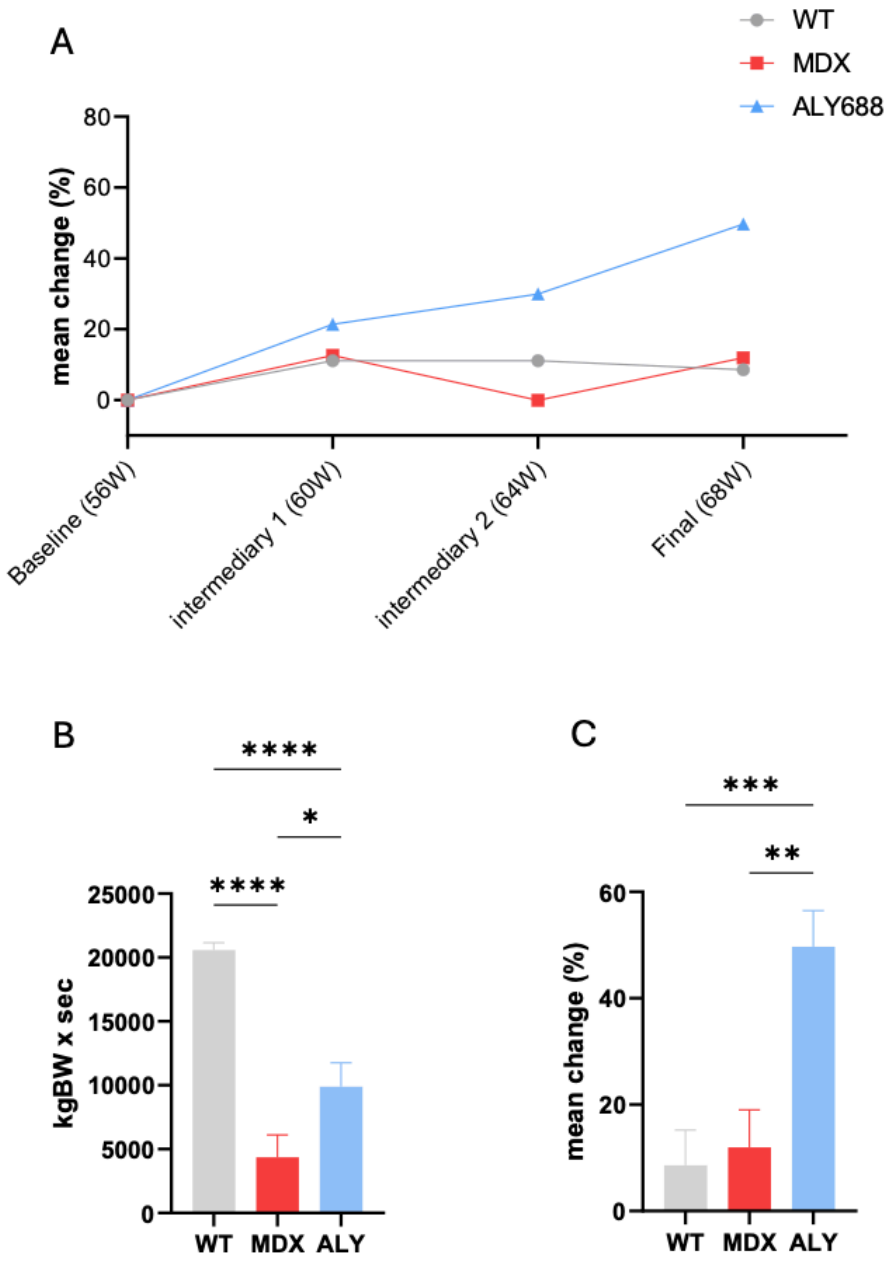

Figure 3. Wire test. *Mice performances were compared from baseline and expressed as the mean change (%) at three different timepoints (intermediary 1, intermediary 2 and final tests) (A). The results of the final test were either normalised to body weight (kgBW × s) (B)*

*or expressed as the mean change compared to baseline (C). Data are means ± SEM; n = 6 mice for all experiments. Statistical analysis was performed using a one-way ANOVA followed by Tukey's test. * p < 0.05, ** p < 0.01, *** p < 0.001, **** p < 0.0001.*

The grip test measures the strength of limb muscles. The force generated by both the upper and four limbs was diminished in mdx mice, but ALY688 partially prevented strength deterioration in the upper limbs (-17% for mdx-ALY vs -24% for mdx) and significantly enhanced it when all four limbs were tested (+6% for mdx-ALY vs -11% for mdx). Specifically, the final test conducted at 67 weeks of age showed an increase of 12% and 13% for the upper and four limbs grip strength, respectively (Figure 4A-F).

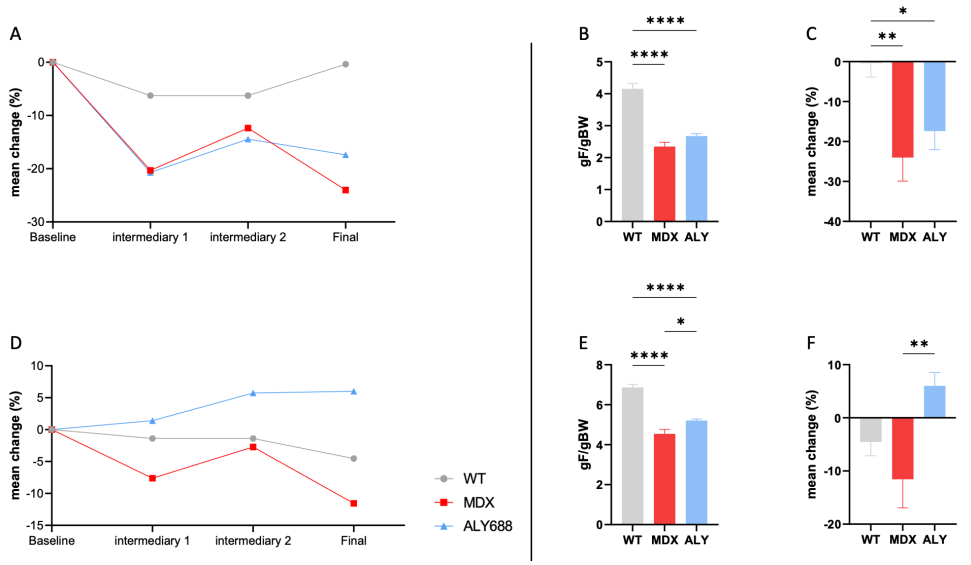

Figure 4. Grip test. *Mice were lowered on a grid connected to a sensor to measure the muscle force of their two upper (upper part) or four limbs (lower part); data were then expressed in gram-force relative to gram-body weight (gF/gBW). Upper and four limbs grip strength were compared from baseline and expressed as the mean change (%) at three different timepoints (intermediary 1, intermediary 2 and final tests) (A and D). The performance of the final test was then either normalised to body weight (kgBW × s) (B and E) or expressed as the mean change compared to baseline (C and F). Data are means ± SEM; n = 6 mice for all experiments. Statistical analysis was performed using a one-way ANOVA followed by Tukey's test. * p<0.05, ** p < 0.01, *** p < 0.001, **** p < 0.0001.*

The uphill treadmill exhaustion test provides valuable data on muscle endurance. The distance covered by mdx mice was significantly reduced in comparison with WT. Although there was a trend toward less endurance decline in the treated group over the study period (-10% for mdx-ALY vs -44% for mdx), no significant differences were observed (Figure 5).

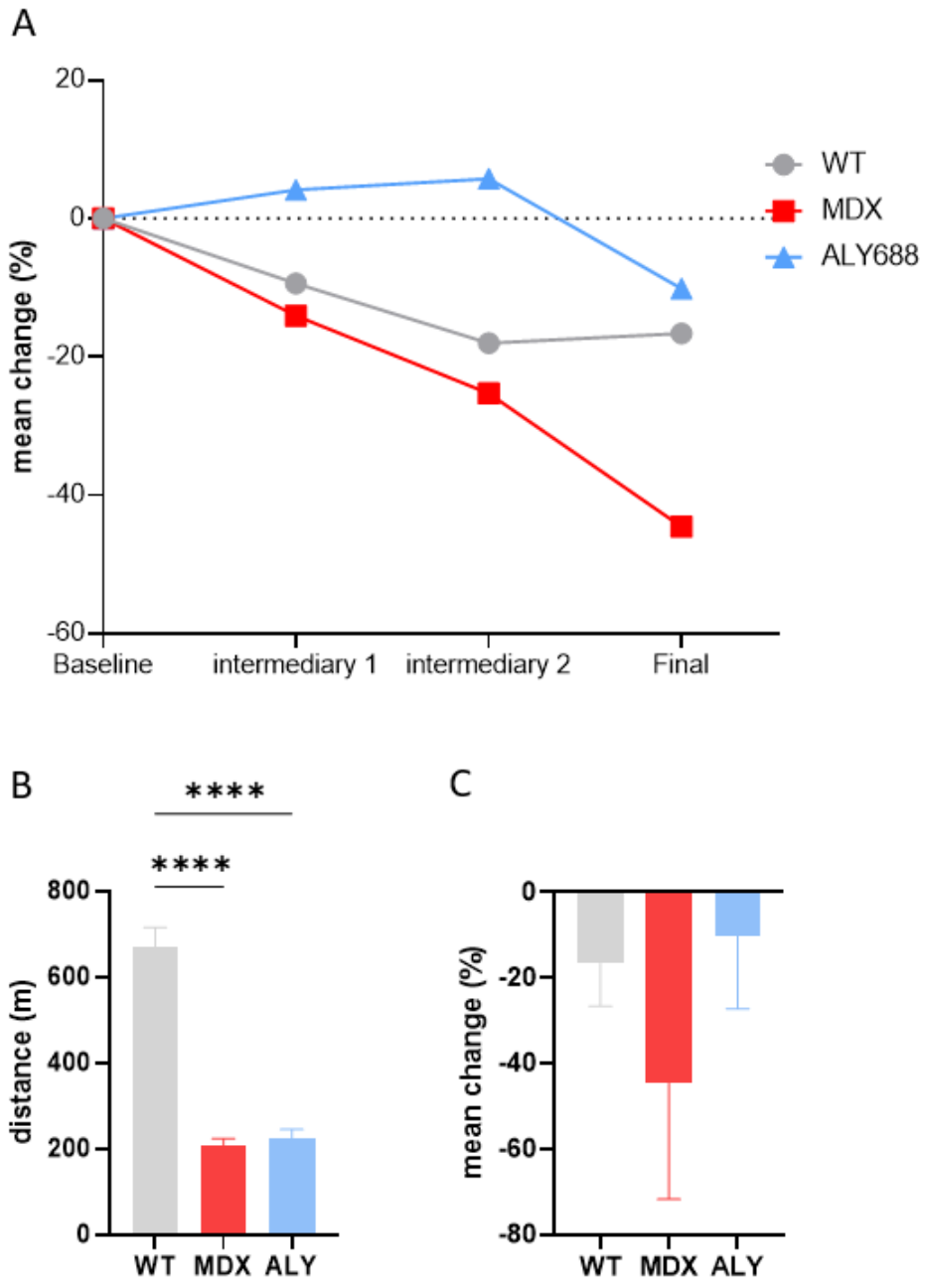

Figure 5. Treadmill exhaustion test. *Mice were placed on a moving belt and encouraged to run to exhaustion with an uphill inclination of 5° and a gradually increasing speed. The mice began by running for 10 minutes at a pace of 20 cm/s. Then, the speed was gradually*

*increased by 1 cm/s every minute until it reached a maximum velocity of 35 cm/s, maintained for another 10 minutes. The distance covered in meters (m) was first recorded either after exhaustion or at the end of the test, then compared to baseline value and finally expressed as the mean change (%) at three different timepoints (intermediary 1, intermediary 2 and final tests) (A). The performance of the final test was also, either normalised to body weight (kgBW × s,) (B) or expressed as the mean change compared to baseline (C). Data are means ± SEM; n = 6 mice for all experiments. Statistical analysis was performed using a one-way ANOVA followed by Tukey's test. *p < 0.05, ** p < 0.01, *** p < 0.001, **** p < 0.0001.*

Taken together, these data indicate enhanced force and resistance to fatigue in dystrophic muscle under ALY688 treatment.

Limitations

The study presented here is limited by the small sample size of mice. Complementary data will soon be available from an additional cohort to reach n=9-10 mice for each group. In addition, the echocardiography data are still not available and might give very interesting results. Finally, it's worth noting that this study encountered several premature deaths, with four mdx mice suffering from muscular tumors. This unfortunate outcome as already been described in aged mdx mice [9]. Importantly, three deaths occurred in the untreated group while only one succumbed in the treated group.

Perspective

After compiling echocardiographic analyses that will give us precious information about heart rate, end-systolic and diastolic volumes, fractional shortening, and left ventricle mass, our next step involves ex vivo analysis to evaluate the impact of ALY688 on cardiac health. Cardiac damages will be assessed through plasma creatine kinase (CK) and lactate dehydrogenase (LDH) levels. Additionally, we'll examine pro-inflammatory and oxidative stress markers, measuring mRNA and protein levels of IL-1β, TNFα, HNE, and PRDX3, complemented by immunohistochemistry analyses.

Subsequently, we will evaluate cardiac fibrosis using Picrosirius red staining, assessing gene expression for αSMA and TGF-β1, along with protein levels of active TGF-β and phosphorylated SMAD2 (P-SMAD2), an effector protein of the TGF-β pathway. The anti-hypertrophic effects of ALY688 will be investigated by examining

gene expression and protein levels of BNP and ANP, two markers of hypertrophy. Mitochondrial biogenesis will also be evaluated by assessing the expression of ERRα and mtTFA, key markers of mitochondrial biogenesis, and the protein levels of TOMM20, a marker of mitochondrial content.

To delve into the mechanisms of action of ALY688 on dystrophic cardiac muscle, we will measure gene expression of its receptors, adipoR1 and AdipoR2, alongside an analysis of the AMPK-PGC-1α-NF-κB pathway. Finally, we wish to test ALY688 on human cardiomyocytes challenged with inflammatory cytokines.

Conclusion

Our preliminary in vivo results demonstrated a significant enhancement in muscle force and resistance to fatigue with 8 mg/kg/day of ALY688ER administered subcutaneously. No safety issue was observed during the study. Additionally, the reduction in heart weight observed at sacrifice is encouraging, particularly in anticipation of the future echocardiography results, which are currently pending.

References

1. Abou-Samra, M., et al., *AdipoRon, a new therapeutic prospect for Duchenne muscular dystrophy.* J Cachexia Sarcopenia Muscle, 2020. **11**(2): p. 518-533.
2. Michel Abou-Samra, N.D., Alice Marino, Camille M. Selvais, Versele Romain, Maria A. Davis-López de Carrizosa, Laurence Noel, Christophe Beauloye, Sandrine Horman, and Sonia M. Brichard, *Striking cardioprotective effects of an Adiponectin Receptor Agonist in an aged mouse model of Duchenne Muscular Dystrophy.* in press, 2024.
3. Dubuisson, N., et al., *The Adiponectin Receptor Agonist, ALY688: A Promising Therapeutic for Fibrosis in the Dystrophic Muscle.* Cells, 2023. **12**(16).
4. Dufeys, C., et al., *AMPKα1 deletion in myofibroblasts exacerbates post-myocardial infarction fibrosis by a connexin 43 mechanism.* Basic Res Cardiol, 2021. **116**(1): p. 10.
5. *<van Putten M. The use of hanging wire tests to monitor muscle strength and condition over time. In DMDM.2.1.004. 2011. httpstreat-nmd.orgwp-contentuploads202106uncategorized-Wire-test.pdf. Accessed 23 Feb 2022..pdf>.*
6. Castro, B. and S. Kuang, *Evaluation of Muscle Performance in Mice by Treadmill Exhaustion Test and Whole-limb Grip Strength Assay.* Bio Protoc, 2017. **7**(8).
7. Quinlan, J.G., et al., *Evolution of the mdx mouse cardiomyopathy: physiological and morphological findings.* Neuromuscular Disorders, 2004. **14**(8): p. 491-496.
8. Peterson, J.M., et al., *NF-κB inhibition rescues cardiac function by remodeling calcium genes in a Duchenne muscular dystrophy model.* Nat Commun, 2018. **9**(1): p. 3431.
9. Chamberlain, J.S., et al., *Dystrophin-deficient mdx mice display a reduced life span and are susceptible to spontaneous rhabdomyosarcoma.* Faseb j, 2007. **21**(9): p. 2195-204.

Part II: List of abbreviation

6MWT six-minute walk test
AAVs adeno-associated vectors
ABD actin-binding domain
ACC Acetyl-CoA carboxylase
ACO acyl-CoA oxidase
AD Alzheimer disease
AdipoAI adipo anti-inflammation agonist
AdipoR ApN muscle receptor
AICAR 5-amino-4-imidazolecarboxamide riboside
ALS amyotrophic lateral sclerosis
ALT alanine transaminase
AMPK AMP-activated protein kinase
AOSD adult-onset Still's disease
ASOs antisense oligonucleotides
AP-1 activator protein 1
ApN Adiponectin
ApN-KO ApN-knockout
ApN-Tg transgenic mice overexpressing ApN
ApN-Tg ob/ob mice obese mice overexpressing ApN
APPL1 adaptor protein containing homology domain, phosphotyrosine binding domain and leucine zipper motif
ASC apoptosis-associated speck-like protein
AST aspartate transaminase
ATP Adenosine triphosphate
BB biceps brachii
BBG bright blue G
BMD Becker Muscular Dystrophy
BMI body mass index
Brg1 *brahma-related gene 1 protein*
BW Body weight
Ca2+ calcium
CaMKKβ Ca2+/calmodulin-dependent protein kinase kinase
CAPS Cryopyrin-Associated Autoinflammatory Syndromes
CARD C-terminal caspase recruitment domain
CCL28 C-C Motif Chemokine Ligand 28
CD cluster of differentiation
CINRG Cooperative International Neuromuscular Research Group
CK creatine kinase
CLI chronic limb ischemia;

COPD chronic obstructive pulmonary disease;
CPPD calcium pyrophosphate dehydrate
CPT1 carnitine palmitoyltransferase 1
CREB cAMP response element binding
CT computed tomography
Cthrc1 collagen triple helix repeat-containing 1
CXMD canine-X-linked muscular dystrophy
DAB 3,3'-Diaminobenzidine staining
DAMPs damage-associated molecular patterns
DAPC dystrophin-associated protein complex
db/db obese and diabetic mice
DGC dystrophin-glycoprotein complex
DIO diet-induced obesity
DMD Duchenne muscular dystrophy
DNHS Duchenne natural history study
EAE experimental autoimmune encephalomyelitis
EBD Evans Blue Dye
ECM extracellular matrix
EDL extensor digitorium longus
EF ejection fraction
EMA European Medicines Agency
ENU N-ethylnitrosourea
ERK extracellular *signal*-regulated kinases
ER Extended release
FAPs fibro/adipogenic progenitors
FCAS Familial cold autoinflammatory syndrome;
FDA *Food and Drug Administration*
FS fractional shortening
G gastrocnemius
gApN globular form of adiponectin
GBP5 guanylate binding protein 5
GCs glucocorticoids
gF gram Force
GLUT-4 Glucose Transporter 4
GPI glycosylphosphatidylinositol
GR glucocorticoid receptor
GREs glucocorticoid response elements
GRMD golden retriever muscular dystrophy
GSDMD Gasdermin D
HES hematoxylin-erythrosin-safran
HFD high-fat diet

HFpEF heart failure with preserved ejection fraction
HFrEF heart failure with reduced ejection fraction
HO-1 heme oxygenase-1
HMGB high-mobility group box 1
HMW high molecular weight complexes
HNE 4-hydroxy-2-nonenal
Hsp heat shock proteins
IFNγ interferon gamma
IGF-1 insulin-like growth factor 1
IκB NF-κB inhibitor
IKK IκB kinase complex
IL- interleukin
IL-1R interleukin 1 receptor
IL-1ra IL-1 receptor antagonist
IL-6R IL-6 receptor
INCA inhibitory CARD
iPSCs induced pluripotent stem cells
IRS-1 insulin receptor substrate 1
K+ potassium
KO ApN knockout mice
LDH lactate dehydrogenase
LGMD2 limb girdle muscular dystrophy type 2
LKB1 liver kinase B1
LMW low molecular weight complexes
LPS lipopolysaccharide
LRR leucine-rich repeat
LV Left ventricle
LVDd Left ventricle end-diastolic
LVDs Left ventricle end- systolic
M1 pro-inflammatory macrophages
M2 anti-inflammatory macrophages
MAPK Mitogen-activated protein kinase
MARK4 microtubule affinity-regulating kinase 4
MCP-1 monocyte chemoattractant protein 1
mdx a murine model of DMD
mdx-ApN mdx mice with ApN overexpression
mdx-AR treated mdx mice
mdx-KO mdx mice with ApN depletion
MI: Myocardial infarction
MIF migration inhibitory factor
miR microRNA

MMW medium molecular weight complexes
MNS 3,4-methylenedioxy-beta-nitrostyrene
Mrf4 myogenic regulatory factor 4
MRFs myogenic regulatory factors
MRI *Magnetic resonance imaging*
MS Multiple Sclerosis
MT mitochondria
mtDNA mitochondrial double-stranded DNA
mTOR mechanistic target of rapamycin
MUFA monounsaturated fatty acids
Myf5 Myogenic factor 5
MyHC myosin heavy chain
MyoD myoblast determination protein 1
Na + sodium
NAFLD nonalcoholic fatty liver disease
NASH nonalcoholic steatohepatitis
NEK7 NIMA Related Kinase 7
NF-κB nuclear factor kappa-light-chainenhancer of activated B cells
NINJ1 nerve injury-induced protein 1
NLRC4 NLR Family CARD Domain Containing 4
NLRP3 nucleotide-binding oligomerization domain, leucine-rich repeat and pyrin domain-containing protein 3
nNOS neuronal nitric oxide synthase
NO nitric oxide
NOD nucleotide-binding oligomerization domain
Nrf2 nuclear factor (erythroid-derived 2)-like 2
NSAIDs non-steroidal anti-inflammatory drugs
P2 × 7R P2X purino-receptor 7 receptor
PAMPs pathogen-associated molecular patterns
P-AMPK phosphorylated AMPK
panx-1 pannexin-1
PD: Parkinson disease
PGC-1α peroxisome proliferator-activated receptor-γ coactivator-1α
PI3K phosphatidylinositol-3 kinase
PKR RNA-dependent protein kinase
POP pyrin-only protein
P-p65 phosphorylated p65 subunit of NF-κB
PPARα the peroxisome proliferator-activated receptor-alpha
PPARγ peroxisome-proliferator-activated receptor-gamma
PRRs pattern recognition receptors
PRDX3/5 peroxiredoxin 3 and 5

PTSD Post-traumatic stress disorder
PYD Pyrin domain
RA Rhumatoid arthritis
RNA Ribonucleic acid
ROS reactive oxygen species
S soleus
sc subcutaneous
SCLC small cell lung cancer
SD standard deviation
SEGRAs selective glucocorticoid receptor agonists
SFA saturated fatty acids
SGT1 *suppressor of G2 allele of skp1*
sIBM sporadic inclusion body myositis
SIRT1 sirtuin 1 SR sarcoplasmic reticulum
SM skeletal muscle
SMAD small mothers against decapentaplegic
SphK-1 Sphingosine kinase 1
sTNFRII soluble tumor necrosis factor receptor type II
T2D Type 2 Diabetes.
TA tibialis anterior
TB triceps brachii
TBI traumatic brain injury
TGFβ transforming growth factor beta
TLR Toll-Like receptors
TNFα tumour necrosis factor alpha
TNFR TNFα receptor
Treg regulatory T cell
TRX from thioredoxin
TWIK2 two-pore potassium channel 2
TXNIP thioredoxin-interacting protein
UTRN utrophin
VCP valosin containing protein
WT Wild-Type mice

Part III: Additional articles

Article 1

Title: Histological Methods to Assess Skeletal Muscle Degeneration and Regeneration in Duchenne Muscular Dystrophy

Authors: Dubuisson N, Versele R, Planchon C, Selvais CM, Noel L, Abou-Samra M, Davis-López de Carrizosa MA.

Abstract: Duchenne muscular dystrophy (DMD) is a progressive disease caused by the loss of function of the protein dystrophin. This protein contributes to the stabilisation of striated cells during contraction, as it anchors the cytoskeleton with components of the extracellular matrix through the dystrophin-associated protein complex (DAPC). Moreover, absence of the functional protein affects the expression and function of proteins within the DAPC, leading to molecular events responsible for myofibre damage, muscle weakening, disability and, eventually, premature death. Presently, there is no cure for DMD, but different treatments help manage some of the symptoms. Advances in genetic and exon-skipping therapies are the most promising intervention, the safety and efficiency of which are tested in animal models. In addition to in vivo functional tests, ex vivo molecular evaluation aids assess to what extent the therapy has contributed to the regenerative process. In this regard, the later advances in microscopy and image acquisition systems and the current expansion of antibodies for immunohistological evaluation together with the development of different spectrum fluorescent dyes have made histology a crucial tool. Nevertheless, the complexity of the molecular events that take place in dystrophic muscles, together with the rise of a multitude of markers for each of the phases of the process, makes the histological assessment a challenging task. Therefore, here, we summarise and explain the rationale behind different histological techniques used in the literature to assess degeneration and regeneration in the field of dystrophinopathies, focusing especially on those related to DMD.

Year: 2022;

Journal: Int J Mol Sci;

Doi: 10.3390/ijms232416080

Article 2

Title: Walking down Skeletal Muscle Lane: From Inflammasome to Disease

Authors: Dubuisson N, Versele R, Davis-López de Carrizosa MA, Selvais CM, Brichard SM, Abou-Samra M.

Abstract:

Over the last decade, innate immune system receptors and sensors called inflammasomes have been identified to play key pathological roles in the development and progression of numerous diseases. Among them, the nucleotide-binding oligomerization domain (NOD-), leucine-rich repeat (LRR-) and pyrin domain-containing protein 3 (NLRP3) inflammasome is probably the best characterized. To date, NLRP3 has been extensively studied in the heart, where its effects and actions have been broadly documented in numerous cardiovascular diseases. However, little is still known about NLRP3 implications in muscle disorders affecting non-cardiac muscles. In this review, we summarize and present the current knowledge regarding the function of NLRP3 in diseased skeletal muscle, and discuss the potential therapeutic options targeting the NLRP3 inflammasome in muscle disorders.

Year: 2021

Journal: Cells

Doi: 10.3390/cells10113023

Article 3

Title: AdipoRon enhances healthspan in middle-aged obese mice: striking alleviation of myosteatosis and muscle degenerative markers

Authors: Selvais CM, Davis-López de Carrizosa MA, Nachit M, Versele R, **Dubuisson N**, Noel L, Gillard J, Leclercq IA, Brichard SM, Abou-Samra M.

Abstract:

Background: Obesity among older adults has increased tremendously. Obesity accelerates ageing and predisposes to age-related conditions and diseases, such as loss of endurance capacity, insulin resistance and features of the metabolic syndrome. Namely, ectopic lipids play a key role in the development of nonalcoholic fatty liver disease (NAFLD) and myosteatosis, two severe burdens of ageing and metabolic diseases. Adiponectin (ApN) is a hormone, mainly secreted by adipocytes, which exerts insulin-sensitizing and fat-burning properties in several tissues including the liver and the muscle. Its overexpression also increases lifespan in mice. In this study, we investigated whether an ApN receptor agonist, AdipoRon (AR), could slow muscle dysfunction, myosteatosis and degenerative muscle markers in middle-aged obese mice. The effects on myosteatosis were compared with those on NAFLD.

Methods: Three groups of mice were studied up to 62 weeks of age: One group received normal diet (ND), another, high-fat diet (HFD); and the last, HFD combined with AR given orally for almost 1 year. An additional group of young mice under an ND was used. Treadmill tests and micro-computed tomography (CT) were carried out in vivo. Histological, biochemical and molecular analyses were performed on tissues ex vivo. Bodipy staining was used to assess intramyocellular lipid (IMCL) and lipid droplet morphology.

Results: AR did not markedly alter diet-induced obesity. Yet, this treatment rescued exercise endurance in obese mice (up to 2.4-fold, $P < 0.05$), an event that preceded the improvement of insulin sensitivity. Dorsal muscles and liver densities, measured by CT, were reduced in obese mice (-42% and -109%, respectively, $P < 0.0001$), suggesting fatty infiltration. This reduction tended to be attenuated by AR. Accordingly, AR significantly mitigated steatosis and cellular ballooning at liver histology, thereby decreasing the NALFD activity score (-30%, $P < 0.05$). AR also strikingly reversed IMCL accumulation either due to ageing in oxidative fibres (types 1/2a, soleus) or to HFD in glycolytic ones (types 2x/2b, extensor digitorum longus) (-50% to -85%, $P < 0.05$ or less). Size of subsarcolemmal lipid droplets, known to be

associated with adverse metabolic outcomes, was reduced as well. Alleviation of myosteatosis resulted from improved mitochondrial function and lipid oxidation. Meanwhile, AR halved aged-related accumulation of dysfunctional proteins identified as tubular aggregates and cylindrical spirals by electron microscopy ($P < 0.05$).

Conclusions: Long-term AdipoRon treatment promotes 'healthy ageing' in obese middle-aged mice by enhancing endurance and protecting skeletal muscle and liver against the adverse metabolic and degenerative effects of ageing and caloric excess.

Year: 2023

Journal: J Cachexia Sarcopenia Muscle

Doi: 10.1002/jcsm.13148

Article 4

Title: Adiponectin and Its Mimics on Skeletal Muscle: Insulin Sensitizers, Fat Burners, Exercise Mimickers, Muscling Pills … or Everything Together?

Authors: Abou-Samra M, Selvais CM, **Dubuisson N**, Brichard SM.

Abstract:

Adiponectin (ApN) is a hormone abundantly secreted by adipocytes and it is known to be tightly linked to the metabolic syndrome. It promotes insulin-sensitizing, fat-burning, and anti-atherosclerotic actions, thereby effectively counteracting several metabolic disorders, including type 2 diabetes, obesity, and cardiovascular diseases. ApN is also known today to possess powerful anti-inflammatory/oxidative and pro-myogenic effects on skeletal muscles exposed to acute or chronic inflammation and injury, mainly through AdipoR1 (ApN specific muscle receptor) and AMP-activated protein kinase (AMPK) pathway, but also via T-cadherin. In this review, we will report all the beneficial and protective properties that ApN can exert, specifically on the skeletal muscle as a target tissue. We will highlight its effects and mechanisms of action, first in healthy skeletal muscle including exercised muscle, and second in diseased muscle from a variety of pathological conditions. In the end, we will go over some of AdipoRs agonists that can be easily produced and administered, and which can greatly mimic ApN. These interesting and newly identified molecules could pave the way towards future therapeutic approaches to potentially prevent or combat not only skeletal muscle disorders but also a plethora of other diseases with sterile inflammation or metabolic dysfunction.

Year: 2020

Journal: Int J Mol Sci.

Doi: 10.3390/ijms21072620